LIPIDS AND CANCER

by

Lesley Catherine Wright, B.Sc. (Queensland), M.Sc. (Macquarie).

A thesis submitted in fulfilment of requirements
for the degree of Doctor of Philosophy in the
Faculty of Medicine, University of Sydney.

Department of Cancer Medicine University of Sydney

March, 1987.

SUMMARY

Transformed, embryonic and malignant cells give a high resolution ^{1}H NMR spectrum which arises from lipids in the plasma membrane. Highly purified plasma membranes were prepared from human acute leukaemic T lymphoblasts (CCRF-CEM) in which the activity of the plasma membrane marker enzyme, 5'-nucleotidase, was enriched 45-fold. Triglyceride and cholesteryl ester each constituted about 4% of the total plasma membrane lipid, and were present in all subcellular membrane fractions isolated. Two-dimensional scalar correlated (COSY) NMR spectroscopy identified triglyceride as the main plasma membrane component giving rise to the NMR spectrum, while soluble non-membrane components accounted for 90% of the remaining resonances in the spectrum of intact cells.

The role of the membranes in multi-drug resistance was investigated using both whole cells and highly purified plasma membranes isolated from human leukaemic lymphoblasts (CCRF-CEM). Cells were made resistant to low levels of vinblastine (up to 20 ng/ml). Despite changes to the high resolution ^{1}H NMR spectrum no consistent changes to the triglyceride or cholesteryl ester content were found in either plasma membranes or whole cells with vinblastine resistance. Free cholesterol and total lipid and protein levels were higher in vinblastine-resistant cells whereas free cholesterol and total phospholipid were more abundant in the plasma membranes. Some of the increased cellular protein and lipid was accounted for by the presence of more mitochondrial profiles and autophagocytic vacuoles in electron micrographs of drug resistant cells.

Ether-linked phospholipids accounted for 13% of the total lipid in sensitive cells and 22% in vinblastine-resistant cells. The increase in

the resistant cells was comprised of 1-O-alkyl phosphatidyl choline and 1-O-alkenyl phosphatidyl ethanolamine. Ether-linked lipids were also present in the purified plasma membranes. 1-O-alkyl triglycerides were present in equal amounts in sensitive and resistant cell membranes, but there was a three-fold increase in 1-O-alkyl phospholipid and a 1.5-fold increase in 1-O-alkenyl phospholipid in the resistant cell membranes.

Freeze-fracture electron microscopy showed alterations to the inner face of the plasma membrane in drug-resistant cells. The presence of bulges indicated that the area of this membrane face could be increased by 4% and the possibility that this structural change could be associated with the higher levels of 1-O-alkyl phospholipid is discussed.

The structure and composition of the neutral lipid domains in the plasma membranes of malignant cells resembles that of serum lipoproteins. A study of lipoproteins in cancer patients was therefore undertaken. An anomolous lipoprotein band (termed "proteolipid") was isolated by density gradient centrifugation from the plasma of an ovarian cancer patient 5 days after surgery. The proteolipid consisted of cholesterol (free and esterified), phospholipid, triglyceride, and contained an abnormally high glycolipid content. Some RNA was possibly present, since two particle sizes (25 - 28 nm and 8 - 11 nm) disappeared after ribonuclease treatment. An abnormal electrophoretic mobility also characterised the proteolipid.

A long T_2 relaxation time (> 800 ms) was recorded by ^1H NMR spectroscopy for the proteolipid fraction. The long relaxation time was associated with a cross-peak (denoted Y), connecting resonances at 1.3 and 4.2 ppm in the 2D spectrum. This cross-peak and the long T_2 have been correlated with the metastatic capacity of cultured cells and human

and rat tumours and arises from molecules on the cells' surfaces. No long T_2 was found in any other lipoprotein fraction or in plasma or serum lipoproteins from normal human subjects. Blood samples taken from the same ovarian cancer patient 7 - 9 months after surgery showed no proteolipid containing a long T_2 and a normal glycolipid content. Moreover the two ribonuclease-sensitive particle sizes were now absent and less of the electrophoretically abnormal band was also detected.

The nature of the resonance with the long T_2 relaxation time was studied in cultured cells of the rat mammary adenocarcinoma line, R13762. Fucosidase treatment decreased the mean T_2 value from 808 to 390 ms and removed the cross-peak Y. When fucosidase-treated cells were injected into Fischer 344 rats the rate of metastasis and the size of the metastatic deposits were markedly reduced. The incorporation of [1-^{14}C] fucose into the non-metastatic variant of the R13762 cells - J clone - was only about half that of the metastatic cells, and in both cases 51% of the label was recovered in a crude ganglioside fraction. NMR analysis of this fraction showed the presence of a long T_2 and cross-peak Y in the sample from the metastatic cells.

It was possible to use serum from Fischer rats to detect the presence of malignancy and identify the presence of metastasis. Normal healthy rats have no ultracentrifugal fraction floating with low density lipoprotein (LDL) density. Rats with primary tumours, whether derived from fucosidase-treated R13762 cells, J clone cells, or R13762 cells before metastasis could be documented, had an LDL fraction with a short T_2 relaxation time (< 400 ms). Rats with macroscopic metastases had not only LDL but also an increased level of very low density lipoprotein (VLDL) and less high density lipoprotein (HDL), especially HDL_2. The LDL fraction from sera of rats with metastases had a long T_2 relaxation

time which could be shortened by fucosidase treatment, and was not found in any other lipoprotein fraction from normal or tumour-bearing rats. NMR analysis of a crude ganglioside fraction from the LDL of sera from rats with metastases demonstrated a long T_2 value, which was again shortened by fucosidase treatment.

Compositional changes were detected in rat lipoprotein fractions after metastasis with the overall trend towards increased triglyceride content at the expense of cholesteryl ester. The presence of a large particle size (24 - 26 nm) with low electrophoretic mobility in the LDL, and unusually small particles (8 - 9 nm) in the HDL_3 was associated with metastasis.

It is concluded that the rat model system, both in vitro and in vivo is useful in studies of metastasis, and may be applicable to human disease. Fucoganglioside in the tumour cell membrane appears to be important in the metastatic process in humans and animals.

Certificate of Originality

I, [redacted] declare that the work presented in this thesis has not been submitted for the award of any other degree to any other University or Institution.

March, 1987.

ACKNOWLEDGEMENTS

This research was performed while the candidate was employed as a member of a multi-disciplinary team in the department of Cancer Medicine (Ludwig Institute for Cancer Research), University of Sydney. My warm thanks to Dr Carolyn Mountford for the many hours she has generously given to helpful discussions and guidance in the design of these experiments and the preparation of the thesis. I also thank Professors Martin Tattersall and Richard Fox for their support and encouragement.

The members of the NMR-Biomembranes group at the Ludwig Institute all gave freely of their time and advice, but special thanks are due to Drs George May, Kerry Holmes and Phil Williams for the performance of the NMR experiments. I am also indebted to Dr Kerry Holmes for the development of the multi-drug resistant lymphoblasts, and the preparation of stimulated lymphocytes and fibroblasts.

The electrophoresis and apo-protein evaluation of the lipoproteins and proteolipids was kindly provided by Dr Dave Sullivan of the Biochemistry Department, Royal Prince Alfred Hospital. I am also grateful to Biotechnology Australia Pty Ltd., for assistance with the isotopic incorporation measurements for RNA and DNA. I wish to thank Pat Gregory and the Animal House staff for providing and treating the rats used in the animal model experiments, and Marlen Dyne and the Electron Microscope Unit, University of Sydney, for the electron microscopy of prepared samples.

Apart from the techniques already mentioned, all experimental work and preparation of samples for NMR spectroscopy was performed by the candidate. Technical assistance in routine lipid analysis and tissue culture was provided by members of the Biomembranes group, but only

after all assay methods had been developed and standardised by the candidate.

I wish to thank Judy Hood for maintaining her sang-froid during the many hours of sun-baking which she missed while typing this manuscript. Last, but certainly not least, I would like to acknowledge the patience and moral support of my husband and children. The latter, for an extortionate fee, were invaluable in chasing up references!

PUBLICATIONS ARISING OUT OF THE WORK DESCRIBED IN THIS THESIS

1. Williams PG, Helmer MA, Wright LC, Dyne M, Fox RF, Holmes KT, May GL and Mountford CE. Lipid domain in cancer cell plasma membrane shown by ^{1}H NMR to be similar to a lipoprotein. FEBS Letters 192:159-164, 1985.

2. Wright LC, Dyne M, Holmes KT and Mountford CE. Phospholipid and ether-linked phospholipid content alter with cellular resistance to vinblastine. Biochemical and Biophysical Research Communications 133:539-545, 1986.

3. May GL, Wright LC, Holmes KT, Williams PG, Smith ICP, Wright PE, Fox RM and Mountford CE. Assignment of methylene resonances in NMR spectra of cancer cells to plasma membrane triglyceride. Journal of Biological Chemistry 261:3048-3053, 1986.

4. Wright LC, May GL, Dyne M and Mountford CE. A proteolipid in cancer cells is the origin of their high resolution NMR spectrum. FEBS Letters 203:164, 1986.

5. Wright LC, Dyne M, Holmes KT, Romeo T and Mountford CE. Cellular resistance to vinblastine is associated with altered respiratory function. Biochemistry International 13:295-305, 1986.

6. Mountford CE, May GL, Wright LC, Holmes KT, Dyne M, Mackinnon WB, Tattersall MHN and Day C. Proteolipid in the serum of a patient with operable cancer: a case history. Lancet (in press), 1987.

LIST OF ABBREVIATIONS

1-O-alkyl PC	=	1 alkyl-2-acyl-sn-glycero-3-phosphocholine
1-O-alkyl PE	=	1 alkyl-2-acyl-sn-glycero-3-phosphoethanolamine
1-O-alkenyl PC	=	1 alk-1'-enyl-2-acyl-sn-glycero-3-phosphocholine
1-O-alkenyl PE	=	1 alk-1'-enyl-2-acyl-sn-glycero-3-phosphoethanolamine
^{1}H	=	proton
^{2}H	=	deuterium
ACS	=	aqueous counting scintillant
ALL	=	acute lymphoblastic leukaemic
Apo A B	=	apoproteins A and B
ATP	=	adenosine 5'-triphosphate
ATPase	=	adenosine 5'-triphosphatase
BHT	=	butylated hydroxytoluene (2,6-di-tertbutyl-p-cresol)
BSA	=	bovine serum albumin
$CDCl_3$	=	deuterated chloroform
cDNA	=	complementary DNA
CL	=	cardiolipin
COSY	=	two dimensional scalar correlated NMR
CPMG	=	Carr-Purcell-Meiboom-Gill
dATP	=	2'deoxyadenosine 5'-triphosphate
diglyceride	=	diacylglycerol
dT	=	deoxythymidine
EBV	=	Epstein-Barr virus
EDTA	=	ethylenediamine tetra-acetic acid
EF	=	exoplasmic face
ESR	=	electron spin resonance
Fatty Acids	=	Numerical symbols are used as in the IUPAC Commission on the Nomenclature of Lipids (1977). First the number of carbon atoms in the fatty acid chain is given, then after the colon, the number of double bonds is stated. The position of the double bonds is placed in brackets e.g. 18:1(11) means a fatty acid chain 18 carbons long, with one double

Fatty Acids (cont'd)

bond situated 11 carbons along from the carboxyl end of the chain.

Sometimes the nomenclature (n - 6) etc.. is used to indicate the position of the double bonds. This refers to the position of the first double bond, counting up from the methyl end of the hydrocarbon chain.

Gangliosides = Abbreviated according to Svennerholm (IUPAC Commission on the Nomenclature of Lipids, 1977).

e.g. $G_{M1} = II^3$ NeuAc - $GgOse_4Cer$
$G_{M2} = II^3$ NeuAc - $GgOse_3Cer$
$G_{M3} = II^3$ NeuAc - LacCer
$G_{D3} = II^3$ $(NeuAc)_2$-LacCer

Other glycolipids are defined in Chapter 2 or text as they occur.

GB = Gaussian broadening
GLC = gas liquid chromatography
GSL = glycosphingolipid
HAc = acetic acid
HDL = high density lipoprotein
Hepes = N-2-Hydroxyethylpiperazine-N'-2-ethanesulfonic acid
H_{II} phase = hexagonal phase
HPTLC = high performance thin layer chromatography
IC_{50} = the dose of drug which inhibits cell growth by 50% after 72 h.
IMPS = intramembranous particles
LB = line broadening
LDL = low density lipoprotein
Lp(a) = lipoprotein(a)
LyPC = lyso-phosphatidyl choline
LyPE = lyso-phosphatidyl ethanolamine
MAL = malignancy-associated lipoprotein

MeOH	=	methanol
mRNA	=	messenger RNA
NMR	=	nuclear magnetic resonance
PA	=	phosphatidic acid
PBL	=	peripheral blood lymphocytes
PBS	=	phosphate buffered saline (Dulbecco's formula, modified, pH 7.4)
PC	=	phosphatidyl choline
PE	=	phosphatidyl ethanolamine
PEI cellulose	=	polyethyleneimine cellulose
PF	=	protoplasmic face
PG	=	phosphatidyl glycerol
PI	=	phosphatidyl inositol
P_i	=	inorganic phosphate
Pipes	=	piperazine-N,N'-bis[2-ethanesulfonic acid]
PL	=	phospholipid
$PolyA^+$ RNA	=	polyadenylated ribonucleic acid
PS	=	phosphatidyl serine
PWM	=	pokeweed mitogen
R_f	=	$\frac{\text{Distance travelled by sample}}{\text{Distance travelled by solvent front}}$
RNase	=	ribonuclease
S.D.	=	standard deviation
S.E.	=	standard error
SPH	=	sphingomyelin
T_2	=	spin-spin relaxation time
TLC	=	thin layer chromatography
triglyceride	=	triacylglycerol
Tris	=	Tris(hydroxymethyl)-aminomethane
VBL	=	vinblastine
VBL7 VBL15 VBL20	=	CCRF-CEM lymphoblasts made resistant to 7, 15 or 20 ng/ml vinblastine
VLDL	=	very low density lipoprotein

TABLE OF CONTENTS

CHAPTER ONE

GENERAL INTRODUCTION

And the end of all our exploring

Will be to arrive where we started;

And to know the place for the first time.

from "Little Gidding", by T.S. Eliot.

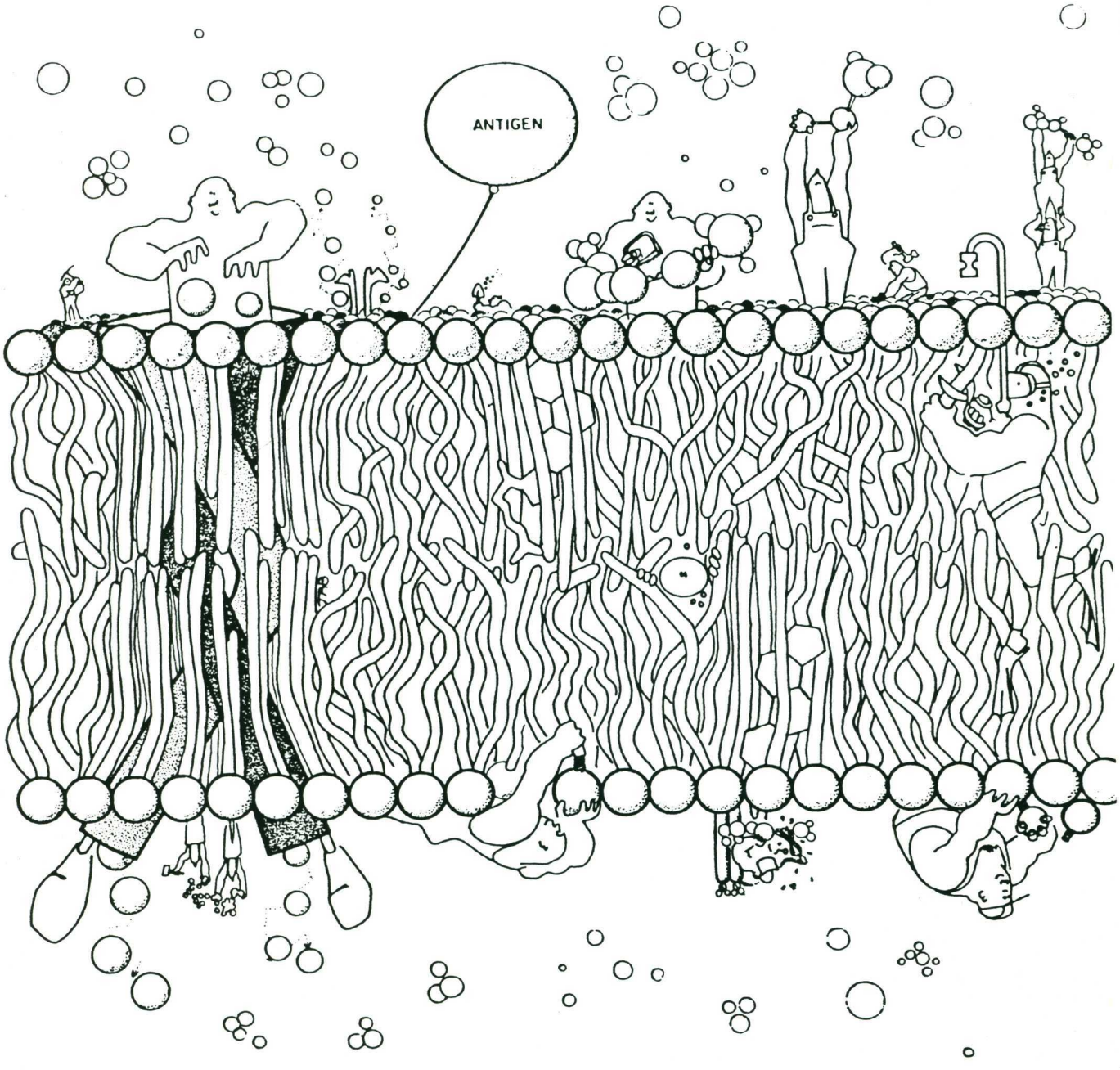

Figure 1.

1.1 MODELS FOR MEMBRANE ORGANIZATION

In 1855 Nägeli first suggested the presence of a membrane on the surfaces of unicellular plants, algae, fungi and mosses (Jain, 1972) and in 1935 Danielli and Davson suggested that plasma membranes consisted of a bimolecular lamellar lipid layer, with protein films and/or saccharides adsorbed on the polar surfaces (Figure 2, from Jain, 1972). In this model, the spread protein completely blanketed the ionic heads of the phospholipids. This model has been known ever since as the "pauci-molecular" or Davson-Danielli model. With the advent of electron microscopy of thin sections of tissues and with X-ray diffraction data, the pauci-molecular model was supported and extended to a general concept of a "unit membrane" structure (Robertson, 1960; 1963). In its original form it suggested that there was one basic

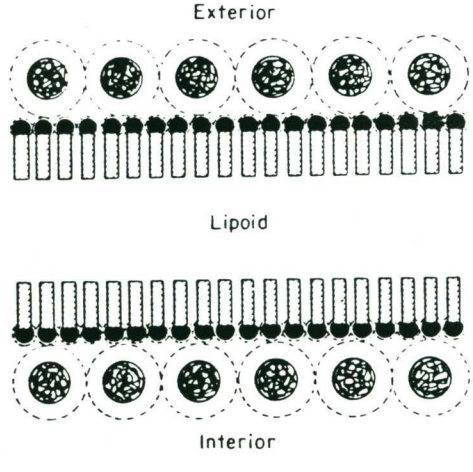

Figure 2. (From Jain, 1972)

structure to which all membranes or most portions of all membranes of all cells and of all species conformed. An electron micrograph of a red

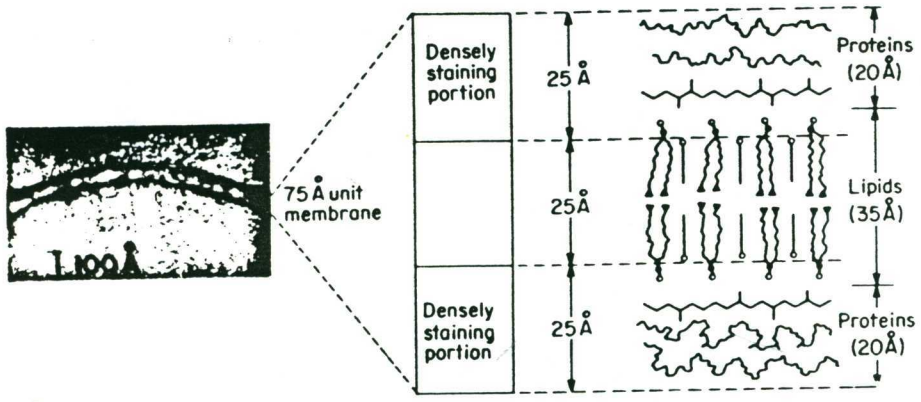

Figure 3. (From Jain, 1972)

cell membrane is shown in Figure 3 (from Jain, 1972). The membrane has a "railway track" appearance of dense lines separated by less dense lines. The interpretation of this observation rests on the assumption that only the polar parts of membranes are accessible to polar staining reagents, which show up as dark lines. Unstained portions are assumed to be due to hydrophobic portions of lipid. The Davson-Danielli-Robertson model did not satisfy requirements for hydrophobic and hydrophilic interactions and required the molecules to be in a high free energy state. This is because the non-polar residues of the proteins are exposed to water molecules and the ionic groups of the lipids and proteins are buried and out of contact with water (Singer, 1971).

A number of other models were proposed to account for membrane structure (Figure 4). Of these, the one developed by Benson (1966), seemed most likely, thermodynamically speaking (Figure 4b, adapted from

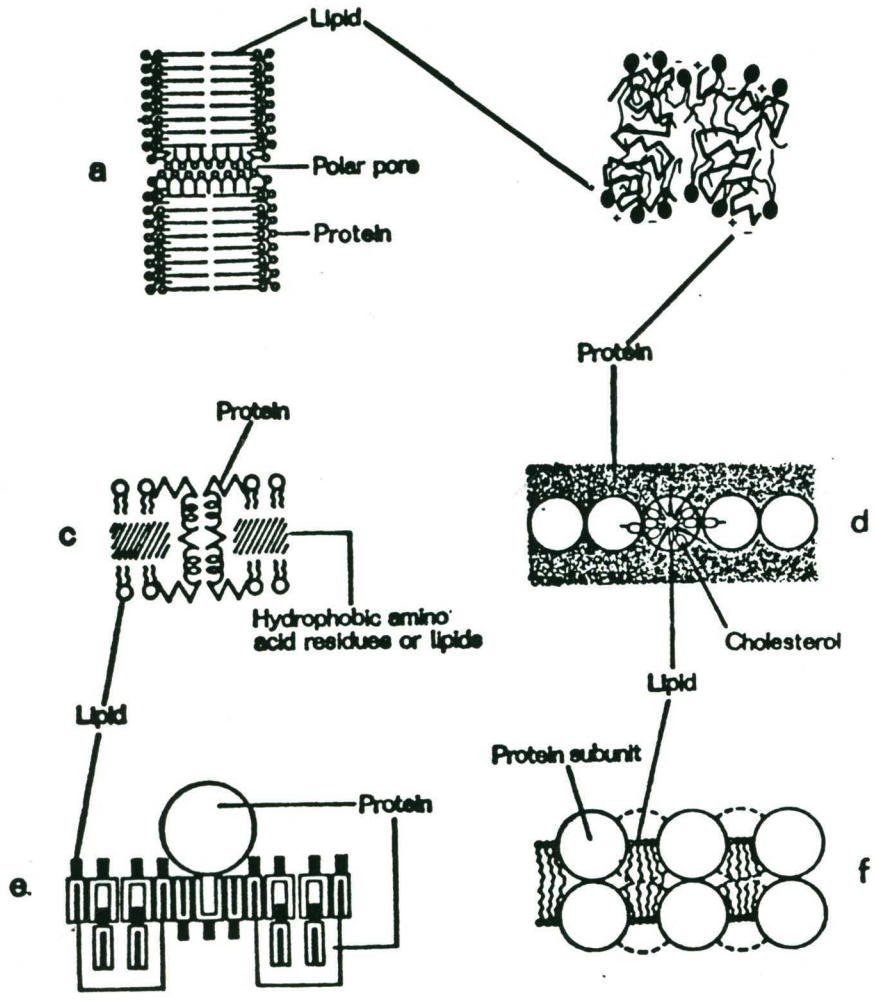

Figure 4. (Adapted from Bretscher, 1973)

1973). In this model, the protein is globular and in the interior of the membrane to maximise hydrophobic interactions. The lipid molecules, however, are not arranged in a bilayer. Their fatty acid chains are individually intercalated into the fold of the protein chains, with the polar heads of the lipids at the exterior surfaces of the membrane in contact with the water. This structure generates a more or less uniform lipoprotein complex, and it was proposed that such complexes exist as morphological subunits held together by hydrophobic interactions in the plane of the membrane.

Intercalation of the fatty acid chains with the proteins, however, still prevents the formation of the maximium number of the interpeptide hydrogen bonds, and this would be thermodynamically unsatisfactory (Singer, 1971).

It was concluded (Singer, 1971) that a mosaic structure of alternating globular proteins and phospholipid bilayer was the only membrane model among those analysed that was simultaneously consistent with thermodynamic restrictions and with all the available evidence on lipid and protein structure, organisation and lateral mobility. For example, proteins that are tightly associated with the membrane (integral membrane proteins) have been found to be structurally amphipathic or asymmetric with regard to the hydrophilic and hydrophobic portions of their structures, as are membrane lipids (Nicolson, 1976; Morawiecki, 1964; Mathews et al., 1971).

The lipid-globular protein mosaic model was developed by Lenard and Singer (1966) and later named the fluid mosaic model by Singer and Nicolson (1972). These models are shown in Figures 5A and B respectively, with proteins floating in a matrix of fluid lipid. The propagation of lipid phase changes over large distances and the unrestricted lateral diffusion of membrane components were implied.

1.2 MODIFICATIONS TO THE FLUID MOSAIC MODEL

1.2.1 Lipid Polymorphism

Most phospholipids spontaneously form the bilayers essential to the fluid mosaic model matrix upon dispersion in aqueous media; however a variety of non-lamellar structures may also be formed with specific lipids under specific conditions (Cullis and de Kruijff, 1979). The individual structures of non-bilayer conformations may be identified

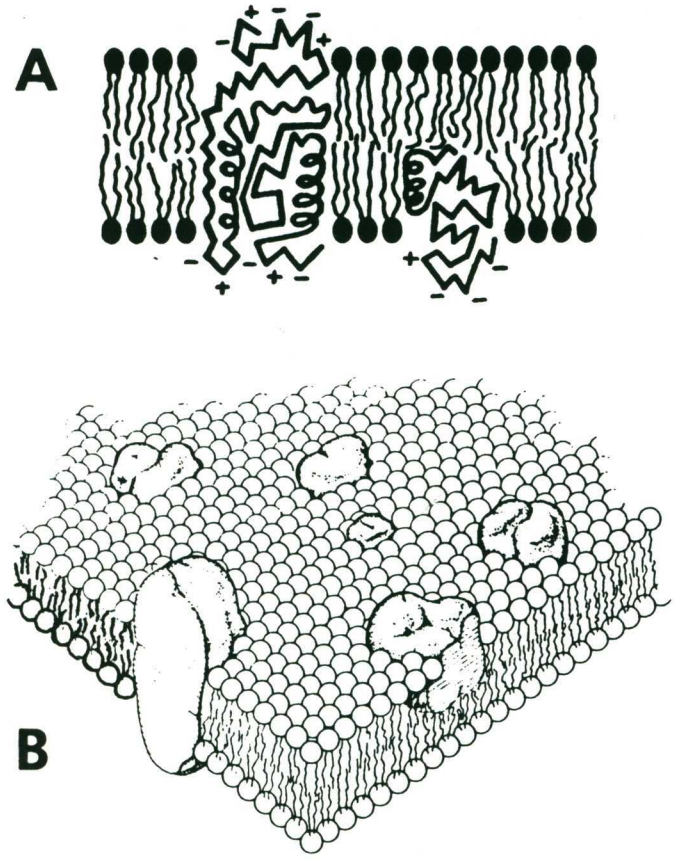

Figure 5. (Singer and Nicolson, 1972)

unequivocally by X-ray-diffraction (Luzzati and Husson, 1962). The inverted hexagonal (H_{11}) phase (Figure 6B) has been the subject of much attention because of its suggested role in cell fusion, exo- and endocytosis, transbilayer movements of lipids (flip-flop), facilitated transport and protein insertion and orientation (Cullis and de Kruijff, 1979).

Phosphorous (^{31}P) NMR spectra and freeze fracture electron-microscopy yield an essentially diagnostic pattern for membrane systems containing hexagonal phase lipid. The added dimension of rotational motion that occurs along the cylindrical axis of the H_{11} phase gives rise to a slightly sharpened line shape (Figure 6B) but with a characteristic ^{31}P NMR spectrum which has reversed asymmetry compared to

bilayer spectra (Figure 6A, Cullis and de Kruijff, 1979). A variety of structures available to phospholipids give rise to narrow, symmetric ^{31}P NMR spectra characteristic of isotropic averaging (Figure 6C). These forms include small bilayer vesicles, micelles, inverted micelles or other lipid phases such as cubic or rhombic (Cullis and de Kruijff, 1979).

Metabolically active membranes, such as rat, beef and rabbit liver microsomes demonstrate isotropic motion for a large fraction of the endogenous phospholipids at 37°C (de Kruijff et al., 1978; Stier et al., 1978). The structure giving rise to isotropic motion is induced by the presence of membrane protein (possibly cytochrome P-450, Stier et al., 1978). Davis and Inesi (1971) concluded on the basis of proton (^{1}H) NMR

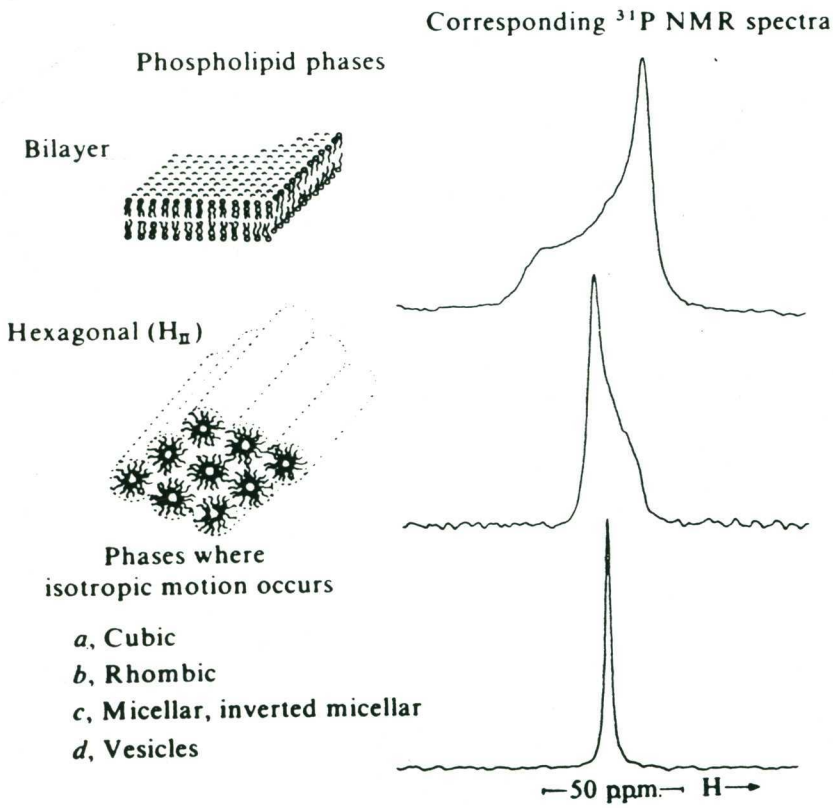

Figure 6. (From Cullis and Dekruijff, 1979)

studies that some 20% of the sarcoplasmic reticulum lipid experienced isotropic motion on the NMR time scale.

1.2.2 Restraints on Lateral Mobility

In many biomembranes the intrinsic proteins are not free to diffuse readily in the plane of the membrane, as proposed in the fluid-mosaic model. They are fixed in position as a result of either high protein concentration, protein aggregation, lipid domain formation, restraint by peripheral membrane components at the inner or outer membrane surfaces or interaction with the underlying cytoskeleton (Nicolson, 1976) or a combination thereof.

The co-operative lattice hypothesis of Changeux et al., 1967 argued for both short-range and long range interactions between protein-lipid units of a membrane lattice. This hypothesis defined the interacting units (protomers) of a membrane lattice as the "intramembranous" segments of membrane protein associated with their boundary layer lipid (Figure 7). In dynamic terms, however, the existence of such a boundary layer is unlikely as evidenced by the rapid exchange (10^{-6} - 10^{-7} s or greater) of molecules between boundary layer lipid and bulk bilayer lipid in ^{2}H NMR studies (Seelig and Seelig, 1978; Oldfield et al., 1978) and the electron spin resonance spectroscopy (ESR) and ^{2}H NMR results of Paddy and Dahlquist, 1982.

Another assumption of the fluid mosaic model is that the lipid hydrocarbon chains in biological membranes are in a fluid, disordered state. However, this is not always so e.g. in Acholeplasma laidlawii and Halobacterium halobium large amounts of ordered lipid are present at temperatures conducive to growth of the organisms (Steim et al., 1969; Chapman and Urbina, 1971; Jackson and Sturtevant, 1978).

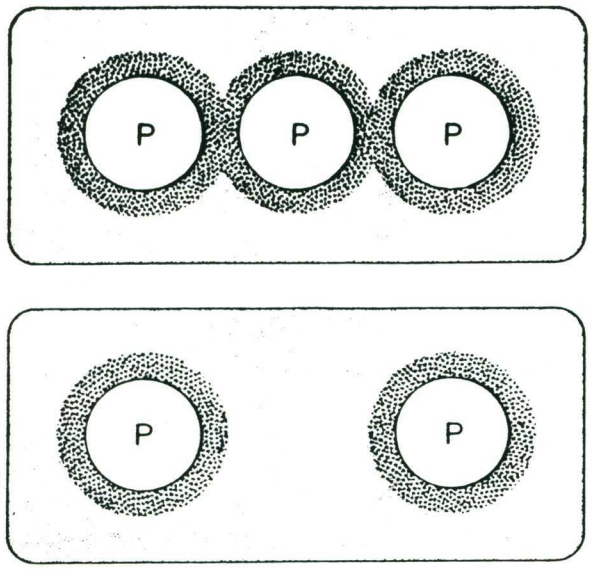

Figure 7. Schematic representation of a section through a hypothetical membrane 'core', showing penetrating membrane proteins, P, with surrounding lipid boundary layers. The proteins are shown as cylinders perpendicular to the membrane plane and the section is parallel to the membrane plane. Top: Merged boundary layers ('coupled' protomers). Bottom: Protomers separated by 'fluid' lipid (from Wallach, 1975).

1.2.3 Asymmetry

Plasma membrane carbohydrates are found to be exclusively associated with the outer half of the bilayer (Gahmberg and Hakomori, 1973). Membrane proteins exhibit an absolute asymmetry in that every copy of a polypeptide chain has the same orientation in the membrane. This asymmetry is maintained by the lack of transmembrane movement of membrane proteins during their lifetime in the membrane (Rothman and Lenard, 1977).

In contrast to the absolute asymmetry of membrane proteins, membrane lipids exhibit partial asymmetry in that most lipid species are found in both halves of the bilayer, but often at different concentrations (Bretscher, 1973; Rothman and Lenard, 1977; Op den Kamp,

1979). The origins, mechanisms for maintenance, and functions of lipid asymmetry are poorly understood. The localization of lipids in some mammalian membranes from normal and malignant cells is presented in Table 1. Most interesting is the destabilization of the lipid bilayer in spicules of sickled red cells, expressed by the enhanced flip-flop of phosphatidyl choline (PC) with the resulting exposure of phosphatidyl serine (PS) in the outer monolayer. The spicules cause an enhanced pro-coagulant activity of sickled cells (Franck et al., 1985).

Table 1. Preferential Location of Lipids in Some Mammalian Cell Membranes

	Location		Equally	
Membrane	Outside	Inside	Distributed	References
Normal Erythrocytes	PC, SPH, LyPC	PE, PS, PI		Renooij et al., 1976
	glycolipids			Gahmberg and Hakomori, 1973
	cholesterol			Fisher, 1976
Sickled Human Erythrocytes	PS	PC		Franck et al., 1985
Blood Platelets	SPH	PC, PE, PS,PI		Chap et al., 1977
	PE	PS, SPH	PC	Otnaess and Holm, 1976
Plasma membrane of malignant mouse cells (LM)	SPH, PS, PI	PE, unsaturated fatty acid	PC	Sandra and Pagano, 1978.
Krebs II ascites cell membranes	diacyl PC, 1-O-alkenyl PC, diacyl PE	1-O-alkyl PC 1-O-alkyl PE	1-O-alkenyl PE	Record et al., 1984.

PC = phosphatidyl choline; PE = phosphatidyl ethanolamine; PS = phosphatidyl serine; PI = phosphatidyl inositol; SPH = sphingomyelin; LyPC = lyso-phosphatidyl choline.

Membrane flip-flop also translocates pro-coagulant phospholipids (mainly PS) in the intact platelet from the inside to the outside. Thus the intact platelet becomes pro-coagulant. The trigger for the flip-flop

mechanism is the simultaneous presence of small amounts of collagen and thrombin (Hemker et al., 1983).

There is also some evidence to suggest that PS exposed on cell surfaces plays a prominent role in the process of macrophage recognition of "non-self", and can serve as a signal for triggering the recognition of effete, damaged and pathological cells such as senescent and sickled red blood cells and perhaps even tumour cells (Fidler, 1985).

1.2.4 Plasma Membrane Domains

Surface membranes have long been known to be heterogeneous in composition (Karnovsky et al. 1982) and in the malignant process they are involved in asocial cell behaviour, invasiveness and metastasis (Nicolson, 1984). These properties will be discussed in more detail in Section 1.6.

Specialized plasma membrane areas clearly exist in cells which have an obvious morphological orientation e.g. dorsal, ventral and intracellular plasma membrane domains have been separated from HeLa cells, a malignant line which adheres to the substratum in culture (Mason and Jacobson, 1985).

Recent evidence suggests the presence of domains in the plasma membranes of cells which do not exhibit an obvious orientation e.g. single cell suspensions such as lymphocytes (Loor, 1980; Hoessli and Rungger-Brändle, 1983). Transformed rabbit and calf thymocytes (Resch et al., 1981, 1983; Szamel et al., 1981) mouse LM fibroblasts (Schroeder et al., 1982) and malignant mouse EL4 lymphoma cells (Szamel et al., 1985) all yielded plasma membrane domains with varying degrees of binding to concanavalin A sepharose columns. The LM fibroblasts were separated into two fractions differing in sialic acid and total lipid content and

5'nucleotidase and Na^+K^+ ATPase activity (Schroeder et al., 1982). The EL4 cells were fractionated into two plasma membrane domains with differing phospholipid fatty acid and enzyme composition (Szamel et al., 1985).

The anchorage of the malignant EL4 cell surface glycoprotein antigen Thy-1 to the membrane is via an association with the 1,2-diacyl-glycerol moiety of phosphatidyl inositol (PI) (Low and Kincade, 1985). This domain is also present in normal mouse thymocytes. The function of Thy-1 is unknown, but it is believed to be associated with cell recognition processes (Williams and Gagnon, 1982; Williams, 1985). It is not clear how and when Thy-1 is released from lymphoid cell surfaces, but it is of interest that phosphatidyl inositol-specific phospholipases C are activated during processes such as the mitogenic stimulation of lymphocytes, resulting in accelerated PI turnover (Berridge, 1984).

The hydrophobic PI membrane anchorage domain has now been associated with a number of proteins of widely differing origin and function and its structure is shown below in (Figure 8), Low et al., 1986.

1.3 MEMBRANE LIPIDS AND MOLECULAR MOTION

1.3.1 Cholesterol

The molecular motion of lipids in membranes can be defined as the reciprocal of the structural order of the lipid components i.e. the greater the disorder of the lipids, the more mobile is the membrane. The structural order is the result of a complex combination of the effects of such parameters as temperature, membrane curvature, the number and position of double bonds and the orientation and motional freedom of the lipid acyl chains (Smith, 1979; Seelig and Seelig, 1980). Of the lipid

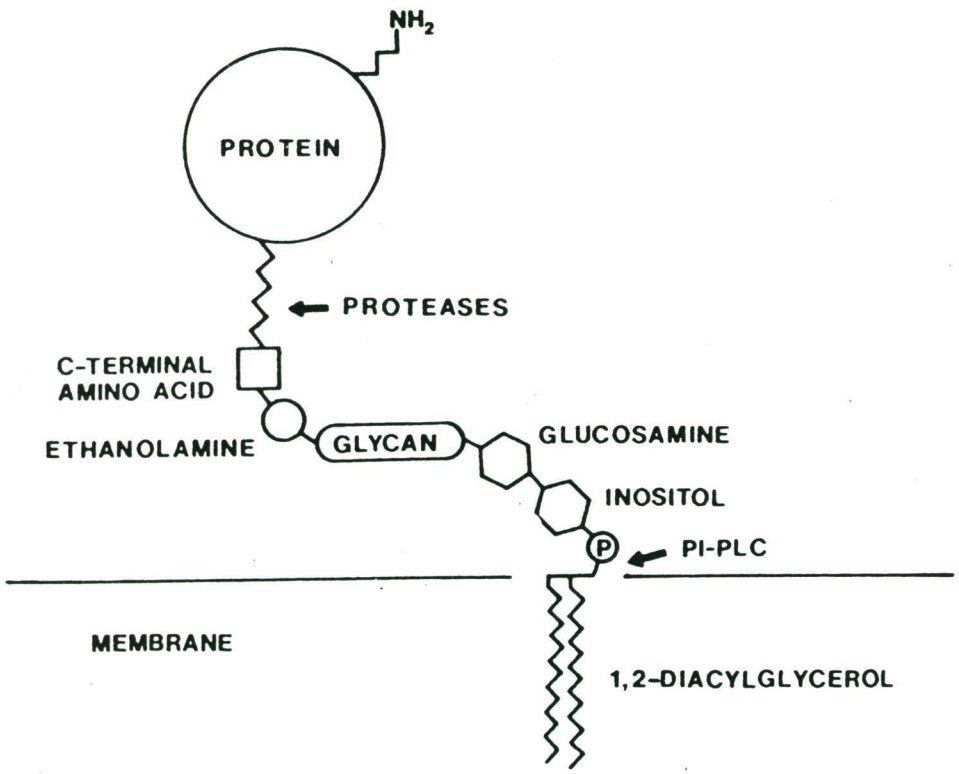

Figure 8. PI-PLC = phosphatidyl inositol-specific phospholipase C (Low et al., 1986)

components free cholesterol is regarded as the most influential in decreasing the molecular motion of lipid acyl chains. It has been demonstrated in artificial systems that cholesterol has a small disordering effect below the phase transition temperature of phospholipids and a large ordering effect above this temperature (Kawato et al., 1978; Oldfield and Chapman, 1972). In biological membranes, cholesterol has an overall ordering effect resulting in decreased molecular motion. The immobilization of acyl chains by cholesterol is enhanced by the presence of oxygenated sterols (Rooney et al., 1985). Up to a certain concentration, it is assumed that cholesterol is distributed evenly between the phospholipids and that the molar ratio of

cholesterol to phospholipid is a good index of lipid molecular motion (Cooper, 1978; van Blitterswijk et al., 1981). Most cellular cholesterol is found in the plasma membrane (Yeagle, 1985).

The cholesterol molecule is believed to be oriented with its polar hydroxyl at C3 abutting the aqueous interface on either side of the bilayer and with its long axis parallel with the phospholipid acyl chains i.e. perpendicular to the plane of the membrane (Figure 9, from Coleman and Lavieties, 1981).

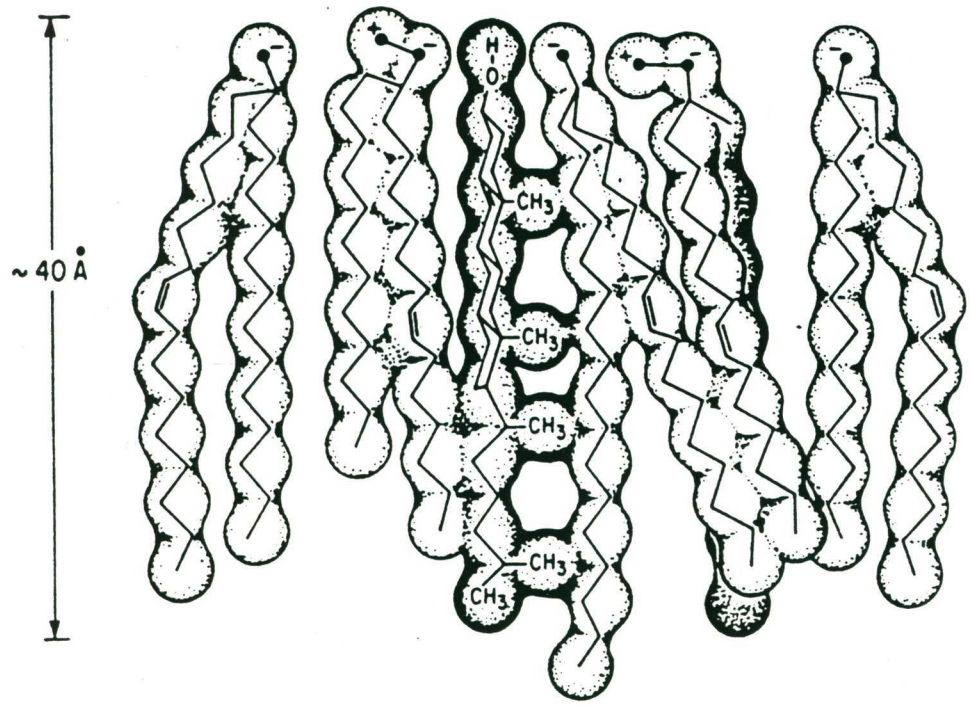

Figure 9. The proposed disposition of cholesterol in one bilayer leaflet of a membrane, illustrating the condensing or clustering of neighbouring polar lipid moieties. Also indicated is the coulombic attraction between polar lipid head groups, as well as the possibility of their H-bonding with the sterol 3-OH group at the aqueous interface (Coleman and Lavieties, 1981).

The weak and non-specific association of cholesterol with phospholipids resembles a solute-solvent type system, with cholesterol being able to diffuse freely from cholesterol rich to cholesterol poor regions of membranes.

Cholesterol metabolism in cancer cells is abnormal. Loss of the feedback regulation of cholesterol synthesis has been demonstrated in hepatomas, precancerous liver, and leukaemias (reviewed by Coleman and Lavieties, 1981), with subsequent accumulation of membrane cholesterol. This increased membrane cholesterol is not always confined to the plasma membrane but may also be found in intracellular membranes, such as those of the mitochondria (Parlo and Coleman, 1984). The rate of cholesterol biosynthesis in leukaemic cells may be 10 - 50 times higher than in normal lymphoid cells and extremely low levels of serum cholesterol have been found in leukaemias (van Blitterswijk et al., 1981). Epidemiological studies have suggested that there is some association, albeit weak, between low serum cholesterol levels and the development of cancer, in particular leukaemias (Dyer et al., 1981) and colon cancer (Sorlie and Feinleib, 1982). More recently, a small positive association between high serum cholesterol levels and colorectal cancers has been established (Mannes et al., 1986).

1.3.2 Acyl Chain Unsaturation

The degree of unsaturation of the membrane phospholipids has also been reported to have important effects on the molecular motion of lipids. For example, the introduction of a cis-double bond into a saturated chain causes an increase in its specific volume with a concomitant increase in the disorder of the surrounding membrane lipids. The double bond has the greatest effect when it is introduced into a

saturated chain e.g. when a stearoyl (18:0) chain is converted to an oleoyl (18:1) chain (Barton and Gunstone, 1975). With the introduction of a second and further double bonds, the effect on molecular motion becomes progressively less pronounced (Stubbs et al., 1981).

The content of polyenoic fatty acids increases during in vivo and in vitro stimulation of rabbit and calf lymphocytes and thymocytes with Concanavalin A and mycobacterium calmette Guerin (Ferber et al., 1975). No particular fatty acid composition has been found to be unique to malignantly-transformed cells, but some trends have been observed. An increase in the ratio of oleic to polyunsaturated fatty acids has been found in several virally transformed cell types (Pessin et al., 1978; Yau and Weber, 1972; Horwitz et al., 1974; Howard and Kritchevsky, 1969). A general trend in hepatoma as compared with normal liver plasma membranes is an increased level of monounsaturated fatty acyl groups, mostly oleic acid (18:1) in the phospholipids (Waite et al., 1977; Bergelson and Dyatlovitskaya, 1973; van Hoeven et al., 1975). An increased ratio of oleic acid to polyunsaturated fatty acid has been demonstrated in microsomes (Waite et al., 1977) and whole cells of Morris hepatoma (Satouchi et al., 1984).

Bergelson and Dyatlovitskaya (1973) found an increased level of 18:1 in the phosphatidyl choline of nephroma as compared with normal kidney. Carruthers (1967) reported a higher degree of fatty acid saturation in phosphatidyl choline, ethanolamine and serine of murine squamous cell carcinoma than in normal or hyperplastic epidermis. Sphingomyelin, however, was more unsaturated. An increased percentage of unsaturated fatty acids is found in acute myeloblastic leukaemia cells compared with normal mature neutrophils (Klock and Pieprzyk, 1979).

The relationship between cancer and dietary fatty acids as described in the literature is confusing. Unsaturated fats were more effective then saturated fats in inducing mammary tumours in rats after a single intragastric dose of 7,12-dimethyl-benz-(a)-anthracine (DMBA) (Hopkins et al., 1976). However, marine oil rich in 20:5 and 22:6 omega-3 fatty acids reduced the amount of rat R3230AC mammary tumours (Karmali et al., 1984), possibly because of inhibitory effects on arachidonic acid metabolism. Many transformed cells lack the ability to convert dietary linoleic acid (18:2, n - 6) to gamma-linolenic acid (18:3, n - 6) (Dunbar and Bailey, 1975). The outline of this pathway and its relationship to prostaglandin (PG) formation is shown below (Figure 10). Some members of the PG 2 series suppress cancer cell proliferation and the administration of gamma-linolenic acid has been found to inhibit tumour growth in rats and some cultured human malignant cell lines (Booyens et al., 1984; Ghayur and Horrobin, 1981). The mechanisms of action of fatty acids on cancer cell metabolism are far from understood.

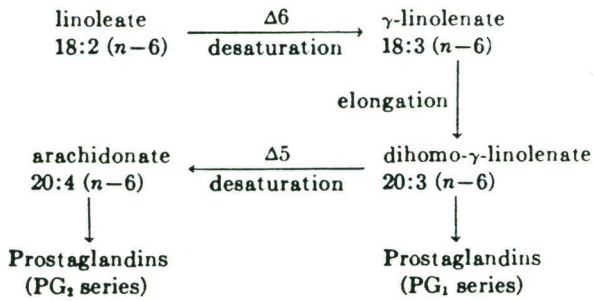

Figure 10. (Dunbar and Bailey, 1975)

1.3.3 Phospholipid Head Groups and Di- and Triacylglycerols

The two choline-containing phospholipids, phosphatidyl choline and sphingomyelin comprise over 50% of the phospholipids of membranes. They are highly dissimilar in physical properties (Barenholz and Thompson, 1980), with natural phosphatidyl choline having a low phase transition temperature compared with sphingomyelin. Besides imparting molecular order to bilayers, sphingomyelin is a powerful coupler of the two lipid monolayers (Schmidt et al., 1978). It can form separate domains under certain conditions (Untracht and Shipley, 1977) and it seems to have affinity to cholesterol in mixtures with other phospholipids (Demel et al., 1977) and proteins (Barenholz and Thompson, 1980). In various processes where the relative content of phosphatidyl choline or sphingomyelin is altered, their total amount remains almost constant (Barenholz and Thompson, 1980). Changes in lipid molecular motion are often expressed as changes to the phosphatidyl choline (lecithin) to sphingomyelin (L/S) ratio. A number of analyses of whole cancer cells and intracellular membranes have shown increased levels of sphingomyelin (Wallach, 1975) when compared with normal cells of the same type. The increases in sphingomyelin are quite dramatic in intracellular membranes, such as mitochondria and nuclei, whereas cardiolipin tends to be lower in tumour cell mitochondria (Wallach, 1975).

Altered phospholipid patterns in neoplasia appear to involve a state of membrane "de-differentiation", that is, the distinctive lipid patterns, which are characteristic of the different membrane types in normal cells e.g. cardiolipin found only in mitochondria and high sphingomyelin content in plasma membranes, are lost (Bergelson et al., 1970; 1974). All membrane subfractions from hepatoma cells have a higher content of phosphatidyl serine than normal liver cells (Bergelson et

al., 1970).

The high metastatic B16-F10 melanoma plasma membranes have lower cholesterol/phospholipid ratios, lower arachidonic acid content and higher phosphatidyl choline/phosphatidyl ethanolamine ratios than their low metastatic counterparts (Schroeder and Gardiner, 1984); see Section 1.6 for a description of metastasis).

The small primary amine headgroup of phosphatidyl ethanolamine forms hydrogen bonds with adjacent phosphate groups resulting in an ordering effect (Shinitzsky, 1984). The conversion of phosphatidyl ethanolamine to phosphatidyl choline by enzymic methylation, as observed during the mitogenic stimulation of lymphocytes, and signal transduction by hormones and neurotransmitters increases the molecular motion of the plasma membrane lipids (Hirata and Axelrod, 1980). The remaining common phospholipids i.e. phosphatidyl serine, glycerol and inositol have relatively unsaturated acyl chains and may be regarded as having a disordering effect similar to phosphatidyl choline (Wallach, 1975).

Diacylglycerol is formed in membranes as a result of phospholipase activity during PI turnover in cellular responses to various stimuli. Its presence can induce hexagonal phases in PE and PC under some conditions and the area per polar lipid group is increased (Das and Rand, 1986). The role of diacylglycerol in malignant transformation is unknown. Diacylglycerol and triacylglycerol are non-bilayer forming lipids (Gorrissen et al., 1982). However high levels of triacylglycerol have been reported in membranes of foetal rat liver mitochondria, which might account for the increased mitochondrial membrane permeability observed in these cells (Harsas et al., 1985).

1.3.4 Glycosphingolipids and Ether Lipids

Glycosphingolipids (GSL) can be subdivided into three major families; neutral GSL, gangliosides and sulfato-GSL. Gangliosides are characterised by the presence of sialic acid, and sulfato GSL's contain carbohydrates substituted with sulfate ester groups. The glycosphingolipids are components of the outer half of the plasma membrane (Gahmberg and Hakomori, 1973; Steck and Dawsen, 1974) with a hydrophobic ceramide region similar to that of sphingomyelin (Figure 11) and therefore they act as promoters of membrane structural order (Feinstein et al., 1975; Sharom and Grant, 1977; Tkaczuk and Thornton, 1979). The hydrophilic head groups containing carbohydrate chains are, in contrast, highly mobile and oriented towards the cell exterior. Those containing sialic acid (gangliosides) carry a net negative charge (Grant, 1984; Lee et al., 1980). They are thus able to participate in hydrogen bonding and ionic interactions (Sharom and Grant, 1978).

Glycerophospholipids and glycerolipids with ether linkages are found in almost all animal cells. These lipids have one or more hydrocarbon chains attached to glycerol through a dehydrated hemiacetal (vinyl ether) or an ether linkage. The terms "alk-1 - enyl" and "alkyl" refer to the presence or absence of unsaturation at the 1 and 2 carbons of the side chain as illustrated below (Figure 12) with the structures of ethanolamine glycerophospholipids (GPE = sn-glycero-3-phosphoethanolamine). The ether-linked glycerophospholipids tend to be concentrated in the plasma membrane (Horrocks, 1972; Cabot and Snyder, 1980). Such lipids tend to pack less closely in a membrane and increase molecular motion (Horrocks and Sharma, 1982). Because they lack a carbonyl group at the 1-position, they have a lower surface potential (Boggs, 1980) and form hydrogen bonds more readily with cholesterol (Brockerhoff, 1974).

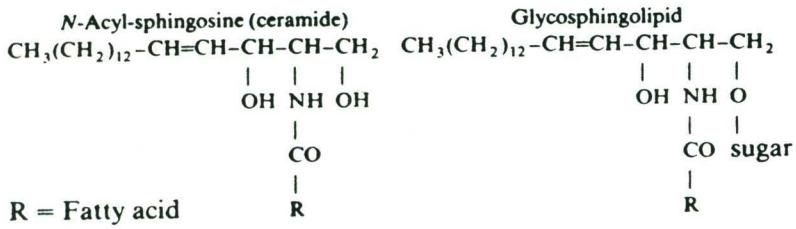

Figure 11. The structure of ceramide and glycosphingolipids (Wiegandt, 1985).

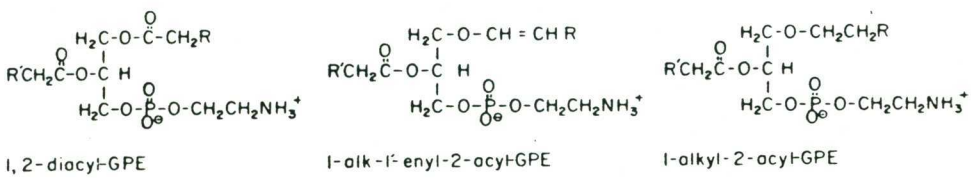

Figure 12. Structures of ethanolamine glycerophospholipids. GPE is an abbreviation for sn-glycero-3-phosphoethanolamine. The common name for diacyl-GPE is phosphatidyl ethanolamine and for alkenyl-GPE is ethanolamine plasmalogen (Horrocks and Sharma, 1982).

Ether-linked lipids generally tend to be present in higher levels in neoplastic tissue, and recently the plasma membrane content of 1-alkyl-2,3,-diacyl-sn glycerols has been linked with metastatic potential (see Section 1.6) in rat mammary carcinomas (Friedberg et al., 1986). Little is known of the functions of ether lipids in either normal or malignant cells. However, platelet activating factor (PAF or PAF-acetether exhibits a broad spectrum of biological activities on various cell types and organs. Specific binding sites have been demonstrated on human platelets, polymorphonuclear neutrophils, macrophages and lung. PAF is critical for the onset and perpetuation of inflammation (Hanahan, 1986).

1.4 CELL SURFACE GLYCOSPHINGOLIPIDS AND CANCER

1.4.1 Alterations in Content and Cell Surface Exposure

Of the approximately 100 glycolipid structures presently known, about half have been reported to be altered in content or cell surface exposure in tumour cells, or not present in normal cells (Reading and Hutchins, 1985). Transformation-associated glycosphingolipid (GSL) alterations were first discovered in cultured cells in 1968 (Hakomori and Murakami) and have been listed extensively in a review by Yogeeswaran (1983). These changes include the reduction in the length of oligosaccharide chains of neutral GSL and gangliosides (Brady and Fishman, 1974; Itaya et al., 1976) and fucolipids (Steiner et al., 1974). However, an elongation of the oligosaccharide chains of GSL was noticed following viral transformation of two 3T3 mouse fibroblast lines (Yogeeswaran et al., 1972). Occasionally precursor GSL accumulates as a consequence of the loss of more complex GSL homologues (Hakomori and Murakami, 1968; Brady and Fishman, 1974). Sometimes transformation

results in the appearance of new GSL's which are present in trace amounts in progenitor cells (Gahmberg and Hakomori, 1975).

With the advent of cell surface labelling techniques e.g. production of antibodies to GSL's, alterations in the organization and cell surface exposure of GSL have been noted in several transformation experiments, e.g. an increase in cell surface exposure of G_{M2} in the transformed state of temperature sensitive SV40-transformed 3T3 cells was correlated with a decrease in the chemical quantity of G_{M2} (Itaya and Hakomori, 1976).

Hepatocarcinomas in animal model systems have elevated total ganglioside levels in all tumours. The ganglioside patterns show a progressive simplification in structure (c.f., above) from hyperplasia to malignant hepatoma. The ganglioside pattern of foetal livers resembled that of poorly differentiated hepatomas (Merritt et al., 1978). Both qualitative and quantitative fucoganglioside changes have been observed in hepatomas compared with normal liver tissues (Baumann et al., 1979).

In contrast to the transformed cultured cells and malignant animal tumours mentioned above, many of the GSL changes in human tumours are quantitative rather than qualitative (Yogeeswaran, 1983). The accumulation of a large variety of fucosylated neutral glycolipids and gangliosides in human cancers to which specific monoclonal antibodies have been raised has been listed in a review by Hakomori (1985). None of these is the specific product of a given tumour. Some are present in small quantities in stem cells or in the normal tissue from which the tumour was derived and others are present in unrelated cells in normal tissues. The GSL antigens are often cryptic and hence immunologically undetectable in normal tissues.

Qualitative changes in GSL do occur in some human cancers, and the most interesting of these are the blood-group antigens. The latter are gene-dependent carbohydrate structural determinants believed to confer "individuality" to cells, just as do histocompatibility antigens (Yogeeswaran, 1983). Alterations of blood group antigens in human tumours can be summarised as follows:-

(a) Deletion of blood group determinants has been noted in certain tumours e.g. a reduction or absence of ABH isoantigenic activity in carcinoma of the cervix, especially when metastatic (Davidsohn et al., 1969).

(b) A second type of change involving the accumulation of precursor blood group substances includes Lewis antigen, precursor blood group core structure, and precursor T antigen of the MN blood group (e.g. Springer and Desai, 1977; Watanabe and Hakomori, 1976; Hakomori and Andrews, 1970). Breast, colon and gastric carcinomas typically involve precursor accumulation (Yogeeswaran, 1983).

(c) The third class of change in blood group determinants involves the appearance of incompatible blood group substances in various human tumours. These include the appearance of A-like antigen in tumours of O and B blood type individuals (Hakomori et al., 1977; Häkkinen, 1970) and an isomer of Le^a seen in Le^b group individuals (Yang and Hakomori, 1971).

1.4.2 Shedding of Cell Surface Components

The shedding of membrane components or domains from the cell surface is generally a selective process which is of widespread occurrence in normal and tumour cells, both in vivo and in vitro (Black, 1980). It may be an important determinant of the cell phenotype and may

play a role not only in intercellular communication but also in the generation and effectiveness of an immune response (Black, 1980; Emersson and Cone, 1981; van Blitterswijk et al., 1975).

Little is known of the differences between normal and tumour cells in the mechanisms and purposes of spontaneous vesicle shedding. Detailed lipid analyses of these vesicles and their parent plasma membranes indicates little difference in composition between the two membranes in normal mouse thymocytes (van Blitterswijk et al., 1982). However, the extracellular membranes exfoliated from leukaemic GRSL cells are significantly different from the corresponding plasma membrane. The cholesterol and sphingomyelin contents are relatively high and the individual phospholipid classes, and their fatty acyl profiles are also different (van Blitterswijk, 1982). In GRSL cells the vesicles form at special domains on the cell surface which are enriched in cholesterol and tumour antigens, as a result of some selective non-random process (van Blitterswijk et al., 1977; 1979).

Gangliosides are shed into the serum of cancer patients in much larger amounts than found in normal controls (Katopodis et al., 1982) and are bound to lipoproteins in the serum (Dawson et al., 1976; van den Bergh and Tager, 1976). The increased level of gangliosides in the plasma of tumour-bearing animals (Kloppel et al., 1977; Lengle, 1979; Skipski et al., 1975b) as well as patients with human cancer (Kloppel et al., 1977; Dnistrian et al., 1982) has been well documented. In human melanoma patients, ganglioside levels are increased both in plasma and in erythrocytes. In particular, G_{D3}, a major component of malignant melanocytes, is increased in patients' plasma (Portoukalian et al., 1978; Gupta et al., 1979) have identified an antigen shed by human malignant melanoma in cell culture which strongly reacted with a

monoclonal antibody against this melanoma cell line.

The amount of gangliosides shed from tumour cells depends on cell density, as demonstrated for mouse ascites hepatoma cells (Shaposhnikova et al., 1984) and Ehrlich ascites carcinoma cells (Prokazova et al., 1984). Highly metastatic cells (Section 1.6, below) shed tumour cell antigens including gangliosides, more readily than those of low metastatic potential (Alexander, 1974; Kim et al., 1975).

Metastatic rat mammary carcinomas have less membrane-associated glycocalyx and higher levels of circulating tumour antigens in serum compared with non-metastatic controls (Kim et al., 1975).

Skipski and co-workers (1975b) noticed that the tumour serum ganglioside profile in malignant hepatoma closely resembled that of tumour tissue and differed from that of normal serum.

1.4.3 Functions in Growth Control and Immune Recognition

Many tumour-associated antigens are GSL often containing large amounts of the carbohydrate, fucose (reviewed by Marcus, 1984). A number of mechanisms exist by which shed cell surface antigens can facilitate tumour escape. A metastatic deposit (Section 1.6, below) of MC-3 sarcoma in rats might avoid destruction by the host because it is enveloped by soluble antigen shed from the cells which intercepts the host defences. The rate of shedding of the antigen may determine the size of the tumour that can escape from the immune defences (Alexander, 1974). On the other hand, gangliosides shed by YAC-1 lymphoma cells surfaces show significant inhibition of mitogen- and antigen-induced T-lymphoproliferation (Ladisch et al., 1983).

Gangliosides substantially inhibit RNA, DNA and protein synthesis and Ca^{2+} uptake into murine T lymphocytes following stimulation by

either Concanavalin A or Ca^{2+} ionophore (Lengle et al., 1979; Krishnaraj et al., 1983). Human leukaemia cell gangliosides have also been found to inhibit mitogen and antigen induced lymphocyte activation (Gonwa et al., 1984). Portoukalian and co-workers (1982) observed that natural killer cell activity can be suppressed by G_{D3} ganglioside in vitro.

Two mutants of murine metastatic tumours (MDAY-D2) which were poorly tumorigenic in normal hosts grew well in immunosuppressed animals. No new antigens were detectable, but relative tumorigenicity was correlated with the rate of tumour cell surface shedding (Dennis et al., 1981).

There is evidence for an antitumour effect of antiglycolipid antibodies in vivo in animal systems (Young and Hakomori, 1981), Urdal and Hakomori, 1980) and in human cancer patients (Hersey et al., 1986).

Shed tumour GSL antigen or antigen-antibody complexes can mediate blocking of cell-mediated immune reactions (Bonavida, 1974; Price and Baldwin, 1977). Immune complexes in the sera of tumour-bearing hosts contain tumour antigens of varying specificities (Loughridge and Lewis, 1971) or foetal antigens (Costanza et al., 1973) or viral antigens (Oldstone et al., 1974). Although the immune complexes have been shown to act as blocking factors in immune reactions the mechanisms are not clear. To quote from Marcus (1984), "a role for gangliosides as modulators of the immune response is an interesting possibility that is not supported by physiologically relevant data at present".

Several lines of evidence, shown in Table 2, indicate that glycolipids may regulate cell growth. A decrease or deletion of ganglioside G_{M3} or G_{M1} in fibroblasts associated with oncogenic transformation may be related to a loss of growth control in those cells, since exogenous addition of G_{M3} or G_{M1} restored normal cell growth (Hakomori, 1985).

Studies of cell growth in chemically defined media indicate that exogenous addition of G_{M3} or G_{M1} alters the binding affinity of cells to platelet-derived growth factor, epidermal growth factor, or fibroblast growth factor via the inhibition of tyrosine-dependent phosphorylation of the receptor (Bremer et al., 1984).

Table 2. Evidence that Glycolipids may Regulate Cell Proliferation (from Hakomori, 1985)

1.	Contact inhibition of cell growth accompanies changes of glycolipid synthesis.
2.	Various glycolipids are more highly exposed at G_1 phase, and some are more highly exposed at G_2 phase.
3.	Butyrate induces cell growth inhibition and enhances ganglioside G_{M3} synthesis.
4.	Retinoids induce contact inhibition, enhance G_{M3} synthesis and glycolipid response.
5.	Antibodies to G_{M3}, but not to globoside, inhibit 3T3 and NIL cell growth and enhance G_{M3} synthesis.
6.	Exogenous addition of glycolipids incorporated into cell membranes inhibits cell growth through the extension of G_1 phase.

The G_1 phase of the cell cycle is the period prior to DNA synthesis and the G_2 phase is the period between DNA synthesis and mitosis (Watson, 1977). The abbreviated representation of gangliosides e.g. G_{M3}, is according to Svennerholm (1963) in the IUPAC-IUB nomenclature of lipids (1977).

1.5 EXTRACELLULAR LIPIDS

1.5.1 Serum Lipoproteins - Normal Structure and Function

All normal human lipoproteins have their origin in the intestine or liver, or both. Four major classes of plasma lipoproteins have been defined (Table 3, from Herbert et al., 1983) and appear to have a pseudomicellar form. Neutral lipids, in particular cholesteryl esters and triglycerides are maintained in the core of particles in a stable form through interactions with the apolipoproteins and phospholipids, which are more polar. Unesterified cholesterol (of intermediate

polarity) is also present in these complexes, and together with phospholipids and apolipoproteins forms an outer shell surrounding the hydrophobic core (Jackson et al., 1976).

Digested dietary fat is incorporated into chylomicra in the intestine and apoproteins of the A group are synthesised there. The C and E apoproteins are acquired from the plasma or lymphatic fluid.

The liver secretes triglyceride into the circulation primarily in very low density lipoprotein (VLDL) particles. A catabolic cascade in the plasma progressively decreases the core triglycerides of VLDL (and hence the particle size) to form intermediate (IDL) and low density lipoproteins (LDL).

Table 3. Chemical and Apolipoprotein Composition of the Lipoprotein Classes as Percent of Dry Weight

	Chylomicrons	VLDL	LDL	HDL
Lipoprotein constituents				
Unesterified cholesterol	1 - 2	4 - 7	5 - 8	3 - 5
Phospholipid	4 - 6	15 - 22	16 - 25	26 - 32
Protein	1 - 2	6 - 10	18 - 22	45 - 55
Esterified cholesterol	1 - 2	15 - 22	45 - 50	15 - 20
Triglyceride	85 - 95	45 - 65	3 - 9	2 - 7
Apolipoprotein components*				
A-I	Major	Minor	Trace	Major
A-II	Major	Minor	Trace	Major
A-IV	Major	Trace	Absent	Minor
B	Major	Major	Major	Minor
C-I	Major	Major	Trace	Minor
C-II	Major	Major	Trace	Minor
C-III	Major	Major	Trace	Minor
D	Unknown	Minor, if present	Trace	Minor
E	Minor	Major	Minor	Minor

* "major" refers to proteins comprising 5 percent or more of the total protein in mesenteric lymph chylomicrons and plasma VLDL, LDL and HDL (from Herbert et al., 1983).

The major protein components of high density lipoproteins (HDL) are synthesized by both liver and intestine but details of the intracellular assembly and transcellular secretion of HDL are not known. HDL particles contain more protein and less lipid than the other classes of plasma lipoproteins (Table 3) and are subdivided into fractions (HDL_3, higher density; HDL_2, lower density). There is evidence for the interconversion of VLDL to HDL_3 and HDL_2 in human plasma (Rye and Barter, 1986) and animal systems (Jansen et al., 1980; Groot et al., 1983) since VLDL and HDL_2 plasma levels are inversely correlated (Patsch et al., 1978).

Most of the apolipoproteins, which are located primarily on the particle surface, readily exchange among lipoproteins (Herbert et al., 1983). The cholesteryl ester exchange protein, identified in the sera of all species but the rat (Barter and Lally, 1978) and the pig (Ha et al., 1981) promotes rapid equilibration between cholesteryl esters in all lipoprotein fractions. Exchange and net transfer of triglycerides between lipoprotein classes is mediated by a separate transfer protein (Rajaram et al., 1980).

The most obvious important function of the plasma lipoproteins is the solublisation and transport of the neutral plasma lipids. Another major function of lipoproteins is in regulating cellular cholesterol metabolism. Most LDL is thought to be catabolized by extrahepatic tissues, approximately one-third by a highly specific receptor-mediated process (Brown and Goldstein, 1976) and the remainder by a receptor-independent pathway (Shepherd et al., 1979). Cellular bound gangliosides enhance the uptake of LDL into human fibroblasts by the receptor-independent pathway (Filipovic et al., 1981) and there is some evidence that glycolipids can be transferred from cells to serum HDL_3 (Kwok et al., 1981). The regulation of cellular cholesterol levels is

achieved by feedback inhibition of β-hydroxy-β-methylglutaryl-CoA reductase, the rate-limiting step on the pathway to cholesterol synthesis, and by down-regulation of LDL receptors (Brown and Goldstein, 1976).

Changes in membrane cholesterol can be brought about by the formation or hydrolysis of cholesteryl esters. The elimination of excessive membrane cholesterol is brought about by its esterification and exclusion from the cell membrane (Brown et al., 1975; Arbogast et al., 1976). Similarly, esterification and de-esterification of serum cholesterol serves to provide a constant cholesterol to phospholipid ratio in membranes of blood cells by cholesterol and phospholipid exchange between serum and the cell membranes (Owen et al., 1984). HDL particles have also been observed to bind to cells (Miller et al., 1977) and to participate in the regulation of cholesterol content by facilitating cholesterol egress.

Lipoprotein triglyceride is a source of acyl chains for membrane lipids. Normally, in vivo, lipoprotein triglyceride is broken down at the endothelial surface by lipoprotein lipase and the resulting fatty acids incorporated into cells (Jackson et al., 1986). However, in cultured cells, especially when grown in medium containing serum from patients with hypertriglyceridaemia, triglyceride from lipoproteins can be accumulated directly into the cells without prior hydrolysis (Howard et al., 1976).

A list of other cellular functions regulated by normal plasma lipoproteins, without uptake of intact lipoprotein particles into the cell is shown in Table 4.

Table 4. Regulation of Cellular Functions by Exogenous Normal Plasma Lipoproteins

Cell Activity	Stimulating or Inhibiting Lipoprotein	Cell or Cellular Function	Selected References
Mg^{2+}-ATPase	VLDL, LDL	Erythrocyte membrane	Shore and Shore, 1975
Adenylate cyclase	VLDL, LDL, HDL	Rat liver plasma membranes,	Ghiselli et al., 1981
Lipogenesis	VLDL	Adipocyte	Thomopoulos et al., 1978
Phosphoprotein phosphatase	LDL, HDL	Erythrocyte membrane	Hui and Harmony, 1979
Prostacyclin production	HDL	Endothelial cells	Fleisher et al., 1982
Immunoregulation	HDL, LDL	Lymphocyte	Hui et al., 1980
Procoagulant monokine production	VLDL, IDL, LDL, HDL	Monocyte (in the presence of lipoprotein-triggered lymphocytes)	Levy et al., 1981
Tumour killing	LDL	Activated peritoneal macrophages	Chapman and Hibbs, 1977
Aggregation	LDL	Platelet	Hassall et al., 1983
Noradrenaline-response	β lipoproteins	Smooth muscle cell	Bloom et al., 1975
Infectious agent	VLDL, HDL	Xenotropic type C virus	Kane et al., 1979
Infectious agent	HDL	Trypanosoma brucei	Rifkin, 1979
Complement-mediated lysis	HDL	Erythrocyte	Rosenfeld et al., 1983
Stimulated by phytohaemagglutinin, pokeweed mitogen and allogenic cells	LDL	Human T lymphocyte	Curtiss and Edgington, 1976
Phosphatidyl inositol turnover, DNA synthesis	LDL	Human T lymphocytes, mitogenically stimulated	Akeson et al., 1984
Pre-replicative protein synthesis, DNA synthesis	VLDL	Foetal rat hepatocytes	Leffert and Weinstein, 1976

1.5.2 Serum Lipoproteins and Cancer

Only a limited number of reports are available regarding plasma lipoprotein levels in cancer patients. Unusually low values for HDL were reported in a variety of cancer patients with a wide range of ages and at different stages of the cancer by Nydegger and Butler (1972). Some of the lowest values obtained were for subjects with intestinal and colon cancer and in advanced breast cancer (Barclay et al., 1970). Many normal subjects who were members of families (first degree relatives) in which there was a high cancer incidence were found to have HDL levels as low as those in patients with overt disease (Barclay and Skipski, 1975; Barclay et al., 1970).

In normal men but not in normal women with positive family histories of cancer, high levels of VLDL co-exist with the low levels of HDL_2. The reciprocal relationship between VLDL and HDL_2 was observed in both men and women with cancer (Barclay and Skipski, 1975) and has also been observed in patients with hyperlipidaemia and severe α-lipoprotein deficiency (Tangier disease), both inherited disorders (Levy et al., 1966), Frederickson et al., 1967).

The same relationship was found between VLDL and HDL_2 in rats with tumours (Barclay and Skipski, 1975), except hepatomas, where the HDL increased (Narayan, 1971; Narayan and Morris, 1970). Similar lipoprotein alterations were found with SV40F tumours in Syrian hamsters (Cox and Gökcen, 1975) and murine leukaemia (Damen et al., 1984).

Lipoproteins also occur in ascites fluid with some intraperitoneal tumours. VLDL, LDL and HDL fractions have been isolated from Ehrlich ascites tumour fluid in mice (Mathur and Spector, 1976). The lipid composition and the electrophoretic patterns of intact particles and apoproteins are similar to lipoproteins of the blood plasma of the

tumour-bearing mice (Mathur and Spector, 1976). These authors suggested that tumour ascites lipoproteins might be derived from the circulation of the tumour-bearing host and supply the growing tumour with lipid. Growth of GRSL ascites tumour in mice was accompanied by alterations in the serum lipoprotein pattern which preceded the same lipoprotein profile in the ascites fluid (Damen et al., 1984).

It is interesting that non-plasma lipoproteins, as well as conventional lipoproteins have been implicated in immunoregulation. Yamazaki and co-workers (1977) demonstrated that VLDL and LDL but not HDL or the delipidated fractions of ascites fluid from MM46 tumour-bearing mice inhibit antibody-dependent macrophage-mediated tumour lysis in vitro. Since human plasma lipoproteins have been implicated in regulation of cytoxic capacity of macrophages (Chapman and Hibbs, 1977), it may be that lipid metabolism is of significance in the biology of neoplasia.

1.6 MALIGNANT TRANSFORMATION AND PROBLEMS IN ITS DETECTION AND TREATMENT

Transformation from health to malignancy is a multi-stage process. The currently accepted first step, initiation, involves alterations at specific sites of genes in normal cells, collectively called proto-oncogenes (Bishop, 1983; Weinberg, 1982; Balmain, 1985). The initiating agent can be any one of a number of chemical agents, viruses or forms of ionizing radiation. If the modification of DNA is perpetuated in subsequent cell generations, then the cells can sometimes become transformed. Transformed cells, and those derived from tumours or premalignant tissue exhibit unlimited proliferative potential (immortality) both in vitro and in vivo (Newbold et al., 1982) in

contrast to normal diploid mammalian cells in culture where the life span is limited and the cells eventually senesce.

Immortality is believed to be a prerequisite for malignant transformation although insufficient by itself (Newbold et al., 1982). The next stage in this process involves further changes to the "initiated" cells caused by agents, either endogenous or exogenous, called tumour promotors. Tumour promotion is partially reversible (Miller and Miller, 1986) and poorly understood. For transformed cells to progress further to the state of malignancy, however, all of the following biological processes must be brought into operation:- (1) biological autonomy (2) uncontrolled cellular proliferation (3) asocial cell behaviour and (4) invasiness and metastasis.

Benign tumours can grow quickly and sometimes be life-threatening, using processes (1), (2) and (3) listed above. However, only malignant tumours have the capacity to invade surrounding tissues and to send cells to begin new tumours at distant sites. This process is called metastasis and it is the major cause of death in patients with cancer. The major obstacle to the treatment of metastases is due, however, to the heterogeneity of the cells populating both primary and secondary neoplasms. Cells obtained from individual tumours exhibit differences with respect to cell surface properties, antigenicity, immunogenicity, growth rate, karyotype, sensitivity to cytoxic drugs and the ability to invade and metastasise (Fidler, 1985).

Different mechanisms have been proposed for the spread of cancer cells (Nicolson and Poste, 1982; Figure 13). "Random" metastasis of tumour cells from a malignant primary tumour populated by cells with similar metastatic properties is shown in Figure 13A. The "non-random" formation of metastases via selective survival of specialized

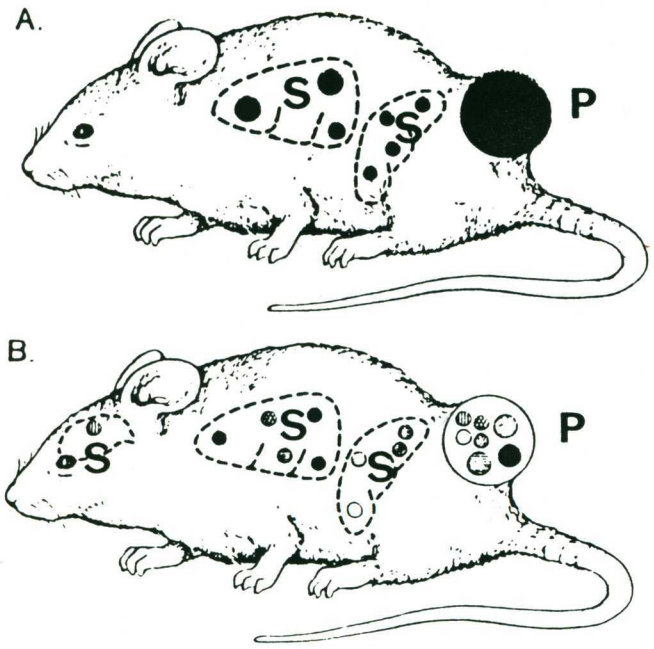

Figure 13. P = primary tumour, S = secondary tumours. In A the primary tumour is homogeneous, but in B it is heterogeneous and contains both metastatic and non-metastatic subpopulations of tumour cells (Nicolson and Poste, 1982).

subpopulations or clones of tumour cells that possess differing metastatic properties is shown in Figure 13B.

Any metastatic cancer cell must have properties which allow it to detach from the tumour mass, invade adjacent tissues and penetrate into the blood or contiguous body cavities. Metastatic cells often travel in the circulation as small clumps of cells called emboli. One single cell can form a metastasis, yet such a tumour then develops the heterogeneity that characterizes malignant tumour cell populations (Fidler, 1985; Fidler and Talmadge, 1986). Blood-borne cancer cells begin their escape from the bloodstream by attachment to the endothelial cells that line the blood vessel. Once attached, the tumour cells induce the endothelial

cells to retract, exposing the underlying basement membrane. The tumour cells invade the space between the endothelium and the membrane and digest the membrane, allowing the cells to pass through. Once through the membrane, they multiply and establish new tumours.

In addition to tumour heterogeneity and metastasis, the development of drug resistance in the cancer patient is also a major limitation to chemotherapy. Despite numerous *in vitro* studies of this phenomenon the mechanisms involved are not fully understood. There have been numerous reports in the literature of mammalian cell lines, selected *in vitro*, that were highly resistant to a cytotoxic antibiotic or plant alkaloid and invariably showed cross-resistance to other compounds structurally unrelated to the initial inducing agent (reviewed by Riordan and Ling, 1985). This phenomenon of multi-drug resistance is a special phenotype the clinical significance of which is slowly being unravelled.

Cell lines resistant to colchicine, vinca alkaloids and anthracyclines have several features in common. These include decreased cellular accumulation of the drugs, cross-resistance to drugs other than the original selective agent, and over production of a 170,000 dalton glycoprotein (the P-glycoprotein where the P stands for "permeability") in the plasma membrane (Juliano and Ling, 1976; Beck *et al.*, 1979; Riordan *et al.*, 1982; Biedler *et al.*, 1983) and overproduction of a 19,000 dalton protein in the cytoplasm (Meyers and Biedler, 1981). There is also a decrease in a family of proteins of molecular weight 70 - 80,000 (Shen *et al.*, 1986). More recently amplification of specific DNA sequences has been shown to correlate with resistance to adriamycin and colchicine in Chinese hamster cells (Roninson *et al.*, 1984; Gros *et al.*, 1986). Although the gene product has not been identified, there is good circumstantial evidence to link it with the P-glycoprotein (Marx, 1986).

Karyotypic features associated with gene amplification have also been associated with multi-drug resistance by Baskin et al., 1981 and Kopnin, 1981.

The currently prevailing hypothesis of multi-drug resistance is that it is the result of the over-expression of the P-glycoprotein genes and others closely associated with it (Riordan and Ling, 1985). Recently a model has been proposed in which P-glycoprotein (the P now stands for "pump") functions as an energy-dependent export pump to reduce intracellular levels of drugs in resistant cells (Gerlach et al., 1986).

1.7 NMR ANALYSIS OF CANCER CELLS

1.7.1 The NMR Experiment

Many of the physical measurements on cancer cells in the past, using fluorescent probes or spin labelling techniques have failed to produce consistent information about the neoplastic state of cells (van Blitterswijk, 1984; Spiegel et al., 1981). In contrast, NMR probes, such as deuterium (^{2}H) are non-perturbing (Chapman and Hayward, 1985) and naturally occurring isotopes e.g. carbon (^{13}C) or protons (^{1}H) may be used for motional studies. Information about membrane dynamic order (i.e. the rate of molecular motion of specific classes of molecules) can be obtained from these NMR experiments.

Basically, three NMR techniques can now be used in the study of tumours and/or cells.

(1) Magnetic Resonance Imaging:- This usually involves ^{1}H NMR and essentially measures ^{1}H density. Special pulse sequences and rapidly changing magnetic field gradients are employed to "see" a slice through a given anatomical part (Valk et al., 1985).

(2) Broadline NMR Spectroscopy:- In large molecules or large assemblies such as membrane bilayers the overall rate of motion is often too slow to average the dipolar interactions effectively and the resonances can be rather broad. The proton magnetic resonance spectrum of R13762 rat mammary adenocarcinoma cells has been separated into its dipolar broadened (("broadline") and non-dipolar-broadened ("high-resolution") contributions (Bloom et al., 1986). Quantitative analysis of the narrow methylene peak, which has been used to characterize the metastatic properties of the R13762 cells showed that it contained 7% of all the protons in the cell (Bloom et al., 1986).

(3) High Resolution NMR Spectroscopy. The NMR spectra obtained from small molecules in non-viscous solvents comprise narrow lines, often one group for each chemically distinct site in the molecule (Abragam, 1983). Figure 14 shows a high resolution ^{1}H NMR spectrum of triolein in chloroform, with assignments. The characteristic frequency of a particular line in the spectrum is usually expressed as the chemical shift in parts per million (ppm). The multiplicity of some of the lines centred around the chemical shift values is due to interaction between the spins themselves. These so-called spin-spin coupling constants occur over only a few bonds, and thus are helpful in characterising the atoms neighbouring that of interest (Farrar and Becker, 1971) e.g. the ^{1}H of the terminal methyl group are coupled to the two protons of the adjacent methylene giving rise to a triplet (Figure 14).

In addition to ^{1}H, there are many other magnetically active nuclei. A partial listing, with relevant properties, is given in Table 5, showing that as the NMR frequency decreases, so does the detection sensitivity. Low isotopic abundances can make nuclei such as ^{13}C and ^{15}N

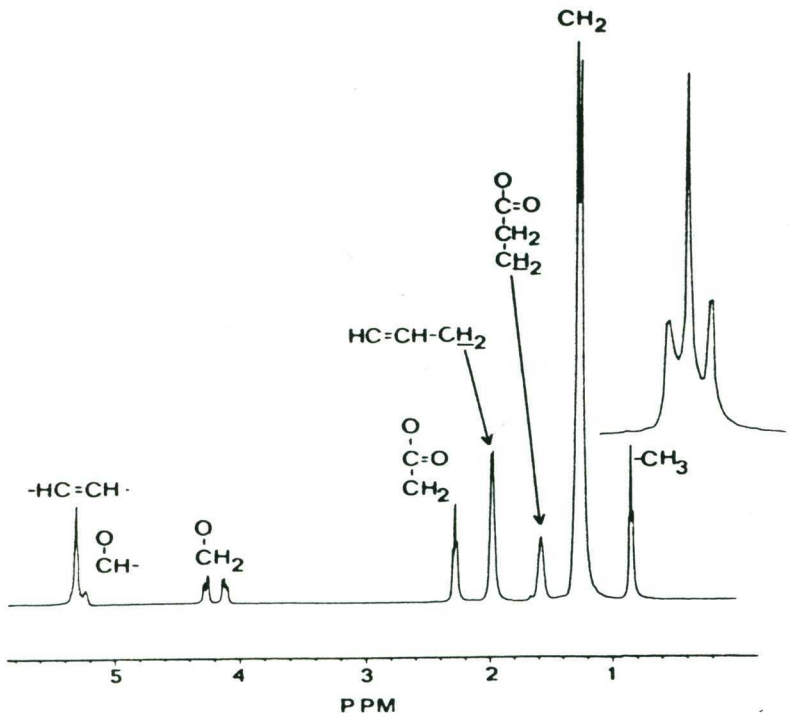

400 MHz ^{1}H NMR spectrum of triolein in $CDCl_3$. The inset is an expansion of the region from 0.77 to 0.92 ppm

Figure 14. (Mountford et al., 1986a)

rather difficult to detect. On the other hand, isotopic enrichment in these elements offers a means to observe particular compounds with little interference from a natural abundance background. The ^{1}H nucleus can be detected with the greatest sensitivity of all to isotopes listed because of its frequency and abundance.

The NMR experiment involves excitation of a nuclear spin system. After excitation the system returns to equilibrium, a process known as relaxation. Two main types of relaxation can be measured:- the T_1 or longitudinal or spin lattice relaxation and the T_2, known as the transverse or spin-spin relaxation. Usually the larger the molecule the less its mobility and thus, the shorter will be its T_2 value and vice

versa. By modification to the pulse sequence it is possible to minimize the contribution from large molecules and observe signals due only to compounds of long T_2 (Brindle et al., 1979).

In ^1H NMR, suppression of the resonance due to H_2O is a major problem. Without some means of suppression, this resonance can dominate the spectrum by factors of thousands (hydrogen in water is 110 M). A variety of methods exists. The simplest method to reduce the intensity

Table 5. Nuclei of Potential Interest for NMR Studies of Cancer Cells

Nucleus	NMR Frequency at 2.35 T (MHz)	Natural Abundance (%)	Sensitivity Relative to ^1H
^1H	100	99.98	1.00
^{19}F	94.1	100.0	0.83
^{31}P	40.5	100.00	6.63×10^{-2}
^{23}Na	26.5	100.00	9.25×10^{-2}
^{13}C	25.1	1.11	1.59×10^{-2}
^2H	15.4	0.015	9.65×10^{-3}
^{15}N	10.1	0.37	1.04×10^{-3}
^{39}K	4.67	93.1	5.08×10^{-4}
^{41}K	2.56	6.88	8.40×10^{-5}

of the water peak is to replace H_2O by heavy water (D_2O). Although deuterium has a magnetic moment, it resonates at a very different frequency from that of ^1H (Table 5). When the heavy water technique is undesirable, or ineffective, various irradiation methods may be used to minimize the height of the H_2O resonance.

1.7.2 High Resolution ^1H NMR Studies of Intracellular Components in Cancer Cells

Agris and Campbell (1982) have used ^1H NMR at 470 MHz to follow the metabolites and changes in lipids in Friend leukaemia cells during their erythroid-like differentiation. Addition of dimethylsulfoxide to these

cells leads to the production of globin and haemoglobin. Using a spin echo technique they were able to follow the time dependence of a variety of resonances. Resonance assignment was made by comparison with the corresponding spectra of cell extracts; in all, some 64 resonances were assigned to 12 amino acids and 19 compounds involved in intermediary metabolism. The most dramatic effect seen during the differentiation was a four-fold increase in the concentrations of glycerophosphorylcholine and phosphorylcholine. A concomitant increase in resonances attributed to the methylene groups of triglyceride was also reported.

^1H NMR of the water in cancer cells was one of the first applications of the NMR technique in oncology (Damadian, 1971). Early reports suggested that cancerous tissue had T_1 and T_2 values for water significantly longer than those of normal tissue (Damadian, 1971; Damadian et al., 1973). Subsequent studies pointed out that cancerous tissue contained increased amounts of water which could be responsible for the longer T_1 values (Inch et al., 1974). As time has gone on, it has become clear that the correlations between water relaxation parameters and pathological states are at best vague, and that significant differences in sample preparation and methods of measurement make comparison of results difficult (Bottomley et al., 1984, 1987; Turner, 1985).

1.7.3 High Resolution ^1H NMR Studies of Lipids in Cancer Cells

Block and co-workers, who first reported the existence in cancer cells of a high resolution NMR spectrum, compared the intact EL4 cell line with extracted cellular lipid. Based on these data they suggested that non-water ^1H NMR signals from tissue might reflect some pathologically relevant information (Block et al., 1974, 1977; Block,

1976). Other reports of a high resolution lipid spectrum include non-transformed cells such as fibroblasts (Nicolau et al., 1975, 1978; Mountford et al., 1980), peripheral blood B lymphocytes, and stimulated T and B lymphocytes (Mountford et al., 1980, 1982b).

Narrow line ^{1}H NMR lipid spectra from intact cells and tumours were considered by most as unlikely, since to generate such a spectrum the lipids had to be able to tumble independently of the cell or tumour. Most scientists familiar with the NMR technique considered that such signals could only be from liposomes or fat droplets in the cytoplasm and therefore would be of little relevance to cellular mechanisms.

The ^{1}H NMR spectrum of an excised solid tumour is remarkably similar to that obtained from a suspension of the same type of cells grown in culture (Mountford et al., 1984b, Figure 15A and B). This spectrum is characteristic of lipid molecules, and can be enhanced in resolution by Lorentzian-Gaussian deconvolution methods to expose at least four resonances under the broad methylene peak at 1.2 ppm (Mountford et al., 1984a, Figure 15C). It is these four resonances which provide information on the cells' ability to metastasise or survive drug therapy i.e. its resistance (Mountford et al., 1984b; Mountford et al., 1986a).

In the resolution-enhanced CPMG spectra of cells of the rat mammary adenocarcinoma metastatic line R13762, four resonances at 1.22, 1.23, 1.25 and 1.27 ppm were resolved under the broad acyl chain envelope (1.2 ppm). Each of these four resonances showed two rates of decay. (These resonances were referenced to the methyl peak at 0.85 ppm. In this thesis the reference is to the external standard of sodium 3-(trimethylsilyl)propanesulfonate which gives a chemical shift of 0.91 ppm for the methyl resonance).

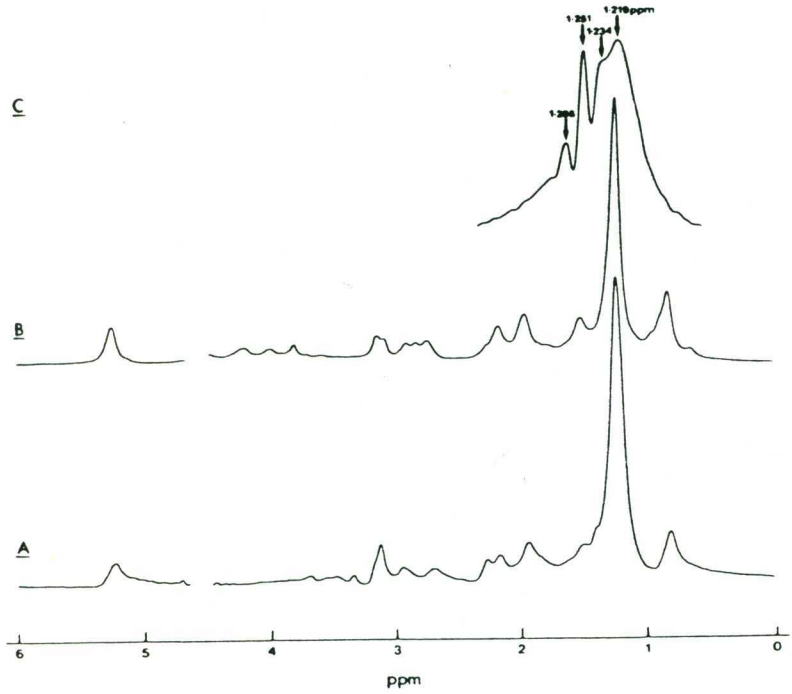

Figure 15. 400 MHz ^{1}H NMR spectra of the mammary adenocarcinoma cell line J clone in PBS-D_2O. Data were recorded with the sample spinning at 37°C. The water peak was suppressed by gated irradiation: 400 Hz sweep width, 1.645 s acquisition time, 64 accumulations. (A) A solid tumour excised from a Fischer rat. The 90° pulse with was 9.5 µs and a line broadening of 3 Hz was applied. (B) J clone cells (1×10^8) were suspended in 0.4 ml of PBS-D_2O, pulse width was 8.5 µs, and a line broadening of 3 Hz was applied. (C) A Lorentzian Gaussian resolution enhancement (k = -11 Hz, g = 0.04 and a = 1.64 s) was applied to the free induction decay recorded for the J clone sample above. The four resonances resolved under the $-CH_2-$ are plotted on an expanded scale (Mountford et al., 1986a)

The long T_2 value (799 ms) of the resonance at 1.25 ppm distinguished the cells with metastatic potential from the non-metastatic variant J clone (Table 6). The resolution-enhanced spectra of the J clone cells also had four resonances at 1.22, 1.23, 1.25 and 1.27 ppm, but the resonance at 1.25 ppm did not have the long T_2 observed in the metastatic parent line (Table 6).

Table 6. Transverse Relaxation Parameter (T_2) for the Methylene Resonance in 13762 and J Clone Cells

Chemical shift (ppm)	T_2 (miliseconds) 13762 cells	J clone cells
	Unmodified Spectra	
1.2	21 ± 3	32 ± 6
	86 ± 16	154 ± 18
	Resolution-enhanced Spectra	
1.22	19 ± 4	50 ± 14
	99 ± 27	136 ± 42
1.23	42 ± 12	63 ± 17
	167 ± 64	224 ± 44
1.25	28 ± 3	55 ± 13
	797 ± 106	117 ± 20
1.27	31 ± 4	38 ± 9
	162 ± 52	157 ± 36

Values for T_2 were calculated by a least-squares method. All values gave an r^2 greater than 0.98. Results are expressed as the mean ± standard error for three experiments (from Mountford et al., 1984b).

The human leukaemic T cell line CCRF-CEM can be made resistant to the anti-cancer drug vinblastine by culturing in an increasing sub-lethal concentration of the drug. Figure 16 shows the spectra of the sensitive parent line compared with lines resistant to 10 and 20 ng/ml vinblastine, called VBL10 and VBL20 respectively. The most notable change is an increase in the intensity of the $-CH_2-$ resonance at 1.2 ppm upon the development of drug resistance. Kinetic studies, in which vinblastine is added directly to the cells in the NMR tube (Mountford et al., 1986a), indicate a difference between resistant and sensitive cells in the behaviour of this resonance on exposure to the drug. Using

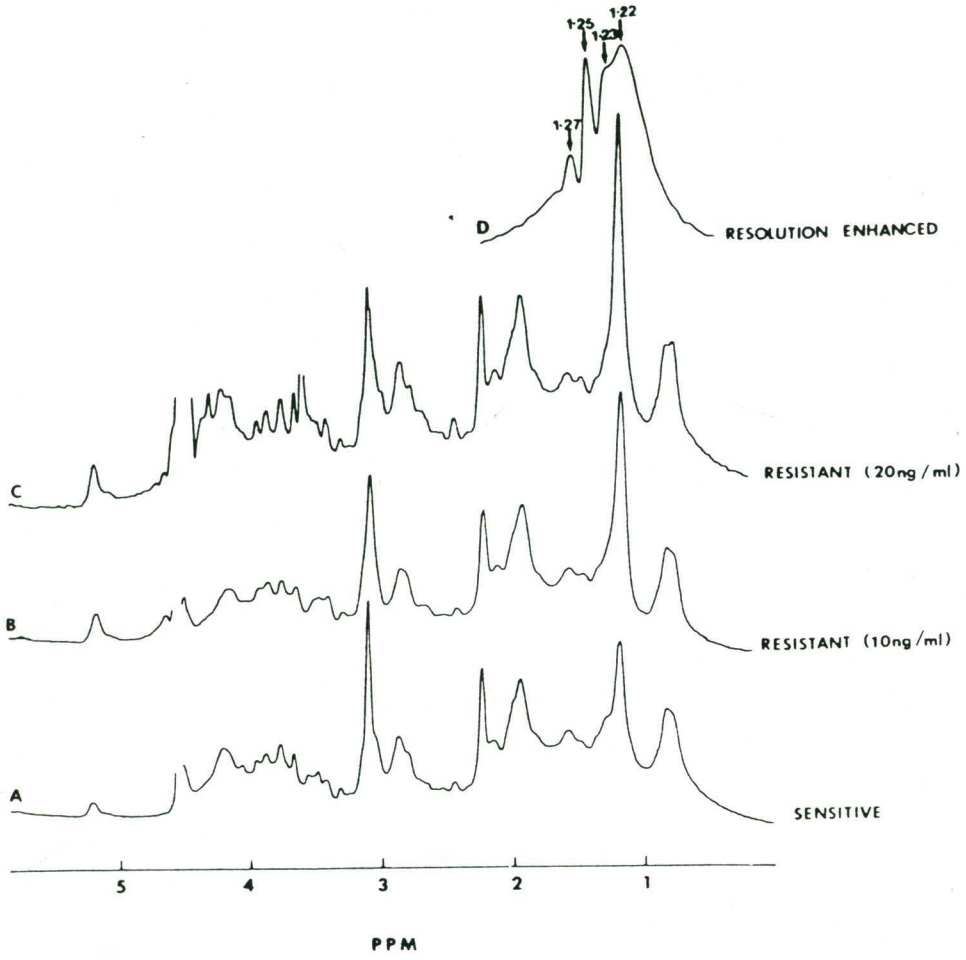

Figure 16. Comparison of the 400 MHz ^{1}H NMR spectrum of CCRF-CEM lines resistant to (A) 20 ng/ml vinblastine, and (B) 10 ng/ml vinblastine with (C) the sensitive parent line. Spectra were collected at 37°C on a Bruker WM 400 MHz spectrometer with the residual water suppressed by selective gated irradiation (Mountford et al., 1986a)

resolution enhancement, changes in intensity of the resonance at 1.25 ppm can be followed for an hour (Figure 17). This peak, generally the most intense and best resolved, is affected by vinblastine differently in the resistant cells compared to the sensitive line. At 40 ng/ml of vinblastine there is a marked decrease in intensity relative to resistant cells in the absence of drug, whereas there is little

difference in the behaviour of this peak in sensitive cells with or without drug.

1.8 THE AIMS OF THIS THESIS

Previous work has established that a high resolution ^{1}H NMR spectrum is typical of transformed or malignant cells but not of resting T lymphocytes (Mountford et al., 1982b). Moreover the resonances in the methylene region are probably from lipid in the plasma membrane of the cell (Mountford et al., 1982b). The existence of rapidly tumbling domains having no diffusive exchange with the rest of the bilayer was

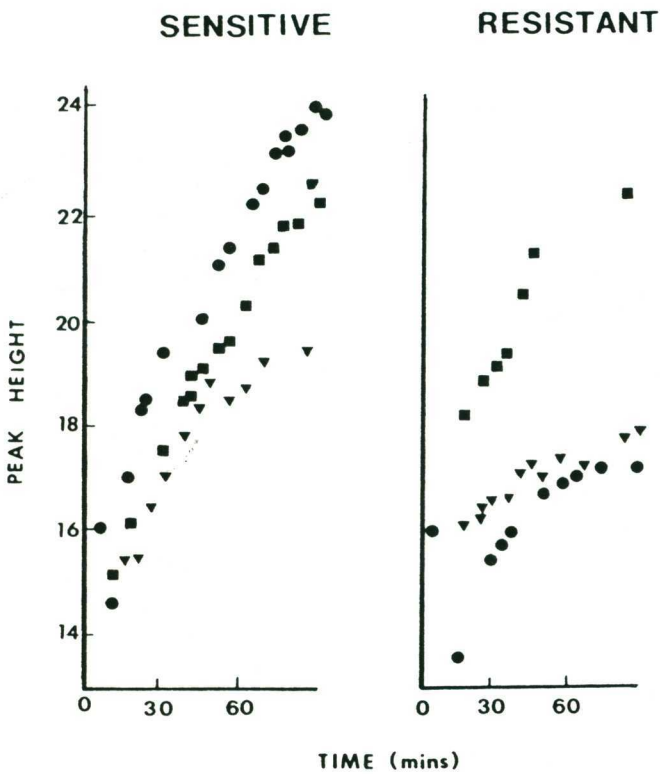

Figure 17. Kinetic effect of vinblastine on the methylene resonance at 1.25 ppm, obtained with Lorentzian-Gaussian resolution enhancement (K = 11 Hz, g = 0.04; a = 1.64 seconds). Vinblastine is added to the NMR tube at 0 min at a concentration of 20 ng (■) and 40 ng (●)/ml. The control sample (▼) has no drug. Sensitive CCRF-CEM cells were compared with cells resistant to 20 ng/ml vinblastine (Mountford et al., 1986a).

suggested by selective and non-selective T_1 measurements on cell suspensions (Mountford et al., 1984a). Such domains could be responsible for the narrow line width of the resonances. A number of questions remain:-

1. What is the identity of the lipid(s) giving rise to the signal in the methylene region and how do such lipids change with the physiological state of the cell i.e. with metastasis and drug resistance?

2. Is the location of such lipids in the plasma membrane of the cell, as has been suggest by paramagnetic probe experiments (Mountford et al., 1982b)?.

3. What is the nature of the rapidly tumbling lipid domains in the membranes? What architecture would allow such motion and how are its lipid components arranged?

4. Is the molecule responsible for the long T_2 relaxation value in metastatic cells part of the same lipid domain and what is the identity of the molecule generating the long T_2 value?

5. What relationship do cancer cells have with surrounding cells, tissues and body fluids, such as blood?

An hypothesis was proposed that the domain should have a lipoprotein-like structure with hydrophobic lipids inside and more polar lipids and proteins in an outside shell. By a combination of lipid

analysis, biochemical techniques, NMR and electron microscopy the presence of such a structure was confirmed on or close to cancer cell membranes and in the serum of cancer patients and rats. The resonance responsible for the long T_2 in tumours and cultured cells was found to be generated by the methyl protons of fucose.

CHAPTER TWO

MATERIALS AND METHODS

2.1 CELL LINES AND CULTURE METHODS

2.1.1 Transformed Lymphocytes and Fibroblasts

Normal T and B lymphocytes were isolated in an interface layer by centrifugation over Ficoll-Paque (Boyum, 1976) from fresh human "buffy coat" supplied by the Red Cross Blood Bank, Sydney, Australia. After dilution in 0.9% NaCl, the lymphocytes were washed free of platelets by repeated centrifugation at 500 g for 5 min. The cells were exposed to pokeweed mitogen (2 μg/ml; Grand Island Biological Co., Grand Island, N.Y.) followed by incubation in medium for 5 days at 37°C.

Chicken embryo fibroblasts were prepared from 10 day old embryonated eggs (Simpson and Hirst, 1961). Primary cultures were used and harvested by mild trypsinisation.

2.1.2 Human T Leukaemic Lymphoblasts and the Establishment of Vinblastine-Resistant Cell Lines

CCRF-CEM human leukaemic T lymphoblasts were originally derived from a patient with acute lymphoblastic leukaemia and have been maintained in culture for many years (Foley et al., 1965). These cells were cultured in RPMI medium containing 10% foetal calf serum, with a doubling time of about 24 h. Dr K.T. Holmes of this laboratory made these cells resistant to $\leq$ 20 ng/ml of vinblastine by culturing cells in the continuous presence of increasing, but sublethal concentrations of the drug. All experiments were performed on cells which had been grown in drug-free medium for at least two weeks, by which time the vinblastine concentration inside the cells was estimated to be less than 0.5 ng/ml.

The vinblastine-resistant CCRF-CEM cells exhibited the "multi-drug" resistant phenotype i.e. they were resistant to a number of other drugs

structurally unrelated to vinblastine. This was quantified by incubating cells at a concentration of 2 x 10^5/ml in the presence of each of the drugs in 3.5 cm^3 well culture plates. Growth at 72 h was determined by hand-counting using a haemocytometer and viability measured by trypan blue exclusion.

The degree of cross-resistance to a range of anti-cancer drugs including vincristine, daunorubicin, VP16, Ara-C and actinomycin D is shown in Table 1 for CCRF-CEM resistant to 20 ng/ml of vinblastine (VBL20) and compared with the sensitive parent cells.

Table 1 Cross-Resistance of CCRF-CEM Cells Resistant to 20/ng/ml VBL

Drug	IC_{50}[a] (ng/ml)	Degree of Resistance[b]
Vinblastine	60	20
Vincristine	65	60
Actinomycin D	40	6
Daunorubicin	90	4
VP16	600	2
Ara-C	3	1

[a] IC_{50} is the dose of the drug which inhibits cell growth by 50% after 72 h. [b] The degree of resistance is obtained by dividing the IC_{50} for the resistant line by the IC_{50} for the sensitive line. VBL = vinblastine.

Vinblastine-resistant lymphoblasts, called VBL7, 15 and 20 in this thesis, grow with a normal doubling time (24 h) in the presence of 7, 15 or 20 ng/ml of vinblastine. The IC_{50} of sensitive CCRF-CEM cells (Beck et al., 1979) is around 3 ng/ml vinblastine, and the IC_{50} values of the sensitive and resistant cells are shown in Table 2, as follows:-

Table 2 Definition of VBL and IC_{50} Values

	IC_{50} (ng/ml)	Maximum VBL Concentration in which Normal Growth Rate occurs (ng/ml)
CCRF-CEM (sensitive cells)	3	5
VBL7	16	7
VBL15	38	15
VBL20	55	20

VBL = vinblastine

Hence the VBL20 cells are eighteen-fold less sensitive to vinblastine than the parent line cells. Measurement of Coulter volume showed no size difference between resistant and sensitive lymphoblasts. Polyacrylamide gel eletrophoresis by Marlen Dyne of this laboratory showed the level of P-glycoprotein in VBL20 cells to be 3-fold higher than in the sensitive cells. Over-production of this glycoprotein is characteristic of the multi-drug resistant phenotype (Juliano and Ling, 1976).

2.1.3 Rat Mammary Adenocarcinoma Lines

The cultured rat mammary adenocarcinoma metastatic cell line, R13762 and the non-metastatic clone "J clone", were supplied by Dr I. Ramshaw, Australian National University (Ramshaw et al., 1982). Cells were grown in RPMI-1640 medium supplemented with 10% foetal calf serum (FCS) at 37°C and were maintained in the logarithmic phase of growth with a doubling time of 17 h. The lightly adherent monolayers could be dislodged by tapping the flask sharply on a padded surface.

2.2 SUBCELLULAR FRACTIONATION

2.2.1 Crude Plasma Membranes

Cells (2×10^8) were washed three times in saline then resuspended in 4 volumes of cavitation buffer (100 mM Tris-HCl pH 7.4, 10 mM $MgCl_2$, 10% (w/v) sucrose and 1 mM phenylmethyl sulfonyl fluoride (PMSF, protease and phospholipase C inhibitor) evaporated from acetone solution. The cells were disrupted in a Parr Pressure Bomb under 800 psi of nitrogen for 15 min. Cellular disruption was monitored by phase contrast microscopy. The suspension was centrifuged for 5 min at 1000 g to remove nuclei and unbroken cells. The pellet was again disrupted in the Pressure Bomb in 4 volumes of cavitation buffer., The bulked supernatants (termed the total homogenate) were centrifuged at 130,000 g for 90 min (Ti 50 rotor, 4°C) to obtain the crude plasma membrane pellet. The 130,000 g supernatant included a floating opalescent lipoidal layer at the top of the liquid (termed floaters).

2.2.2 Purified Plasma Membranes

Cells ($4 - 6 \times 10^9$) were treated as above with the addition of 10 µM leupeptin (a protease inhibitor) as well as PMSF to obtain a total homogenate and a crude plasma membrane pellet. This pellet was resuspended in 3 ml phosphate buffered saline (PBS) pH 7.4 per 10^9 cells by four up-and-down strokes at 1100 rpm in a Braun homogenizer at 4°C. The suspension was further fractionated by sucrose density gradient centrifugation according to the method of Iwanik *et al*, (1984). A discontinuous gradient was formed using 7 ml of 60% sucrose, 7 ml of 48% sucrose, 8 ml of 30% sucrose and 8 ml 10% sucrose in PBS pH 7.4. 3 ml of crude membrane suspension was layered on top of each gradient and centrifugation carried out at 4°C for 2 h in a Beckman SW28 rotor at

106,000 g. The membrane bands from the gradients were removed by aspiration and diluted 1:4 with 10 mM Hepes, pH 7.2, before re-centrifugation at 130,000 g for 60 min (Beckman Ti 70 rotor, 4°C). The membrane pellets were resuspended in 10 mM Hepes, pH 7.2 for marker enzyme assay. All marker enzyme activities except 5'nucleotidase and NADPH cytochrome c reductase were assayed on membranes which had been frozen overnight at -70°C. Little loss of activity occurred.

2.2.3 Marker Enzymes

The purity of the plasma membrane preparations was assessed by calculating the specific activity of the marker in the membrane and dividing by that in the homogenate. Enzyme activities were used only over the range of linearity with membrane or homogenate concentration and time. Protein content was measured with the Bio-Rad Coomassie Blue protein assay kit using bovine serum albumin as a standard. The following three enzymes were used as plasma membrane markers:- (1) 5'nucleotidase (E.C.3.1.3.5) assayed by the radiometric method of Newby et al., 1975. (2) Na^+K^+ adenosinetriphosphatase (E.C.3.6.1.3) measured as the difference in activity obtained in the presence and absence of ouabain in the following reaction:-

50 µl 5 mM ATP, 2 mM EGTA in reaction buffer (see below),

10 µl 20 mM $MgCl_2$ in 10 mM Hepes pH 7.2,

15 µl 7 mM ouabain or H_2O,

25 µl sample.

Incubation was for 30 min at 37°C and Pi release was measured colorimetrically by the method of Ames (1965). Minus enzyme and minus substrate blanks were included. The reaction buffer consisted of 100 mM Hepes pH 7.2 containing 160 mM NaCl and 60 mM KCl. (3) γ-Glutamyl

transpeptidase (E.C.2.3.2.2). This was measured colorimetrically according to the method of Jacobs (1971).

The lysosomal marker, acid phosphatase (E.C.3.1.3.2) was measured in the following reaction mixture:-

50 µl p-nitrophenyl phosphate (10 mM) in Pipes Buffer,
100 mM, pH 5.3 containing 2 mM $MgCl_2$,
25 µl membrane preparation,
25 µl H_2O.

Incubation was for 30 min at 37°C and Pi release was measured by the method of Ames (1965). Minus enzyme and minus substrate controls were included.

Cytoplasmic contamination was determined by lactate dehydrogenase (E.C.1.1.1.27) (Boehringer-Mannheim GmbH diagnostica lactate dehydrogenase test kit, catalogue No.124907).

Spectrophotometric methods were used to determine NADPH-cytochrome c reductase (E.C.1.6.2.4), the marker for endoplasmic reticulum (Sottocasa et al., 1967), and cytochrome c oxidase (E.C.1.9.3.1), the mitochondrial marker (Wharton and Tzagoloff, 1967). Nuclear contamination was assessed by the presence of DNA, measured fluorimetrically by ethidium bromide binding (Brunk et al., 1979).

2.2.4 Supernatant from VBL20 Cell Homogenates

Cells (2×10^8) were washed three times in 0.9% NaCl, then lysed for 20 min at 4°C in 2 ml D_2O. The resulting homogenate was centrifuged at 130,000 g for 60 min at 4°C to sediment the membrane pellet, and the supernatant fraction was removed and used immediately for NMR spectroscopy.

2.3 LIPID ANALYSES

2.3.1 Lipid Extraction and Total Lipid Weight

Membranes or homogenates were extracted with 7 volumes of distilled methanol containing 0.1 mg per ml sample of butylated hydroxytoluene (BHT) for 15 min with stirring, followed by the addition of 14 volumes of chloroform (Mallinckrodt, nanograde). Stirring was continued for 1 h at room temperature (Gottfried, 1967). After filtration through a sintered glass filter, the non-lipid contaminants were removed with coarse Sephadex G25 chromatography (Williams and Merrilees, 1970). The sample was evaporated to dryness on a rotary evaporator and taken up in $CHCl_3$: MeOH (19:1 v/v) for storage at -20°C in the dark. An aliquot was pumped dry and weighed on a Mettler HK60 electronic balance.

2.3.2 Cholesterol

The total cholesterol was measured after saponification of dried lipid with 33% ethanolic KOH for 16 h at 37°C. The hydrolysate was diluted 1 in 10 with freshly distilled isopropanol and the total cholesterol was measured by the fluorimetric method of Heider and Boyett (1978). Free cholesterol was measured on unhydrolysed lipid and cholesteryl ester content calculated by subtracting free cholesterol from total cholesterol.

2.3.3 Di- and Triacylglycerols

Triacylglycerol was determined colorimetrically (Sigma Diagnostic Kit 405) using the molecular weight of triolein (885). Diacylglycerol was measured in neutral lipid extracts obtained from total lipids by silica gel column chromatography. Neutral lipids were eluted with 10 ml chloroform/gm adsorbant, concentrated under vacuum and applied to a 0.5

mm thin layer chromatography (TLC) plate (Merck Silica gel G 60). The solvent system used was benzene:isopropanol:H_2O (100:10:0.25 by volume). After visualisation of the bands with iodine vapour the area corresponding to 1,2 diacylglycerols was scraped from the plate and eluted with equal volumes of diethyl ether, chloroform and methanol. Diacylglycerol was then quantitated with the Sigma Diagnostic Kit 405. No 1,3-diacylglycerol was detected.

2.3.4 Fatty Acids

Fatty acids were estimated as methyl esters, prepared by hydrolysis of total lipids dissolved in benzene for 1.5 h at 110°C with 14% boron trifluoride in methanol (Morrison and Smith, 1964). Analysis was by gas liquid chromatography on a Carbowax 20 M Capillary column using a Hewlett Packard 5890 Gas Chromatograph. The temperature was programmed for 1 min at 80°C followed by an increase at 3°C/min to 220°C. The temperature was then maintained at 220°C until the completion of the analysis. 25:0 fatty acid was added to each sample before methylation as an internal standard.

2.3.5 Total Lipid Phosphorus and Phospholipid Composition

Total lipid phosphorus was determined colorimetrically on the total extracts (Duck-Chong, 1979) based on a phosphorus content of 4% by weight and a mean molecular weight for phospholipid of 750.

Polar lipids were separated from total cell lipids by chromatography on a silica gel 60 (Merck) column. Neutral lipids were eluted with 10 ml $CHCl_3$/g adsorbant and polar lipids were eluted with 15 ml MeOH (+ a drop of H_2O) per g adsorbant. The polar lipid fraction was evaporated to dryness, redissolved in a small volume of $CHCl_3$:MeOH (2:1

by volume) and up to 200 µg was loaded on one corner of a 10 x 10 cm plastic-backed TLC sheet (Merck), which was developed in two dimensions. The solvent systems used were (i) $CHCl_3$:MeOH:HAc:H_2O (25:8:8:1 by volume) and (ii) tetrahydrofuran:dimethoxymethane:MeOH:H_2O (20:12:8:2 by volume). The spots were visualised by dipping the TLC sheets in spray reagent (Dittmer and Lester, 1964). Since phosphatidic acid and cardiolipin do not separate well in this solvent system, the identity of cardiolipin was confirmed using $CHCl_3$:MeOH:NH_4OH (7.5 N) (65:25:5 by volume) as the second solvent. Each spot was cut out of the sheet and the silica gel eluted from its backing into a test tube with $CHCl_3$:MeOH (2/1). After evaporation of the solvent, the phosphorus content was estimated in the presence of the silica gel by the method of Duck-Chong (1979). The TLC sheets were run in duplicate.

2.3.6 Total Ether-linked Lipids

Total lipid extracts (1 - 2 mg) were fractionated by silica gel Sep-Paks (Waters), with the neutral lipids eluting in 10 ml $CHCl_3$ and the polar lipids in 15 ml MeOH containing a drop of H_2O. 1-O-alkenyl and 1-O-alkyl lipids were estimated in both the neutral and polar fractions by the colorimetric method of Blank et al., 1975.

2.3.7 Ether-linked Phospholipid Species

Guinea pig pancreas was homogenized and freed of low molecular weight contaminants by Sephadex G-25 column chromatography to obtain a crude preparation of phospholipase A_1, which was stored at -70°C until required (El Tamer et al. 1984; Fauvel et al. 1981). Each polar lipid sample was split into three fractions of about 200 µg of lipid, and analysed by methods based on that of El Tamer et al., 1984. Sample A was

chromatographed by TLC in two dimensions using the solvent systems (i) $CHCl_3$:MeOH:NH_4OH (7.5 N) (90:54:11 by volume) and (ii) $CHCl_3$:MeOH:HAc:H_2O (90:40:12:2 by volume). The phosphorus content of the spots was estimated as in Section 2.3.5 and this analysis provided a measure of the total phospholipid content. Two samples, B and C, were then treated with phospholipase A_1 for 4 h (El Tamer et al., 1984) to remove the acyl chain from position 1 of the diacyl phospholipids. Corresponding lyso-compounds were formed. One enzyme-treated sample, B, was subjected to TLC as for sample A. The difference between the phosphorus content of the spots in A and B gave a measure of the diacyl content of the component phospholipids. Sample C was run first in the acidic solvent (ii), then the TLC sheet was placed in a closed container with HCl fumes for 10 min to hydrolyse the 1-alkenyl-2-acyl species. The 1-alkyl-2-acyl species remained intact. The TLC sheet was then run in solvent (1) in the second direction and the difference between the phospholipid components of B and C was due to the 1-alkenyl-2-acyl moieties (the plasmalogens) in the original sample. The phospholipids measured in sample C were the 1-alkyl-2-acyl species. Only the choline and ethanolamine glycerophospholipids contained 1-alkyl and 1-alkenyl species. The remaining phospholipid species were degraded fully by phospholipase A_1, in agreement with the findings of El Tamer et al. (1984) and Diagne et al. (1984), for phospholipids from a number of human, rat and guinea pig tissues.

2.3.8 Gangliosides and Neutral Glycosphingolipids

Washed cells (5×10^8) or lipoprotein fractions were extracted with $CHCl_3$:MeOH by the method of Gottfried (1967). The filtered extracts were evaporated to dryness and partitioned three times between $CHCl_3$:MeOH

(2:1) (5 volumes) and H_2O (1 volume). The organic phase was kept aside for neutral glycosphingolipid analysis, whereas the aqueous phase was evaporated to a small volume (rotary evaporator, 50°C) and dialysed overnight against distilled H_2O at 4°C. The dialysate was evaporated to dryness and transferred to a small vial in $CHCl_3$:MeOH (2:1) through an Acrodisc filter for storage at -20°C. This fraction is the crude ganglioside fraction. Quantitation of gangliosides (by the colorimetric resorcinol method) was performed as described by Bergelson (1980) for the plasma specimen on day 5 (Chapter 5). Neutral glycolipid was estimated by the colorimetric orcinol method (Hildebrand et al., 1971). The more sensitive and specific fluorimetric determination for sphingosine was required for detection and quantitation of both acidic and neutral glycolipids at 9 months (Naoi et al., 1974; see Chapter 5). Sphingomyelin was removed from the organic phase lipids before sphingosine determination by silica gel column chromatography. The column was poured in diethyl ether and washed with $CHCl_3$. Neutral lipids were eluted with 15 ml $CHCl_3$/g adsorbant and glycolipids with 35 ml/g of acetone:MeOH (9:1, v/v).

The ganglioside fraction was spotted on high performance thin layer chromatography (HPTLC) plates (Merck Silica Gel 60), developed in $CHCl_3$:MeOH:0.02% aqueous $CaCl_2$, 55:45:10 by volume, and sprayed with resorcinol reagent. Plates were heated at 100°C for 15 min (Svennerholm, 1957). The organic phase glycolipid fraction was spotted on HPTLC plates also and developed in $CHCl_3$:MeOH:H_2O, 50:21:3 by volume and sprayed with diphenylamine reagent to detect neutral glycolipids (Vance and Sweeley, 1967).

Ganglioside standards were purchased from Supelco (G_{M1}, G_{D1a}, G_{T1b} + G_{D1b} and bovine brain mixture). These abbreviations for gangliosides

follow the nomenclature system of Svennerholm (1963), IUPAC-IUB Commission on Biochemical Nomenclature (1977). G_{M1} = II^3 Neu Ac $GgOse_4Cer$; G_{d1a} = IV^3 Neu AcII^3 Neu Ac $GgOse_4Cer$; G_{D1b} = II^3 (Neu Ac)$_2$-$GgOse_4Cer$; G_{T1b} = IV^3 Neu Ac, II^3 (Neu Ac)$_2$-$GgOse_4Cer$.

Neutral glycolipid standards were also purchased from Supelco and included stearoyl sphingosine, monogalactosyl and glucosyl stearates, globotriaosyl ceramide = Gal (α1-4) Gal (β1-4) GlcCer and globotetraosyl ceramide = GalNAc (β1-3) Gal (α1-4) Gal (β1-4) GlcCer.

2.4 ELECTRON MICROSCOPY

2.4.1 Transmission Electron Microscopy of Cells and Membranes

Membrane fractions (Chapter 3) were fixed by suspension in 1.8% glutaraldehyde in 50 mM phosphate buffer pH 7.4. They were then sedimented by centrifugation at 40,000 g for 30 min at 4°C, post-fixed with 1% osmium tetroxide in PBS, and stained *en bloc* with aqueous uranyl acetate, dehydrated through a graded series of acetone/H_2O and embedded in Spurrs resin. Ultra-thin sections were cut, stained with uranyl acetate and lead citrate, and examined in a Philips 400 electron microscope at 100 kv.

The pellets of 10^6 cells were washed with phosphate buffered saline (PBS) and then fixed with 2% glutaraldehyde in PBS, and post-fixed with 1% osmium tetroxide in PBS. The remaining procedure was the same as that for membrane fractions.

2.4.2 Freeze Fracture of Whole Cells

For freeze fracturing, unfixed cell concentrates in PBS were frozen in liquid nitrogen-cooled Freon 22 and fractured at -100°C in a Balzer Freeze Etch Unit (BAF300). Replicas were examined in a Philips 400

electron microscope operating at 100 kV. The terminology of Branton et al. (1975) is used in referring to membrane fracture faces.

The increase in surface area of the plasma membrane of the resistant cells (Chapter 4) was modelled as a number of hemispheres, and calculated by measuring distance (X) in the direction of the shadow through to midpoint of the elevated areas (bulges). The radius (r) of the hemispheres was derived trigonometrically from the platinum shadow arriving at an angle of 45°. The surface area of a hemisphere would contribute an increase in surface area of $2\pi r^2 - \pi r^2 = \pi r^2$. A second measurement was made to ensure that in most cases the value of X which is the area of shadow plus the diameter was greater than the diameter of the hemisphere at right angles to the direction of shadowing. A total of 2 μ^2 of a cell membrane was measured containing 67 bulges. Stereo pairs at ± 6° were taken of the area measured and the cell curvature was found to be negligible therefore calculations were of a non-curved surface.

2.4.3 Sizing of Lipoprotein Particles by Negative Staining

Lipoprotein fractions were dialysed against 0.9% NaCl for 2 h at 4°C. The preparations were stained with 1% sodium phosphotungstate (pH 7.3) and the electron micrographs obtained with a Philips 400 electron microscope operating at 100 Kv and a maximum working magnification of X 92,000. Calibration of the magnification scales was performed using crystalline catalase. For the distribution of particle diameters 300 - 400 particles were measured from electron micrographs using an ocular magnifier (X 8) with a scale of 0.1 mm divisions.

2.5 ELECTROPHORESIS OF LIPOPROTEINS, AND DETERMINATION OF APOPROTEIN CONTENT

Isolated lipoproteins and proteolipid were examined by electrophoresis on 1% agarose with 1 M barbital buffer, pH 9.0. Gels were stained with oil red O and positions of apo-A and apo-B containing lipoproteins were ascertained from a normal plasma control. Apo A and B were quantitated in human samples using antibodies (Muir and Hensley, 1977).

2.6 TOTAL PROTEIN ESTIMATION

Cells, homogenates and membranes were dissolved in 0.16 N NaOH for 30 min at 37°C, neutralised with HCl, then the protein content was estimated using the Bio-Rad Coomassie Blue Reagent (Bio-Rad 500-0001) with bovine serum albumin as standard. Lipoproteins were assayed without NaOH treatment.

2.7 LACTATE ASSAY METHOD AND RIBONUCLEASE AND LIPOPROTEIN LIPASE TREATMENTS OF PROTEOLIPIDS

A U.V. spectrophotometric method was used to measure lactate (Boehringer-Mannheim U.V.-Test Kit (L-lactic acid) No. 137984) in cell supernatants and lipoprotein fractions.

Either ribonuclease A (RNase A) 0.024 IU, Sigma, E.C.3.1.1.34) or lipoprotein lipase (4.2 IU, bovine pancreas, Boehringer-Mannheim, E.C.3.1.27.5) was added to 1 ml of proteolipid complex (Chapter 5) which contained 367 µg protein, and then incubated for 1 h at 37°C prior to study.

2.8 RNA AND DNA ANALYSIS OF LIPOPROTEINS

2.8.1 RNA

In the 5 day sample (Chapter 5) RNA was determined by the orcinol method on intact lipoprotein and corrected for glycolipid content (Almog and Shirey, 1978). RNA was also extracted from lipoproteins and proteolipids as described by Wieczorek et al. (1985) and the absorption at 260 nm measured.

A variety of standard methods such as phenol-$CHCl_3$ and guanidine-HCl extraction was used to assess the presence of RNA in the 9 month lipoprotein specimens in Chapter 5 (Maniatis et al., 1982; Cheley and Anderson, 1984). Similar methods were employed on the rat lipoprotein fractions in Chapter 7. In addition, nucleic acid was determined by following the exact procedure of Wieczorek et al. (1985), to the conclusion of the oligo-dT column chromatography stage.

More specific methods were also applied. Lipoprotein samples were extracted to remove lipid and protein and taken to the final ethanol precipitation stage (Wieczorek et al., 1985). The samples were evaporated to dryness and suspended in 10 µl of 10 mM Tris-HCl 1 mM disodium EDTA pH 7.5. An aliquot (1 µl) of each sample was used to test for the initiation of cDNA synthesis. This procedure was carried out at Biotechnology Australia Pty Ltd. Globin mRNA (50 ng) was allowed to react alone and mixed together with the proteolipid fractions from the patients (Chapter 5) to check that there was no inhibition of the incorporation of [^{32}P]-d-ATP into the globin mRNA/cDNA hybrid. A reaction mixture containing no RNA or sample was included as a blank. The samples were spotted on a PEI cellulose TLC plate (Merck) and resolved in 0.2 M KH_2PO_4, pH 3.5. ^{32}P incorporated into DNA/RNA hybrids remains at the origin and radioactivity was detected by autoradiography

of the TLC plate. The plate was cut into pieces and the ^{32}P-cpm in each fraction was determined by Cherenkov counting.

2.8.2 DNA

The lipoprotein fractions in Chapter 5 were tested for the presence of DNA at Biotechnology Australia Pty Ltd. An aliquot (1 µl) of the same extracts as used for RNA determination was digested with restriction endonucleases EcoR1 and BamH1. The fragments were tested for incorporation of [^{32}P]-dATP into DNA with DNA polymerase 1 using chromatography on 1% agarose gels (Maniatis et al., 1982). Undigested controls were included, and control DNA (17 ng pUR291) was run separately in the presence and absence of proteolipid fractions to test for inhibition of the reaction. The incorporation of radioactivity was detected by autoradiography.

2.9 THE DISTRIBUTION OF LABEL FROM ^{14}C FUCOSE IN R13762 AND J CLONE CELLULAR COMPONENTS

Cells were grown for 48 h in RPMI medium with 10% foetal calf serum containing 0.2 µCi L-[1-^{14}C] fucose (Amersham) (55 mCi/mmol) per 100 ml of cell suspension. Cells were split into 2 batches.

1. The first batch was washed in saline, disrupted by sonication, and protein was precipitated with 1% tungstophosphoric acid in 0.5 M HCl. The precipitate was washed twice with tungstophosphoric acid and twice with $CHCl_3$:MeOH (2/1, v/v). The organic solvents were evaporated to dryness in a scintillation vial and aqueous supernatant (1.5 ml) added to it, together with 10 ml ACS scintillant. The protein pellets were dissolved in 400 µl 3N NaOH at 60°C and neutralised after 1 h with 600 µl 2.7 N HCl then mixed with 10 ml of ACS scintillant. Samples were

counted on a Rack-Beta scintillation counter. No quenching was observed with a blank containing tungstophosphoric acid.

2. The second batch of washed cells was extracted with $CHCl_3$:MeOH by the method of Gottfried (1967). The filtered extract was evaporated to dryness and partitioned three times between $CHCl_3$:MeOH (2:1) (5 volumes) and H_2O (1 volume). The organic layer was dried over $Na_2 SO_4$, then evaporated to dryness in a scintillation vial, to which 1 ml H_2O and 10 ml ACS scintillant were added. The methanol-H_2O phase was dialysed overnight against distilled H_2O at 4°C, evaporated to 1 ml and mixed with 10 ml ACS scintillant. The samples were counted in a Rack-Beta scintillation counter.

2.10 ISOLATION OF LIPOPROTEINS AND PROTEOLIPIDS

2.10.1 Cancer Patients and Controls

The total lipoprotein was isolated from plasma collected into EDTA by flotation as described by Goldstein et al. (1983). A NaCl solution of density 1.006 g/ml at 20°C containing 0.01% EDTA was prepared according to the method of Hatch and Lees (1968). This solution was adjusted with solid KBr to make density solutions of 1.221, 1.063 and 1.019 g/ml at 20°C. These solutions were chilled to 4°C, then layered above 3 ml of total lipoprotein adjusted to density 1.225 with solid KBr and chilled to 4°C. The gradient steps were each about 2.2 ml. The gradients were centrifuged at 4°C at 105,000 g (max.) for 17 h using a Sorvall AH627 or Beckmann SW28 head with 17 ml buckets. The proteolipid fraction was visible as a white band between the LDL (orange) and HDL (yellow) fractions. All bands were collected at 4°C by aspiration and dialysed overnight against 0.9% NaCl containing 0.24 mM disodium EDTA (pH 7.4) and 0.01% sodium azide at 4°C. They were stored at this temperature

until chemical analysis or NMR spectroscopy was carried out. Samples (0.5 ml) for NMR were further dialysed for 2 h against D_2O - 0.9% NaCl containing 0.01% azide.

2.10.2 The Rat Model System

Sera were collected from blood clotted at room temperature. Solid KBr was added to the sera at the rate of 0.3517 g/ml, and the solution was then chilled to 4°C. A NaCl solution of density 1.0063 g/ml at 20°C containing 0.01% EDTA was prepared according to the method of Hatch and Lees (1968). This solution was adjusted with solid KBr to make density solutions of 1.125, 1.085 and 1.063 g/ml at 20°C. These solutions were chilled to 4°C, then layered above 4 ml of serum per 17 ml ultracentrifuge tube. The gradient steps were each 4 ml and the tubes were filled to the top with d 1.063 g/ml solution. The serum in one tube per treatment was pre-stained with Sudan black (Terpstra et al., 1981) to aid in the location of the lipoprotein bands, which are colourless in rats. The gradients were centrifuged at 105,000 g for 24 h. Lipoprotein fractions were collected at 4°C by aspiration.

The fractions were dialysed overnight against 0.9% NaCl containing 0.24 mM disodium EDTA (pH 7.4) and 0.01% sodium azide at 4°C and stored at this temperature until chemical or NMR analysis was carried out. Samples (0.5 ml) for NMR were further dialysed for 2 h against 0.9% NaCl-D_2O containing 0.01% azide.

2.11 ANIMAL EXPERIMENTS

2.11.1 Animals

Female Fischer 344 rats were bred in the Ludwig Institute for Cancer Research (Sydney Branch). Rats used in experiments were 12 - 16

weeks old. They were fed standard rat chow and acidified water ad libitum.

2.11.2 Fucosidase Treatment of Cells

R13762 cells (1×10^8) were incubated at 37°C with α-L-fucosidase in PBS (Sigma, bovine epididymus E.C.3.2.1.51, 0.125 unit) for 30 min and then cells were washed several times in phosphate buffered saline (PBS), or PBS-D_2O for NMR experiments. Viability of the cells as determined by trypan blue exclusion was not diminished by this treatment despite a temporary clumping of the cells during incubation.

Fucosidase was used without further purification. Less than 0.06% proteinase activity was detected using bovine serum albumin as substrate, and β-N-acetylglucosaminidase activity was less than 0.1%. α and β-galactosidase, α-mannosidase, and β-fucosidase activities were all < 0.2% of the α-fucosidase activity. The latter activities were supplied by Sigma.

2.11.3 Experimental Metastasis

Fucosidase-treated R13762 cells (called FT) were suspended (1×10^7/ml) in RPMI-1640 medium and injected into the mammary line of ten rats. Similarly, R13762 cells were washed as above and incubated in the absence of enzyme for 30 min in PBS at 37°C prior to injection into ten control rats (MET 2). A second set of controls consisting of unwashed cells was injected into a further ten animals (MET 1). Untreated J clone cells (10^7) were also injected into ten animals as above (called JC).

Primary tumours were first evident in the inguinal area of the mammary line approximately 10 days after injection of cells. Animals were sacrificed 4 weeks after inoculation. Tumour diameters were

measured with calipers and all animals were examined for macroscopic metastases in the lymph nodes, lungs, gut, liver and mesentery with metastases being found only in axial lymph nodes. No examination for micrometastases was carried out.

Untreated R13762 cells (MET 1) injected into the mammary line of the rats resulted in an 80% rate of lymph node metastasis, compared to 70% for the cells incubated in PBS for 30 min (MET 2). All animals in each treatment bearing secondary tumours were exsanguinated and the sera bulked separately. Cells incubated in fucosidase prior to injection had only a 20% metastasis rate and the sera from the eight rats with tumours but no metastases were bulked (FT). No J clone-treated rats formed metastases and sera from all tumour-bearing animals was bulked (JC).

All the bulked serum samples were then subjected to density gradient centrifugation to obtain lipoprotein fractions.

2.12 NUCLEAR MAGNETIC RESONANCE SPECTROSCOPY

2.12.1 Preparation of Samples

(a) Cells ($0.5 - 1.0 \times 10^8$) were washed three times in PBS-D_2O, then resuspended in about 400 µl of PBS-D_2O and transferred to the NMR tube. Cell viability was assessed both before and after each experiment by the Trypan blue exclusion test. Only data obtained from cells with at least 90% viability were used. The longest time for which this was achieved was 3 - 4 h.

(b) Triolein (Sigma) was dissolved (20 mg/ml) in $CDCl_3$ (99.96% isotopic purity, supplied by Wilmad Glass Co.) and the solution was degassed while freeze-thawing four times with liquid nitrogen.

(c) Liproproteins and Proteolipids: Samples (0.5 ml) were dialysed at 4°C for 2 h against a small volume of D_2O-NaCl containing 0.01%

azide.

(d) Crude Ganglioside Fractions and Organic Phase Lipids: These samples were evaporated to dryness in a small vial and dispersed in 0.5 ml D_2O with alternate vortexing and heating (60°C). They were then rapidly transferred to the NMR tube. When ganglioside fractions or proteolipids were treated with fucosidase, they were re-dialysed against D_2O or D_2O-NaCl (0.9%) to remove free fucose before NMR spectra were acquired.

2.12.2 T_2 Relaxation Times

This method is described in Mountford et al. (1984a). ^1H NMR spectra were recorded at 37°C unless stated otherwise using a Bruker WM 400 spectrometer equipped with an Aspect 2000 computer. All peaks were referenced to aqueous sodium 3 -(trimethylsilyl)propanesulfonate, as an external standard. This substance gives a chemical shift of 0.91 ppm for the methyl resonance used as a reference. In $CDCl_3$ solutions the residual $CHCl_3$ resonance at 7.26 ppm was used as an internal chemical shift reference. Spectra were recorded with the ^2HOH peak suppressed by selective gated irradiation (Jesson et al., 1973).

The CPMG pulse sequence (Brindle et al., 1979) was used for spin-spin relaxation measurements, $90^\circ_x-(\tau-180^\circ_y-\tau)_n$-echo. A delay of 7.5 seconds was left between pulse trains to allow re-equilibration of magnetisation. An interpulse delay, τ, of 1 ms was employed. The frequency domain spectrum was obtained for different values of n from the Fourier transform of the trailing edge of the nth echo. Eight echoes were recorded for each value of n, and the delay list repeated a further seven times to give a total of 64 accumulations for each value of n. The initial value of n was repeated at the end of the list to confirm that

the sample had not altered over the time taken to collect the data. Selective and non-selective inversion-recovery spin-lattice relaxation experiments were carried out as described by Brown and Davis (1981) and Farrar and Becker (1971) respectively, in the absence of water suppression. A selective pulse of 12 ms ($\gamma B_1/2\pi \sim 20$ Hz) was calibrated to 90° for the water peak and used to irradiate the $-CH_2-$ peak at 1.2 ppm.

The FID obtained was manipulated by either a line broadening of 3 Hz or a Lorentzian-Gaussian resolution enhancement. The latter is of the form $\exp[-\pi\kappa(t - t^2/(2\ ga) - ga/2)]$, where κ is the usual line broadening function, g is the fraction of the free induction decay (FID) to be resolution-enhanced, and a is the acquisition time for the FID. Typical values were κ = -11 Hz, g = 0.04 - 0.08, a = 1.64 s.

2.12.3 Two-dimensional Scalar-correlated Spectroscopy (COSY)

^1H NMR spectra were recorded on a Bruker WM-400 spectrometer equipped with an aspect 2000 computer. Spectra were measured at 37°C and were referenced to aqueous sodium 3-(trimethylsilyl)propanesulfonate as an external standard. COSY spectra were recorded with a pulse sequence modified as described in Cross et al. (1984) to compensate for rf inhomogeneity. The complete sequence is:-

$$[(\pi/2)_\phi(\pi/2)_{\phi+90°}]\text{-}t_1\text{-}[(\pi/2)_\psi(\pi/2)_{\psi-90°}(\pi/2)_\psi(\pi/2)_{\psi+90°}]\text{-}t_2$$

where phase angles ϕ and ψ are cycled as in a conventional COSY experiment (Bax et al., 1981). The compensated COSY pulse sequence gives greatly improved results with inhomogeneous suspensions of cells compared to the conventional uncompensated pulse sequence. The duration of 2D experiments is limited by cell viability. Acquisition of 32 free induction decays for each 200 increments in t_1 resulted in a total acquisition time of approximately 3 h. The resulting 200 x 2048 data

point matrix was zero filled and Fourier transformed to 1024 x 1024 data points for each two-dimensional spectrum. A Lorentzian-Gaussian window function (Ferrige and Lindon, 1978) was used in the t_2 domain with sine-bell weighting in the t_1 domain. The choice of window function in the t_2 domain was dictated by the requirement that the resolution enhancement of procedure used did not substantially degrade the signal to noise ratio.

NOTE: In previous publications, e.g. Mountford et al., 1984b, resonances have been referenced to the methyl peak at 0.85 ppm. In this thesis and associated publications however, references are to the external standard of sodium 3-(trimethylsilyl)propanesulfonate which gives a chemical shift of 0.91 ppm for the methyl resonance.

CHAPTER THREE

NEUTRAL LIPIDS IN THE PLASMA MEMBRANE OF MALIGNANT CELLS

3.1 INTRODUCTION

The high resolution ^{1}H NMR spectrum obtained from a suspension of cancer cells or an excised solid tumour is characteristic of lipids (Mountford et al., 1982b). Other rapidly dividing cells have been shown to give a similar high resolution ^{1}H NMR spectrum (Block, 1973; Nicolau et al., 1975, 1978; Mountford et al., 1982a). The first evidence that the lipids responsible were located in the plasma membrane was obtained by comparing the ^{1}H NMR spectrum of isolated membrane ghosts with that of the intact viable cells (Mountford et al., 1982b). To further determine if the cellular lipid present in the high resolution ^{1}H NMR spectrum was part of the plasma membrane, intact cells were exposed to either $^{153}Gd^{3+}$ or $^{54}Mn^{2+}$. The location of these radioactively labelled metals indicated that $^{54}Mn^{2+}$ was able to pass through the plasma membrane whereas the $^{153}Gd^{3+}$ selectively bound to the membrane (Mountford et al., 1982b). These experiments parallel those described by Bergelson and Barsukov (1977) where Gd^{3+}, unable to pass through the vesicle bilayer, broadened only the external lipid molecules. In contrast Mn^{2+}, which is able to pass through the bilayer, broadened all resonances.

Most lipid molecules in the plasma membranes of cells should generate a ^{1}H NMR spectrum of width about 10 KHz, even when the membranes are in the liquid-crystalline state (Wennerström and Lindblom, 1977; Ulmius et al., 1975; Bloom et al., 1977), due to the lack of averaging of dipolar interactions to zero. In contrast, the narrow lines originating from the membranes of cancer cells are less than 10 Hz wide.

There are two potential mechanisms that can account for the narrow lines associated with the protons in this system. The first involves lipid molecules located at positions in the plasma membrane such that

the principal axis of motional averaging makes an angle θ with the external magnetic field close to the "magic angle". The second possibility is that the narrow lines are quasi-Lorentzian in nature (Bloom et al., 1978; Wennerström and Ulmius, 1976), and arise from small structures which retain their integrity within the plasma membrane, or closely associated with it, but allow molecules within them to tumble isotropically and produce narrow resonances. To test these two possibilities selective and non-selective T_1 experiments were undertaken on a suspension of cells (Mountford et al., 1984a). Similar values were obtained for the selective and non-selective T_1 measurements, indicating that lipids at the "magic angle" were not the source of the narrow ^1H resonances. The probability is that the lipids giving rise to the narrow lines tumble isotropically, and are in domains which are not in diffusive exchange with other lipids in the plasma membrane bilayer (Mountford et al., 1984a).

A major problem encountered in studies of cell or tissue samples is the resolution and assignment of proton resonances to particular cellular constituents. Lorentzian-Gaussian resolution enhancement of the lipid methylene proton resonances near 1.2 ppm resolves four peaks, at 1.22, 1.23, 1.25 and 1.28 ppm, each of which can be examined separately in an NMR relaxation experiment (Mountford et al., 1984a, Chapter 1.7.3). However assignment of the resonances to specific protons is difficult from one-dimensional spectra. Chemical shifts may be displaced for molecules within the cell or tissue as a result of interactions between cellular constituents (Daniels et al., 1976, 1978). Differences in magnetic susceptibility inside and outside the cell can also lead to perturbation of chemical shifts (Fabry and San George, 1983).

In contrast two-dimensional scalar correlated spectroscopy (COSY)

provides much information not available from a one-dimensional spectrum (Wagner et al., 1981; Arseniev et al., 1982) by generating spectra which allow spin system assignments based on spin-spin (scalar) coupling. By use of a modified pulse sequence (Cross et al., 1984) it has been found that suspensions of intact viable cancer cells may be studied by two-dimensional NMR methods.

In this Chapter, two-dimensional scalar correlated spectroscopy shows that the NMR spectrum in rapidly dividing cells arises predominantly from triacylglycerol. Since cells in tissue culture have a tendency to accumulate cytoplasmic lipid droplets containing triacylglycerol (Rosenthal, 1981; Schneeberger et al., 1971; Stubbs et al., 1980) or diacylglycerol (Homa et al., 1983; Rosenthal, 1981) it was necessary to develop a methodology for the preparation of highly purified plasma membranes to confirm the cell surface as a location for the isotropically tumbling lipid domain.

3.2 RESULTS

3.2.1 Chemical Analysis of Crude Plasma Membranes

The chemical analyses of the crude plasma membranes isolated from cancer cells and other embryonic or transformed cells known to give narrow NMR lines are shown in Table 1. The triacylglycerol (triglyceride) contents of the membranes are comparable in most cases, with chicken fibroblasts and stimulated human lymphocytes showing the highest values and greatest variation. Cholesteryl ester levels were variable, with large standard errors for each cell type. The free cholesterol levels were more uniform, both within and between cell types.

Table 1. Neutral Lipid Composition of Membranes from Different Cell Types.

Crude plasma membranes were isolated from 2.5 x 10^8 cells as described in Chapter 2.2.1. Membranes from the 13762 and J clone cell lines were purified 4-fold with respect to plasma membrane markers. The values represent the mean ± S.E. as determined from assays run in duplicate on the number of experiments indicated in parentheses. Data are expressed as nmol/mg of lipid. The abbreviations used are: PBL, peripheral blood lymphocytes; PWM, pokeweed mitogen; VBL, vinblastine.

Cell Type		Triglyceride	Free Cholesterol	Cholesteryl Ester
			nmol/mg lipid	
Rat mammary adenocarcinoma				
Metastatic line 13762	(3)	43 ± 4	278 ± 21	45 ± 7
Non-metastatic J Clone	(3)	38 ± 3	236 ± 9	6 ± 6
CCRF-CEM				
Sensitive	(5)	47 ± 2	167 ± 31	28 ± 11
Resistant to 20 ng/ml (VBL20)	(5)	44 ± 8	182 ± 41	48 ± 23
Chicken Fibroblast	(2)	81 ± 18	191 ± 22	55 ± 25
Human PBL stimulated with PWM	(2)	245 ± 15	256 ± 17	14 - 290[a]

[a]The range of values has been indicated due to large variation in results.

3.2.2 Isolation of Purified Plasma Membranes from VBL7 Cells

Subcellular fractionation was carried out on CCRF-CEM cells made resistant to 7 ng/ml vinblastine (VBL7) (Chapter 2.1.2). Discontinuous sucrose gradient centrifugation of crude membrane preparations resulted in the formation of three visible bands (B1 - 3) and a pellet (B4) on the bottom of the tube (flow diagram, Figure 1; details, Chapter 2.2.2). B1 contained the most highly purified plasma membrane fraction.

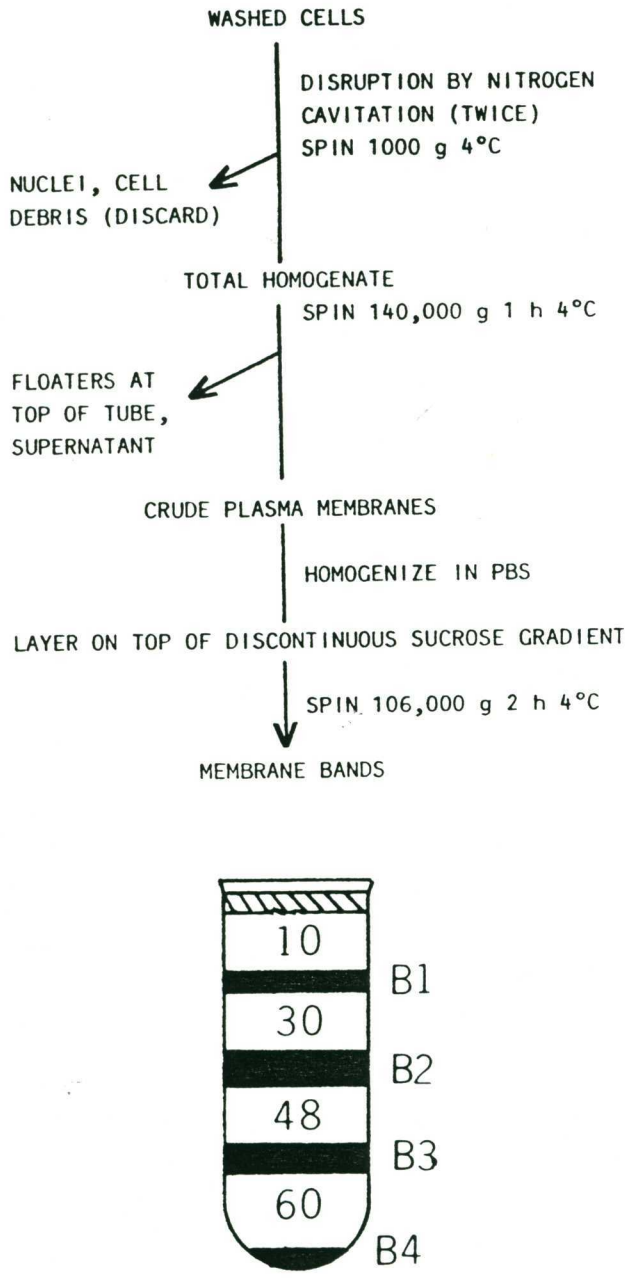

Figure 1. Flow diagram of the steps involved in the isolation of purified plasma membranes.

The extent of the purification was determined by markers for plasma membrane and other cell constituents (Table 2). Band 1 (B1), at the junction of the 10 - 30% sucrose layers had the highest enrichment in the plasma membrane marker, 5'nucleotidase (45-fold), and was enriched in the other two plasma membrane markers to the same extent as band 2 (B2). Band 1 was therefore regarded as the purest plasma membrane-containing fraction. Recovery of 5'nucleotidase activity in this fraction was 45 ± 9% of that in the homogenate and recovery of protein was 1.5 ± 0.4%. Although the enrichment of 5'nucleotidase activity above that in the homogenate was approximately 45-fold, the ratio of plasma membrane markers to cytoplasmic, mitochondrial, and nuclear markers was many times greater. The major contamination appeared to stem from endoplasmic reticulum as evidenced by the enrichment of NADPH cytochrome c reductase activity. Even so, the ratio of 5'nucleotidase activity to endoplasmic reticulum marker in band 1 was 11:1. Bands 2 - 4 were mixed membrane bands containing varying levels of mitochondrial, endoplasmic reticulum, lysosomal, and/or nuclear membranes in addition to plasma membrane.

3.2.3 Electron Microscopy of Purified Plasma Membranes

Additional confirmation of the purity of the plasma membrane fraction was obtained by transmission electron microscopy. Band 1 was comprised of membrane vesicles and whorls, some containing electron dense material (Figure 2A). No lipid droplets were seen in the membrane preparations. They were visible however in sections of whole VBL7 cells (Figure 2B). Electron dense material was always seen around the outsides of the plasma membrane vesicles (Figure 2A). This type of material has been reported before in leukaemic lymphoblast plasma membranes (e.g.

Table 2. Marker Enzyme Activity of Membrane Fractions from VBL7 Lymphoblasts. Plasma membranes were isolated from 4.5 x 10^9 cells by disruption using nitrogen cavitation followed by fractionation on a sucrose density gradient. The enzyme activities were determined as described in Section 2.2.3 for the initial suspension (homogenate) after cell disruption and the four density gradient bands as well as the supernatant from the density gradient centrifugation and a band of lipid which separated on top of the supernatant (designated floaters). The enrichment was calculated by the specific activity of the marker in each fraction divided by that in the homogenate. The values represent mean ± S.E. of two experiments. Band 1 is at the interface of the 10 and 30% sucrose layers; band 2 is at the interface of the 30 and 48% layers; band 3 is at the interface of the 48 and 60% sucrose layers; and band 4 is the pellet at the bottom of the 60% sucrose layer. (N.D. = not detected).

	Enrichment					
Enzyme Marker	Band 1	Band 2	Band 3	Band 4	Floaters	Supernatant
5'-Nucleotidase	44.9 ± 17.7	19.4 ± 5.0	15.5 ± 2.2	14.6 ± 5.3	0.46 ± 0.09	ND
γ-Glutamyltranspeptidase	12.6 ± 3.3	11.1 ± 2.9	5.0 ±.0.4	0.6 ± 0.6	ND	0.15 ± 0.15
Na^+, K^+ adenosine-triphosphate	10.5 ± 3.4	14.4 ± 5.0	5.8 ± 2.5	2.4 ± 0.3	ND	ND
Acid phosphatase	1.2 ± 0.4	1.9 ± 0.1	1.4 ± 0.1	1.0 ± 0.4	1.1 ± 0.3	2.0 ± 0.9
Lactate dehydrogenase	0.009 ± 0.001	0.08 ± 0.01	0.087 ± 0.005	0.035 ± 0.004	3.0 ± 1.2	2.5 ± 0.7
NADPH cytochrome c reductase	4.0 ± 0.2	6.8 ± 1.4	9.0 ± 0.6	6.7 ± 2.6	1.5 ± 0.2	0.9 ± 0.2
Cytochrome c oxidase	0.39 ± 0.3	3.5 ± 0.7	7.2 ± 1.2	6.4 ± 0.6	ND	ND
DNA	0.079 ± 0.007	0.11 ± 0.02	0.39 ± 0.03	1.1 ± 0.5	0.021 ± 0.004	0.015 ± 0.003

Figure 2. Transmission electron microscopy of (A) purified plasma membranes (B1) from VBL7 cells and (B) sections of VBL7 cells, showing nucleus (N) lipid droplets (LD), mitochondria (M), endoplasmic reticulum (E), autophagocytic vacuoles (AV) and Golgi apparatus (G). The bars = 1 μM.

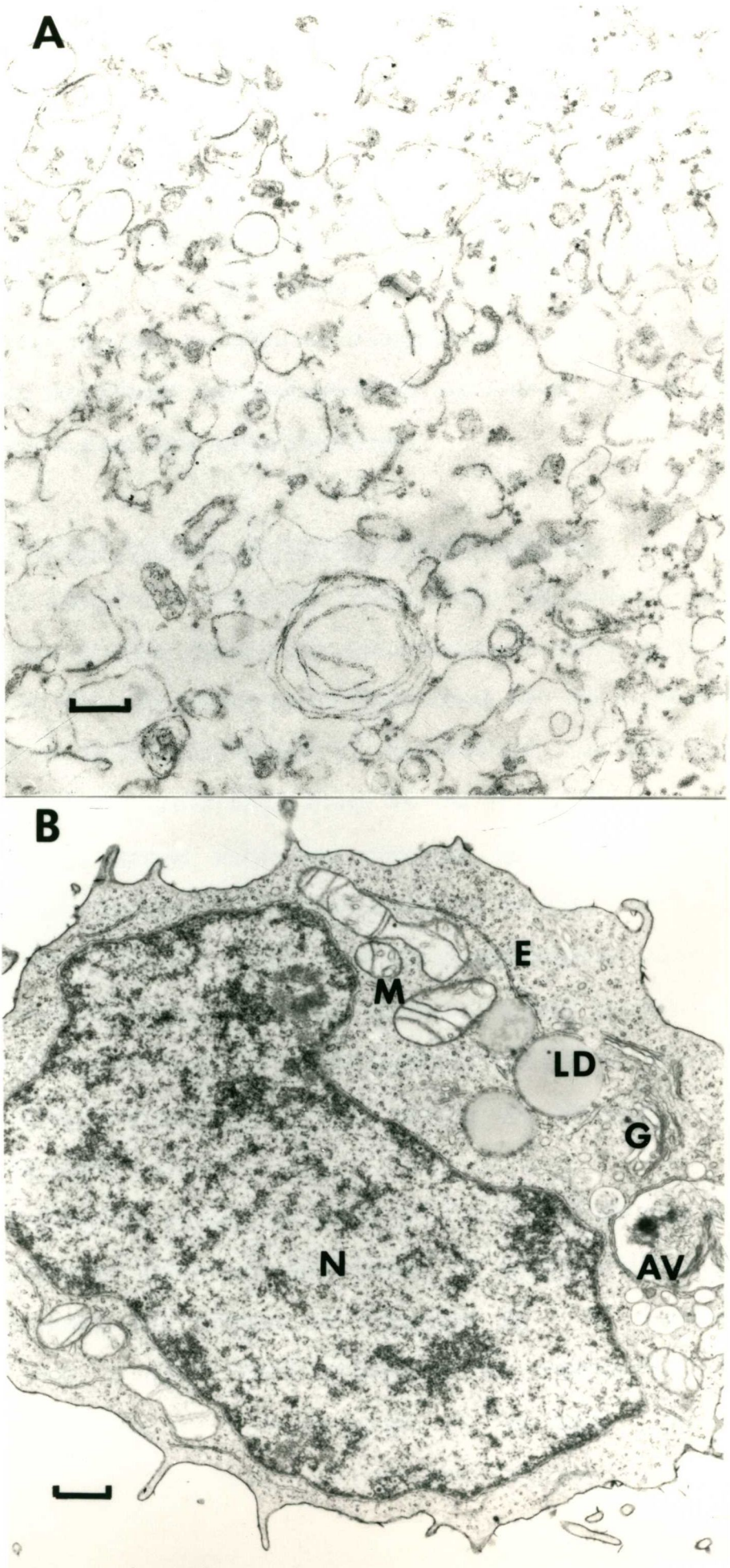
A
B
E
M
LD
G
N
AV

Torrent-Quetglas et al., 1981) and since Melera and Cronin-Sheridan (1976) reported cytoplasmic RNA associated with purified human lymphocyte plasma membranes the possibility that it was RNA was investigated. Band 1 membranes from VBL7 cells were incubated for 30 min at 37°C with RNase A (0.24 IU, Sigma, E.C.3.11.34) before fixation, but subsequent thin sections revealed no disappearance of the electron-dense particles. No significant DNA contamination was present in band 1 (Table 2) and all cells used were mycoplasma-free.

3.2.4 Chemical Analysis of Purified Plasma Membranes

Chemical analysis of the major lipids (Table 3A) demonstrated that the mean levels of free cholesterol and cholesteryl ester in the mixed membrane bands (B3 - 4) approximated those found for the crude membrane preparations of VBL20 cells (Table 1). In contrast, the mean level of free cholesterol and cholesteryl ester in the B1 and B2 fractions was higher. Some cholesteryl ester was detected in all the bands. The presence of large amounts of free cholesterol is in itself an indication of membrane purity (Yeagle, 1985) since the plasma membrane is the major site of cholesterol accumulation. The decrease in free cholesterol from B1 to B4 reflected the level of plasma membrane enrichment. In contrast, the cholesterol-to-phospholipid ratio showed an increase over the homogenate in bands 1 and 2.

The triglyceride content of bands 1 - 3 (Table 3B) was similar within experimental error but the content of triglyceride in B4 was elevated. Recovery was highest in fractions B1 - B3 (fraction B4 represents only a very small proportion of recovered protein). Triglyceride accounts for 4.2% by weight of the total lipid in the plasma membrane (B1). It is very unlikely that triglyceride was trapped

Table 3A Cholesterol and Phospholipid Composition of Membranes from VBL7 Lymphoblasts. The lipid composition was determined for the homogenate and membrane bands obtained by density gradient centrifugation, as well as for the supernatant fraction and a band of lipid which separated on top of the supernatant (designated floaters). The values represent the mean ± S.D. as determined from assays run in duplicate on up to 8 different extractions (data are expressed as nmol per mg of lipid).

Fraction	Free Cholesterol	Cholesterol Ester	Phospholipid	Cholesterol to Phospholipid Ratio
Homogenate	121 ± 23	56 ± 24	577 ± 154	0.22 ± 0.02
Floaters	16 ± 4	20 ± 9	125 ± 34	0.11 ± 0.01
Supernatant	93 ± 34	21 ± 7	426 ± 131	0.22 ± 0.01
B1	222 ± 26	67 ± 19	719 ± 8	0.28 ± 0.01
B2	202 ± 25	54 ± 13	617 ± 139	0.34 ± 0.05
B3	165 ± 29	68 ± 6	708 ± 97	0.23 ± 0.05
B4	178 ± 3	17 ± 2	943 ± 30	0.19 ± 0.01

Table 3B Triglyceride Composition of Membranes from VBL7 Lymphoblasts. (data are expressed as nmol per mg of lipid or protein).

Fraction	Lipid	Protein	Recovery[a]
Homogenate	120 ± 44	70 ± 17	-
Floaters	303 ± 25	132 ± 76	37 ± 12
Supernatant	152 ± 54	18 ± 1	39 ± 14
B1	48 ± 8	73 ± 12	10 ± 4
B2	49 ± 12	72 ± 10	10 ± 2
B3	55 ± 8	69 ± 2	11 ± 2
B4	77 ± 5	92 ± 36	7 ± 3

[a]Distribution of triglyceride was measured as a % of the total triglyceride recovered. The 1000 g pellet was not assayed. Molecular weights of triglyceride = 885, cholesterol = 387, cholesteryl ester = 650, phospholipid = 750.

in the membrane bands from the triglyceride-rich floaters and supernatant fractions since for B1 the ratio of the plasma membrane marker 5'nucleotidase to the cytoplasmic marker lactate dehydrogenase was 5000:1. Moreover no lipid droplets were seen in B1 by electron microscopy (Section 3.2.3).

3.2.5 Comparison of ^{1}H NMR Spectra of Intact Cells and Purified Plasma Membranes

The fraction (B1) was obtained from cells of the EBV-transformed B cell line (JP) lysed hypotonically in 10 mM Hepes, pH 7.2 rather than by nitrogen cavitation as in Chapter 2.2.2. It was enriched about 30-fold in the plasma membrane marker 5'nucleotidase and was re-suspended in PBS-D_2O for NMR analysis. The ^{1}H NMR spectra of JP cells and purified plasma membranes are compared in Figure 3A and B and can be seen to be almost identical in the 0 - 2.5 ppm regions. The region of 2.5 - 4 ppm in the purified membranes was obscured by residual sucrose, hence that portion of the spectrum is not included for comparison.

3.2.6 Identity of the Resonances in the ^{1}H NMR Spectrum of Cells

The ^{1}H NMR spectrum of a suspension of VBL20 cells is compared with the 400 MHz COSY spectrum of the same cells in Figures 4A and B. The 400 MHz COSY spectrum of triolein in $CDCl_3$ is presented in Figure 4C. The off-diagonal cross-peaks, labelled A-G, indicate spin-spin coupling between protons on adjacent carbon atoms. The connectivities corresponding to each acyl chain cross-peak (A-F), summarized in Structure 1 (phospholipid) and Structure 2 (triglyceride), can be seen in the spectrum of the leukaemic T cell line VBL20 (Figure 4B) confirming the assignment of lipid acyl chain resonances in the spectrum

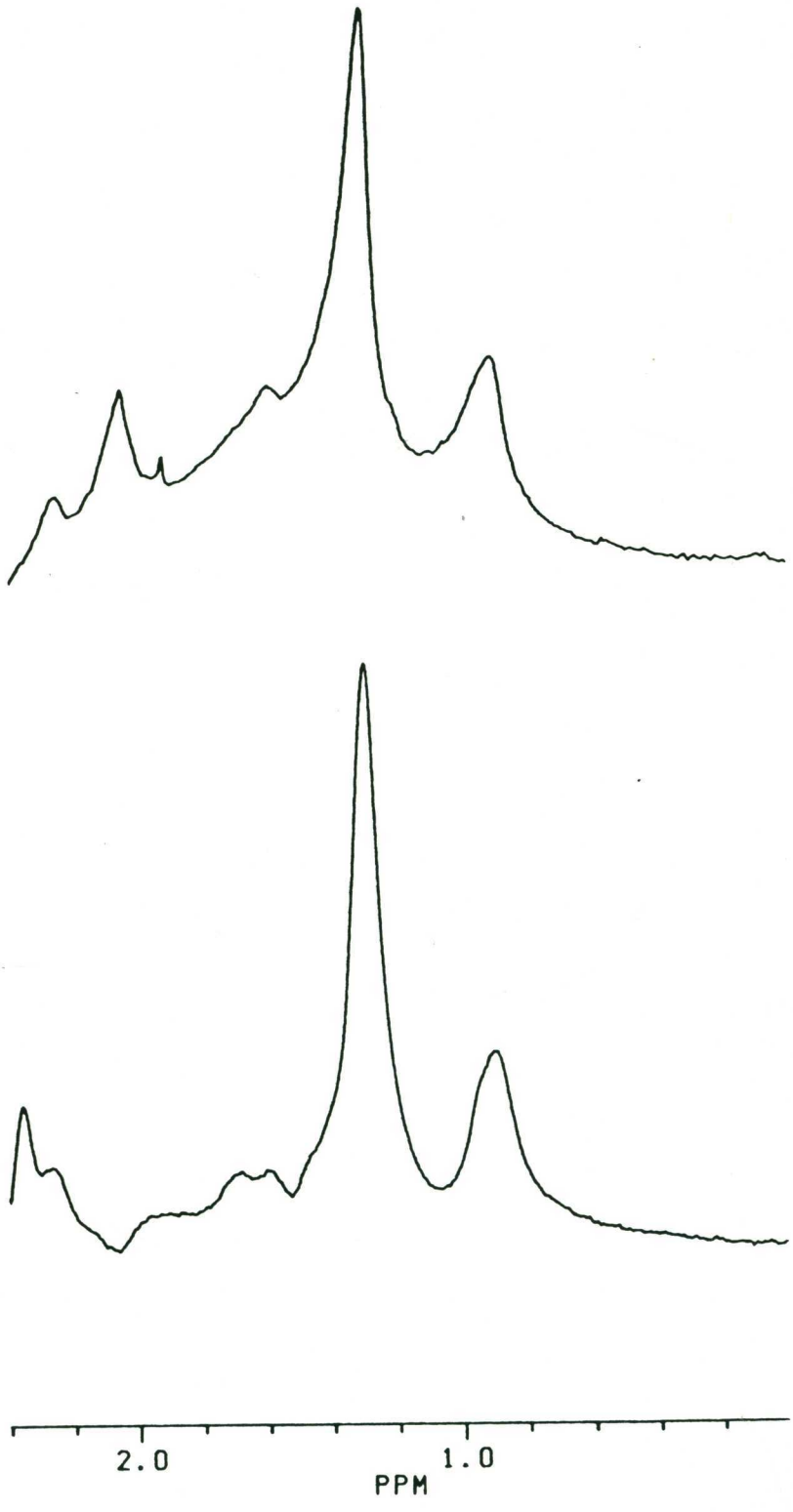

Figure 3. 400 MHz ^{1}H NMR spectra of (A) purified plasma membranes from JP cells, suspended in PBS-D_2O; (B) JP cells (1×10^{8}) suspended in PBS-D_2O.

1

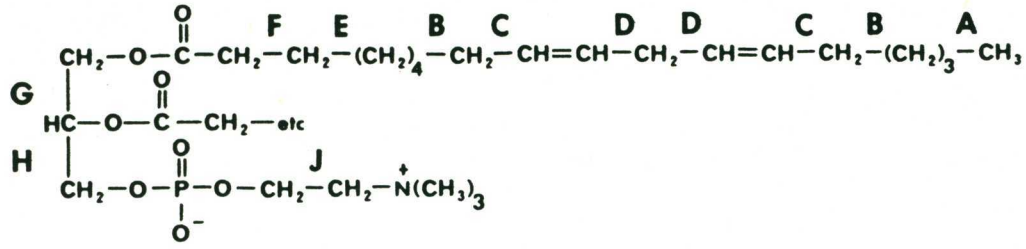

2

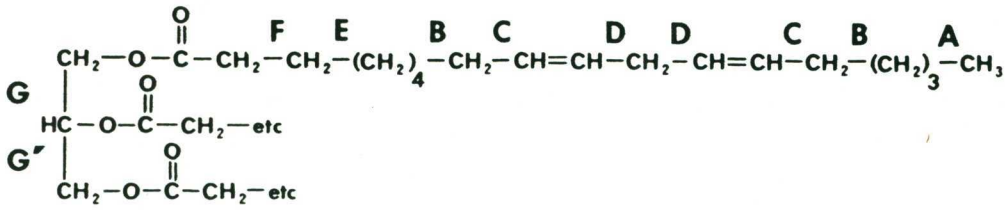

of cancer cell plasma membranes. Two-dimensional NMR spectroscopy also identified the lipid acyl chains as components of triglyceride. Triglyceride possesses a unique cross-peak G' at 4.3 ppm resulting from the geminal protons of carbons 1 and 3 of the glycerol backbone (Structure 2 and Figure 4C). This resonance is 0.1 ppm downfield from the corresponding glycerol resonance (Structure 1) in the phosphatidylcholine spectrum. Furthermore, no cross-peaks from a glycerol methylene adjacent to a phosphatidylcholine group, H, (Cross et al., 1984) were in evidence in the cell spectrum, nor was the cross-peak J due to the choline head group. The cross-peak group D is not present in Figure 4C as triolein has only one olefinic group in each acyl chain. However, the absence of C in the cell spectrum (Figure 4B) was unexpected and while this cannot be due to the complete absence of carbon-carbon double bonds (evident by the presence of D) it may suggest a low level of olefinic

Figure 4. Symmetrized COSY Spectra. (A) ^{1}H NMR spectrum (400 MHz) of a suspension of VBL20 cells (1×10^{8}) in PBS-D_2O. (B) COSY spectrum of the same VBL20 cell suspension. (C) Triolein in $CDCl_3$ solution (20 mg/ml). Lipid acyl chain and glycerol backbone connectivities are indicated. (D) Supernatant from VBL20 cells (2.0×10^{8}). The COSY spectrum was recorded as for VBL20 cells. The assignments of the cross-peaks are shown in Structure 2 which is described in the text. All spectra were obtained at 37°C except for triolein which was measured at 25°C. Sine-bell and Gaussian (line broadening = -16, Gaussian broadening = 0.22) window functions were applied in the t_1 and t_2 domains, respectively (Cross et al., 1984 and Chapter 2.12.3). Lipid acyl chain and glycerol backbone connectivities are indicated.

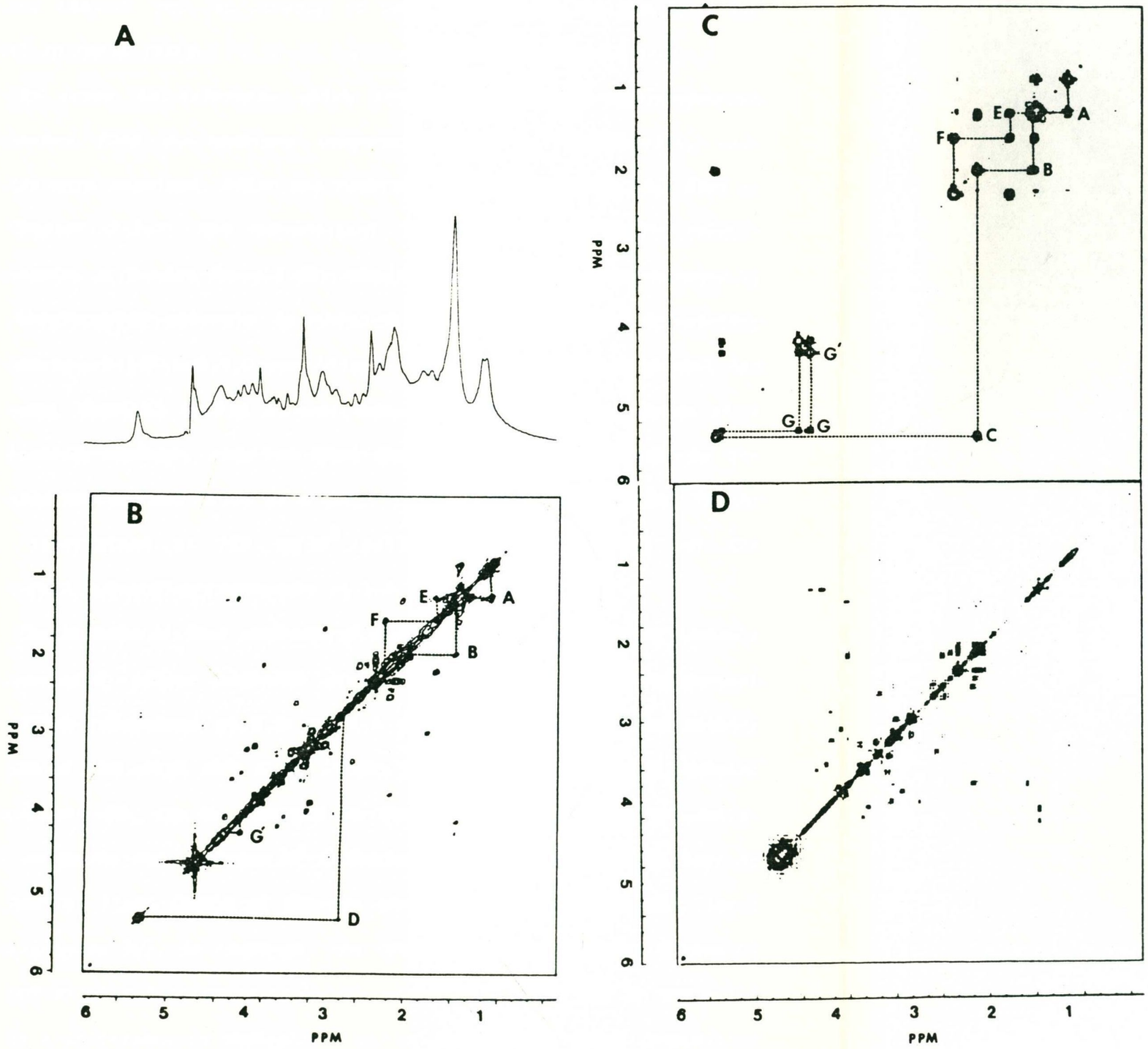
A
B
C
D
E
A
F
B
G'
G
G
C
D
PPM
PPM
PPM
PPM
6
5
4
3
2
1

groups or that this cross-peak was not observed for dynamic reasons. The cross-peak G is rarely observed in cell systems. However in the 2D spectrum of triolein in $CDCl_3$ (Figure 4C) this cross-peak is much less intense than G' and its absence in cell spectra may be due to a low signal to noise ratio.

In order to determine which cross-peaks in the cell spectrum originated from non-membrane components such as metabolites, cell lysates were examined. After the membranes and nuclei were spun down as in Chapter 2.2.4, the supernatant, which contained only soluble components, accounted for all the remaining cross-peaks not generated by the triglyceride molecule in this cell line except that connecting resonances at 1.7 and 3.0 ppm (Figure 4D). This latter cross-peak had the same chemical shifts as one occurring in the 2D spectrum of a ganglioside mixture, and had thus been tentatively assigned to the oligosaccharide head group of a ganglioside. Lactate was present in the cell supernatant at 220 $\mu g/10^8$ cells and might account for the cross-peak connecting resonances at 1.3 ppm and 4.2 ppm.

The amounts of free cholesterol and cholesteryl ester were variable in the crude plasma membrane preparations (Table 1). A cross-peak connecting resonances at 0.9 and 1.4 ppm from the methyl and methine protons of the alkyl side chain of the cholesterol ring system, denoted Z in Figure 5B, can be observed in the spectra of many cancer cells. This suggests the presence of cholesterol and/or cholesteryl ester in the neutral lipid domain of the rat mammary adenocarcinoma cell line J clone (Figure 5B). In contrast, the VBL20 cell line (Figure 4B and C) did not display this cross-peak, the absence of which may be accounted for by a difference in cholesterol and/or cholesteryl ester composition or by the location of the free cholesterol in the bilayer rather than in

the neutral lipid domains.

Human lipoproteins are rich in cholesteryl ester and triglyceride. A possibility for the anomalously narrow ^{1}H NMR lines in cancer cells is that the neutral lipid domains may be akin to those in lipoproteins. The COSY spectrum in Figure 5A shows that, except for the cross-peaks G and D (which has a very low intensity in the J clone cells and is not always observed), the cell spectrum was accounted for in terms of the triglyceride-rich VLDL spectrum plus that of the cellular metabolites.

The two-dimensional NMR spectra of diacylglycerols (diglycerides) were essentially indistinguishable from those of triglycerides since the acyl chain connectivities were identical. TLC quantitation of 1,2 diglycerides in the crude membranes of the J clone and VBL20 cell lines (Methods, Chapter 2.3.2) has shown levels less than 5% of the triglyceride content. 1,3 diglycerides and monoglycerides were not detected.

3.3 DISCUSSION AND CONCLUSIONS

For the first time, a highly purified plasma membrane fraction has been prepared from an ALL cell line. The nitrogen decompression method of cellular disruption was found to provide a better yield of broken cells and intact nuclei than other disruption techniques, such as hypotonic lysis, or mechanical homogenisation. Moreover large cell numbers ($4 - 6 \times 10^{9}$) could be treated as one batch thus speeding up the isolation procedure. Other advantages of the method were the inert atmosphere used, the lack of localised heating, and the isosmotic conditions during lysis of the cells (Wallach and Kamat, 1964, 1966).

A comparison of membrane preparations from lymphoid cells of various types was published by Monneron and d'Alayer (1978). The purity

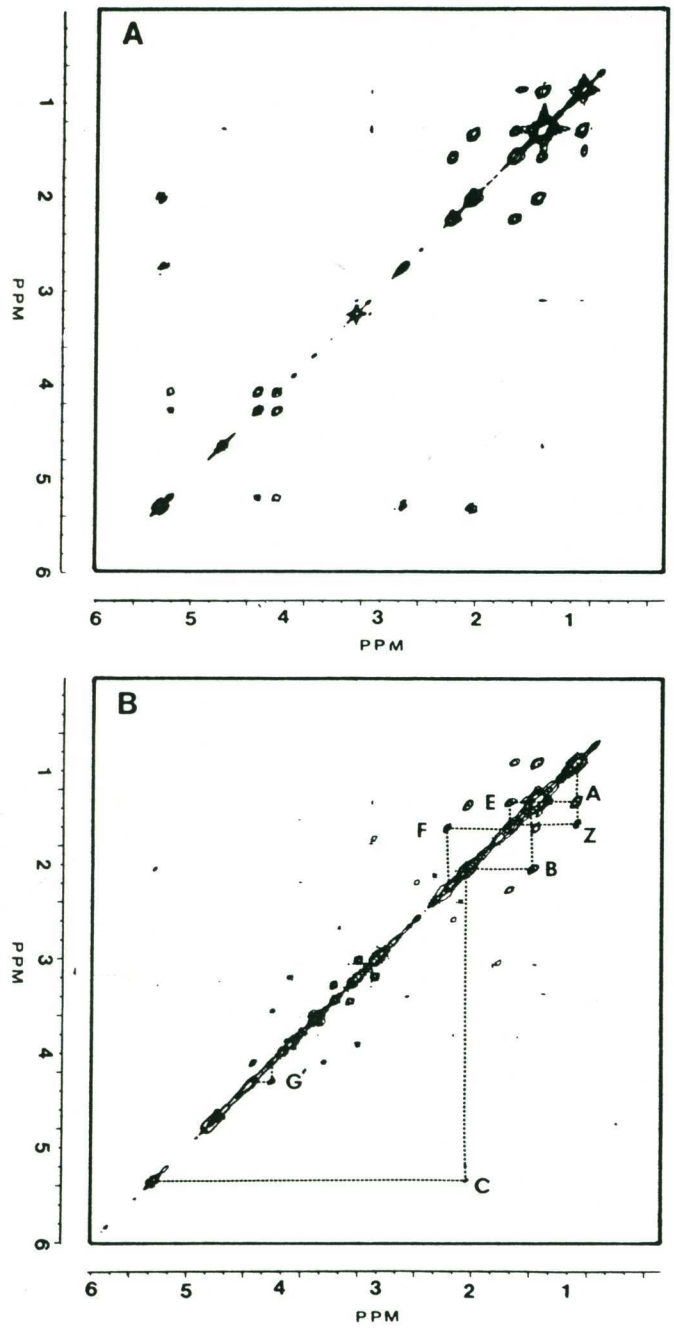

Figure 5. Symmetrised COSY Spectrum. (A) VLDL in NaCl-D_2O (from healthy human donors) (B) A suspension of J clone cells (1×10^8) in PBS-D_2O. Window functions (line broadening = -16, Gaussian broadening = 0.22) were applied in the t_1 and t_2 domains, respectively. Lipid acyl chain and glycerol backbone connectivities are as indicated. Z denotes the cross-peaks between the methyl and methine protons of the alkyl side chain of the cholesterol ring system.

and yield of the VBL7 membranes compared favourably with the best membrane preparations described. The VBL7 membranes were enriched 45-fold in 5'nucleotidase with a 45% recovery of activity and 1.5% recovery of total protein. Enrichment of other lymphoid plasma membranes in the activity of 5'nucleotidase above that in the homogenates varied from 3.9 - 36-fold. Recovery of 5'nucleotidase activity in plasma membranes ranged from 0.7 to 55% of that present in the homogenate and recovery of protein ranged from 0.5 - 2.1% (Monneron and d'Alayer, 1978).

No extrinsic plasma membrane marker was used such as ^{125}I-labelling by lactoperoxidase-catalysed radioiodination or wheat germ agglutinin, thus the possibility of some activation of 5'nucleotidase during purification cannot be ruled out.

The cholesterol to phospholipid ratio of the most highly purified plasma membrane fraction, B1 was 0.28. This is lower than published values for other human lymphoid cells, both cultured and circulating (Table 4). The parameter usually quoted to describe membrane "fluidity" or molecular motion is the cholesterol/phospholipid ratio (Van Blitterswijk, 1984). By this criterion VBL7 leukaemic lymphoblasts have unusually mobile lipids in their plasma membrane.

The triglyceride and cholesteryl ester content of plasma membranes has been reported only rarely in the literature and then only for rat and mouse liver. Some of the few available data are listed in Table 5A so that they can be compared with the data in Table 3B. There is a wide range of values for rat liver and hepatomas obtained in different laboratories.

Triglyceride and cholesteryl ester comprised 4.2% and 4.4% of the total lipid weight in lymphoblast plasma membranes. The corresponding

Table 4 Cholesterol/Phospholipid Molar Ratios in Plasma Membranes from Human Lymphoid Cells

Non-cultured Human Cells		
Leukaemic		
CLL	0.38	Marique and Hildebrand, 1973.
	0.54	Liebes et al., 1981.
ALL	0.39	Petitou et al., 1978.
Hairy Cell	0.66	Liebes et al., 1981.
Cultured Human Lymphoblastoid Cell Lines		
Molt 4F	0.4	Pratt et al., 1978
Burkitt's Lymphoma	0.56	Boland and Tweto, 1980.
Normal		
Lymphocytes	0.67	Petitou et al., 1978.
	0.55	Liebes et al., 1981.
Monocytes	0.60	Liebes et al., 1981.

CLL = chronic lymphoblastic leukaemia; ALL = acute lymphoblastic leukaemia.

figures are 7.0% and 2.5% for mammalian liver plasma membranes (Table 5B). On a protein basis the amount of triglyceride in lymphoblast plasma membranes (73 nmol/mg) is comparable with that of most hepatomas (Table 5A). On a lipid weight basis the amount of triglyceride (48 nmol/mg) is about half of the mean value for the livers and hepatomas, but the cholesteryl ester (67 nmol/mg) is equal to the highest value on Table 5A.

Chang liver cells (a virally-transformed human cultured cell line) and fresh rat liver hepatocytes were donated to this laboratory by the Commonwealth Health Department. Both gave high resolution ^{1}H NMR spectra, similar to those of the cells listed in Table 1. This is consistent with their having a relatively high triglyceride content in their plasma membranes such as found by van Hoeven and Emmelot (Table 5A).

Table 5.

A. Triglyceride and Cholesteryl Ester Content of Plasma Membranes from Mammalian Liver

	Triglyceride (n/mol/mg protein)	Cholesteryl Ester (n/mol/mg protein)	Triglyceride (n/mol/mg lipid)	Cholesteryl Ester (n/mol/mg lipid)
Rat Liver	35	3	77	8
Rat Hepatoma 484A	111	61	122	67
Mouse Liver	43	8	85	16
Mouse Hepatoma 147042	45	21	81	37
Mouse Hepatoma 143066	65	32	122	56
(Data calculated from van Hoeven and Emmelot, 1972)				
Rat Liver	5.6	2.1		
Rat Hepatoma 7288TC	0.7	0.9		
(Data calculated from Upreti et al., 1983)				
Rat Liver			96	47
(Data calculated from Keenan and Morré, 1970)				
Rat Liver			61	23
(Data calculated from Lee et al., 1973)				

B. Triglyceride and Cholesteryl Ester Profiles of Isolated Subcellular Membrane Structures of Mammalian Liver (taken from van Hoeven and Emmelot, 1972)

	Weight % of Total Lipid	
	Triglyceride	Cholesteryl Ester
Plasma Membranes	7.0	2.5
Lysosomal Membranes	2.5	8.0
Nuclear Membranes	4.0	1.0
Endoplasmic Reticulum Membranes	5.0	1.0
Golgi Membranes	16.0	4.5
Mitochondrial Membranes	9.0	
	(triglyceride, cholesteryl ester and fatty acid)	

Elevated levels of triglyceride have been found in a 9-fold enriched plasma membrane preparation from the rat mammary adenocarcinoma J clone subline. Chemical analysis showed the B1 fraction to contain 183 nmol/mg of lipid which is higher than the levels for liver in Table 5A.

The data thus support the NMR assignments in Figure 5.

The data in Table 3B suggest that triglyceride is present in all membrane fractions and indeed increased amounts of triglyceride have been found recently in mitochondrial membranes of rat liver, the rapidly dividing foetal cells containing four times as much as the adult cells (Harsas et al., 1985). Triglyceride is present as a major component in all other membrane fractions in mammalian liver (Table 5B, data from van Hoeven and Emmelot, 1972). Cholesteryl ester is present in smaller amounts.

There is biochemical evidence for heterogeneity in protein and lipid components of plasma membranes (de Pierre and Karnovsky, 1973). The use of multiple plasma membrane markers is widespread, so that the distribution of all the fragments of the plasma membrane can be followed during gradient separations. The enrichment of band 1 in Table 2 is 45-fold with respect to 5'nucleotidase activity but only 13-fold and 11-fold with respect to γ-glutamyl transpeptidase and Na^+K^+ ATPase respectively. Both of these last two enzymes appeared uniformly distributed in bands 1 and 2. Moreover the cholesterol/phospholipid ratio appeared to be higher in band 2 than band 1 (Table 3A). The non-uniform recovery and enrichment of plasma membrane markers has often been reported in cell membranes from lymphoid cell lines (e.g. Koizumi et al., 1981; Maler and Riordan, 1980; Monneron and d'Alayer, 1978). While differences in stability of marker enzymes during the isolation procedure might contribute, the domain structure of the plasma membrane predisposes toward the isolation of membrane vesicles of different enzymic composition, such as those separated from murine T lymphocytes by Hoessli and Rungger-Brändle (1983).

CONCLUSIONS

Chemical analysis of VBL7 plasma membranes from T leukaemic lymphoblasts has detected the presence of unusually high levels of triglyceride and cholesteryl ester. The presence of these lipids provides an explanation for the narrow ^{1}H NMR resonances originating from the plasma membranes of embryonic and transformed cells. Since triglycerides and cholesteryl esters are regarded to be non-bilayer components, they are likely to exist as separate neutral lipid domains in or attached to the plasma membrane. These neutral lipids are also the major components of the serum lipoproteins which bind to receptors on cellular surfaces (Brown et al., 1975). The ^{1}H NMR spectrum of cancer cells is accounted for mainly in terms of the triglyceride - rich very low density lipoprotein spectrum plus that of the cellular metabolites. Properties of the various lipoproteins and their resemblance to cell surface domains will be considered further in later Chapters.

CHAPTER FOUR

VINBLASTINE RESISTANCE IN LEUKAEMIC LYMPHOBLASTS

Page

4.1 INTRODUCTION

Vinblastine (Figure 1) is an alkaloid from the plant, Vinca rosea linn., which has been extensively employed in cancer chemotherapy because of its wide spectrum of activity. The antitumour effect has been attributed to its high affinity for tubulin, the basic protein subunit of microtubules. As a result the mitotic spindle is disrupted and cells are arrested in metaphase (Jackson and Bender, 1978).

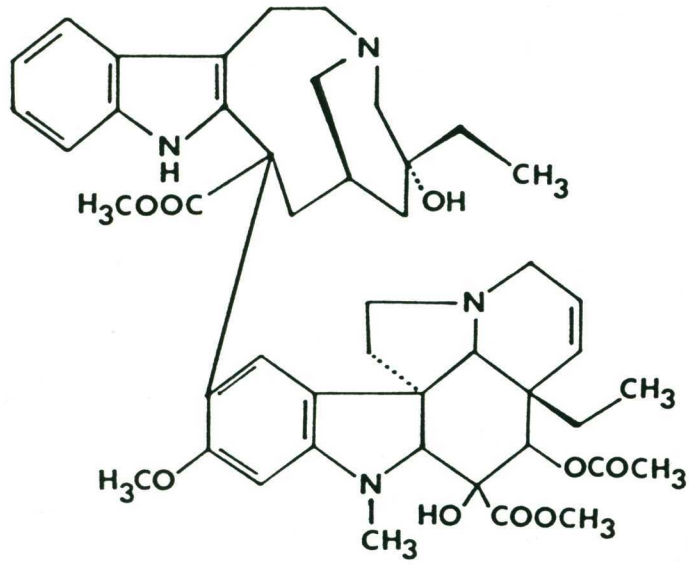

Figure 1. Structure of vinblastine.

One feature associated with the use of vinblastine is the development of multi-drug resistance (Chapter 1.6). This means that tumour cells become resistant not only to vinblastine, but also to structurally unrelated drugs such as the anthracyclines and colchicine.

Most studies of vinca alkaloid resistance in vitro are undertaken on cultured cells resistant to very high levels of drug e.g. in the μg-mg/ml concentration range which is 100 - 1000-fold more resistant than the sensitive cell lines. However, resistance to lower levels of

drug is more likely to be encountered in cancer patients.

Increased vinblastine binding has been reported in membrane vesicles from multi-drug resistant human KB carcinoma cells, compared with sensitive cells (Cornwell et al., 1986). It is possible that the binding site is the P-glycoprotein, which is over-produced in drug-resistant cells (Juliano and Ling, 1976) and which may function as an ion pump on the plasma membrane (Gerlach et al., 1986).

When human leukaemic lymphoblasts (CCRF-CEM) are made resistant to very low levels of vinblastine (10 - 20 ng/ml; 5 - 20-fold) changes in the cellular lipid spectrum can be detected by ^{1}H NMR spectroscopy (Chapter 1.7.3; Mountford et al., 1986a). An immediate effect was noticed on the methylene resonances in cells challenged with vinblastine. This effect was different in sensitive and resistant cells.

The methylene resonance in the spectrum of leukaemic lymphoblasts made resistant to 7 ng/ml vinblastine (VBL7) originates from neutral lipid forming part of an isotropically-tumbling plasma membrane domain (see previous Chapter). A comparison of the lipid composition of plasma membranes from vinblastine-resistant cells with those from the sensitive parent line CCRF-CEM is reported in this Chapter.

The development of drug resistance has been associated with the appearance of altered microtubule and mitochondrial-associated proteins (Gupta and Gupta, 1984; Gupta et al., 1985). Moreover, in multi-drug resistant cells, active transport mechanisms have been proposed to account for the reduced accumulation of drugs such as daunomycin, vincristine and vinblastine which is typical of such cells (reviewed by Danø et al., 1983). This suggests that not only the permeability of the plasma membrane and the production of the P-glycoprotein, but also the functional integrity of the intracellular membranes involved in energy

production are important in the mechanism of multi-drug resistance. To this end the composition of whole cells, both sensitive and resistant, was investigated in addition to plasma membrane studies.

Evidence is provided in this chapter for alterations to the lipid content of both whole cells and purified plasma membranes when leukaemic lymphoblasts are made resistant to low levels of vinblastine. Cellular accumulation of the drug might consequently be affected.

4.2 RESULTS

4.2.A COMPARISON OF THE LIPID COMPOSITION OF SENSITIVE AND RESISTANT WHOLE CELLS

4.2.A.1 The Neutral and Total Phospholipid Composition of Whole Cells

The generation and characterisation of human acute leukaemic lymphoblasts resistant to 7, 15 and 20 ng/ml of vinblastine (called VBL7, 15 and 20) is described in Chapter 2.1.2.

The total lipid, protein and cholesterol content were all significantly higher in VBL20 cells than the sensitive parent line CCRF-CEM. Phospholipid, cholesteryl ester and triglyceride mean values were also higher, but more samples need to be analysed to establish a statistical difference. The raised lipid, protein, cholesterol and phospholipid content suggested that membrane material might be increased inside resistant cells since the size of these cells is not larger (Chapter 2.1.2).

Table 1 Whole Cell Lipid and Protein Composition of Sensitive and VBL20 Cells. Results are means ± S.D. from at least 5 experiments. * Indicates results significantly different by the Mann-Whitney U Test. For the purposes of calculation, phosphorus was assumed to constitute 4% of phospholipid. The molecular weights of phospholipid, triglyceride, and cholesteryl ester were taken as 750, 885 and 650 respectively.

	SENSITIVE	RESISTANT
Total lipid ($mg/10^8$ cells)	1.37 ± 0.23	1.97 ± 0.46*
Free cholesterol ($nmol/10^8$ cells)	231 ± 40	320 ± 135*
Ester cholesterol ($nmol/10^8$ cells)	142 ± 53	162 ± 56
Phospholipid ($nmol/10^8$ cells)	940 ± 185	1245 ± 261
Triglyceride ($nmol/10^8$ cells)	135 ± 25	172 ± 48
Protein ($mg/10^8$ cells)	2.62 ± 0.4	4.54 ± 0.7*
$\frac{\text{Cholesterol (mol)}}{\text{Phospholipid (mol)}}$	0.22 ± 0.05	0.29 ± 0.05

4.2.A.2 Transmission Electron Microscopy of Thin Sections of Cells

The observation that VBL20 cells contained more lipid and protein and hence possibly more membranes (Table 1) led to the examination of sensitive and resistant cells by transmission electron microscopy. Two major differences were observed. The sensitive cells appeared to have mitochondrial profiles where the cristae were either absent or poorly developed (Figure 2A), despite the double membrane remaining intact. This is normal for mitochondria of leukaemic lymphoblasts (Schumacher et al. 1973). In contrast, the mitochondrial profiles of the resistant

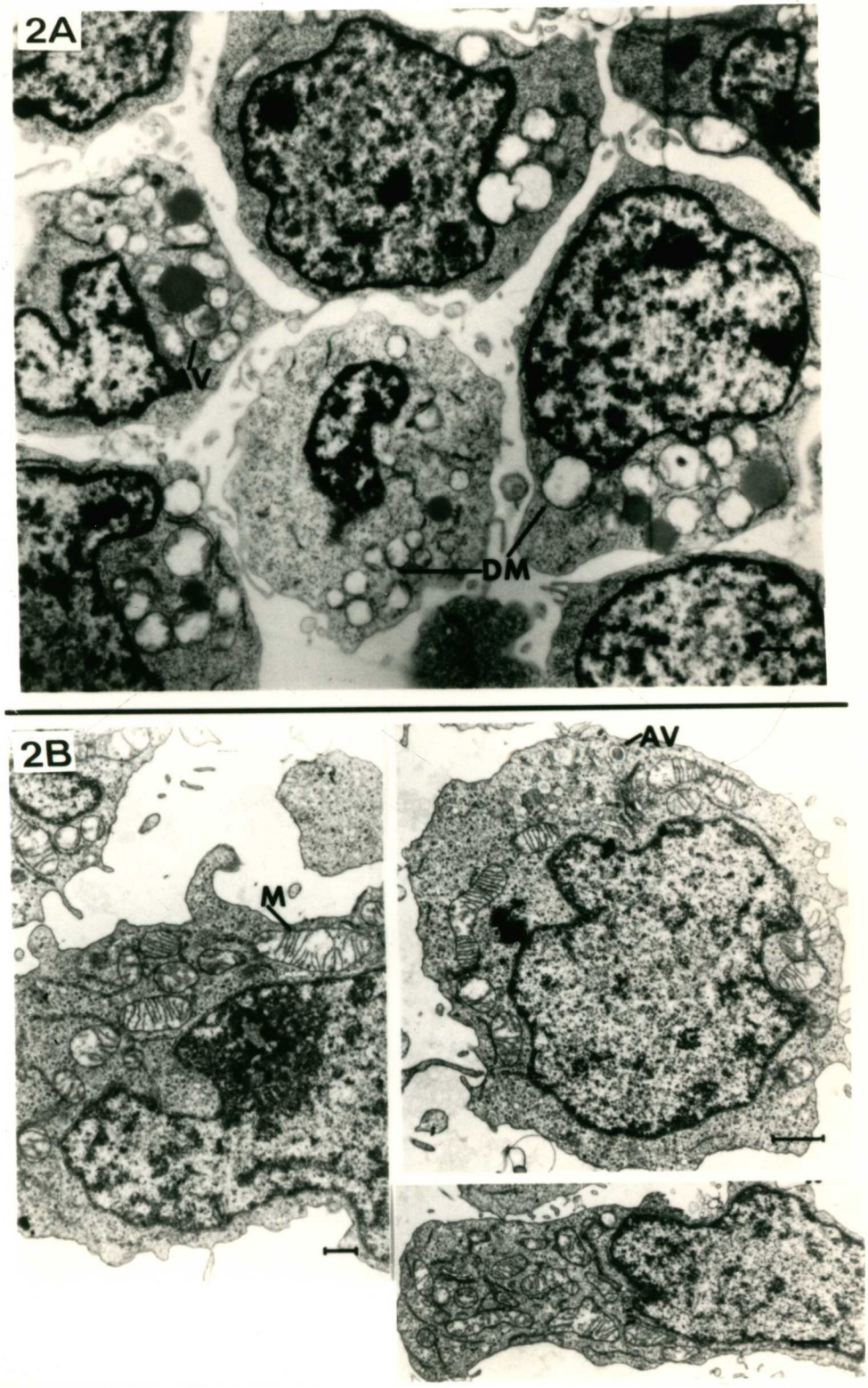

Figure 2. (A) Transmission electron micrograph of sensitive CCRF-CEM cells illustrating degenerate mitochondrial profiles (DM) and an autophagocytic vacuole (AV). Bar = 1 μ m. (B) VBL20 cells showing increased numbers of mitochondrial profiles (M). A number of small autophagocytic vacuoles (AV) can be seen in the top right hand cell. Bar = 1 μm.

cells appeared more numerous and to have well developed cristae (Figure 2B). Vinblastine-resistant cells were found to have increased respiratory capacity when compared with sensitive cells. This study is included in Appendix 1. In addition, autophagocytic vacuoles bounded by a single membrane were seen more frequently in resistant cells. Thus increased organellar content was consistent with the increased cholesterol, total lipid, total protein and phospholipid levels (Table 1).

4.2.A.3 Phospholipid Species Composition of Whole Cells

The total lipid of most membranes consists of 50 - 80% by weight of phospholipids and changes in these can affect membrane permeability. Differences in the relative quantities of phospholipid species between sensitive and VBL20 cells were observed (Table 2). The resistant cells contained 2.5% more SPH, 2% more CL, 4% less PE and 1% less PS, but no significant differences in PI or PG content. The increase by 4% in the positively charged phospholipids (PC + SPH) was balanced by a 5% decrease in negatively charged phospholipid (PE + PS). The increase in cardiolipin, a mitochondrial inner membrane marker (Krebs et al., 1979) is in accord with the suggestion in Figure 2A that there are more mitochondria with cristae in VBL20 cells.

4.2.A.4 Ether-linked Phospholipid Species Composition of Whole Cells

The structure of ether-linked lipids is shown in Chapter 1.3.4. The ether-linked phospholipid content of the resistant cells was 34% of the total phospholipid compared with 24% in the sensitive cells. In terms of total cell lipid these figures were 22% for resistant cells and 13% for

Table 2 Phospholipid Species Composition of Sensitive and VBL20 Whole Cells

	Sensitive	Resistant
	(% by weight of total)	
Origin + Lyso PC	0.3 ± 0	0.2 ± 0.1
Sphingomyelin (SPH)	3.0 ± 0.2	5.5 ± 0.3
Phosphatidyl Choline (PC)	44.3 ± 0.1	45.5 ± 1.4
Phosphatidyl Ethanolamine (PE)	30.7 ± 0.1	26.6 ± 0.4
Phosphatidyl Serine (PS)	5.8 ± 0.4	4.9 ± 0.1
Phosphatidyl Inositol (PI)	7.7 ± 0.4	8.1 ± 0.1
Phosphatidyl Glycerol (PG)	1.3 ± 0.9	0.9 ± 0.4
Cardiolipin (CL)	6.8 ± 0.1	8.7 ± 1.2

sensitive cells.

Differences were also found when the individual phospholipids were separated into their 1,2-diacyl, 1-O-alkenyl-2-acyl and 1-O-alkyl-2-acyl components (Methods, Chapter 2.3.7). Resistant cells had 10% more 1-O-alkyl-2-acyl PC and 27% more 1-O-alkenyl-2-acyl PE with concomitant decreases in 1,2-diacyl PC (10%) and 1,2-diacyl PE (27.5%). The amounts of 1-O-alkenyl-2-acyl PC and 1-O-alkyl-2-acyl PE remained the same (Table 3). Of the phospholipid assayed in Table 2, only PE and PC contained measurable amounts of ether-linked species.

Table 3 Distribution of Acyl and Ether-linked Chains in Whole Cell Phospholipid Analyses of Sensitive and Resistant Lymphoblasts

	(% by weight of phospholipid)			
	Sensitive		Resistant	
	% of PC or PE	% of PL	% of PC or PE	% of PL
PC				
1,2-diacyl	80.2 ± 4.9	35.5	70.6 ± 4.7	32.1
1-O-alkenyl	5.1 ± 1.4	2.3	5.1 ± 3.4	2.3
1-O-alkyl	14.7 ± 3.4	6.5	24.3 ± 1.6	11.1
PE				
1,2-diacyl	50 ± 7.5	15.4	22.5 ± 9.0	5.9
1-O-alkenyl	42.8 ± 7.2	13.1	69.7 ± 9.2	18.5
1-O-alkyl	7.1 ± 0.3	2.2	7.8 ± 0.2	2.1

PL = phospholipid.

4.2.B COMPARISON OF THE LIPID COMPOSITION OF PURIFIED PLASMA MEMBRANES FROM SENSITIVE AND VINBLASTINE-RESISTANT CELLS

4.2.B.1 The Isolation of Purified Plasma Membranes from Sensitive and VBL15 Cells

Since lipid changes were observed in whole cells made resistant to vinblastine, it was pertinent to examine which of these was located in the plasma membrane. Alterations to the structure or composition of this membrane might affect permeability to the drug.

Membrane fractions were obtained by sucrose density gradient centrifugation (Methods, Chapter 2.2.2) from sensitive CCRF-CEM cells. The distribution of marker enzyme activity from the sensitive cells is shown in Table 4. Band 1 at the junction of the 10 - 30% sucrose layer

was the purest plasma membrane-containing fraction and although the enrichment over the homogenate is 32-fold, the ratio of plasma membrane markers to cytoplasmic, mitochondrial, and nuclear markers is many times greater. The major contamination arose from the endoplasmic reticulum as is evident by the enrichment of NADPH cytochrome c reductase activity. Even so, the ratio of plasma membrane to endoplasmic reticulum markers in band 1 was 19:1. There was no mitochondrial contamination in band 1 since no cytochrome c oxidase activity was detected.

Bands 2 - 4 were mixed membrane bands containing varying levels of mitochondrial, endoplasmic reticulum, lysosomal, and/or nuclear membranes in addition to plasma membrane. The recovery of 5'-nucleotidase in band 1 of the sensitive cell membranes was 59.5% and the sensitive cell membrane purification was comparable with that for VBL7 cell membranes (Chapter 3.2.2).

Membrane fractions were also obtained from cells which were more resistant to vinblastine (VBL15) compared with those used in Chapter 3 (VBL7). The distribution of marker enzymes and degree of purification of the plasma membrane fraction, B1, from VBL15 cells was similar to that obtained from both the sensitive and VBL7 cells.

4.2.B.2 The Neutral, Total Phospholipid and Ether-linked Lipid Composition of Purified Plasma Membranes

A comparison of the composition of all subcellular fractions obtained from sensitive cells and resistant (VBL15) cells is presented in Table 5. Fraction B1 was the purest plasma membrane band in both cases.

Table 4 Marker Enzyme Activity of Membrane Fractions from Sensitive Lymphoblasts. Plasma membranes were isolated from 4.5×10^9 cells by disruption by nitrogen cavitation followed by fractionation on a sucrose density gradient. The enzyme activities were determined as described in Section 2.2.3 for the initial suspension (homogenate) after cell disruption and the four density gradient bands as well as the supernatant from the density gradient centrifugation and a band of lipid which separated on top of the supernatant (designated floaters). The enrichment was calculated by the specific activity of the marker in each fraction divided by that in the homogenate. The values represent mean ± S.E. of two experiments. Band 1 is at the interface of the 10% and 30% sucrose layers; band 2 is at the interface of the 30% and 48% layers; band 3 is at the interface of the 48% and 60% sucrose layers; band 4 is the pellet at the bottom of the 60% sucrose layer. ND = not detected

	ENRICHMENT					
Enzyme Marker	Band 1	Band 2	Band 3	Band 4	Floaters	Supernatant
5'-Nucleotidase	32.5 ± 7.5	23.3 ± 7.9	18.2 ± 6.5	20.4	0.065 ± 0.065	0.22 ± 0.04
γ-Glutamyl transpeptidase	7.1 ± 0.8	10.1 ± 1.2	2.8 ± 0.1	1.1 ± 0.2	ND	0.075 ± 0.075
Na^+, K^+ adenosinetriphosphatase	8.0 ± 0.1	9.4 ± 1.5	3.1 ± 0.3	2.5 ± 1.7	ND	ND
Acid phosphatase	0.62 ± 0.12	1.65 ± 0.20	0.43 ± 0.01	0.15 ± 0.15	0.5 ± 0.1	0.83 ± 0.07
Lactate dehydrogenase	0.0029 ± 0.0010	0.051 ± 0.003	0.026 ± 0.002	0.0032 ± 0.0032	2.2 ± 0.1	2.5 ± 0.3
NADPH Cytochrome c reductase	1.7 ± 0.3	5.6 ± 1.7	3.58 ± 0.08	2.25 ± 0.10	0.73 ± 0.34	1.66 ± 1.10
Cytochrome c oxidase	NIL	2.0 ± 0.6	3.6 ± 0.6	2.3 ± 0.1	ND	ND
DNA	0.06 ± 0.01	0.09 ± 0.03	0.39 ± 0.02	1.5 ± 0.7	0.009 ± 0.002	0.008 ± 0.002

Triglyceride was present in all membrane fractions of both sensitive and resistant cells, although the highest concentration was again in the supernatant and floaters fractions (c.f. Chapter 3). No difference was observed between sensitive and resistant cells in the levels of triglyceride present in any of the membrane fractions although the floaters and homogenate from the sensitive cells had a higher content (Table 5).

Small amounts of cholesteryl ester were present in all membrane fractions from the sensitive cells, but none was detected in the VBL15 membrane fractions (Table 5). Since cholesteryl ester was present in VBL7 membranes (Chapter 3), it is unlikely that the cholesteryl ester content of the membranes is correlated with drug resistance. In contrast to cholesteryl ester, free cholesterol was present in larger amounts in all VBL15 membrane fractions, including the plasma membrane (B1). Total phospholipid was also higher in the plasma membrane fraction (B1) and B3 and B4 membrane fractions from VBL15 cells.

The cholesterol to phospholipid ratio was highest in the B1 and B2 fractions in both sensitive and resistant cells (Table 6) as a consequence of their high plasma membrane content. There was no difference in this ratio between sensitive and resistant plasma membranes (B1). The triglyceride to phospholipid ratio was lower in the B1 fraction from the VBL15 cells than in the sensitive cell B1 fraction. This was the result of an increased phospholipid content rather than decreased levels of triglyceride (Table 5). Similar amounts of triglyceride were recovered in membrane fractions from both sensitive and VBL15 cells.

Table 5 Lipid Composition of Membrane Fractions from Sensitive and VBL15 Lymphoblasts. The lipid composition was determined for the homogenate and membrane bands from the density gradient centrifugation, as well as for the supernatant fraction and a band of lipid which separated on top of the supernatant (designated floaters). The values represent the mean ± S.D. as determined from assays run in duplicate on up to 8 different extractions (data are expressed as nmol per mg of lipid). Values marked (*) are regarded as being significantly different in sensitive and resistant plasma membranes. ND = Below the level of detection i.e. < 1.0 nmol/mg lipid.

A. SENSITIVE CELL MEMBRANES

Fraction	Free Cholesterol	Cholesteryl Ester	Triglyceride	Phospholipid
Homogenate	127 ± 25	52 ± 19	157 ± 41	677 ± 29
Floaters	20 ± 8	21 ± 1	540 ± 86	88 ± 43
Supernatant	60 ± 33	34 ± 8	189 ± 85	215 ± 136
B1	* 186 ± 41	22 ± 3	63 ± 19	* 585 ± 54
B2	204 ± 13	34 ± 7	51 ± 16	642 ± 129
B3	156 ± 44	21 ± 6	62 ± 24	653 ± 138
B4	66 ± 26	40 ± 20	68 ± 31	294 ± 80

B. VBL15 CELL MEMBRANES

Fraction	Free Cholesterol	Cholesteryl Ester	Triglyceride	Phospholipid
Homogenate	206 ± 7	ND	82 ± 2	622 ± 3
Floaters	46 ± 27	12 ± 9	288 ± 16	252 ± 80
Supernatant	77 ± 22	70 ± 10	291	201 ± 30
B1	* 273 ± 4	ND	66 ± 1	* 770 ± 25
B2	272	ND	53 ± 6	578 ± 191
B3	281 ± 13	ND	76 ± 5	1027 ± 56
B4	178 ± 45	ND	71 ± 1	850 ± 114

Table 6 Lipid Ratios and Triglyceride Recovery in Membrane Fractions from Sensitive and VBL15 Lymphoblasts.

A. SENSITIVE CELL MEMBRANES

Fraction	Cholesterol to Phospholipid Ratio	Triglyceride to Phospholipid Ratio	% Triglyceride[a] Recovery
Homogenate	0.19 ± 0.02	0.20 ± 0.04	-
Floaters	0.24 ± 0.04	3.86 ± 0.76	37 ± 9
Supernatant	0.27 ± 0.07	0.39 ± 0.08	34 ± 4
B1	0.32 ± 0.08	0.12 ± 0.02	8 ± 3
B2	0.33 ± 0.05	0.08 ± 0.03	10 ± 4
B3	0.24 ± 0.08	0.10 ± 0.05	6 ± 3
B4	0.23 ± 0.02	0.10 ± 0.06	5 ± 3

B. VBL15 CELL MEMBRANES

Fraction	Cholesterol to Phospholipid Ratio	Triglyceride to Phospholipid Ratio	% Triglyceride[a] Recovery
Homogenate	0.31 ± 0.002	0.012 ± 0.00	-
Floaters	0.23 ± 0.05	1.43 ± 0.13	* 26
Supernatant	0.30 ± 0.07	1.15	52
B1	0.35 ± 0.009	0.09 ± 0.003	6
B2	0.47 ± 0.10	0.09 ± 0.03	5
B3	0.27 ± 0.01	0.07 ± 0.003	6
B4	0.21 ± 0.03	0.08 ± 0.009	6

[a]Distribution of triglyceride is measured as a % of the total triglyceride recovered. The 1000 g pellet was not assayed. *Since one supernatant assay for triglyceride was lost, a recovery for only one membrane fractionation was obtained in the VBL15 cells.

The lipid and protein contents of the plasma membrane (B1) fractions isolated from sensitive cells and cells with varying degrees of resistance are presented in Table 7. The cholesterol to phospholipid ratio was similar, within experimental error, in all lines. Triglyceride and cholesteryl ester levels showed no trends, but free cholesterol and total phospholipid were higher in the plasma membranes of all the drug resistant cells (VBL7 - 20). The ether-linked lipids showed some significant differences, with almost three times the 1-O-alkyl phospholipid content in the resistant cell membranes. A smaller increase in 1-O-alkenyl phospholipid was observed also (Table 7).

Table 7 The Lipid Composition of Lymphoblast Purified Plasma Membranes Showing Varying Degrees of Resistance to Vinblastine. All comparisons are made with B_1 fractions isolated from cells as in Chapter 2.2.2. The results are means and standard deviations of at least three experiments and are expressed as nmol/mg total lipid. The values for the ether lipids and protein/lipid ratios are presented as a composite of resistant and sensitive cell membrane values as indicated by the brackets. Two sets of data were obtained from sensitive cells analysed some years apart and grown in different batches of foetal calf serum. TG = triglyceride; CHOL = free cholesterol, CE = cholesteryl ester; PL = phospholipid. Molecular weights assumed for ether-linked TG = 871 and for ether-linked PL = 736.

	Protein to	Cholesterol					1-O-alkyl		1-O-alkenyl	
Sample	Lipid Ratio	to PL ratio	TG	CHOL	CE	PL	TG	PL	TG	PL
Sensitive cells	0.78 ± 0.19	0.23 ± 0.02	51 ± 25	140 ± 2	18 ± 0	596 ± 67	96 ± 26	99 ± 41	< 1	32 ± 5
		0.32 ± 0.08	63 ± 19	186 ± 41	22 ± 3	585 ± 54				
VBL7	0.48 ± 0.13	0.31 ± 0.002	48 ± 8	222 ± 26	67 ± 19	719 ± 8	85 ± 19	275 ± 78	< 1	41 ± 4
VBL15		0.35 ± 0.01	66 ± 1	273 ± 4	< 1	770 ± 25				
VBL20		0.32 ± 0.04	70 ± 15	263 ± 50	< 1	807 ± 71				

A comparison of the ether-linked phospholipid content of purified plasma membranes and whole cells, calculated from Tables 3 and 7 in this Chapter, is presented in Table 8. In both cases the content of 1-O-alkyl phospholipid was higher in drug-resistant cells. The 1-O-alkyl phospholipid formed a higher proportion of the total phospholipids in purified plasma membranes than in whole cells. Conversely the alkenyl phospholipid was lower in plasma membranes.

4.2.B.3 The Fatty Acid Composition of Plasma Membrane Lipids

Alterations to the fatty acyl chain composition also occurred in cells with low level resistance to vinblastine (Table 9). The total fatty acid content of the purified plasma membrane fraction, B1, was about 7% higher in the proportion of unsaturated chains which was spread over the following fatty acids:- 16:1, 18:1 (11), 20:4, 22:5, 22:6 and 24:1. This was largely at the expense of a 4.1% decrease in the content of a single fatty acid, 18:0. The double bond index for plasma membranes from sensitive cells was lower than that from resistant cells (Table 9).

4.2.B.4 Plasma Membrane Structural Studies using Freeze-fracture Electron Microscopy

Studies on the structure of the inner and outer bilayer halves of lymphoblast plasma membranes were pursued by freeze-fracture electron microscopy (Figure 3A, B).

The faces developed from the fracture through the hydrophobic interior of the lipid bilayer of the plasma membrane are the outer or exoplasmic face (EF) and the inner or protoplasmic face (PF). Smooth fracture faces are considered to be formed by lipid bilayers (Verkleij and Ververgaert, 1978) and the intramembranous particles (IMPS) observed

Table 8 Distribution of Acyl and Ether-linked Phospholipid Chains in Purified Plasma Membranes Compared with Whole Cells. Results are as % of total phospholipid weight. Values for the whole cells were calculated as PE+ PC only; however most ether-linked phospholipid is associated with these head groups (El Tamer et al., 1984)

	1-O-alkyl	1-O-alkenyl	1,2-diacyl
Sensitive plasma membranes	16.7	5.4	77.9
Resistant plasma membranes (VBL7, 15, 20)	35.8	5.4	58.8
Sensitive whole cells	8.7	15.4	75.9
VBL20 whole cells	13.2	20.8	66.0

Table 9 Total Fatty Acid Composition of Plasma Membranes from Sensitive and VBL15 Cells.

FATTY ACID METHYL ESTER	% COMPOSITION IN PLASMA MEMBRANE	
	SENSITIVE	VBL15
14:0	2.4 ± 0.2	2.2 ± 0.4
16:0	29.0 ± 1.0	29.7 ± 1.5
16:1	1.1 ± 0.1	1.5 ± 0.2*
18:0	18.7 ± 0.3	14.6 ± 0.4+
18:1(9)	17.4 ± 0.8	17.0 ± 0.5
18:1(11)	5.4 ± 0.4	6.6 ± 0.1*
18:2	1.7 ± 0.1	1.9 ± 0
18:3(6,12)	2.7 ± 0.5	2.2 ± 0.2
20:4[20:3(8,14)]	4.9 ± 0.2	5.8 ± 0.3*
22:4	1.9 ± 0.3	2.1 ± 0.14
22:5	3.4 ± 0.3	4.7 ± 0.7*
22:6	4.0 ± 0.2	5.7 ± 0.9*
24:1	1.0 ± 0.2	2.2 ± 0.7*
Double Bond Index	35.3 ± 1.0	41.2 ± 3.7

Less than 1% of the following fatty acids was detected:- 8:0, 9:0, 12:0, 15:0, 17:0, 18:3 (9,15), 20:0, 20:1, 20:3 (11,17), 20:5, 22:0, 24:0. * denotes a significant increase; + denotes a significant decrease. Values are means and standard deviations of three experiments. Double Bond Index = $\varepsilon \frac{N_i W_i}{M_i}$

N_i = number of bonds in fatty acid chain; M_i = molecular weight

W_i = percentage by weight of fatty acid in a given mixture.

appear to be proteins intercalated in the membrane (Murphy and Swift, 1983). IMPS can also be formed by lipopolysaccharides in the outer membrane of E. coli and by artificial lipid model systems (Verkleij, 1980).

The PF and EF faces of the resistant cells (VBL20) had 56% and 68% more IMPS respectively than the sensitive cells (Figure 3A and B). This increase in intramembranous particles could possibly reflect the increased P-glycoprotein content of the membranes, which has previously been associated with altered drug uptake (Beck et al., 1979). The PF face of the plasma membrane of resistant cells was characterised by the presence of elevated IMP free regions or bulges (Figure 3B). The PF face of the sensitive cells did not have these elevated regions (Figure 3A). The additional surface area provided by the bulges was calculated to be approximately 4% (method of calculation is in Chapter 2.4.2).

4.3 DISCUSSION AND CONCLUSIONS

Changes in cellular and plasma membrane phospholipids are observed in vinblastine-resistant CCRF-CEM cells. The multi-drug resistant phenotype is associated with a 3-fold increase in 1-O-alkyl phospholipid in the plasma membrane, probably phosphatidyl choline, by analogy with the changes in whole cells lipids. Ether-linked phospholipids account for 13% of the total lipid in sensitive cells and 22% in resistant cells.

The changes in cellular ether-linked phospholipid composition due to drug resistance can be considered in the light of the distribution of phospholipids found in the plasma membranes of the neoplastic Krebs II ascites cells (Record et al., 1984). Differences in phospholipid

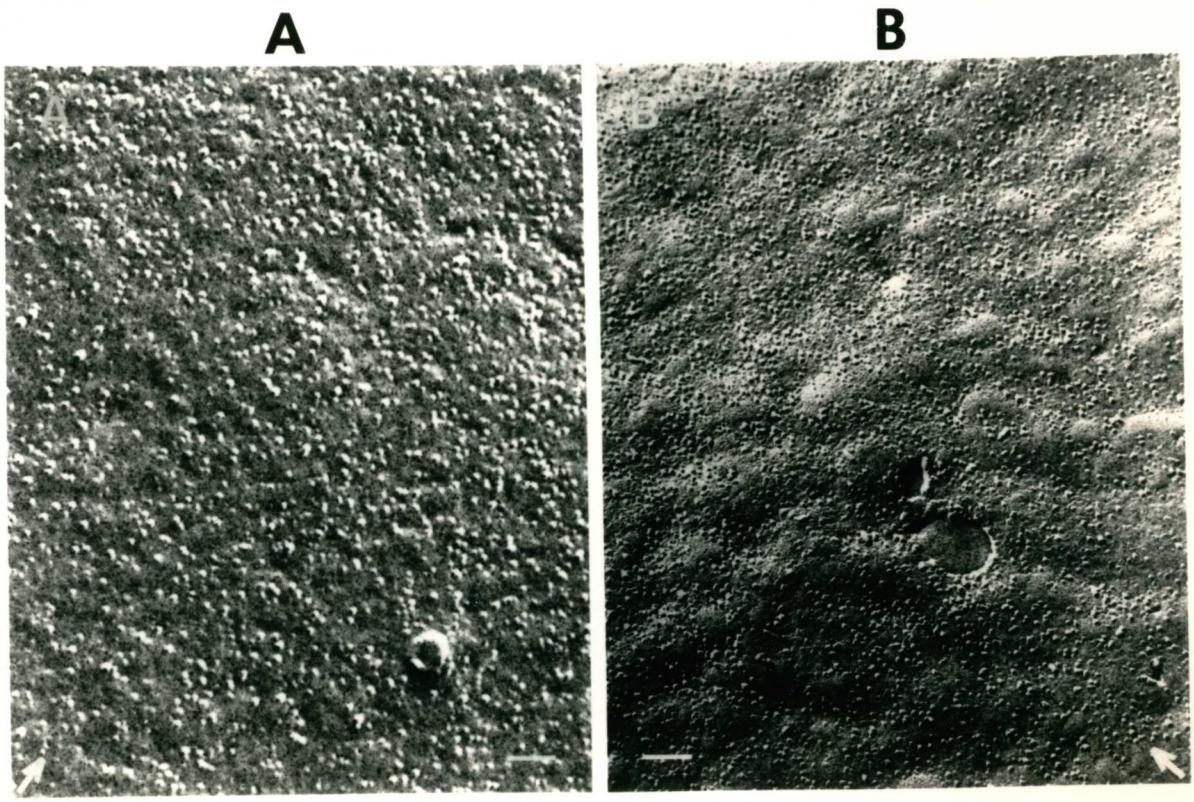

Figure 3. Freeze fracture replicas of the protoplasmic face of the plasma membrane of CCRF-CEM. A (left): Sensitive cells. B (right): Vinblastine resistant cells (VBL20). Arrow indicates the direction of shadowing. Bar = 1 µm.

subclasses between resistant and sensitive cells reflect differences in total membrane composition and are expressed both as a percentage of the phospholipid species and as a percentage of the total phospholipid in Table 3.

Some interesting speculations can be made if the known asymmetry of the ether-linked phospholipids in Krebs II ascites plasma membranes is applied to vinblastine-sensitive and -resistant lymphoblasts (Table 10). The 1,2-diacyl PE and PC found on the external face is decreased by 12.9% when the cells become resistant to vinblastine (sum of -3.4 and -9.5, Table 10). The 1-alkyl, 2-acyl PC (an inner face phospholipid) increases by 4.6%. The 1-O-alkenyl PE (plasmalogen), located on both faces, increases by 5.4% and if there is an even distribution, this implies a 2.7% increase in both halves of the bilayer. The net loss of major phospholipids from the outer half of the bilayer is therefore 10.2% and there is a concomitant gain of 7.2% lipid to the inner half of the bilayer (Table 10).

When the asymmetry of the phospholipids in Krebs II ascites plasma membranes is applied to the purified lymphoblast plasma membranes, there has been a 19.1% increase in an inner face component (1-O-alkyl phospholipid) at the expense of an outer membrane component (1,2-diacyl phospholipid) with vinblastine resistance (Table 8).

Thus analyses of both whole cell and plasma membrane lead to one possible explanation for the increased area of the inner half of the bilayer due to the elevated particle free regions or "bulges" seen by freeze fracture electron microscopy, viz. an increase in 1-O-alkyl phosphatidyl choline in the inner half of plasma membrane (Figure 3). Detailed studies on the asymmetry of phospholipids in lymphoblast plasma membranes are need to confirm this hypothesis. 1-O-alkyl phosphatidyl

Table 10 Distribution of Acyl and Ether-linked Chains in Whole Cell Phospholipid Analyses of Sensitive and Resistant Lymphoblasts and Their Hypothetical Asymmetry in the Plasma Membrane

	(% by weight of phospholipid)				Difference[+]	
	Sensitive		Resistant		Expressed As %	Membrane
	% of PC or PE	% of PL	% of PC or PE	% of PL	Total PL	Face[*]
PC						
1,2-diacyl	80.2 ± 4.9	35.5	70.6 ± 4.7	32.1	- 3.4	outer
1-O-alkenyl	5.1 ± 1.4	2.3	5.1 ± 3.4	2.3	nil	outer
1-O-alkyl	14.7 ± 3.4	6.5	24.3 ± 1.6	11.1	+ 4.6	inner
PE						
1,2-diacyl	50 ± 7.5	15.4	22.5 ± 9.0	5.9	- 9.5	outer
1-O-alkenyl	42.8 ± 7.2	13.1	69.7 ± 9.2	18.5	+ 5.4	both
1-O-alkyl	7.1 ± 0.3	2.2	7.8 ± 0.2	2.1	- 0.1	inner

[+]Difference between resistant and sensitive; [*] Lipid as located in Krebs II ascites cells (Record et al., 1984); PL = phospholipid.

choline is thought to be a precursor of platelet-activating factor (Diagne et al., 1984), but its significance in drug resistance awaits further investigation.

Ether-linked lipid levels are often elevated in cancer cells (Snyder, 1972). Diacyl and ether-linked phospholipids are membrane components, and plasma membranes, in particular, are rich in ether-linked phospholipids (Record et al., 1984). Ether-linked phospholipids pack less tightly in membranes and could increase molecular motion (Horrocks and Sharma, 1982). Increased impermeability of membranes has been linked with increased ether- lipid content because of the lower surface potential of these lipids and their capacity to form hydrogen bonds with cholesterol (Brockerhoff, 1974). A mixture of diacyl and ether-linked phospholipids can also increase the stability of plasma

membranes because of the resistance of ether lipids to phospholipases (Horrocks and Sharma, 1982).

Since no larger cell size was apparent for the resistant cells, their increased levels of protein, total lipid, free cholesterol and phospholipid suggest two possibilities: (1) that more membranes were present per cell or (2) that existing membranes were packed with more lipid and protein. Transmission electron microscopy suggested the presence of more mitochondrial profiles and autophagocytic vacuoles within resistant cells (Figure 2). The appearance of "bulges" on the internal face of the plasma membrane of the resistant cells and a greater number of intramembranous particles on both faces in freeze-fracture electron micrographs are also consistent with these membranes containing more lipid and protein (Figure 3).

No difference in cholesterol to phospholipid ratio was observed in vinblastine-resistant lymphoblast plasma membranes (Table 6). Thus membrane lipid order by this criterion (van Blitterswijk, 1984), is unchanged. Attempts by others to correlate the physical state of the bilayer with drug resistance have produced conflicting results (Ramu et al., 1983; Wheeler et al. 1982; Rintoul and Center, 1984). There are few data in the literature relating lipid changes to multi-drug resistance in purified plasma membranes. One report showed that phosphatidyl serine in the plasma membranes of sensitive murine fibroblasts treated for 4 h with 100 μm vinblastine decreased by 4% (Schroeder et al., 1981).

No change in cellular (or plasma membrane) triglyceride content was found in resistant leukaemic lymphoblasts (Tables 1 and 7). Most studies on lipids have used whole cell analyses. In one study, a 3.6-fold increase in cellular triglyceride content was observed in doxorubicin-resistant P388 mouse leukaemic cells (Ramu et al., 1984).

Cellular cholesterol and phospholipid both increased in resistant lymphoblasts (Table 1), resulting in a constant cholesterol to phospholipid ratio. These findings are similar to those for doxorubicin resistance in rat glioblastoma cells (Vrignaud et al., 1986).

An increased sphingomyelin content and a decrease in the negatively-charged phospholipids, PE and PS were found in drug resistant lymphoblasts (Table 2). No change in phospholipid species was observed in rat glioblastoma cells made resistant to doxorubicin (Vrignaud et al., 1986). An increased sphingomyelin content was, however, observed by Ramu et al. (1984) with drug resistance. Sphingomyelin is found in greater concentration in the outer leaflet of plasma membranes, with the ratio of SPH to PC being proportional to the phospholipid structural order (Barenholz and Thompson, 1980). Decreased membrane permeability has been linked with increased sphingomyelin content (Brockerhoff, 1974).

No differences were found in whole cell fatty acids between sensitive and vinblastine-resistant lymphoblasts (data not shown) and only small differences in the purified plasma membrane lipids (Table 9), with polyunsaturates increasing at the expense of 18:0. However, Vrignaud et al. (1986) found that drug resistant cell lipids were characterised by a decrease in 20:3 fatty acid and 2- to 3-fold increase in the polyunsaturated fatty acids, especially 20:4 and 22:6.

The lipid analyses in this Chapter were undertaken to investigate the changed intensity of the lipid methylene resonance detected by ^{1}H NMR spectroscopy with drug resistance (Mountford et al., 1986a). Triglyceride indicating the presence of neutral lipid domains (Chapter 3) was found to an equal extent in both sensitive and resistant cells and membranes. Bilayer or monolayer lipid acyl chains, because of their

relative immobility do not contribute substantially to the high resolution spectrum, but constitute much of the broad, low resolution portion of the spectrum (Bloom et al., 1986). Although the location of ether lipids in the neutral lipid domains of the plasma membrane is unknown, it seems unlikely that the NMR spectral changes can be explained by gross compositional changes, but rather result from a subtle rearrangement of membrane components as demonstrated by freeze-fracture electron microscopy (Figure 3).

CONCLUSIONS

The lipid analysis of whole cells and plasma membranes, combined with electron microscopic studies as presented in this Chapter have shown that membrane lipids are involved in the multi-drug resistance and that the lipid content, especially the ether-linked phospholipids, sphingomyelin and cholesterol might alter membrane permeability. In a recent publication, Gerlach and co-workers (1986) have proposed that the P-glycoprotein functions as an ATP-dependent pump at the plasma membrane which effects rapid drug efflux. While undoubtedly this pump would contribute to the diminished accumulation of vinblastine in resistant lymphoblasts (it is overproduced 3-fold in these cells; Chapter 2.1.2) it cannot be regarded as the sole mechanism. The structural and lipid compositional changes in the plasma membrane discussed in this Chapter and the increased mitochondrial function (Appendix I) may also play an important role.

CHAPTER FIVE

A PROTEOLIPID IN CANCER CELLS IS THE ORIGIN OF THEIR HIGH RESOLUTION NMR SPECTRUM AND IS FOUND IN THE PLASMA OF A PATIENT WITH MALIGNANT DISEASE

5.1 INTRODUCTION

Triglyceride-rich domains were shown to be present in or on the plasma membrane of embryonic and transformed cells, including cancer cells, in Chapter 3. Since serum lipoproteins contain a core of triglyceride and cholesteryl ester, surrounded by a shell of phospholipid, protein and cholesterol (Herbert et al., 1983; Chapter 1.5.1), normal human blood lipoproteins were characterised by ^{1}H NMR methods and chemical analysis. Comparisons were made between the properties of the triglyceride-rich domain found in cancer cells, and the serum lipoproteins (Williams et al., 1985; and Chapter 3). The 2D scalar correlated NMR spectra of cancer cells or solid tumours were similar to those obtained from very low and low density lipoproteins (VLDL and LDL). However, the long T_2 relaxation value observed for neutral lipids in the methylene region of spectra from metastatic cancer cells (> 400 ms, Mountford et al., 1984b), was not observed for any of the normal serum lipoproteins studied. None of the lipoprotein classes gave a T_2 longer than 250 ms (Williams et al., 1985). It was therefore proposed that an abnormal lipoprotein is responsible for the ^{1}H NMR spectrum in metastatic cancer cells.

Lipoprotein metabolism is deranged in patients with cancer (Barclay and Skipski, 1975). A correlation between cancer in humans and experimental animals and a new type of particle, "neoproteolipid", was established in the 1970's (Skipski et al., 1971). The properties of the isolated complex met the definition given by Folch and Lees (1951) viz:- "Proteolipids are lipoproteins having as constituents a lipid moiety and a protein moiety but, while other known lipoproteins are soluble in water or salt solution, proteolipids are insoluble in water and soluble in chloroform-methanol mixtures; i.e. their solubilities are

akin to those of lipids". Neoproteolipids were found in lipid extracts of tumours, and in larger amounts in tissues and sera from tumour-bearing animals or patients compared with healthy individuals. The complexes contained polypeptide, fatty acids, sphingosine bases, carbohydrates, cholesterol and phosphorus (Skipski et al. 1975a).

An RNA-proteolipid complex containing phospholipid, cholesterol, peptide, RNA and a high proportion of neutral glycolipid was recently isolated from the serum of patients with malignant diseases and from the medium from cultures of malignant cells (Wieczorek et al., 1985). Since the high resolution ^{1}H NMR spectrum from malignant, transformed and embryonic cells arises predominantly from neutral lipids (Chapter 3) and the neutral lipid domain in the plasma membrane resembles a lipoprotein-like entity (Williams et al., 1985), the origin of the long T_2 relaxation value was sought among lipoproteins and proteolipids in the serum of patients with cancer.

In this Chapter, the isolation and characterisation of the proteolipids and other lipoproteins from the plasma of a patient with a borderline ovarian tumour is described. In addition, NMR methods have been used to define the properties of the tumour biopsy and the lipoproteins and proteolipids, which have been further studied by lipid analysis, electron microscopy and biochemical assays. The plasma lipoproteins and proteolipids of the patient were studied 5 days after a total hysterectomy and salpingo-oophorectomy and again at 7 and 9 months after surgery.

Biopsy samples of tumours on both ovaries of this patient were examined and long T_2 values of 850 and 650 ms recorded. These figures are consistent with the malignant and metastatic phenotype. In previous

work in this laboratory (Mountford et al., 1986b), one hundred and fifty human biopsy samples excised from patients with malignant primary tumours in the colon, breast and ovary have been examined by NMR methods. Only two samples (both colon) were shown to have the malignant but non-metastatic phenotype (Mountford et al., 1986a; Mountford et al., 1986b).

5.2 RESULTS

5.2.1 The Patient

A 31 year old nulliparous woman (C) presented in September 1985 with a 12 month history of intermittent pain in the right iliac fossa. Clinical examination revealed a right ovarian mass. At laparotomy, there were multilobulated tumours involving both ovaries with adherent omentum, and peritoneal nodules over the rectosigmoid and bladder. Total abdominal hysterectomy, bilateral salpingo-oophorectomy and infracolic omentectomy were performed, and the post-operative recovery was uneventful. Histological examination revealed bilateral proliferating serous cystadenomas of the ovary with omental implants and florid reactive mesothelial proliferation. She remains well without therapy, and there have been no clinical signs of recurrent tumour. Preoperative CA 125 level was 123 U/ml and levels have fluctuated between < 6 - 66 U/ml in the past 12 months.

5.2.2 Separation of Plasma Lipoproteins: T_2 Relaxation Values

5 days after surgery: Total lipoproteins were isolated from plasma collected within 5 days of surgery by methods described in Chapter 2.10.1. Subfractionation of the total lipoprotein on a KBr gradient revealed the presence of an opaque band below the LDL band but above the

HDL at approximately 1.085 g/ml density. This opaque band is called a proteolipid, to distinguish it from the normal lipoproteins and to be consistent with the literature e.g. Wieczorek et al., 1985. All lipoprotein fractions and the regions between visible bands on the KBr gradient were collected (Figure 1A and B).

NMR studies, including T_2 relaxation times, were performed on all fractions. The ^1H NMR spectra and T_2 relaxation profiles for resonances in the methylene region are shown in Figure 2 for the total plasma lipoprotein fraction (including the proteolipid), the isolated proteolipid complex and LDL and VLDL from the patient. A long T_2 of 852 ms was recorded for the opaque proteolipid band. The region between the opaque band and the HDL also generated a long T_2 of 970 ms (Table 1A, Figure 2). None of the conventional lipoproteins generated a long T_2 relaxation value (Table 1A, Figure 2). This long T_2 was measured not only in the isolated complex and total lipoprotein fraction, but also in the excised tumours (T_2 850 and 650 ms) from this patient. The opaque band was named proteolipid 1, and the region below, where no bands were visible, was named proteolipid 2. The two proteolipid fractions, and the normal lipoproteins were further studied by electron microscopy, NMR and chemical analysis. Proteolipids and 1 and 2 were pooled for lipid analysis.

VLDL and chylomicra ran together at the top of the KBr gradient. This fraction had a T_2 value of 199 ms 5 days after surgery (Figure 2). Insufficient sample was recoved to carry out a complete lipid analysis.

9 months after surgery: Proteolipid 1 was visible to the naked eye on the KBr gradient in plasma taken 7 and 9 months after surgery. Again nothing was visible in the area between the proteolipid 1 band and HDL. Both proteolipid 1 and proteolipid 2 were collected for study. Similar

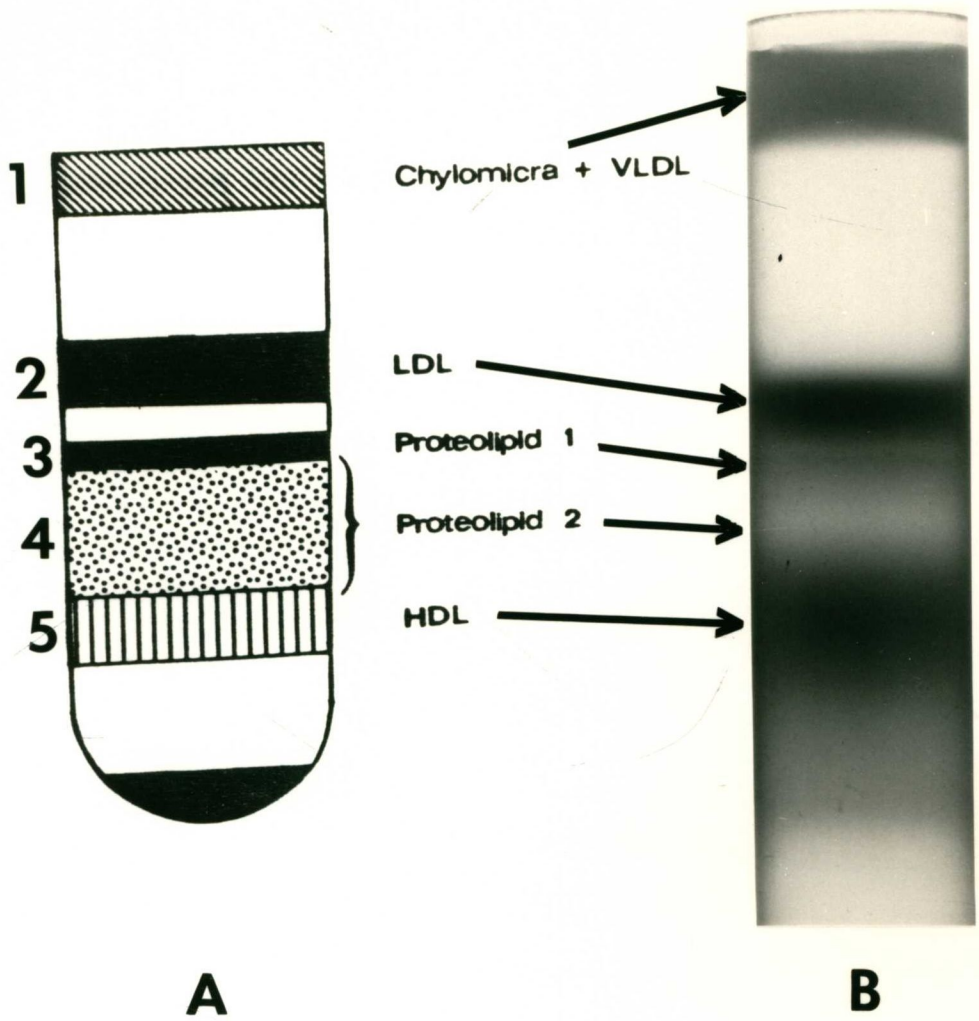

Figure 1. (A) A schematic representation of the location of the various plasma lipoprotein and proteolipid complexes when the total lipoprotein of a patient with malignant disease is fractionated on a KBr gradient, showing fractions 1 - 5 collected for further analyses. (B) A photograph of the gradient, stained with Sudan black, obtained from the patient 9 months after surgery.

Table 1 Plasma Lipoproteins from a Patient with Operable Ovarian Tumour

A. T_2 Relaxation Values (ms) of Resonances in the 1.30 - 1.35 ppm Region

Post Operative	LDL	Proteolipid 1	Proteolipid 2	HDL
5 Days	111	852	970	154
9 Months	N.M	167	N.D	N.M

B. Total Plasma Lipid (µg/ml plasma)

Post Operative	LDL	Proteolipids (1 + 2)	HDL
5 Days	580	486	1062
9 Months	761	301	1112

N.D = not detected; N.M = not measured.

fractions were observed in gradients from both the 7 and 9 month samples. However, less proteolipid 1 and increased amounts of LDL and HDL were visible compared with the 5 day sample. These visible differences in lipoprotein and proteolipid content have been quantified and are shown in Table 1B. The T_2 relaxation time of proteolipid 1 nine months after surgery was 167 ms (Table 1A). The amount of proteolipid 2 was insufficient for the acquisition of an NMR spectrum.

5.2.3 ^{1}H 1D and 2D COSY NMR Spectroscopy of Proteolipids and Lipoproteins

5 days after surgery: The 1D ^{1}H and 2D COSY NMR spectra of proteolipids 1 and 2 were similar, and the spectrum of proteolipid 2 is shown in Figure 3A. 2D COSY methods allow assignments of resonances

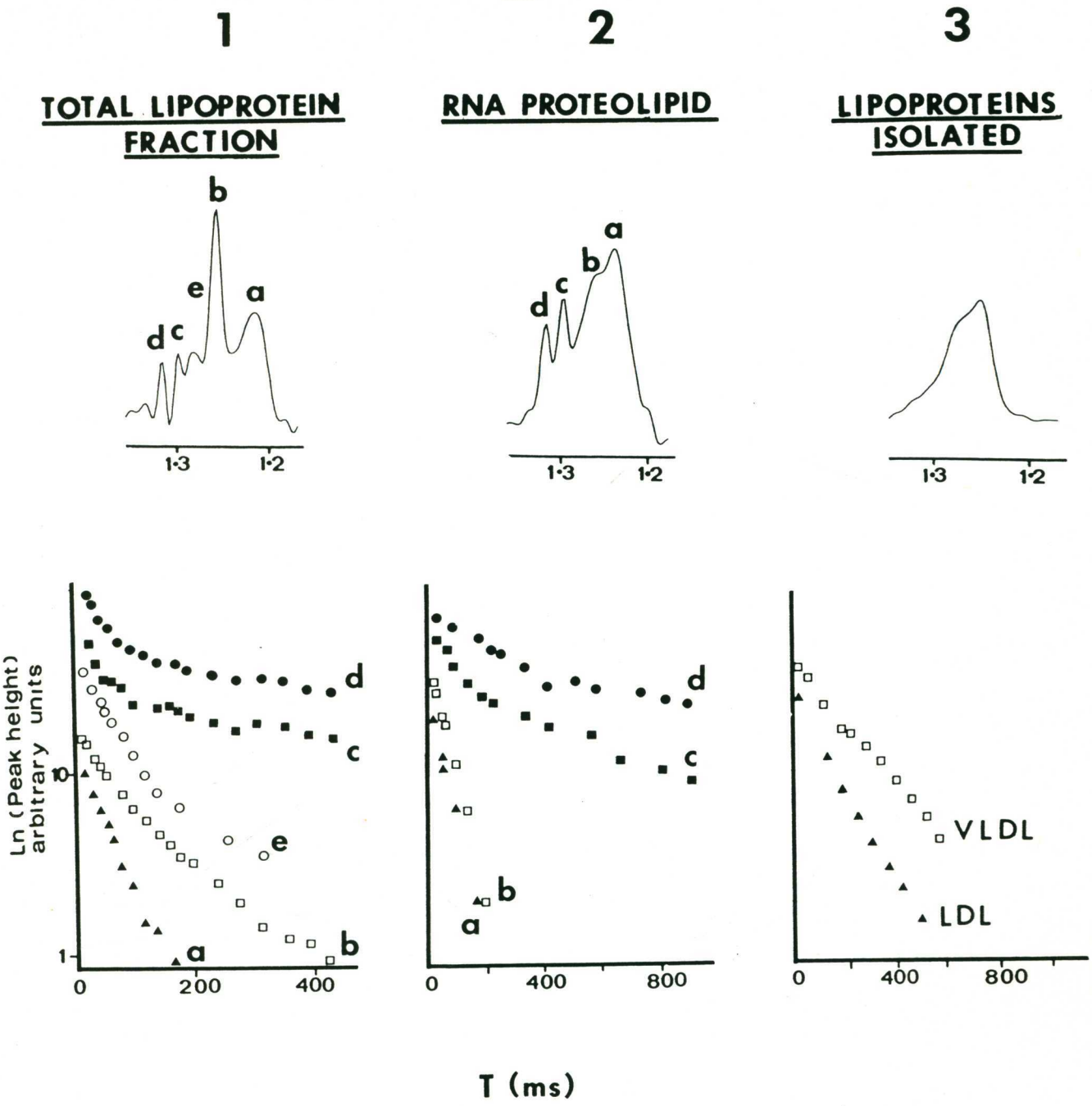

Figure 2. 400 MHz ^{1}H NMR spectra of the methylene region of: (1) total lipoprotein fraction (including proteolipid) isolated from the plasma 5 days after surgery; (2) proteolipid 2; (3) lipoproteins (LDL and VLDL) which were isolated from the same plasma sample. The spectra are resolution enhanced by the Lorentzian-Gaussian method using LB = -12; GB = 0.08. Below the NMR spectra are the results of the CPMG T_2 relaxation experiment (Mountford et al., 1984a). The natural log of each peak height is plotted against the delay between the first pulse and the n'th echo. The T_2 values are calculated using a least squares method where $r^2 \geq 0.98$. The longest T_2 (ms) values of each profile are as follows: (1) a = 84, b = 181, c = 730, d = 660, e = 226; (2) a = 68, b = 63, c = 671, d = 970, (3) VLDL = 199, LDL = 111.

based on spin-spin (scalar) coupling. The off diagonal cross-peaks denoted A-G indicate spin coupling between protons on adjacent atoms. The presence of cross-peaks A-E (as summarised in Structure 2, Chapter 3) and cross-peak G' (at 4.3 ppm) which is unique to triglyceride, indicated the presence of this neutral lipid in proteolipid samples both 5 days and 9 months after surgery (Figures 3A, B). Cross-peak Z denotes scalar coupling between methine and methyl groups on cholesterol. It remains to be determined if this is due to free or esterified cholesterol or both. In contrast to the cell spectrum (Figure 3C), the assignments for which have been documented previously (Chapter 3), cross-peak F was not observed in the spectra of the proteolipid complexes (Figure 3A and B).

The main difference between the spectra obtained from the proteolipid fractions at 5 days and the normal plasma lipoproteins is a cross-peak (Y) connecting resonances at 1.3 and 4.2 ppm. This doublet which is clearly seen in the resolution-enhanced 1D spectra of proteolipid complexes (Figures 4A and B) was not present in the 1D spectra of the VLDL, LDL or HDL fractions from this patient or from normal subjects (Williams et al., 1985). Cross-peak Y indicates covalent linkage between a methine and methyl group in a compound such as fucose rhamnose, threonine or lactate and was evident in the spectrum of cells from the metastatic rat mammary adenocarcinoma line, R13762 (Figure 3C). Lactate was found only in the ultracentrifugal residue at the bottom of the tube in gradients used to isolate proteolipids.

9 months after surgery: Neither the long T_2 relaxation value nor cross-peak Y, connecting resonances at 1.3 and 4.2 ppm was observed in any of the fractions isolated from the KBr gradient, including proteolipid 1 (Figure 3B, Table 1A). Resolution enhancement of the

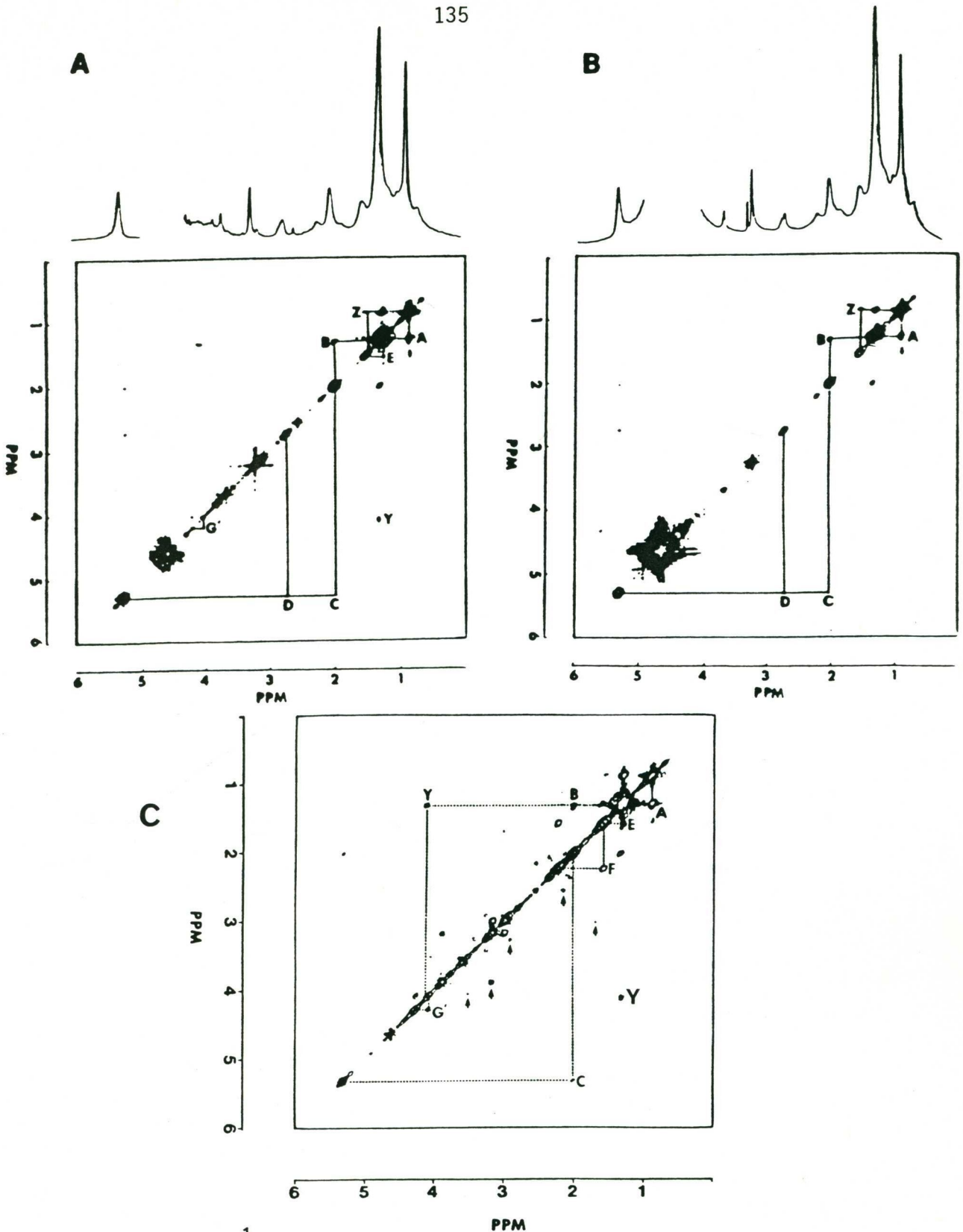

Figure 3. 400 MHz ^{1}H NMR 1D and 2D COSY spectra of proteolipid particles suspended in NaCl/D_2O, and a suspension of cultured cells. Sine-bell and Gaussian (LB = -30, GB = 0.25) window functions were applied in the t_1 and t_2 domains respectively. Cross-peaks are assigned as previously described (Chapter 3), with reference to the labelled Structure 2. (A) Proteolipid 2 isolated from the plasma of the patient 5 days after surgery. (B) Proteolipid 1 isolated 9 months after surgery. (C) A suspension of rat mammary adenocarcinoma R13762 cells (1×10^8) in PBS/D_2O. The arrows indicate cross-peaks due to metabolites.

methylene region of the proteolipid spectrum showed that the resonances at 1.33 and 1.35 which were responsible for the long T_2 relaxation value were no longer present (Figure 4C).

The 2D NMR spectrum of the proteolipid complex obtained at 9 months was much weaker than that obtained from the 5 day proteolipid fractions. Cross-peak G' from the triglyceride backbone was not present nor is cross peak E at this contour level. The latter cross-peak could be observed at a lower contour level.

Attempts were made to identify RNA and the lipid contributions to the four methylene resonances which occurred at 1.33, 1.31, 1.28 and 1.26 ppm in the spectrum of the proteolipid complex (Figures 2 and 4). Ribonuclease (RNase A), an enzyme which hydrolyses ribonucleic acids, had no effect on any of these resonances. Lipoprotein lipase, which degrades triglycerides to monoglycerides plus free fatty acids caused resonances a and b at 1.26 and 1.28 ppm to decrease significantly in intensity. These two resonances had a short T_2 of less than 200 ms.

5.2.4 RNA and DNA Content of Proteolipids and Lipoproteins

5 days after surgery: Using the orcinol method on intact proteolipid, with corrections for glycolipid, 4.1% by weight of the proteolipid was found to consist of RNA. This is considerably lower than the 11 - 14% quoted by Wieczorek et al. (1985). Since the orcinol method only detects ribose, this assay does not establish the presence of intact mRNA. RNA was therefore also extracted by the method reported by Wieczorek and the absorbance at 260 nm recorded. No nucleic acid was found. The presence of a residue, insoluble in aqueous solutions, was noted.

9 months after surgery: Several conventional extraction techniques

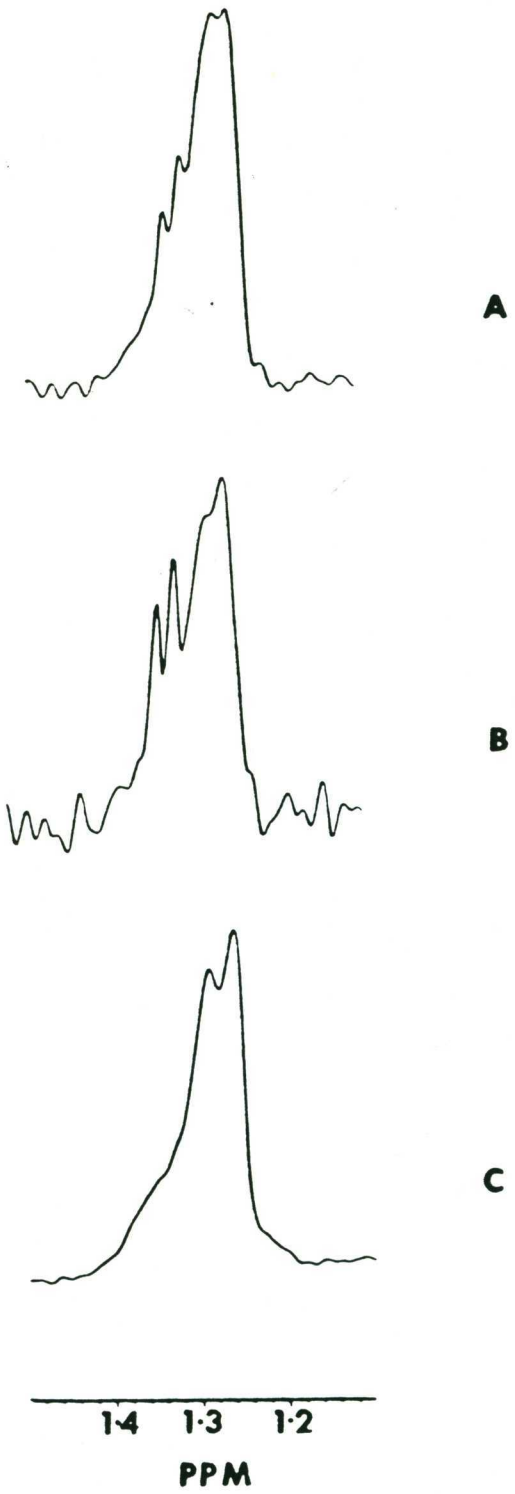

Figure 4. 400 MHz ^{1}H NMR spectra of proteolipids:- the resonances under the composite ($-CH_2-$) peak were resolved by application of the Lorentzian-Gaussian enhancement technique (Mountford et al., 1984a). The methylene region (1.2 - 1.4 ppm) of the resolution enhanced spectrum is plotted on an expanded scale. (A) Proteolipid 1 from plasma 5 days after surgery. (B) Proteolipid 2 from plasma 5 days after surgery. (C) Proteolipid 1 from plasma 9 months after surgery.

(Methods, Chapter 2.8.1) were employed and followed by measurement of the absorbance at 260 nm. No RNA was detected. The method of Wieczorek, to the completion of the oligo-dT cellulose chromatography stage was also unsuccessful.

More specific methods were employed in an effort to detect RNA. The results of oligo-dT primed cDNA synthesis experiments used to detect polyA$^+$ mRNA in the proteolipid and lipoprotein fractions 1 - 5 (Figure 1) isolated from the patient (C) are shown in Figure 5A (Methods, Chapter 2.8.1). Lipoprotein fractions (1 - 5, see Figure 1) from the serum (not plasma) of another cancer patient, P, are also included. By comparison with the blank and the globin standards little or no oligo-dT primed cDNA synthesis was catalysed by any of the gradient fractions from patients C or P and there is no indication of any larger amounts present in the proteolipid fractions C3 and P3. Given that about 5 ng of globin mRNA can readily be detected by this method and that the samples were extracted from 3 - 11 ml of plasma or serum it is possible to establish a mRNA content of less than 20 - 90 ng/ml serum. This is well below the lower limit of 200 ng/ml set for cancer patients by Wieczorek et al. (1985). Similarly low values were obtained in fresh sera from cancer patients and media from cultured cancer cells.

The presence of DNA was sought in extracts of lipoprotein and proteolipid fractions C and P (1 - 5) after digestion with restriction endonucleases. The ability of the fragments to initiate the incorporation of [^{32}P]-dATP into DNA using DNA polymerase 1 (Methods, Chapter 2.8.2) is shown in Figure 5B. Significant incorporation of radioactivity is visible in fractions C2, 4 and 5, but little is seen in the proteolipid fraction C3, or in C1. Some incorporated radioactivity is visible in all bands P1 - 5, but most seems to be in P5 (HDL). The

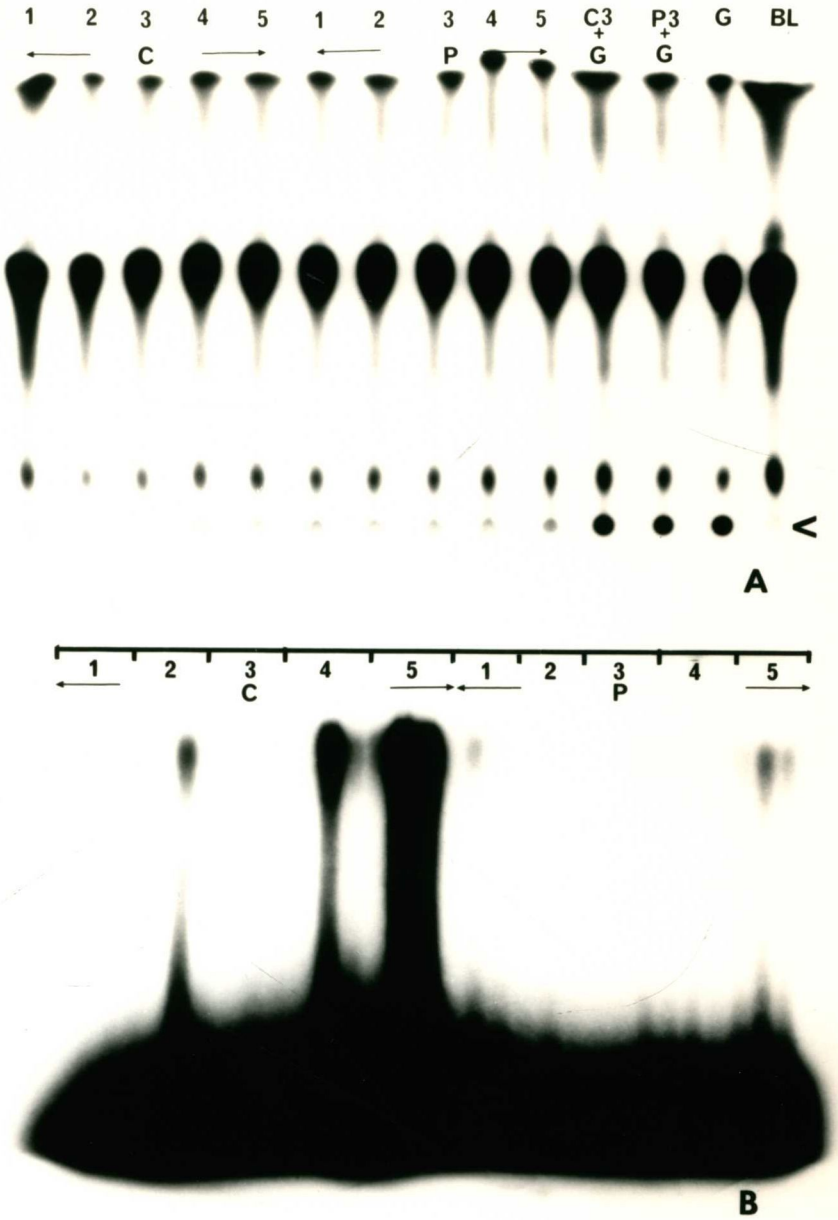

Figure 5. (A) Incorporation of [^{32}P]-dATP into cDNA using RNA extracted by the method of Wieczorek et al. (1985), from lipoprotein fractions isolated by density gradient centrifugation. C1 - 5 are VLDL, LDL, proteolipid 1, proteolipid 2 and HDL samples taken from the ovarian patient 9 months after surgery; P1 - 5 are similar samples taken from another ovarian patient. G = globin mRNA (50 ng), included as a control. BL = blank containing no RNA. The position of the cDNA/RNA hybrids is marked by <. (B) The incorporation of [^{32}P]-dATP into DNA using DNA polymerase and fragments of the same extracts used in (A). Each sample was run as three lanes. From the left, these were undigested, EcoR1 digested and BAMH1 digested.

smearing of the radioactivity indicated on the gel shows that the DNA did not consist of discrete species, but was similar to genomic complex DNA which might originate from cellular debris. DNA was also found in fresh unfractionated serum from cancer patients and in supernatants from cultured cancer cells. A very small amount was also detected in sera from normal volunteers. Accurate quantitation was not possible by this method.

5.2.5 Sizing of Proteolipid Particles by Electron Microscopy

5 days after surgery: From electron micrographs two main particle sizes, 16 - 23 and 25 - 28 nm, were identified in proteolipid 1 (Table 2). In contrast, proteolipid 2 contained equal amounts of 8 - 11 and 16 - 23 nm diameter particles plus a smaller number of the 25 - 28 nm size particle (Table 2).

Both proteolipid samples were treated with RNase and the NMR signals did not change (Section 5.2.3, above). However after RNase treatment, proteolipid 1 lost most of the 25 - 28 nm sized particles and proteolipid 2 lost all the 8 - 11 nm sized particles.

7 months after surgery: The proteolipid 1 band contained only 16 - 23 nm particles. Over 50% of the particles in the proteolipid 2 band contained 16 - 23 nm sized particles (Table 2). The particles not present in the plasma taken 7 months after surgery are those removed by RNase treatment of the day 5 sample.

5.2.6 Apoproteins and Electrophoretic Mobility of Proteolipids

5 days after surgery: Proteolipid 1 contained only apoprotein B whereas proteolipid 2 had equal amounts of both apoproteins A and B. Both proteolipids 1 and 2 had a component of unusual electrophoretic mobility which ran ahead of pre-β (Table 3 and Figure 6).

Table 2 Particle Sizes (nm) of Plasma Lipoprotein Fractions Determined by Electron Microscopy

	% of Total Counted*				
	4 - 7	8 - 11	13 - 5	16 - 23	25 - 28
DAY 5					
LDL			3	84	12
Proteolipid 1 untreated				48	40
+ RNase		1	5	80	9
Proteolipid 2 untreated		41	6	38	13
+ RNase		3	2	84	
HDL	49	37	3	9	
7 MONTHS					
LDL			1	92	5
Proteolipid 1		1	4	91	3
Proteolipid 2		28	5	53	11
HDL			not done		

*At least 200 particles were sized in each sample.

7 months after surgery: Only apoprotein B was present in proteolipid 1 (Table 3), but trace amounts of apoproteins A and B were recorded in the proteolipid 2 fraction. The component with the unusual mobility was also decreased in proteolipid 1 and had disappeared from proteolipid 2.

Table 3 Apoprotein Content of Plasma Lipoproteins (mg protein/ml plasma)

	Apo A_1	Apo B	Unknown (> pre β mobility)
DAY 5			
LDL	< .002	.124	-
Proteolipid 1	.002	.072	+++
Proteolipid 2	.016	.013	+++
HDL	1.648	< .002	-
7 MONTHS			
LDL	< .002	.129	-
Proteolipid 1	< .002	.021	+
Proteolipid 2	< .002	.008	-
HDL	not done		-

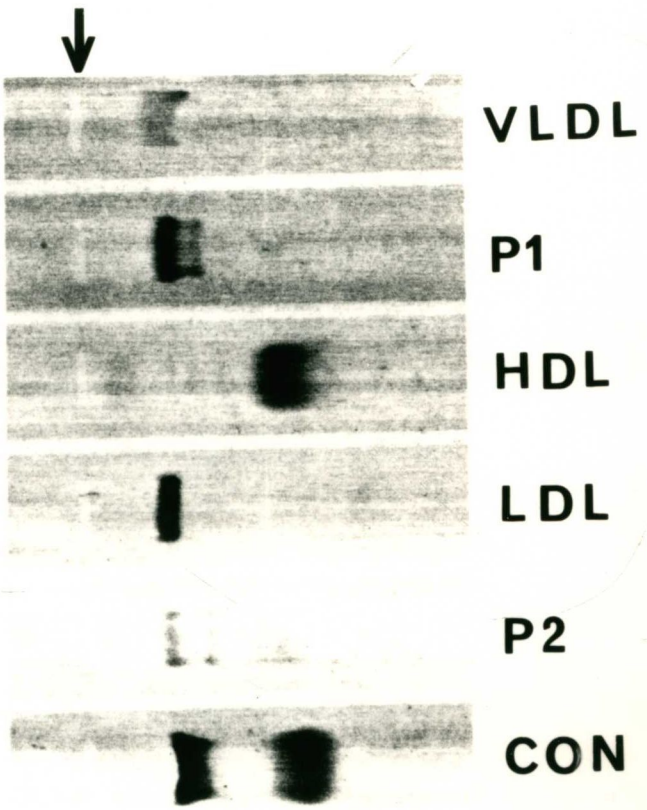

Figure 6. Electrophoresis patterns of lipoproteins isolated by KBr density gradient centrifugation from the plasma of an ovarian cancer patient 5 days after surgery. Samples were run on agarose and stained with oil red O. From the top the samples are VLDL, proteolipid 1 (P1), HDL, LDL, proteolipid 2 (P2) and a normal patient's serum as a control. The arrow indicates the origin.

5.2.7 Chemical Analyses of LDL, HDL and Proteolipids

The lipid and protein content of the proteolipid 1 + 2 complexes and the adjacent LDL and HDL fractions from the plasma of the ovarian tumour patient are shown on Table 4. Small amounts of ether-linked lipids (0.4 - 0.6%) were found in all fractions listed in Table 4.

The proteolipid composition in both 5 day and 9 month specimens resembled that of the patient's LDL samples obtained at the same times, except that the protein content of each of the proteolipid samples was higher than its corresponding LDL fraction (Table 4). Lipoprotein (a) which floats with a density similar to the proteolipids (Kostner, 1983) also resembles normal LDL in composition, except for a higher protein content. This lipoprotein is included for comparative purposes in Table 4. No tests were performed to ascertain its presence in the patient's plasma.

Substantially elevated levels of glycolipid, both neutral and acidic, were identified in all lipoprotein and proteolipid fractions in the day 5 plasma specimen. No glycolipids were present in the proteolipid complexes 9 months after surgery and the lipoproteins had only trace amounts, comparable with normal levels (Table 4). The composition of all plasma fractions changed between the 5 day and 9 month specimens. The cholesteryl ester levels increased to the upper limits of normal whilst the protein levels dropped to below normal (Table 4). Free cholesterol and triglyceride levels remained unchanged and within the normal range throughout the time period. HDL phospholipid was markedly increased after 9 months. The contribution of total lipid from the proteolipid fraction to the plasma lipid decreased after 9 months (Table 1B) with a concomitant increase in LDL and HDL.

Table 4 % Lipid Composition by Weight of Plasma Lipoproteins from a Patient with Borderline Ovarian Tumour Compared with those from Healthy Females

	Protein	Triglyceride	Cholesterol Ester	Cholesterol	Phospholipid	Glycolipid Acidic	Glycolipid Neutral
LDL							
5 Days	17	8	14	7	29	1	24
9 Months	8	7	51	10	24	0.2	0.1
NORMAL[a]	18 - 22	3 - 9	18 - 50	5 - 12	16 - 28	0.2	0.3
Proteolipid 1 + 2							
5 Days[b]	21	7	12	7	27	5	17
9 Months	12	8	42	9	29	< 0.1	< 0.1
Lipoprotein (a)[c]	26	3	32	11	20	0.15	0.25
HDL							
5 Days	47	5	9	2	25	1	10
9 Months	25	6	25	3	42	0.2	0.2
NORMAL[a]	45 - 55	2 - 7	15 - 21	3 - 7	26 - 42	N.F	0.15

[a]Literature values see references Barclay and Skipski, 1975; Herbert et al., 1983; Clarke et al., 1976 and Simons et al., 1970. [b]4% of total weight allocated to RNA as determined by the Orcinol method. [c]See references Kostner, 1983, Albers et al., 1975 and Simons et al., 1970.

N.F = quantitative data not found in literature.

Little change was noted in the fatty acid content of the plasma lipoproteins over the 9 month period. However, significant changes were noted in the fatty acid composition of the combined proteolipid fractions. Increases were recorded for 16:0 (21 to 46%), 18:0 (8 to 22%), 18:1(11) (< 1 to 6%) with corresponding decreases in 18:1(9) (17 to 6%), 18:2(6) (26 to 5%), 18:3 (5 to < 1%) and 20:4 (8 to 3%). The double bond index was subsequently calculated and noted to decrease from 51% to 15%.

5.3 DISCUSSION AND CONCLUSIONS

Magnetic resonance spectroscopy can identify abnormal lipoproteins in the plasma or serum of patients with premalignant and malignant tumours. Two proteolipid complexes, containing a high proportion of particles 8 - 11 nm and 25 - 28 nm in size respectively, were isolated from the plasma of a patient with a borderline ovarian tumour 5 days after surgery. These complexes which generated a characteristically long T_2 relaxation value (> 400 ms) were disrupted by RNase. None of the conventional lipoproteins had a T_2 value in excess of 200 ms. Chemical analysis of the proteolipid complexes showed a 22% glycolipid component. The composition of the isolated proteolipid complexes (shown in Table 4) is similar to that reported by Wieczorek et al. (1985), except that these authors did not document the presence of triglyceride or acidic glycolipids (gangliosides) and found little apoprotein A or B (Table 5). The presence of these proteins (Table 3) might indicate contamination of the proteolipids with adjacent LDL and HDL fractions.

The RNA in the proteolipid complex cannot be isolated and quantified by normal procedures (Wieczorek, personal communication), since the lipid and polypeptide moieties are particularly difficult to

Table 5 Composition of RNA-proteolipid Complex in Serum and in the Media of Cultured Malignant Cell Lines (from Wieczorek et al., 1985).

	% of Total Weight			
	RNA-proteolipid			
Component	In Serum (n = 62)	Secreted by Cells (n = 8)	LDL in Serum	HDL_2 in Serum
Oligopeptide	12.8 - 15.1	15.4 - 18.1		
RNA	11.5 - 11.8	13.9 - 14.3		
Cholesterol	2.3 - 3.9	4.2 - 6.5	8	8.5
Cholesteryl Ester	8.4 - 9.7	0.8 - 1.7	37	18
Phospholipids*	29.9 - 37.4	28.5 - 34.1	22	21.5
Glycosphingolipids+	24.1 - 37.6	28.1 - 32.2	NP	NP
Apolipoprotein A++	> 2			50
Apolipoprotein B++	> 2		25	

NP = not present; *Spingomyelin, phosphatidylcholine and inositol phospholipids; +Ceramide hexasaccharides; ++Detected by the use of rabbit antisera (Behring).

remove. Without adequate purification the RNA is insoluble in aqueous media and is lost. Since the extraction procedures used were probably inadequate, the presence of RNA in the proteolipids isolated from patients with malignant disease has not yet been confirmed.

Nine months after surgical resection of all tumour a visible lipoprotein band, possibly Lp(a), persisted in the plasma but neither the long T_2 relaxation value nor the 8 - 11 or 25 - 28 nm sized particles were present.

The proteolipid particles which remained after 9 months (16 - 23 nm size) contained less of the unusual component with > pre-β mobility and no measurable glycolipid. Collectively these data suggest that it was the 8 - 11 and/or 25 - 28 nm particle sizes which carried the glycolipid and long T_2 value. The disruption of these particles by RNase suggests that RNA was indeed present in these complexes. These data thus support the report of Wieczorek and colleagues that mRNA is associated with

certain proteolipid complexes. However they reported that RNase did not affect the RNA in the intact complex, findings which are not in agreement with the observations above.

Lipoprotein (a) (Lp(a)) has many characteristics which are comparable with proteolipids 1 and 2 (Kostner, 1983; Albers et al., 1975), viz. it floats between LDL and HDL_2 at a density of 1.085 g/ml; it contains mostly apo B as well as a peptide named apo (a) (sometimes called sinking pre-β) and moves with an electrophoretic mobility of pre-β, which is similar to that assigned for proteolipids 1 and 2. Antibody tests for apo (a) have not yet been carried out on proteolipids 1 and 2.

LP(a) is acidic, subject to self-aggregation and ready degradation and is 25 nm in size - slightly larger than conventional LDL. The origin and function of the LP(a) particle are unknown but raised levels constitute a risk factor for myocardial infarction (Kostner, 1983; Albers et al., 1975). No study has linked LP(a) with cancer, however it is reported to adsorb plasma proteins. The above factors suggest that proteolipid 1 might be LP(a) aggregated with a malignancy-associated proteolipid constituting the opalescent band on the KBr gradient at 5 days.

Elevated levels of glycolipid, both neutral and acidic, were identified in lipoprotein and proteolipid fractions in the first plasma specimen (day 5). Neutral glycolipid represented 24 - 38% of serum proteolipid as described by Wieczorek (Table 5) and was also a major component of neoproteolipids W and S (Skipski et al., 1975a). Accumulation of a large variety of fucosylated glycolipids and their sialosylated derivatives (fucogangliosides) has been found in a wide variety of human cancers, particularly those originating from such

endodermal epithelia as the gastrointestinal tract and lung and from mammary epithelium which are the sites of the most common human cancers (reviewed by Hakomori, 1985). Tumour cells shed their surface components (membrane vesicles, glycolipids, glycoproteins and certain enzymes) to a greater extent than normal cells (Yogeeswaran, 1983) and in plasma, glycolipids are usually associated with lipoproteins (van den Bergh and Tager, 1976). The increased level of gangliosides in plasma of tumour-bearing animals (Kloppel et al., 1977; Lengle, 1979; Skipski et al., 1975b) and in cancer patients (Dnistrian et al., 1982; Kloppel et al., 1977; Portoukalian et al., 1978) has been well documented. The functions of glycolipids in growth control and immune recognition have been reviewed in Chapter 1.4.3.

CONCLUSIONS

High resolution ^{1}H NMR studies have shown that the spectrum of a proteolipid complex, isolated from the plasma of a patient with malignant disease, is directly comparable with that obtained from intact cancer cells and solid tumours. The long T_2 relaxation time and cross-peak Y in 2D COSY spectra have been shown previously to be linked with the metastatic potential of cancer cells (Mountford et al.,1984b; Mountford et al., 1986a). The proteolipid contains cholesterol, phospholipid, triglyceride, glycolipids, ether-linked lipids and an apoprotein of unusual electrophoretic mobility. Two different particle sizes are associated with the proteolipid fractions (8 - 11 and 25 - 28 nm). The presence of mRNA has yet to be confirmed. In the one patient studied in detail, the serum proteolipid disappeared within 7 months of removal of the tumour.

CHAPTER SIX

INHIBITION OF METASTATIC POTENTIAL BY FUCOSIDASE: AN NMR STUDY IDENTIFIES FUCOGANGLIOSIDE AS A CELL SURFACE METASTASIS MARKER

6.1 INTRODUCTION

Plasma membrane turnover i.e. the synthesis, incorporation, and release of surface macromolecules ("shedding") from viable cells is of particular importance to tumour cells (Black, 1980). Several steps in cancer metastasis have been identified as involving the plasma membrane (Poste and Nicolson, 1980; Fidler, 1985; Nicolson, 1984; Holmes et al., 1986; Chapter 1.6). Shedding phenomena important to the metastatic process include the release of cell surface components such as proteases, adhesion molecules, tumour associated antigens which block the hosts' immune mechanisms, and factors which promote tumour embolus formation (Black, 1980).

Highly metastatic cells, for example, shed antigenic glycoproteins and gangliosides more readily than those of low metastatic potential (Alexander, 1974; Kim et al., 1975). By the inhibition of antigen-induced lymphoproliferation (Ladisch et al., 1983) such antigens might protect the tumour cells from immune destruction during circulation in the bloodstream. In another example, plasma membrane vesicles shed into the blood of guinea pigs, mice and humans bearing tumours were found to have pro-coagulant activity (Dvorak et al., 1983). The ability to form emboli is typical of cells with the highly metastatic phenotype.

High resolution ^{1}H NMR signals (T_2 relaxation times > 400 ms) indicating metastatic potential have been located in the plasma membrane of R13762 rat mammary adenocarcinoma cells (Mountford et al. 1984b) and human tumours (Mountford et al., 1986b). Cells which were not capable of generating secondary deposits (non-metastatic J clone) had a T_2 of less than 400 ms. High resolution signals with a T_2 relaxation time > 400 ms have been found in the plasma of a patient with malignant disease (Chapter 5). The origin of the NMR resonances has been identified as a

6.2 RESULTS

6.2.1 Removal of the Cell Surface Marker In Vitro by Fucosidase Treatment

The 1D ^{1}H NMR spectrum of the rat mammary adenocarcinoma R13762 cell line is shown in Figure 1. The composite resonance at $\sim$ 1.25 ppm is predominantly due to fatty acyl chain ($-CH_2-$) resonances of neutral lipids. This resonance can be resolved into several components (Mountford et al., 1984a), by Lorentzian-Gaussian deconvolution techniques (Figure 1A) and the T_2 values of these component peaks measured by the CPMG pulse sequence. The long T_2 value (> 400 ms) of the resonance at 1.33 ppm has previously been shown to correlate with metastatic behaviour in the experimental rat model. A contour plot of the 400 MHz 2D COSY spectrum of R13762 metastatic cells is shown in Figure 2. The lipid connectivities have been described previously (Chapter 3).

Cross-peak Y is of particular interest since it connects resonances at 1.3 ppm and 4.2 ppm and appears in the spectra of all metastatic cells and tumours studied so far. It coincides with the resonance at 1.33 ppm observed in the resolution enhanced spectrum (Figure 1A). Cross-peak Y is consistent with a methyl-methine coupling on either fucose, rhamnose, lactate or threonine.

To distinguish between the four molecules possibly responsible for cross-peak Y, the R13762 cells were treated with fucosidase. The treated cells were then washed to remove any free fucose. Two control samples were also studied. The first was untreated in any way and the second was incubated in the absence of the fucosidase for the same time as the enzyme treated cells in order to control for possible loss of the relevant molecule by surface shedding.

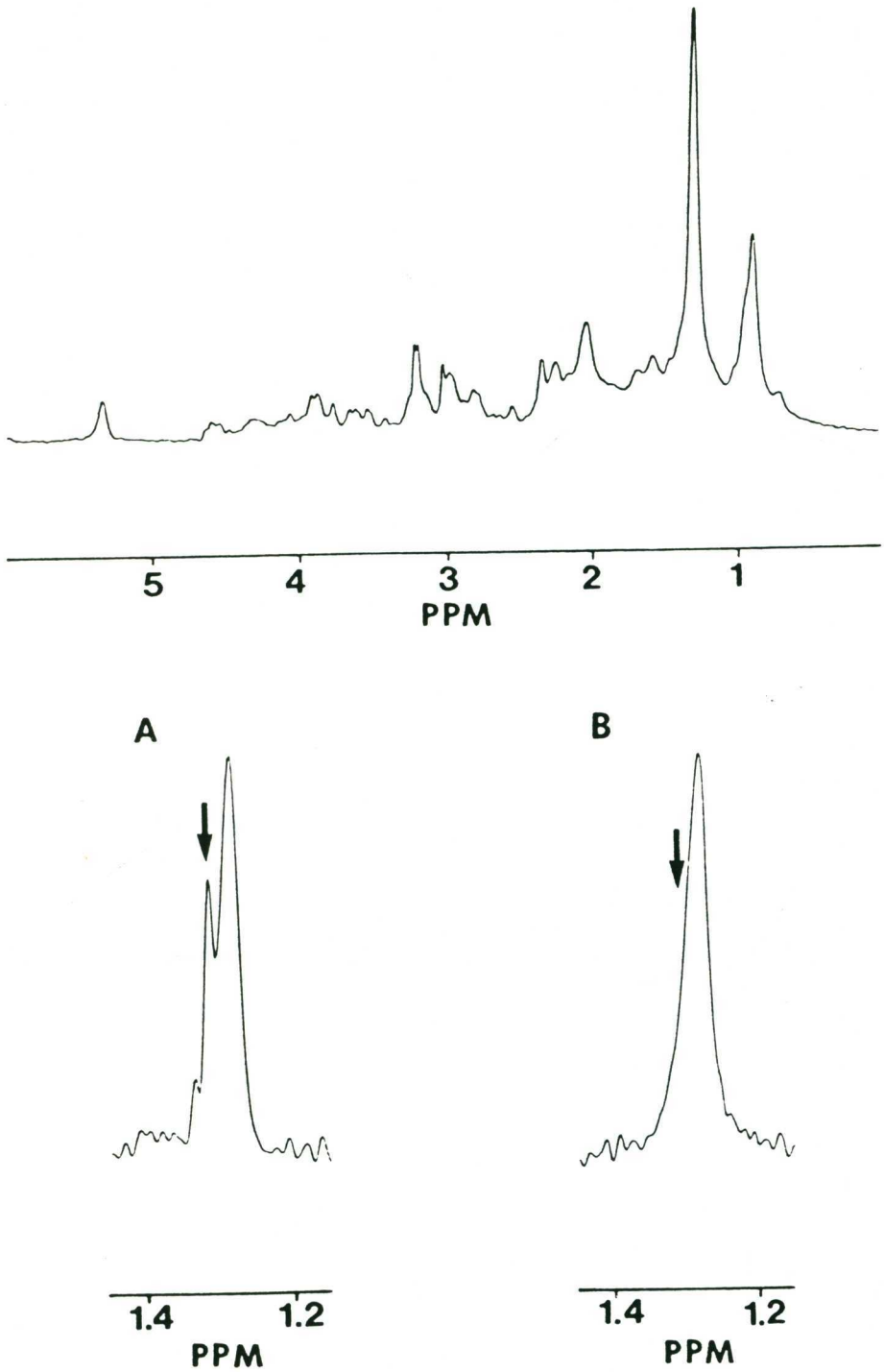

Figure 1. 400 MHz ^{1}H NMR spectra of a suspension of R13762 cells (1×10^{8}) in PBS-D_2O. The resonances under the composite ($-CH_2-$) peak were resolved (Mountford et al., 1984b) by application of the Lorentzian-Gaussian enhancement technique. The methylene region (1.2 - 1.4 ppm) of the resolution enhanced spectrum is plotted on an expanded scale. (A) Untreated cells. (B) Cells treated with fucosidase.

The resonance at 1.33 ppm remained in both control samples (Figure 1A) but was significantly reduced in intensity after fucosidase treatment (Figure 1B). The measured T_2 values for both control samples were > 700 ms, whereas the cells treated with fucosidase gave a mean T_2 of 390 ms (Table 1).

When a vertical slice was taken through the COSY contour plot at 4.2 ppm, cross-peak Y (at 1.3 ppm) was clearly observed in the untreated R13762 cells (Figure 2A). However this cross-peak was not seen in cells after treatment with fucosidase (Figure 2B). Although the enzyme contains minor contamination from different glycosidases, other carbohydrate molecules do not have a resonance in this region of the NMR spectrum. Rhamnose, an isomer of fucose, occurs only in plants (Wiegandt, 1985).

Threonine was eliminated as a possibility because the cross-peak connecting the α and β CH protons at 4.1 and 4.3 ppm respectively was absent. Free lactate in the medium surrounding the cells in the NMR tube has been measured biochemically and found to be the same concentration in both the metastatic R13762 and non-metastatic J clone cells, under the conditions of the NMR experiment (263 $\pm$ 1 $\mu g/10^8$ cells). Despite similar levels of free lactate, the T_2 value for R13762 cells was more than double (760 ms) that measured for J clone cells (325 ms), indicating that lactate is not responsible for the long T_2 of the resonance at 1.33 ppm.

It appears therefore that the nucleus responsible for generating the long T_2 and cross-peak Y is removed by fucosidase treatment.

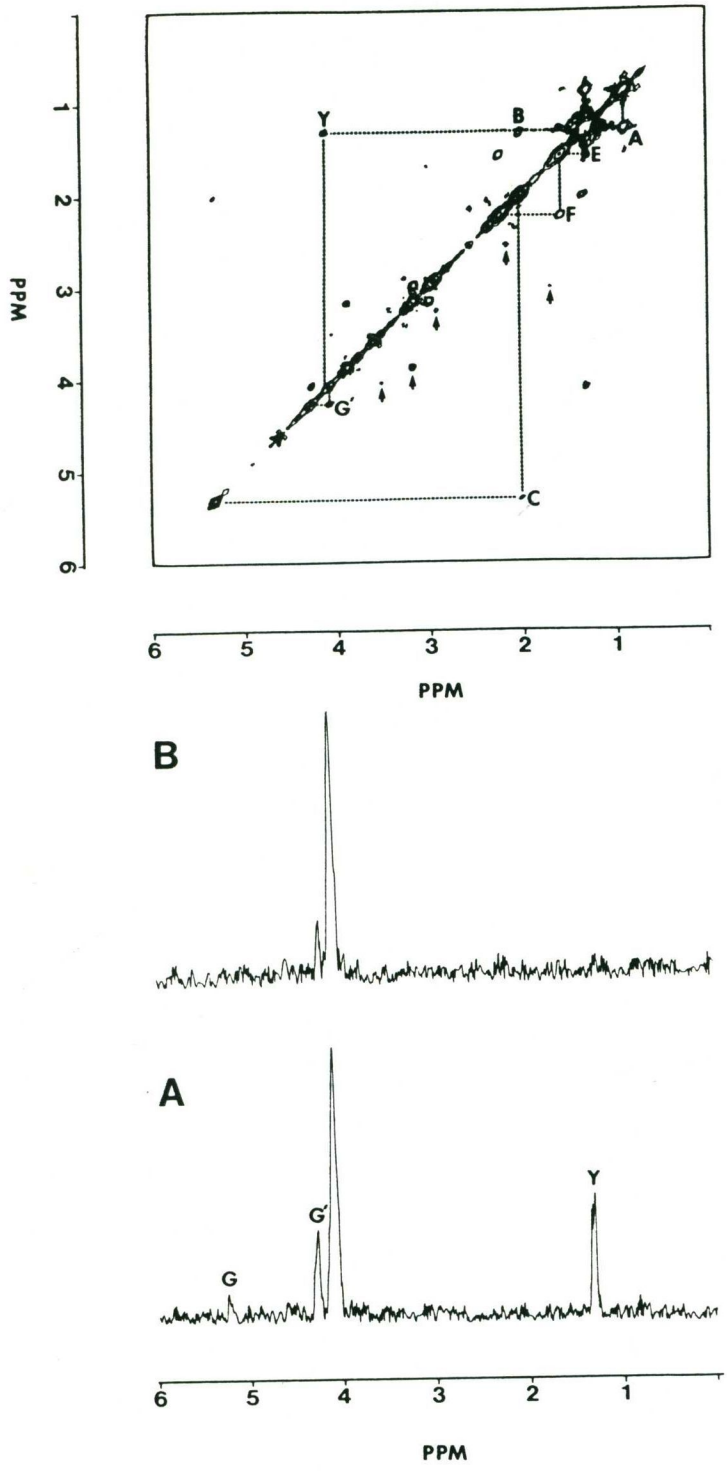

Figure 2. 400 MHz ^{1}H NMR 2D COSY spectrum of a suspension of R13762 cells (1×10^{8}) in PBS-D_2O. Sine-bell and Gaussian (LB = -30, GB = 0.25) window functions were applied in the t_1 and t_2 domains respectively. Cross-peaks are assigned as previously described (Chapter 3). Cross-peaks due to metabolites are marked with arrows. A vertical slice through the COSY contour plot at 4.2 ppm yields the chemical shifts of all the protons coupled to that peak. Crosspeaks G and G' are the vicinal methylene-methine and geminal methylene couplings respectively, in the glycerol portion of the triglyceride molecule. (A) Untreated cells. (B) Cells treated with fucosidase.

6.2.2 Removal of Metastasic Capacity In Vivo by Fucosidase Treatment of Cells Prior to Inoculation

Animals were divided into three groups of ten. Untreated R13762 cells injected into the mammary line of the rats subsequently resulted in the formation of macroscopic lymph node metastases in eight out of ten animals, compared with seven out of ten from the cells incubated in PBS for 30 minutes (Table 1). The sizes of the resulting primary tumours were similar in each case after four weeks (4 - 5 cms).

Cells incubated with fucosidase prior to injection produced smaller primary tumours after four weeks (3 - 4 cm) and only two out of the ten rats had visible lymph node metastases, and these were in a single lymph node. Metastatic deposits in these two animals were 1.0 cm^3 in volume compared to a mean of 63 cm^3 in the two control groups (Table 1).

Table 1 Effect of Fucosidase on the Metastasising Capacity of R13762 Cells

Treatment of Cells	Diameter Primary Tumour (cm)	Metastatic Deposits (cm^3)	Rats with Metastases (10/group)	T_2 (ms)[+]
None	4 - 5	64 ± 6	8	760 ± 48
Incubated in PBS at 37° for 30 min without enzyme	4 - 5	62 ± 6	7	857 ± 80
Incubated in PBS at 37° for 30 with 0.07 units fucosidase	3 - 4	1 ± 0.1	2	390 ± 65

Cells (1×10^7) were injected into the mammary line fat pad of Fischer rats. Animals were sacrificed 4 weeks after the initial injection and examined for macroscopic metastases. The volumes of the metastatic deposits are means ± standard deviations of the total secondary tumour volumes in the animals bearing metastases. The differences in sizes of metastatic deposits between the two control groups and the fucosidase treated group was found to be significant ($P < 0.01$) by the Wilcoxon ranking test. [+]Mean ± S.D. of 3 samples.

Thus the exposure of R13762 cells to fucosidase prior to injection into the fat pad of the mammary line reduced their metastatic but not tumorigenic property *in vivo*. It therefore seemed important to investigate how long these cells took to refucosylate cell surface molecules *in vitro*.

6.2.3 Regeneration of the Cell Surface Marker In Vitro

The R13762 cells which had been treated with fucosidase were cultured in enzyme free medium for a further 24 hour period and the NMR experiments repeated. The long T_2 relaxation value and cross-peak Y in the 2D COSY spectra were again apparent after 24 hours in tissue culture and the doubling time of these cells was the same as the parent cells (approximately 17 hours).

6.2.4 Cellular Uptake of ^{14}C Fucose

The highly metastatic R13762 cells and the non-metastatic J clone cells were incubated with L-[1-^{14}C] fucose. Other workers have previously shown that there is insignificant conversion of labelled fucose into other sugars, amino acids or glycogen in cultured cells or rat tissues (Atkinson and Summers, 1971; Coffey *et al.*, 1964; Kaufman and Ginsberg, 1968; Bosmann *et al.*, 1969; Bekesi and Winzler, 1967). The R13762 cells incorporated almost twice as much label, although the same distribution among the various lipid and protein components of the cell was recorded for both cell lines (Table 2). The majority of the fucose was incorporated into the non-protein fraction (mean of 62%) and a mean of 87% of this was found in the crude ganglioside preparation.

Table 2 Distribution of ^{14}C Fucose in R13762 and J Clone (JC) Cellular Components. Cells were incubated with 0.2 μ Ci L-[1-^{14}C]fucose per 100 ml of medium for 48 h and the uptake of label recorded in the total protein and lipid components of the cells. The incorporation of label was further measured in the neutral and ganglioside subfractions of the lipid components. (dpm = disintegrations per minute). Results are means ± S.E. of duplicates.

	R13762 (Metastatic)	JC (non-metastatic)
Total uptake (dpm per 10^8 cells)	25341 ± 1925	14892 ± 751
% dpm in protein	38.5 ± 0.1	37.0 ± 2.7
% dpm in lipid	61.5 ± 0.1	63.0 ± 2.7
% dpm in subfractions of lipids		
gangliosides	86 ± 6	88 ± 2
other lipids	14 ± 6	12 ± 2

6.2.5 NMR Spectroscopy of a Crude Ganglioside Fraction

The gangliosides isolated from the R13762 cells were found by TLC to be a mixture, but the dominant band had the same Rf as the GM_1 standard. NMR analysis of the total ganglioside fraction showed the presence of a long T_2 ($\sim$ 1000 ms) and the cross-peak Y was present in the 2D COSY spectrum. No long T_2 was found in the organic phase lipids, which would include neutral lipid, neutral glycolipid and phospholipid.

These data indicate that fucogangliosides are key molecules in the metastatic process and have a long T_2 relaxation value comparable with that of the intact cells.

6.3 DISCUSSION AND CONCLUSIONS

The rat R13762 metastatic cell line has a long T_2 relaxation value not observed in the non-metastatic phenotype J clone (Mountford *et al.*, 1984b), whether grown *in vitro* or *in vivo*. Since fucosidase treatment of R13762 cells removes the fucose resonance and the associated long T_2 for one generation of cells only, daughter cells produced after injection of the original 1×10^7 cells into the rat should have the fucose-containing molecule on their surface if cellular fucosylation capacity is normal. This suggests that the state of the cells' surface at the time of injection into the animal is critical in the generation of metastases.

When the cells were grown *in vitro* in medium supplemented with ^{14}C fucose, twice as much ^{14}C fucose was incorporated into the highly metastatic R13762 cells compared to the non-metastatic JC cell line. Subfractionation of the R13762 cellular components located 62% of the label in the lipids, 87% of which was located in the ganglioside fraction. The long T_2 relaxation value which has proven to be an excellent metastatic marker in the rat mammary adenocarcinoma model can therefore be generated by the methyl protons on fucogangliosides.

Fucosyltransferase A and B activity is present in the plasma membranes of malignant cells (Chatterjee and Kim, 1978) and the fucosyltransferase B activity has previously been shown to be 7-fold higher in metastasising tumours (Chatterjee and Kim, 1978), an observation not confirmed by Dennis and Kerbel (1981). The former report is consistent with the significantly higher incorporation of ^{14}C fucose in the R13762 metastasising cells.

The glycolipids of a murine lymphoma line with low and high metastatic variants has been investigated (Murayama *et al.*, 1986).

Differences in the position of their sialic acid residues were revealed, as well as the presence of high quantities of the neutral glycolipids (Gg_3Cer and Gg_4Cer) in the low metastatic variant, Eb. A comparison of rat and murine cell lines with different metastatic potential showed that higher degrees of sialylation could be linked to metastatic potential (Yogeeswaran and Salk, 1981), although this simple correlation was not found in all studies (reviewed by Nicolson, 1982). The wheat germ lectin-resistant variant of MDAY-D2 showed greatly reduced metastatic potential correlated with lack of fucosylation (Dennis and Kerbel, 1981). These observations are consistent with the finding that the metastatic R13762 cell line incorporates more ^{14}C fucose into fucoganglioside than the non-metastatic J clone cell line. Increased ganglioside levels have been found also in plasma membranes of primary and secondary tumours of rats bearing metastatic mammary carcinomas (Skipski et al., 1981).

Migratory inhibition factor (MIF) plays an important role in cellular immune systems by modulating the function of the macrophages. L-fucose has been found to inhibit the MIF present in ascites fluids of ovarian cancer patients (Fahlbusch and Tittel, 1986). Low levels of serum α-L-fucosidase have been associated with epithelial ovarian cancer (Barlow and Bhattacharya, 1983). It can be postulated that there would be a resultant increase in serum fucose and cellular surface fucose (Lynch et al., 1985) which might render the surrounding macrophages unresponsive to MIF. Others have reported that serum fucose levels in patients are a guide to recurrent malignant disease (Wallack et al., 1978).

The role of fucoproteins in the generation of the long T_2 and the metastatic process has yet to be evaluated. Alterations to the cell

surface glycoproteins have been described in metastatic clones of the R13762 NF rat mammary adenocarcinoma line (Steck and Nicolson, 1984). Fucosylated derivatives of the major sialoglycoprotein (ASGP1) on R13762 cell surfaces have now been sequenced (Hull et al. 1984). Cells from DMBA8 and MAT13762 rat mammary lines showed increased binding of fucose-specific lectin to more highly metastatic variants (Ramshaw and Badenoch-Jones, 1985).

Proteolipids have been isolated from the plasma of a patient with malignant disease (Chapter 5) which contained a high percentage of glycolipid, a long T_2 relaxation time and a cross-peak Y when examined by 2D NMR spectroscopy - all observations consistent with the involvement of fucolipids in these complexes. If the fucose is shed in the form of proteolipid complexes from malignant cells, it is possible that the proteolipids might contribute to the immunosuppression of the host (Marcus, 1984; Chapter 1.4.3).

CONCLUSIONS

The NMR data presented in this Chapter indicate that the long T_2 relaxation value (500 - 800 ms) observed in metastatic rat mammary adenocarcinoma cells is removed by treatment with fucosidase. 2D scalar correlated NMR (COSY) spectra of fucosidase-treated cells show that a cross-peak, consistent with scalar coupling between the methyl and methine groups on fucose and usually associated with malignancy and metastatic ability, is absent. Metastases were observed in only two out of ten rats injected subcutaneously with fucosidase-treated cells compared to eight out of ten with untreated cells. NMR studies on isolated cellular lipids identified the long T_2 relaxation value only in the ganglioside fraction. This fraction accounts for 51% of the total ^{14}C labelled fucose incorporated into the cells.

CHAPTER SEVEN

RAT SERUM LIPOPROTEINS ARE MARKERS FOR BOTH MALIGNANCY AND METASTASIS

7.1 INTRODUCTION

Rat mammary adenocarcinoma cells (R13762), and solid tumours grown along the mammary line of Fischer rats by injection of R13762 cells have a high resolution ^1H NMR signal containing resonances with a long T_2 relaxation time (Mountford et al., 1984b). A range of human tumours in patients with metastases was also found to have T_2 values of > 400 ms (Mountford et al., 1986b) as did proteolipid complexes found in the plasma of a cancer patient (Chapter 5). These resonances disappeared after removal of the tumour (Chapter 5) and proteolipids have been detected in the medium from cultured malignant cell lines (Wieczorek et al., 1985). It is likely, therefore, that the source of the molecules generating the long T_2 in serum is the tumour tissue.

The spectrum of fucolipid exhibits resonances responsible for the long T_2 in R13762 cultured cells (Chapter 6). Fucose was also present in one class of the "neoproteolipids" described by Skipski et al. (1975a). These particles were found in large amounts in lipid extracts of various human and animal tumours, including mouse mammary adenocarcinoma. Neoproteolipids found in red blood cell lipids and serum lipoproteins from both humans and experimental animals were quantitatively related to tumour growth (Skipski et al., 1975a).

Plasma hyperlipidaemia is a well documented phenomenon associated with tumour growth in both humans and experimental animals, with reports of increased VLDL lipid and decreased HDL_2 being the most frequent (Barclay and Skipski, 1975). However no detailed study of the effects of tumour progression and metastasis on lipoprotein distribution has been reported.

Experiments investigating the possibility that there are proteolipid complexes in the serum of rats with mammary adenocarcinoma

which are involved in the metastatic process are presented in this Chapter. There are differences in lipoprotein biochemistry between the rat model system and that of humans e.g. rats and mice (especially females) frequently have little or no low-density lipoproteins because of the high efficiency of chylomicron and VLDL remnant clearance from the circulation and the absence of cholesteryl ester exchange proteins (Oschry and Eisenberg, 1982; Barclay and Skipski, 1975). Nevertheless, the cell surface signal for metastasis (the long T_2 relaxation time) has now been identified in the LDL fraction of serum from rats with secondary tumours.

7.2 RESULTS

7.2.1 Alterations to Serum Lipoproteins in Tumour-bearing Rats and Further Changes Associated with Metastasis

When pre-stained serum bulked from ten normal, healthy Fischer 344 female rats was subjected to density gradient centrifugation only three lipoprotein bands were visible:- VLDL (d < 1.063 g/ml), HDL_2 (d 1.125 - 1.083 g/ml) and HDL_3 (d 1.225 - 1.125 g/ml) (Figure 1A; Methods, Chapter 2.10.2). The HDL_2 and HDL_3 layers formed a continuous staining zone above d 1.225 g/ml. There were no visible LDL or HDL_1 bands and the ultracentrifugal residue at the bottom of the tube (d 1.225 g/ml) showed little staining (not included in Figure 1).

Eight out of ten rats injected with the highly metastatic cell line, R13762, had macroscopic axillary node metastases by 4 weeks after inoculation. However, two out of ten of the animals still had primary tumours and no visible metastases. Lipoproteins isolated from the bulked sera of animals with primary tumours only showed the presence of a new band in the LDL region (d 1.083 - 1.063 g/ml) (Figure 1B). The top half

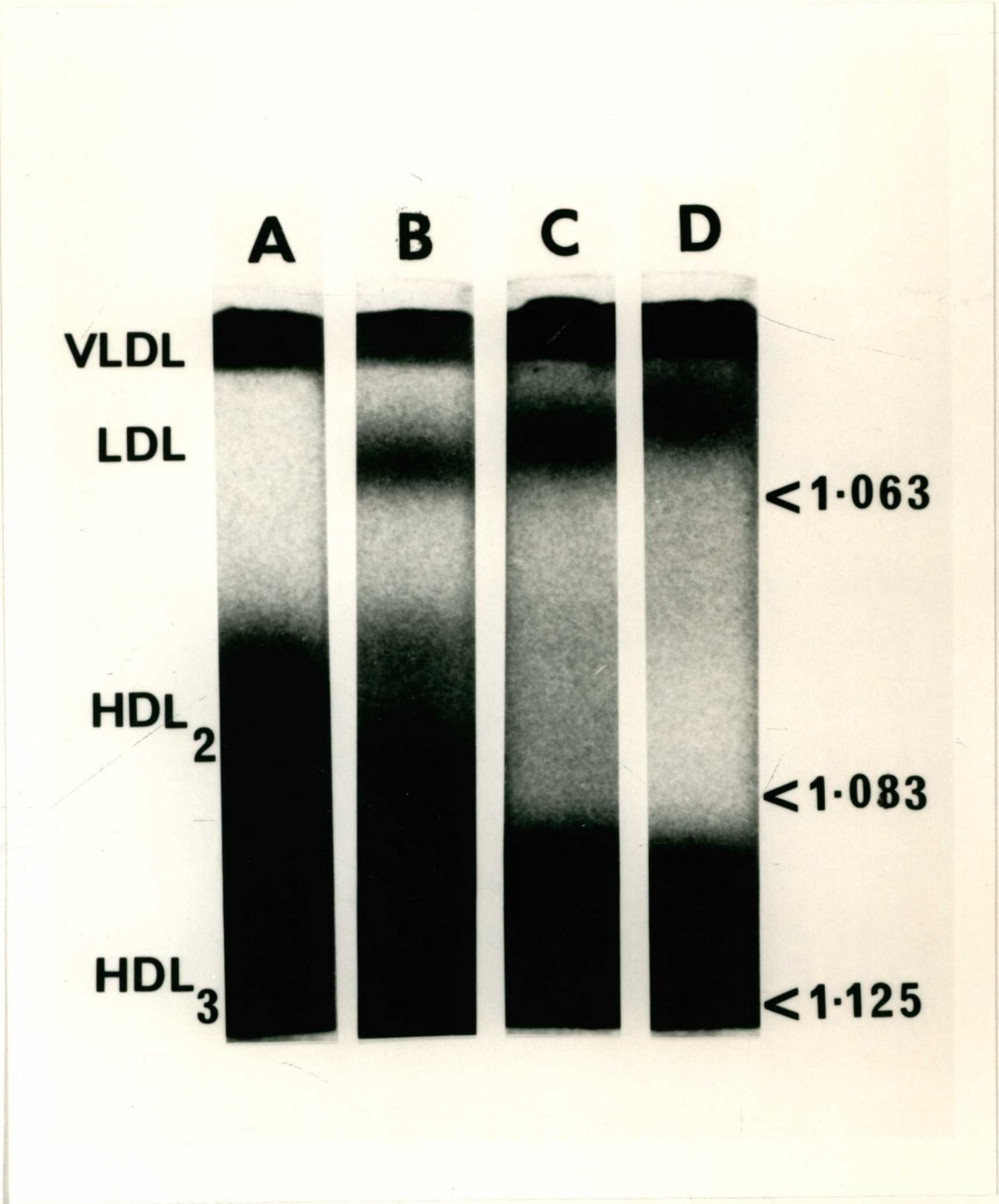

Figure 1: Lipoprotein fractions isolated from rat sera by KBr density gradient centrifugation. From the left the gradients are from (A) control rats; (B) rats injected with R13762 cells, but with primary tumours only; (C) rats injected with R13762 cells and bearing metastases in the lungs and lymph nodes; (D) rats injected with R13762 cells bearing 2.5 times the burden of metastases with some found in the liver in addition to the lymph nodes. The position of the bottom of each step on the density gradients is indicated (<).

of the HDL_2 region was less heavily stained, and the lower half was distinguishable as separate from the HDL_3 band.

Lipoproteins isolated from the bulked sera of rats with metastases contained visibly larger amounts of particles in the LDL region and the entire HDL_2 region became only faintly visible (Figure 1C). In serum fractionated from an animal 5 weeks after injection of cells and showing advanced metastatic disease with liver involvement, 2.5 times the volume of metastatic deposits shown in Table 2 were present. The HDL_2 region had disappeared completely and the LDL band was even more pronounced and floated with a slightly lower density (Figure 1D).

The VLDL band became more heavily stained in a thin film at the top in animals bearing primary tumours only, compared with controls. The entire band became heavily stained in the animals with metastases (Figure 1C and D). When these animals were near to death their serum became of milky appearance and most of the HDL region disappeared. The VLDL band became milky and the LDL band slightly reduced in intensity (not shown in Figure 1). Overnight fasting did not alter the distribution of lipoproteins in sera from either normal or tumour-bearing rats.

7.2.2 Quantitation of the Hyperlipidaemia in Tumour-bearing Rats

Changes to the lipoprotein components were quantified in the sera of rats injected with non-metastatic J clone cells (JC) and R13762 cells rendered non-metastatic by fucosidase treatment (FT). The results were compared with those obtained from rats injected with untreated R13762 cells (MET 1) and bearing macroscopic metastases. As a control for fucosidase treated cells, animals were injected with R13762 cells which were washed and incubated in phosphate buffered saline in the absence of

enzyme. These animals also bore metastases (MET 2).

All rats with primary tumours but no metastases had LDL in their serum whether they were injected with malignant but non-metastatic J clone cells (JC), with fucosidase-treated R13762 cells (FT) or with untreated R13762 cells, where serum was collected prior to the observation of metastases (Figure 1B). The relationship between tumour burden and amount of the various lipoproteins as judged by their total lipid content is quantified in Table 1.

Table 1 The Distribution of Lipid in Rat Lipoproteins According to Tumour Burden

Animals (10 per Treatment)	Diameter of Primary Tumour (cm)	Volume of Secondary Tumours (cm^3)	Total Lipid (µg/ml serum) VLDL	LDL	HDL_2	HDL_3	TOTAL
Control	NIL	NIL	304	112*	1284	1717	3417
JC	2	NIL	405	222	1055	1495	3177
FT	3 - 4	NIL	863	384	406	1404	3057
MET 1	4 - 5	64	2251	690	99	990	4030
MET 2	4 - 5	62	2250	566	426	1266	4778

*No band visible. Control: healthy rats. JC: rats injected with J clone cells. Primary tumours present only, and regressing. FT: rats injected with 13762 cells treated with fucosidase. Primary tumours present only. MET 1: rats injected with 13762 cells; primary and secondary tumours present. MET 2: as for MET 1, but cells were washed in PBS before injection.

In animals injected with the non-metastatic J clone cells (JC) a small burden of regressing primary tumours was evident after four weeks. VLDL lipid was increased by 50%, LDL was doubled and HDL_2 and HDL_3 were decreased to 82% and 87% when compared with the levels in the control rats (Table 1).

Rats injected with fucosidase-treated R13762 cells (FT) to remove their metastatic potential (Chapter 6) carried a greater tumour burden than the JC rats, but no metastases. VLDL and LDL lipids were almost 3-fold higher than in control animals and HDL_2 and HDL_3 lipids were reduced to one third and 82%, respectively, of those found in control animals (Table 1).

Even more dramatic changes were observed in both groups of animals with metastases (MET 1 and MET 2). VLDL and LDL levels were increased an average of 8-fold and 6-fold respectively. HDL_2 and HDL_3 lipids decreased on average to 20% and 66% of those in the controls (Table 1). The total serum lipoprotein lipid was raised (hyperlipidaemia) in MET 1 and MET 2 rats.

The primary tumour size ranges and mean volumes of secondary tumours produced are shown in Table 1. Ten rats were used for each treatment. Overnight fasting did not alter the distribution of lipoproteins in sera from either normal or tumour-bearing rats.

7.2.3 Size Distribution of Particles in Lipoprotein Fractions

The sizes of the lipoprotein particles in each fraction on the KBr gradients were measured from electron micrographs and the variations were associated with tumour burden. The particle diameters measured in the LDL, HDL_2 and HDL_3 fractions are plotted as a function of percentage distribution in Figure 2. The ranges of sizings used for reporting the results approximate the ranges for rat and mouse lipoproteins in the literature (e.g. Camus *et al.*, 1983; Oschry and Eisenberg, 1982). Insufficient numbers of particles were found in the gap region of gradients from normal animals (corresponding to LDL in tumour-bearing animals) for accurate sizing.

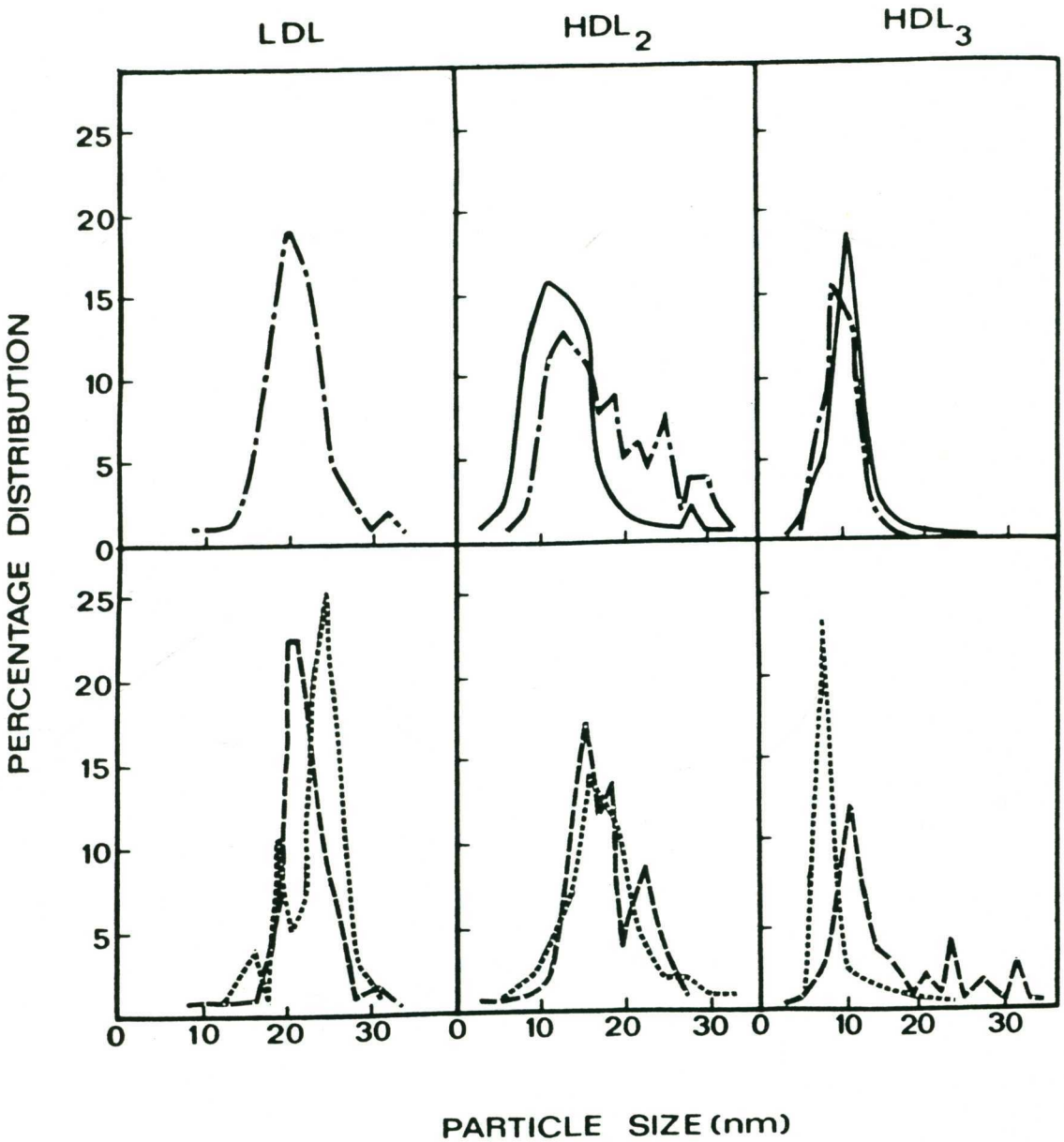

Figure 2. Size Distribution of Lipoprotein Particles Isolated by Density Gradient Centrifugation. Lipoprotein fractions were dialysed against 0.9% NaCl for 2 h at 4°C. The lipoprotein particles were examined by negative staining electron microscopy.

Control ——————— ; J Clone — - — - — ;

Fucosidase Treated — — — — ; R13762 with Metastases ·····.

The VLDL fraction from all treatments contained a vast range of particle sizes with no real maximum in the percentage distribution of any particular size. Most particles fell within the expected range for VLDL (> 28 nm). Most LDL particles also fell within the expected range for LDL (18 - 27 nm). However examination of the size which occurred most frequently revealed a change with the appearance of visible metastases. In animals with primary tumours only (JC and FT) the maximum in the percentage distribution (modal value) occurred at 20 - 22 nm (Figure 2). This shifted to a larger size (24 - 26 nm) in the LDL from animals with metastases (Figure 2).

The HDL_2 fraction for the control rats lay mostly in the range expected for HDL_1 and HDL_2 (9 - 17 nm). In animals with small primary tumours (JC) there was an increase in larger HDL_2 particles (18 - 27 nm) and an increase in modal value from 11 nm in the control to 13 nm (Figure 2). With higher tumour burden (FT) and metastasis, however, there was a pronounced shift to larger particle sizes with modal value of 16 nm.

The HDL_3 fractions of the control rats and those with primary tumours only (JC and FT) had a modal value of 9 - 11 nm (Figure 2). In metastatic samples there was a marked shift to a smaller particle size (8 - 9 nm), which resembles that of chylomicron remnants (Redgrave, 1970).

7.2.4 Electrophoresis of Rat Lipoproteins

Changes in apoprotein composition were not evaluated but differences in electrophoretic mobility on agarose gels were observed in fractions from rats with metastases. Lipoprotein fractions isolated from rats bearing primary tumours only (JC) differed from those of control

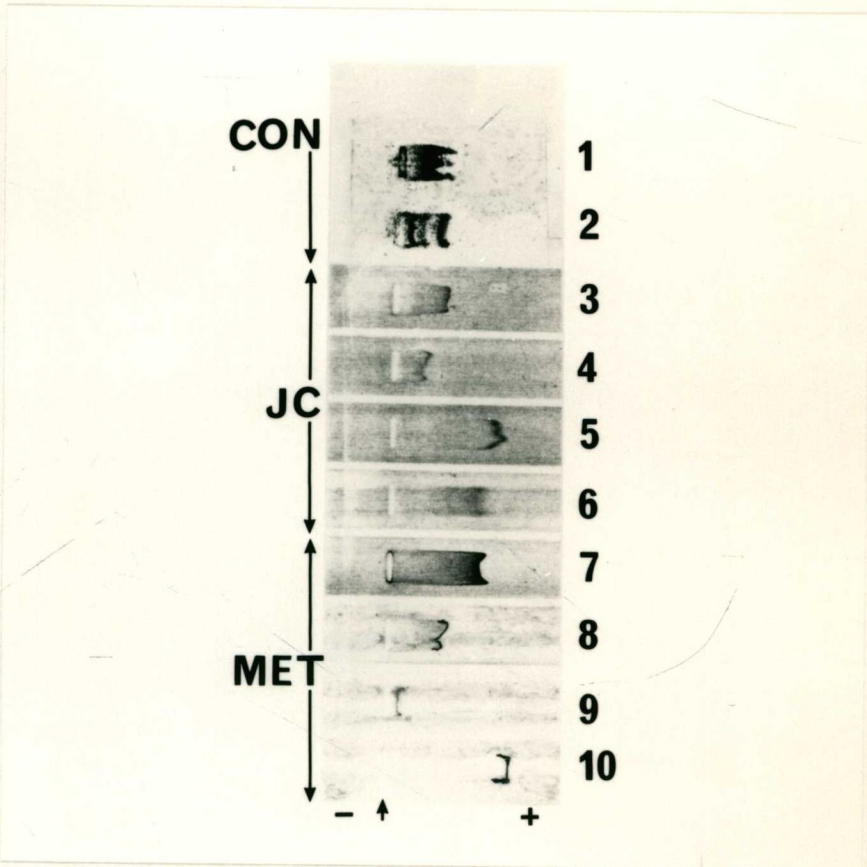

Figure 3. Electrophoresis of Rat Serum Lipoproteins Isolated by Density Gradient Centrifugation. The samples from the top are:- (1) VLDL and (2) the area in the region of LDL from normal rats. Tracks 3 - 6 are VLDL, LDL, HDL_2 and HDL_3 from rats injected with non-metastatic J clone (JC) cells and tracks 7 - 10 are HDL_3, VLDL, LDL and HDL_2 from rats injected with metastatic R13762 cells (MET 1). The arrow indicates the origin.

rats only in the mobility of the LDL fraction (Figure 3). The differences are not quantitative as a very heavy load was applied to the gel to show the presence of triple bands in the control LDL area, probably representing trace amounts of a mixture of VLDL, LDL and chylomicra (Chalvardjian, 1971). Only one band could be detected in the J clone LDL fraction running in the β position, which was typical of LDL (Koga et al., 1969).

The LDL isolated from animals with metastases also migrated as a single band but was much less mobile than the JC LDL (Figure 3). It barely moved from the origin, which could reflect the larger particle size (Figure 2), or a lesser particle charge. HDL_2 from animals with metastases was more mobile than that from JC or control animals despite the larger particle size (Figure 2).

7.2.5 NMR Identifies the Presence of a Metastasis Marker similar to that on Tumour Cell Surfaces in the Serum LDL Fraction from Rats Bearing Metastases

The methylene resonance of cancer cells and serum proteolipids can be resolved into several components by Lorentzian-Gaussian deconvolution techniques (Chapters 5 and 6). LDL isolated from rats with metastases had a similarly composite resonance which could be resolved into three main components (Figure 4A). In the same animals the VLDL fraction could be resolved into two components (Figure 4B). The resonances in HDL fractions from animals with metastases could not be further resolved. All lipoproteins isolated from normal rats or from animals with primary tumours only (JC, FT) produced a single resonance around 1.25 ppm (Figure 4C). When the LDL sample in Figure 4A was treated with fucosidase, and redialysed before NMR spectroscopy to remove free

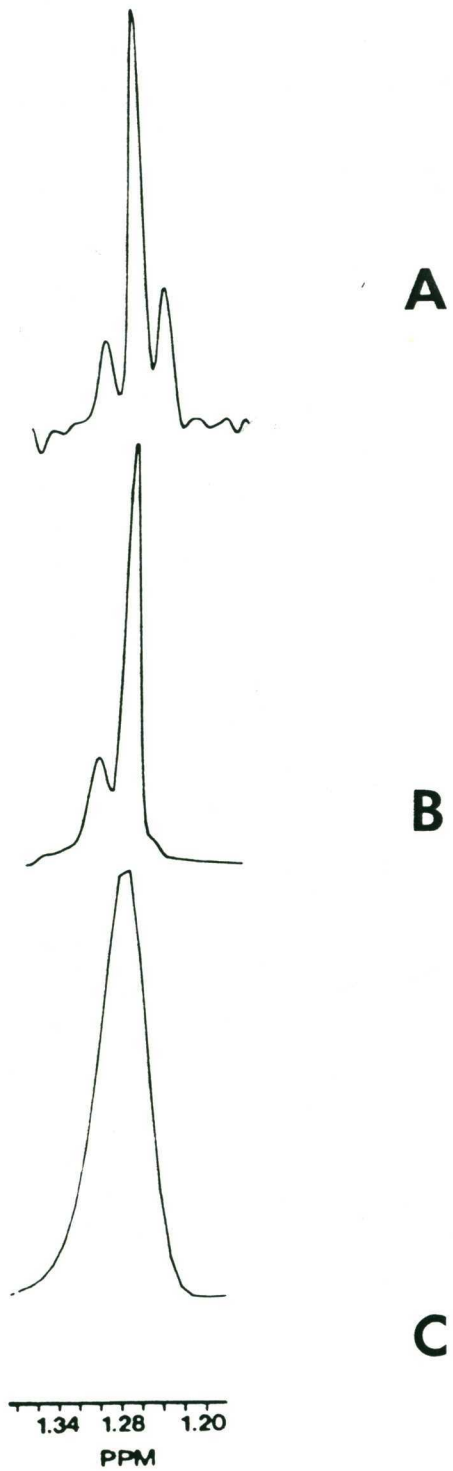

Figure 4. 400 MHz ^{1}H NMR Spectra of Lipoproteins Dialysed against NaCl - D_2O for 2 h. Resolution enhanced spectra were plotted over the methylene region (1.2 - 1.4 ppm) on an expanded scale for (A) LDL from rats injected with metastatic R13762 cells; (B) VLDL from rats injected with metastatic R13762 cells; (C) LDL from rats injected with non-metastatic J clone cells (JC).

fucose, the spectrum changed to resemble that in Figure 4B, with only two components resolved.

The T_2 relaxation times of the resonances around 1.33 ppm for lipoproteins isolated from normal, primary tumour-bearing and metastasis-bearing rats are shown in Table 2. Only the LDL fraction from rats with metastases had a T_2 of > 400 ms, which is the same as that from metastatic R13762 cells (Mountford et al., 1984b). When this fraction was treated with fucosidase, as above, the T_2 decreased from 522 - 96 ms.

Table 2 T_2 Values (ms) for Lipoproteins Isolated from Rats with Differing Tumour Burdens

Treatment	VLDL	LDL	HDL_2	HDL_3
Control	288	-*	193	170
JC	265	237	165	195
FT	278	272	251	118
MET 1	294	522	250	242
MET 2	270	502	268	250

*Insufficient sample to give ^1H NMR signal. The treatments and tumour burdens of the rats are the same as in Table 1.

Two dimensional COSY experiments on the isolated lipoproteins resulted in 2D spectra dominated by lipid connectivities from triglyceride i.e. A,B,C,E,F,G,G' (Chapter 3; Figure 5). Cross-peak Y, connecting resonances at 1.3 and 4.2 ppm, appeared in the spectra of all malignant and metastatic cells and tumours studied thus far, and was removed by treatment with trypsin (Holmes et al., 1986) and α-L-fucosidase (Chapter 6). This cross-peak was present in the 2D spectrum of LDL in Figure 5, but was very difficult to distinguish from the background noise.

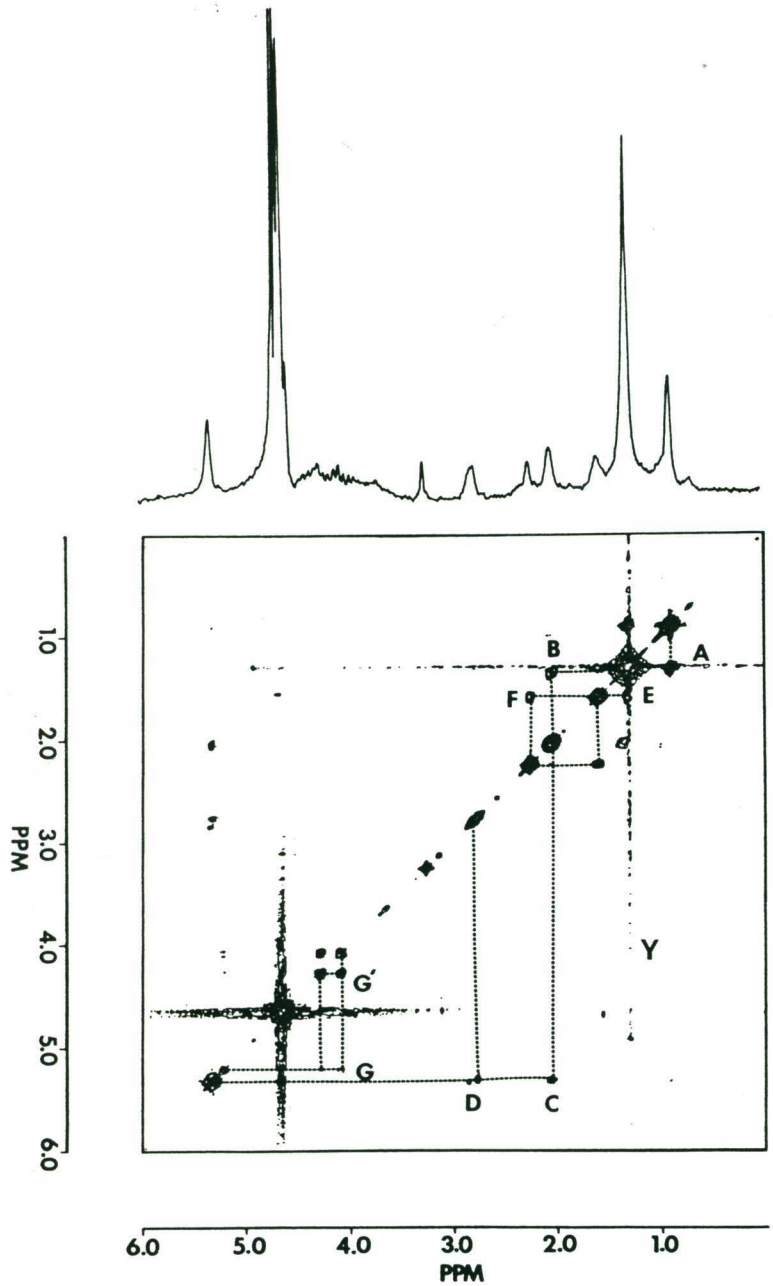

Figure 5. 1D and Symmetrised COSY Spectra of LDL in NaCl - D_2O from Rats Injected with Metastatic R13762 Cells (MET 1). A Sine-bell window function was applied in both the t_1 and t_2 domains. Lipid acyl chain and glycerol backbone connectivities are indicated A-G' (see Chapter 3 for structure to indicate connectivities).

7.2.6 NMR Identifies the Serum Metastasis Marker in a Crude Ganglioside Fraction Isolated from LDL

A crude ganglioside preparation was made from the LDL of rats with metastases derived from injected R13762 cells. Two main resonances could be resolved in the methylene region at 1.27 and 1.24 ppm (Figure 6A and B). The longest T_2 value was 600 ms. After treatment with fucosidase the resonance at 1.27 ppm was greatly diminished and the T_2 was now 190 ms (Figure 6C). The resonance giving rise to the long T_2 in R13762 cells has been identified as derived from fucose and has been isolated from a crude ganglioside fraction extracted from these cells (Chapter 6).

7.2.7 Lipoprotein Compositional Changes in Relation to Tumour Burden

With the exception of VLDL and the ultracentrifugal residue, the lipid and protein composition of the individual lipoproteins was found to vary substantially with increasing tumour burden. Although no lipoprotein bands were visible by staining in the LDL region from control rats, this area of the gradient was collected and analysed.

A decrease in total protein content compared with the control is apparent in the HDL and LDL fractions from rats with even the smallest tumour burden (JC) (Table 3). This was most evident in the HDL_2 fraction, where a further decrease occurred with metastasis.

Triglyceride levels in the HDL fractions were altered little with the presence of small primary tumours (JC) but were elevated substantially with increasing tumour burden in FT, MET 1 and MET 2 samples. Again the most obvious increase was with the HDL_2 fraction in animals bearing metastases (x 13.5 of the control, Table 3). The LDL fraction showed a progressive increment in triglyceride content from JC

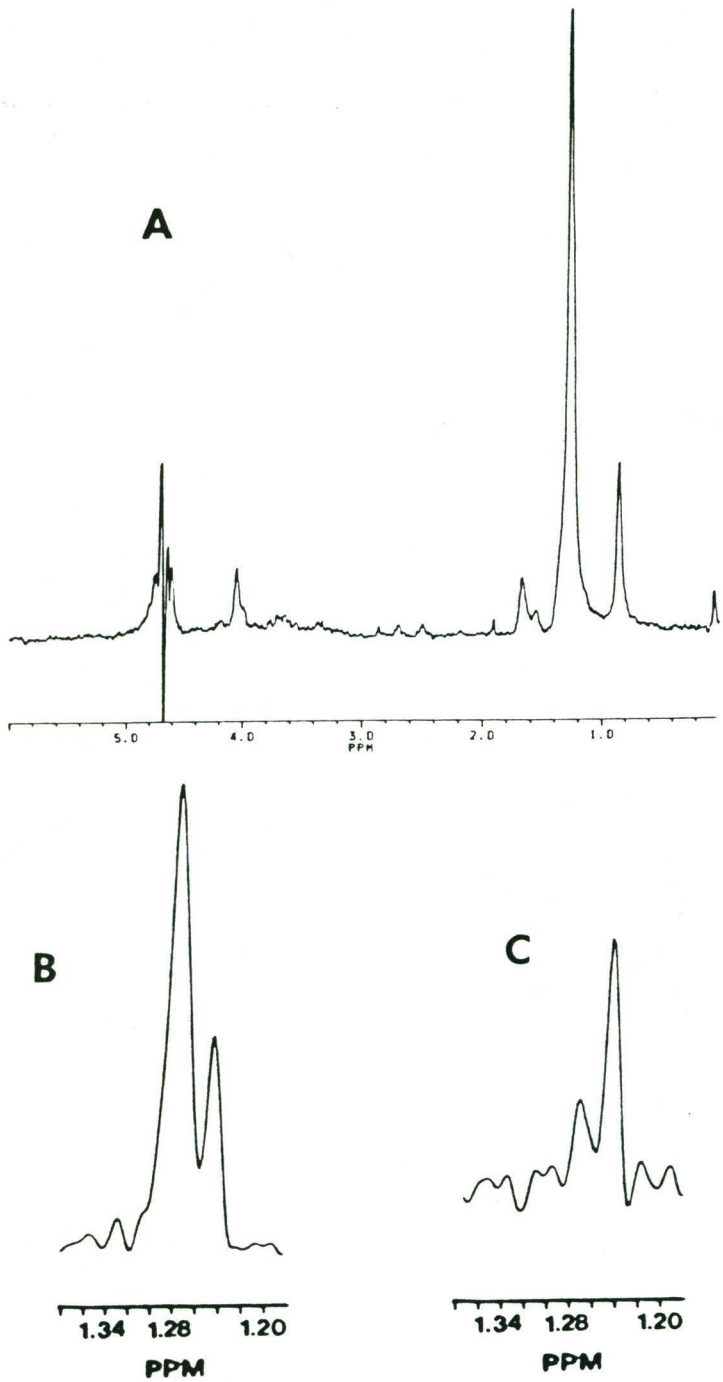

Figure 6. 400 MHz ^{1}H NMR Spectra of:- (A) a crude ganglioside fraction (in D_2O) isolated from the LDL of rats injected with metastatic R13762 cells (MET 1) and resolution enhanced on an expanded scale in (B). The resolution enhanced spectrum of the same ganglioside sample after fucosidase treatment is shown in (C).

to MET 2 and MET 1 where the level reached twice that of the control.

Increased triglyceride tended to be compensated by decreased cholesteryl ester in all LDL fractions from animals with tumours, but only in the HDL fractions from animals with metastases. In these animals the cholesteryl ester was reduced to an average of 25% and 89% of the controls in the HDL_2 and HDL_3 fractions respectively. Some reduction in cholesteryl ester was also noted in the VLDL fractions from all tumour-bearing animals.

Free cholesterol levels were lower than the control in the HDL fractions of animals with metastases (Table 3), but higher in the LDL fractions of all animals with tumours. Phospholipids showed no uniform changes in the HDL_3 and LDL fractions but decreased about 3.5-fold in the HDL_2 fraction of animals with metastases. Some increase in phospholipid occurred in the VLDL from all animals with tumours.

The most curious feature of the HDL_2 fractions (Table 3) was the marked change in composition with metastasis from HDL_1-like (Oschry and Eisenberg, 1982) to VLDL-like particles with very high triglyceride and very low protein and cholesteryl ester levels. These particles were smaller than VLDL (Figure 2) but must contain some unusual molecular packing or some other component, such as glycolipid to make them float at HDL_2 density.

7.2.8 Fatty Acid Profiles of LDL Fractions

The fatty acid composition of lipoproteins isolated from rats with the differing tumour burdens described in Table 2 was examined to ascertain if any particular fatty acid was associated with the long T_2 value (Table 2). Considering their different compositions (Table 3), the

Table 3 Percentage Composition of Rat Lipoproteins with Increasing Tumour Burden

	Protein	TG	CE	CHOL	PL
VLDL					
Control	2	82	8	2	5
JC	3	81	4	4	8
FT	4	80	3	4	9
MET 1	6	78	5	3	9
MET 2	2	84	2	3	9
LDL					
Control	13	37	41	2	7
JC	< 0.1	53	27	7	13
FT	2	65	15	6	12
MET 1	4	75	12	3	7
MET 2	5	69	12	4	11
HDL_2					
Control	31	6	30	7	26
JC	15	8	33	9	34
FT	13	22	31	8	26
MET 1	3	82	6	2	7
MET 2	< 0.1	80	9	3	8
HDL_3					
Control	48	5	19	4	24
JC	27	5	29	4	35
FT	22	31	19	3	25
MET 1	24	31	17	2	25
MET 2	29	32	17	1	21
RESIDUE					
Control	94	5	< 1	< 1	1
JC	98	1	< 1	< 1	< 1
FT	80	19	< 1	< 1	1
MET 1	96	3	< 1	< 1	< 1
MET 2	73	27	< 1	< 1	< 1

TG = triglyceride; CE = cholesteryl ester; CHOL = free cholesterol; PL = phospholipid. The treatments listed are the same as in the legend to Table 1.

fatty acid composition of all LDL fractions was remarkably similar with the dominant species being 16:0, 18:1(9), 18:0, 18:2, 20:4 and 22:6 (Table 4). In LDL from control rats the level of 18:2(6) was reduced to 73% of the average for tumour-bearing rats in favour of the appearance of small amounts of 12:0, 14:0, 15:0, 20:3 and 22:3. The content of 20:4 was highest in the JC rats.

Table 4 The Fatty Acid Composition (%) of LDL Isolated from Normal and Tumour-bearing Rats

	Treatment				
Fatty Acid	Control	JC	FT	MET1	MET 2
12:0	1.9	< 1	< 1	< 1	-
14:0	2.9	< 1	< 1	< 1	< 1
15:0	1.5	< 1	< 1	< 1	< 1
16:0	24.7	20.4	22.1	22.8	23.6
16:1	1.8	1.2	1.1	< 1	< 1
18:1(9)	16.3	16.1	18.7	20.1	17.9
18:1(11)	2.9	2.3	2.4	3.2	2.2
18:0	11.4	9.7	8.9	10.6	9.0
18:2(6)	15.9	19.7	23.2	22.1	21.4
18:3(6,12)	-	-	-	< 1	1.5
20:3(11,17)	1.9	< 1	< 1	< 1	-
20:4 + 20:3 (8,14)	11.9	20.2	12.4	9.1	11.4
20:3(8,14)					
22:3	1.4	< 1	< 1	< 1	< 1
22:6	4.8	4.8	6.5	4.7	9.7

The treatments of the rats and their tumour burdens are described in Table 1.

7.3 DISCUSSIONS AND CONCLUSIONS

Some surface molecules on R13762 cells are characterised by a long T_2 relaxation time. When Fischer 344 rats were injected with these cells, metastases formed, and the serum LDL fraction isolated from the animals contained the same resonances which were responsible for the long T_2 value in the injected cells. The presence of cross-peak Y, as detected by 2D NMR experiments, and which connects the resonances believed to be responsible for generating the long T_2 value (Holmes *et al.*, 1986) could not be ascertained unequivocally. Nevertheless the occurrence of a fucosidase-sensitive resonance with a T_2 of 600 ms in a ganglioside fraction derived from the LDL of R13762-injected rats suggests that fucolipid might be responsible for the signal in serum as it is on the cell surface (Chapter 6). The differences in chemical shift between the resonance responsible in the serum LDL (1.33 ppm) and the isolated ganglioside fraction (1.27 ppm) might be explained by environmental differences.

The lipid and protein composition of the individual lipoproteins was found to vary substantially with increasing tumour burden. This is in contrast to the hepatoma 7288C in rats when no compositional changes were recorded (Clarke and Crain, 1986). The hepatomas grew *in situ* and did not form metastases.

The LDL fraction of rats with metastases is peculiar in that the triglyceride to cholesteryl ester ratio is higher than in the control rats or those injected with the non-metastatic J clone or fucosidase-treated cells (Table 3). There was no sign of particles with HDL_1 mobility in the LDL fraction (α1, Chapman, 1980). The decreased cholesteryl ester with secondary tumour burden is consistent with changes in the cholesteryl ester levels in the human proteolipid

monitored in the serum of a patient after surgical resection of a borderline ovarian tumour (Chapter 5).

Further comparisons can be made between the LDL and HDL fractions from rats with metastases and the proteolipid 1 and 2 fractions isolated from the plasma of an ovarian tumour patient (Chapter 5). Both proteolipids 1 and 2 contained glycolipid and showed a long T_2 relaxation time. Proteolipid 1 contained a high proportion of a particle (25 - 28 nm) larger than conventional LDL as did the rat LDL fraction. The proteolipid 2 ran closer to HDL on the density gradient and had a high proportion of very small particles (8 - 11 nm) as in the rat HDL_3 fraction. However no long T_2 was noted in the rat HDL_3 fraction.

Attempts by conventional techniques to find RNA in the lipoproteins isolated from rat sera were unsuccessful (Materials and Methods, Chapter 2.8). However, as in Chapter 5, this result cannot be regarded as a true negative, since conventional techniques cannot be used to isolate proteolipid-bound RNA (Wieczorek, personal communication). Both human proteolipids (Chapter 5) and LDL from rats with metastases showed electrophoretic abnormalities when compared with normal LDL.

In rat mammary adenocarcinoma the increase of VLDL and LDL at the expense of HDL_2 and HDL_3 was proportional to the tumour burden with marked changes following metastasis. Increases in low density lipoprotein levels have also been reported in in mice bearing the GRSL ascites tumour (Damen et al., 1984), to a minor extent in Morris hepatoma-bearing rats (Clarke and Crain, 1986), and in some human cancer patients (Barclay and Skipski, 1975).

The relationship between the HDL and lower-density lipoproteins is not well understood. Increased serum triglyceride levels are believed to be the result of defective catabolism rather than elevated hepatic

synthesis of triglyceride-rich lipoproteins (Damen et al., 1984). Lipoprotein lipase is the key enzyme responsible for the hydrolysis of triglycerides in chylomicrons and VLDL (Nilsson-Ehle et al., 1980). During hydrolysis of the triglyceride core the redundant surface constituents e.g. phospholipids and cholesterol form discoid particles which are transferred to HDL (Patsch et al., 1978). HDL will also accept cholesterol and phospholipid from plasma membranes of tissues (Damen et al., 1985).

The phospholipids and cholesterol in HDL become substrates for lecithin-cholesterol acyltransferase (LCAT) and generate cholesteryl esters which are then systematically removed from the HDL by a process in which hepatic lipase is thought to be involved (van Tol et al., 1980). Hepatic lipase has been proposed to act in opposition to lipoprotein lipase in a cycle of HDL_3 - HDL_2 interconversions (Jansen et al., 1980; Groot et al., 1983).

In mice bearing GRSL tumours [^{14}C]cholesteryl ester labelled HDL was converted into lipoproteins of low density (LDL + HDL_1 (Damen et al., 1985). The cause was postulated to be impaired removal of HDL by decreased hepatic lipase activity. Both overall tissue lipoprotein lipase (Damen et al., 1984) and adipose tissue lipoprotein lipase (Lanza-Jacoby et al., 1982) decrease in GRSL murine tumours and AC33 rat mammary tumours respectively. Deficiency in both hepatic and lipoprotein lipases is supposed to cause an accumulation of HDL which is then converted, by some as yet unidentified process to LDL or HDL_1. The possibility that the extra LDL or some part of it might arise from the tumour cells in rats and mice has not been addressed in the literature on the subject.

CONCLUSIONS

The chemical, morphological and magnetic resonance properties of rat serum lipoproteins allow the distinction to be made between healthy rats, those bearing only a primary tumour and those with macroscopic secondary malignant deposits (metastases). Female Fischer 344 rats bearing malignant primary mammary adenocarcinomas have low density lipoprotein (LDL) present in their serum whereas in the normal healthy controls this lipoprotein is absent. After the primary tumour has metastasised the LDL particles increase in size from 20 - 22 to 24 - 26 nm, decrease in electrophoretic mobility, and NMR spectroscopy records a T_2 relaxation parameter in excess of 500 ms from a molecule on the particles' surface. A combination of NMR and lipid isolation methods identifies a source of the long T_2 value as fucoganglioside. The NMR signal unique to animals bearing metastases was not detected in any other lipoprotein fractions and was removed by fucosidase treatment of both the LDL particles and the isolated gangliosides.

CHAPTER EIGHT

CONCLUSIONS

"If ye kin make a model, ye understand it,

if ye kanna ye dinna"

Attributed to Lord Kelvin

8.1 TUMOUR CELLS HAVE "MAL"-ADJUSTED MEMBRANES

Plasma membrane domains containing neutral lipid have been identified in embryonic, transformed and malignant cells (Chapter 3). A modification of the fluid mosaic model, described in Chapter 1.2.1 is suggested to accommodate the chemical and NMR data presented in this thesis.

Only a very small proportion of triglyceride can be incorporated into bilayers where it exhibits motional behaviour similar to that of phospholipid acyl chains (Gorrissen et al., 1982) and would therefore not give a high resolution ^{1}H NMR spectrum. ^{2}H NMR studies have shown that a maximum of 0.7 mol percent of triolein can be incorporated into egg lecithin bilayers in the presence of cholesterol (Gorrissen et al., 1982). However, triglyceride accounts for 4.9 mol percent of the major lipids in VBL20 plasma membranes (Chapter 3), and thus a non-bilayer structure is required to account for its presence.

The most appropriate non-bilayer structures containing triglyceride with a high resolution spectrum are the serum lipoproteins. It is proposed that particles similar to lipoproteins are found in or attached to the plasma membranes of malignant cells. In Figure 1 these are shown incorporated into the Fluid Mosaic Model structure, and it is suggested that they be termed Malignancy-associated Lipoproteins (MAL). The term "lipoprotein" is used in preference to "proteolipid" (Wieczorek et al.,

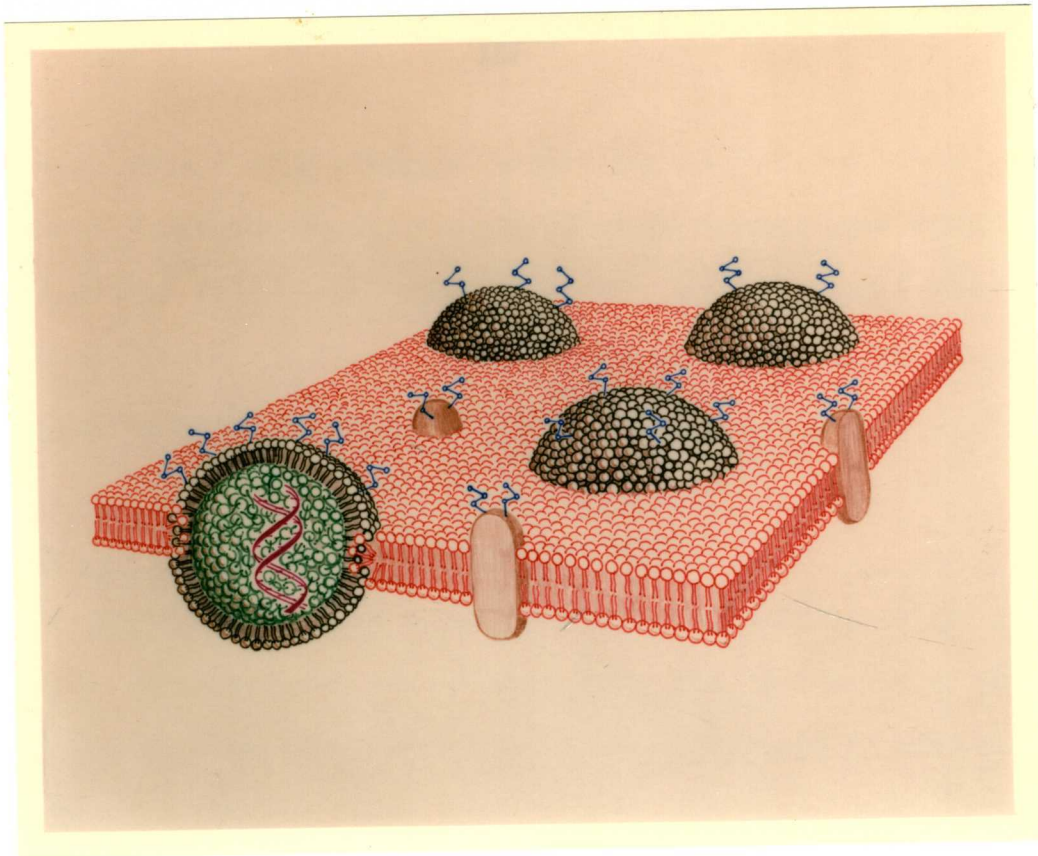

Figure 1. Malignancy-associated Lipoproteins accommodated in the fluid mosaic model.

1985) because there is no precedent for the use of the latter word to denote the abnormal LDL fraction from rats. Furthermore, it is desirable to use the same terminology for rats and humans, since the particles are malignancy and metastasis markers in both.

From experiments using radiolabelled and paramagnetic metal ions (Mountford et al., 1982b) it can be deduced that the MAL are either embedded in, or attached to the outer surface of the malignant cell membrane. The geometry of the attachment of the MAL to the bilayer remains to be elucidated, as does the existence of specific receptors for MAL.

In Figure 1 the size of the MAL membrane domain has been drawn as slightly larger than conventional LDL i.e. 25 - 28 nm in a membrane about 9 nm thick. The data in Chapters 5 and 7 indicate that the ^{1}H NMR signal for MAL in serum is associated with either an HDL-sized particle

(8 - 11 nm diameter) or a slightly larger than LDL-sized particle (25 - 28 nm diameter) or both. Whilst the MAL particle has not been visualised on cell surfaces by methods other than NMR, it is assumed that the dimensions are similar to those identified in the serum and the diameter is thus proposed be in the range of 8 - 28 nm.

8.2 COMPARISON WITH THE METAMORPHIC MOSAIC MODEL

Cullis et al. (1986) have also proposed a modification to the fluid mosaic model for membranes which they term the "metamorphic mosaic model" (Figure 2). The term "metamorphic" was introduced to acknowledge the ability of lipids to adopt a variety of structures e.g. inverted micelles, cylinders and the H_{11} phase, in addition to the bilayer. The original term "mosaic" in the Singer-Nicolson model was used to describe

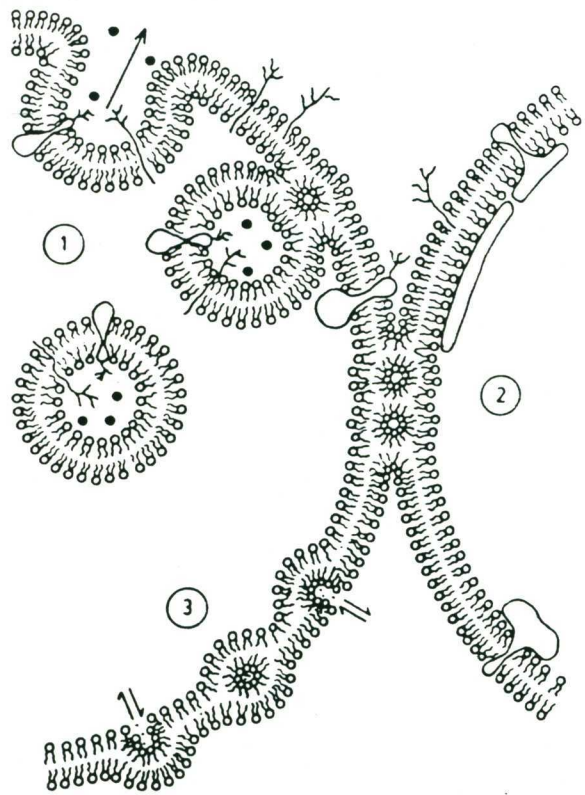

Figure 2. Metamorphic mosaic model (Cullis et al., 1986).

the varied pattern created by the proteins situated, in and protruding through, the lipid bilayer.

The metamorphic mosaic model presents explanations for a variety of membrane events e.g in region 1, Figure 2, an exocytotic event is proceeding via an intermediate inverted micellar or inverted cylinder structure, whereas in region 2, an inverted cylinder structure allows a stable, semi-fused interbilayer connection to exist, possibly corresponding to a tight junction. In region 3 enhanced permeability to divalent cations is proposed to proceed via an inverted micellar intermediate.

In contrast to the predominantly neutral lipids found in the MAL domains (Figure 1), the lipids which can induce such non-bilayer structures as in Figure 2 are the phospholipids PE, PS, PA and CL, or cholesterol and long-chain fatty acids under some conditions. Also, in contrast to Figure 1, the formation of non-bilayer structures is proposed in normal as well as neoplastic cells and is believed to be both localised and/or transitory during such processes as membrane fusion and other membrane contact phenomena (Cullis et al., 1986).

8.3 THE COMPOSITION OF MAL

The chemical and physical structure of MAL as determined in Chapters 5 and 7 is believed to be similar to conventional serum lipoproteins (Herbert et al., 1983). The neutral lipids (triglycerides and cholesteryl ester) tumble isotropically in a central spherical core, surrounded by a shell of glycolipid, phospholipid, free cholesterol and protein. The main differences from normal lipoproteins are the large amounts of glycolipid on the particle surface (the antenna-like projections in Figure 1) and the presence of DNA. DNA (Chapter 5) has

been depicted in Figure 1 as being in the core of the particle where it is protected it from destruction by deoxyribonucleases.

The nature of the protein in the MAL particles is unknown. The presence of Apo A and B might indicate contamination by LDL and HDL. Apo (a) content has yet to be determined. The abnormal electrophoretic mobility of both human and rat MAL suggests the presence of protein or lipid of unusual charge or an unusual particle size, or both.

DNA of unknown origin was found in MAL and other lipoproteins in human serum (Chapter 5). No convincing evidence for the presence of intact RNA was found. This finding differs with that of Wieczorek et al. (1985), who reported polyA$^+$ mRNA inside proteolipid particles, but not in conventional serum lipoproteins from cancer patients. The extrusion of DNA and RNA from cells is a controversial topic, with some critics claiming that the nucleic acids are debris from dead cells. However evidence has accrued over the years that DNA and RNA can leave living, intact eukaryote cells, both normal and malignant (Stroun et al., 1977; reviewed by Adams, 1985). RNA and DNA are released both separately and together as complexes (Stroun et al., 1977; Khandijian and Turian, 1976) with lipid and protein (Adams, 1985). Biological functions have also been recorded for this type of complex, involving the alteration of immune responses (Valentine and Lawrence, 1969; Heller et al., 1973) and increases in the proliferation rate of normal bone marrow cells (Wieczorek, 1983). The origin and function of DNA, and the presence of RNA in MAL have not been resolved at present.

One component on the surfaces of metastatic cancer cells which is unique to MAL is fucose (Figure 1). The NMR profile of this MAL shows a long T_2 relaxation time and the presence of cross-peak Y in 2D COSY experiments. Both of these parameters are fucosidase-sensitive (Chapter

6). The fucosylated molecule has been identified by NMR spectroscopy in the crude ganglioside fraction of metastastic R13762 cells. However the contribution of protein-bound fucose to the NMR experiments is not known. Chemical confirmation of the presence of fucose and the identity of the fucomolecule(s) responsible for cellular metastatic potential await completion of further experiments.

8.4 THE ORIGIN OF MAL

There is circumstantial evidence presented in this thesis that MAL in the serum is shed from MAL on the surface of tumour cells. Moreover, MAL in the serum has been used to model the characteristics of MAL on the cells. Wieczorek et al. (1985) identified proteolipid in the medium from cultured malignant cells and concluded that the particles were extruded by the cells. The composition of proteolipid in the cell media was the same as that in patients' serum. The NMR parameters characteristic of fucomolecules associated with the metastatic process in cells are also present in MAL found in the serum of human cancer patients or rats bearing metastatic tumours (Chapters 5 and 7). Fucosidase treatment of the serum MAL resulted in the same spectral changes as shown by the cell-associated MAL. MAL was only found in the serum of rats with tumours and in patients with tumours or shortly after their removal.

Many questions remain to be answered on the origins of MAL. At what stage of tumour development does the fucosylated molecule appear which is a marker for metastasis? Is the complete MAL shed intact from cells into the blood or only some components of it? Since there is interconversion of normal lipoproteins in serum it is possible that MAL formation, or some part of the process, is the result of deranged

lipoprotein metabolism in cancer patients.

8.5 CELL SURFACE PROPERTIES AND METASTASIS

Treatment of metastatic cells with fucosidase reduced their metastatic but not their tumorigenic capacity, both *in vivo* and *in vitro*. The possible importance of the cell surface in determining the particular properties of metastatic cells has been the basis for a number of investigations in recent years (reviewed by Turner, 1982). Some of these experiments are listed in Table 1. Turner concluded that

Table 1 Effect of Modifying the Cell Surface on the Subsequent Metastatic Behaviour

Treatment	Change in Surface Properties - In Vitro	Change in Metastatic Behaviour - In Vivo
Trypsin*	decreased ^{1}H NMR signal	decreased number of lymph nodules
Trypsin	decreased surface charge	decreased number of lung nodules
Neuraminidase	decreased surface charge	decreased lung retention of labelled cells
In Vitro culture	decreased ConA agglutination	increased number of lung nodules
Heparin	increased surface charge	increased organ retention of labelled cells
Cytoskeletal disrupting agents	decreased cell adhesion, migration, and ability to aggregate	decreased retention of labelled cells in lungs and in the number of of lung nodules
Vesicle fusion	increased sensitivity to immune lymphocytes	increased retention of labelled cells in lungs and in the number of lung nodules
Tunicamycin	decreased cell adhesion and the expression of surface glycoproteins	decreased the number of lung nodules
Trasylol	increased cell adhesion	increased retention of labelled cells in lungs and in the number of lung nodules

Except for Holmes *et al.* (1986)*, all references are listed by Turner (1982).

no evidence exists to suggest that metastatic transformation is accompanied by the appearance of any common specific surface feature.

The occurrence of an NMR signal from fucosylated molecules has been noted in many human tumours (Mountford et al., 1986b), in cultured cancer cells with metastatic potential, and in the serum from rats with metastatic tumours derived from the same cultured cells. Although no metastases were detected outside the pelvic region in the patient with borderline ovarian cancer in Chapter 5, it is still possible that the tumours had the potential for metastasis. The latter is a multi-stage process, as described in Chapter 1.6, with one step involving the invasion of surrounding tissues. Histologically the cells from the ovarian tumours apparently lacked invasive capacity and the prognosis for this patient is good. However multiple foci were present in the pelvis, so that either the tumours were multifocal in origin, or cells had become detached from the primary tumour and seeded elsewhere. No invasive property would be required for this migration. (It is conceivable therefore that borderline ovarian tumours carry the ability to immunosuppress the host but not the capacity to invade).

Many fucoproteins and fucolipids defined by monoclonal antibodies have been listed as tumour-associated markers (reviewed by Hakomori, 1985). MAL have been found in the plasma and serum of a number of other cancer patients, but the study is incomplete and has not been included in this thesis. Extensive clinical trials are needed to determine if the presence of MAL in human sera is a reliable indicator of the metastatic potential of tumours. It is likely that fucosylation is one of the steps necessary for metastasis, and that it affects the host's immune response (references are provided in Chapter 6). However, both of these hypotheses await proof.

8.6 A MODEL FOR SURFACE MEMBRANES IN DRUG-RESISTANT CELLS

Changes to the lipid composition and structure of plasma membranes from vinblastine-resistant leukaemic lymphoblasts have been identified in this thesis. Cholesterol, phospholipid and ether-linked phospholipids are all present in greater quantities and might affect the permeability of the bilayer. The inner half of the bilayer of resistant cell membranes contains 4% extra lipid detectable as particle-free bulges by freeze-fracture electron microscopy (Chapter 4). A likely candidate for inclusion in the membrane lipid bulges is 1-O-alky-2-acylphosphatidyl choline, if its plasma membrane distribution is similar to that found in another malignant cell line (Record et al., 1984). Asymmetric distribution of the extra cholesterol and phospholipid found in the vinblastine-resistant lymphoblast membranes is also possible. None of these lipids gives a high-resolution ^{1}H NMR spectrum, thus any direct effects of their increased membrane content would not produce spectral changes.

The structure of the P-glycoprotein in the plasma membranes of cells with the multi-drug resistant phenotype has been depicted by Marx (1986), Figure 3.

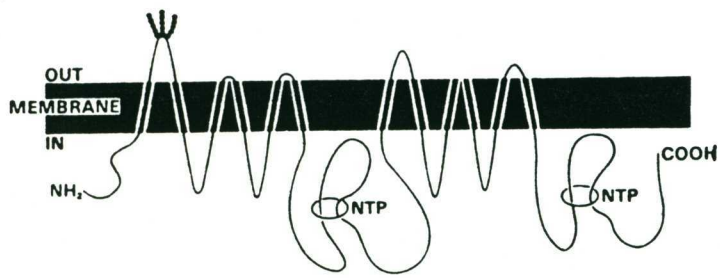

Figure 3. Model of the human P-glycoprotein. NTP = binding sites for nucleoside triphosphates (Marx, 1986).

To this membrane model, MAL, as depicted in Figure 1, can now be added, as well as bulges to the inner half of the bilayer. The function of MAL in drug resistance is not known, although alterations to this domain were detected by ^{1}H NMR in vinblastine-resistant cells (Chapter 1.7.3). Whether the membrane lipid bulges are related to the increased P-glycoprotein content of the membranes or to cytoskeletal changes induced by vinblastine remains to be elucidated.

It is hoped that the work presented in this thesis will lead to the development of a simple serum test for the detection and monitoring of malignancy and metastasis. In addition, trials will assess the possibilities of improved combination chemotherapy, using the knowledge gained of lipid and mitochondrial alterations in multi-drug resistant cells.

REFERENCES

Abragam A (1983): in: Principles of Nuclear Magnetism. Clarendon Press, Oxford

Adams DH (1985): Int J Biochem 17:1133-1141

Agris PR, Campbell ID (1982): Science 216:1325-1327

Akeson AL, Scupham DW, Harmony JAK (1984): J Lipid Res 25:1195-1205

Albers JJ, Cabana VG, Warnick GR, Hazzard WR (1975): Metabolism 24:1047-1054

Alexander P (1974): Cancer Res 34:2077-2082

Almog R, Shirey TL (1978): Anal Biochem 91:130-137

Ames BN (1965): Methods Enzymol 8:115-118

Arbogast LY, Rothblat GH, Leslie MH, Cooper RA (1976): Proc Natl Acad Sci USA 73:3680-3684

Arseniev AS, Wider G, Jonbert FJ, Wüthrich K (1982): J Mol Biol 159:323-351

Atkinson PH, Summers DF (1971): J Biol Chem 246:5162-5175

Balmain A (1985): Br J Cancer 51:1-7

Barclay M, Skipski VP (1975): Prog Biochem Pharmacol 10:76-111

Barclay M, Skipski VP, Terebus-Kekish O, Greene EM, Kaufman RJ, Stock CC (1970): Cancer Res 30:2420-2430

Barenholz Y, Thompson TE (1980): Biochim Biophys Acta 604:129-158

Barlow JJ, Bhattacharya M (1983): Clin Obstet Gynaecol 10:187-196

Barter PJ, Lally JI (1978): Biochim Biophys Acta 531:233-236

Barton PG, Gunstone FD (1975): J Biol Chem 256:4470-4476

Baskin F, Rosenberg RN, Dev V (1981): Proc Natl Acad Sci USA 78:3654-3658

Baumann H, Nudelman E, Watanabe K, Hakomori S (1979): Cancer Res 39:2637-2643

Bax A, Freeman R, Morris G (1981): J Magn Reson 42:164-168

Beck WT, Mueller TJ, Tanzer LR (1979): Cancer Res 39:2070-2076

Bekesi JG, Winzler RJ (1967): J Biol Chem 242:3873-3879

Benson AA (1966): J Amer Oil Chemists' Soc 43:265-270

Bergelson LD (1980): in: Lipid Biochemical Preparations, LD Bergelson (ed.). Elsevier/North Holland, Amsterdam, pp.244-245

Bergelson LD, Barsukov LI (1977): Science 197:224-230

Bergelson LD, Dyatlovitskaya EV (1973): in: Symposium on Tumour Lipids, R Wood (ed.) American Oil Chemists' Society, Champaign, Ill, Chapter 9, pp.111-125

Bergelson LD, Dyatlovitskaya EV, Sorokina IB, Gorkova NP (1974): Biochim Biophys Acta 360:361-365

Bergelson LD, Dyatlovitskaya EV, Torkhovskaya TI, Sorokina IB, Gorkova NP (1970): Biochim Biophys Acta 210:287-298

Berridge MJ (1984): Biochem J 220:345-360

Biedler JL, Chang T, Peterson RHF, Mebra PW, Meyers MB, Spengler BA (1983): in: Rational Basis for Chemotherapy, BA Chabner (ed.). Alan P. Liss Inc., New York, pp.71-92

Bishop JM (1983): Annu Rev Biochem 52:301-354

Black PH (1980): Adv Cancer Res 32:75-199

Blank ML, Cress EA, Piantadosi C, Snyder F (1975): Biochim Biophys Acta 208:208-218

Block RE (1973): FEBS Lett 34:109-112

Block RE (1976): in: The Nuclear Resonance Effect in Cancer, R Damadian (ed.), Chapter 10. Pacific Publishing Co., Portland, Oregan, pp.

Block RE, Maxwell GP, Irvin GL, Hudson JL, Prudhomme DL (1974): in: Membrane Transformation in Neoplasia, H Schultz, Block RE (eds.). Academic Press, New York, p.244

Block RE, Maxwell GP, Prudhomme DL, Hudson JL (1977): J Natl Cancer Inst 58:151-156

Bloom D, McCalden TA, Rosendorff C (1975): Br J Pharmacol 54:421-427

Bloom M, Burnell EE, Roeder SBW, Valic MI (1977): J Chem Phys 66:3012-3020

Bloom M, Burnell EE, MacKay AL, Nichol CP, Valic MI, Weeks G (1978): Biochemistry 17:5750-5762

Bloom M, Holmes, KT, Mountford CE, Williams PG (1986): J Magn Reson 69:73-91

Boggs JM (1980): Can J Biochem 58:755-770

Boland JD, Tweto J (1980): Biochim Biophys Acta 600:713-729

Bonavida B (1974): J Immunol 112:926-934

Booyens P, Engelbrecht P, Le Roux S, Louwrens CC (1984): Prostaglandins Leukotrienes and Medicine 15:15-33

Bosmann HB, Hagopian A, Eylar EH (1969): Arch Biochem Biophys 130:573-583

Bottomley PA, Foster TH, Argersinger RE, Pfeifer LM (1984): Med Phys 11:425-448

Bottomley PA, Hardy CJ, Argersinger RE, Allen-Moore G (1987): Medical Physics 14:in press

Boyum A (1976): Scand J Immunol 5:9-15

Brady RO, Fishman PH (1974): Biochim Biophys Acta 355:121-148

Branton D, Bullivant S, Gilula NB et al. (1975): Science 190:54-56

Bremer EG, Hakomori S, Bowen-Pope DF, Raines E, Ross R (1984): J Biol Chem 259:6818-6825

Bretscher M (1973): Science 181:622-629

Brindle KM, Brown FF, Campbell ID, Grathwohl C., Kuchel PW (1979): Biochem J 180:37-44

Brockerhoff H (1974): Lipids 9:645-650

Brown MF, Davis JH (1981): Chem Phys Lett 79:431-435

Brown MS, Goldstein JL (1976): Science 191:150-154

Brown MS, Faust JR, Goldstein JL (1975): J Clin Invest 55:783-793

Brunk CF, Jones KC, James TW (1979): Anal Biochem 92:497-500

Cabot MC, Snyder F (1980): Biochim Biophys Acta 617:410-418

Camus M, Chapman MJ, Forgez P, Laplaud PM (1983): J Lipid Res 24:1210-1288

Carruthers C (1967): Cancer Res 27:1-6

Chalvardjian A (1971): J Lipid Res 12:265-269

Changeux JP, Thiery J, Tung Y, Kittel C (1967): Proc Natl Acad Sci USA 57:335-341

Chap HJ, Zwaal RFA, van Deenen LLM (1977): Biochim Biophys Acta 467:146-164

Chapman D, Hayward JA (1985): Biochem J 228:281-295

Chapman D, Urbina J (1971): FEBS Letts 12:169-172

Chapman HA, Hibbs JB (1977): Science 197:282-285

Chapman MJ (1980): J Lipid Res 21:789-828

Chatterjee SK, Kim U (1978): J Natl Canc Inst 61:151-162

Cheley S, Anderson R (1984): Anal Biochem 137:15-19

Clarke JTR, Stoltz JM, Mulcahey MR (1976): Biochim Biophys Acta 431:317-325

Clarke RW, Crain RC (1986): Cancer Res 46:1894-1903

Coffey JW, Miller ON, Sellinger OZ (1964): J Biol Chem 239:4011-4017

Coleman PS, Lavietes BB (1981): CRC Critical Reviews in Biochemistry 11:341-393

Cooper RA (1978): J Supramol Struct 8:413-430

Cornwell MM, Gottesman MM, Pastan IH (1986): J Biol Chem 261:7921-7928

Costanza ME, Pinn V, Schwartz RS, Nathanson L (1973): N Engl J Med 289:520-522

Cox RA, Gökcen M (1975): J Natl Cancer Inst 54:379-386

Cross KJ, Holmes KT, Mountford CE, Wright PE (1984): Biochemistry 23:5895-5897

Cullis PR, de Kruijff B (1979): Biochim Biophys Acta 559:399-420

Cullis PR, Hope MJ, Tilcock CPS (1986): Chem Phys Lipids 40:127-144

Curtiss LK, Edgington TS (1976): J Immunol 116:1452-1458

Damadian R (1971): Science 171:1151-1153

Damadian R, Zaner K, Hor D, Di Maio T, Minkoff L, Goldsmith M (1973): Ann NY Acad Sci 222:1048-1076

Damen J, de Widt J, Hengeveld T, van Blitterswijk WJ (1985): Biochim Biophys Acta 833:495-498

Damen J, Van Ramshorst JV, Van Hoeven RP, Van Blitterswijk WJ (1984): Biochim Biophys Acta 793:287-296

Danielli JF, Davson H (1935): J Cell Comp Physiol 5:495

Daniels A, Williams RJP, Wright PE (1976): Nature (London) 261:321-323

Daniels A, Williams RJP, Wright PE (1978): Neuoroscience 3:573-585

Danø K, Skøvsgaard T, Nissen NI, Fricke E, Di Marco A (1983): 13th International Cancer Congress, Part C, Biology of Cancer (2), Alan R. Liss Inc., New York, pp.231-246

Das S, Rand RP (1986): Biochemistry 25:2882-2889

Davidsohn I, Kovarik S, Ni LY (1969): Arch Pathol 87:306-314

Davis DG, Inesi G (1971): Biochim Biophys Acta 241:1-8

Dawson G, Kruski AW, Scanu AM (1976): J Lipid Res 17:125-131

de Kruijff B, van den Besselaar AMHP, Cullis PR, van den Bosch H, van Deenen LLM (1978): Biochim Biophys Acta 514:1-8

Demel RA, Jansen JWCM, van Dijck PWM, van Deenen LLM (1977): Biochim Biophys Acta 465:1-10

Dennis JW, Kerbel RS (1981): Cancer Res 41:98-104

Dennis JW, Donaghue TP, Kerbel RS (1981): J Natl Cancer Inst 66:129-139

De Pierre JW, Karnovsky ML (1973): J Cell Biol 56:275-303

Diagne A, Fauvel J, Record M, Chap H, Douste-Blazy L (1984): Biochim Biophys Acta 793:221-231

Dittmer JC, Lester RL (1964): J Lipid Res 5:126-127

Dnistrian AM, Schwartz MK, Katopodis N, Fracchia AA, Stock CC (1982): Cancer 50:1815-1819

Duck-Chong CG (1979): Lipids 14:492-497

Dunbar LM, Bailey JM (1975): J Biol Chem 250:1152-1153

Dvorak HF, Van de Water L, Bitzer AM, Dvorak A, Anderson D, Harvey VS, Bach R, Davis GL, de Wolf W, Carvalho ACA (1983): Cancer Res 43:4434-4442

Dyer AR, Stamler J, Paul O, et al. (1981): J Chronic Diseases 34:249-260

El Tamer A, Record M, Fauvel J, Chap H, Douste-Blazy L (1984): Biochim Biophys Acta 793:213-220

Emerson SG, Cone RE (1981): J Immunol 127:482-486

Fabry ME, San George RC (1983): Biochemistry 22:4119-4125

Fahlbusch B, Tittel R (1986): Biomed Biochim Acta 45:359-370

Farrar TC, Becker ED (1971): in: Pulse and Fourier Transform NMR, Academic Press, New York

Fauvel J, Bonnefis MJ, Chap M, Thouvenot JP, Douste-Blazy L (1981): Biochim Biophys Acta 666:72-79

Feinstein MB, Fernandez SM, Sha'afi RI (1975): Biochim Biophys Acta 413:354-370

Ferber G, De Pasquale G, Resch K (1975): Biochim Biophys Acta 398:364-376

Ferrige AG, Lindon JC (1978): J Magn Reson 31:337-340

Fidler IJ (1985): Cancer Res 45:4714-4726

Fidler IJ, Talmadge JE (1986): Cancer Res 46:5167-5171

Filipovic I, Schwarzmann G, Buddecke E (1981): Biochim Biophys Acta 647:112-118

Fisher KA (1976): Proc Natl Acad Sci USA 73:173-177

Fleisher LN, Tall AR, Witte LD, Miller RW, Cannon PJ (1982): J Biol Chem 257:6653-6655

Folch J, Lees M (1951): J Biol Chem 191:807-817

Foley GE, Lazarus H, Farber S, Uzman BG, Boone BA, McCarthy RE (1965): Cancer 18:522-529

Franck PFH, Bevers EM, Lubin BH, Comfurius P, Chiu DTY, Op den Kamp JAF, Zwaal RFA, van Deenen LLM, Roelofsen B (1985): J Clin Invest 75:183-190

Frederickson DS, Levy RI, Lees RS (1967): New Engl J Med 276:34-44. 94-103, 148-156, 215-225, 273-281

Friedberg SJ, Smajdek J, Anderson K (1986): Cancer Res 46:845-849

Gahmberg CG, Hakomori S (1973): J Biol Chem 248:4311-4317

Gahmberg CG, Hakomori S (1975): J Biol Chem 250:2438-2446

Gerlach JH, Endicott JA, Juranka PF, Henderson G, Sarangi F, Deuchars KL, Ling V (1986): Nature 324:485-489

Ghayur T, Horrobin DF (1981): IRCS Med Sci 9:582-586

Ghiselli G, Sirtori CR, Nicosia S (1981): Biochem J 196:889-902

Goldstein JL, Basu SK, Brown MS (1983): Methods Enzymol 98:241-260

Gonwa TA, Westrick MA, Macher BA (1984): Cancer Res 44:3467-3470

Gorrissen H, Tulloch AP, Cushley RJ (1982): Chem Phys Lipids 31:245-255

Gottfried EL (1967): J Lipid Res 8:321-327

Grant CWM (1984): Can J Biochem Cell Biol 62:1151-1157

Groot PHE, Scheek LM, Jansen H (1983): Biochim Biophys Acta 751:393-400

Gros P, Ben Neriah Y, Croop JM, Housman DE (1986): Nature 323:728-731

Gupta RS, Gupta R (1984): J Biol Chem 259:1882-1890

Gupta RS, Venner TJ, Chopra A (1985): Can J Biochem Cell Biol 63:489-502

Gupta RS, Irie RF, Chee DO, Kern DH, Morton DL (1979): J Natl Cancer Inst 63:347-356

Ha YC, Calvert GD, McIntosh GH, Barter PJ (1981): Metabolism 30:380-383

Häkkinen I (1970): J Natl Cancer Inst 44:1183-1193

Hakomori S (1985): Cancer Res 45:2405-2414

Hakomori S, Andrews HD (1970): Biochim Biophys Acta 202:225-227

Hakomori S, Murakami WT (1968): Proc Natl Acad Sci USA 59:254-261

Hakomori S, Wang SM, Young WW Jr (1977): Proc Natl Acad Sci USA 74:3023-3027

Hanahan D (1986): Annu Rev Biochem 55:483-509

Harsas W, Murdoch S, Pollak JK (1985): Biochem Int 10:487-494

Hassall DG, Owen JS, Bruckdorfer KR (1983): Biochem J 216:43-49

Hatch FT, Lees RS (1968): Adv Lipid Res 6:111-168

Heider JG, Boyett RL (1978): J Lipid Res 19:514-518

Hemker HC, van Rijn JLML, Rosing J, van Dieijn G, Bevers EM, Zwaal RFA (1983): Blood Cells 9:303-317

Heller P, Bhoophalam N, Cabana V, Costea N, Yakulis V (1973): Ann NY Acad Sci 207:468-480

Herbert PN, Assmann G, Gotto AM Jr, Fredrickson DS (1983): in: The Metabolic Basis of Inherited Disease, 5th Edition, JB Stanbury, JB Wyngaarden DS, Fredrickson, JL Goldstein, MS Brown (eds.), Chapter 29, MacGraw Hill Inc., pp.589-597

Hersey P, Schibeci SD, Townsend P, Burns C, Cheresh DA (1986): Cancer Res 46:6083-6090

Hildebrand J, Stryckmans P, Stoffyn P (1971): J Lipid Res 12:361-366

Hirata F, Axelrod J (1980): Science 209:1082-1090

Hoessli DC, Rungger-Brändle E (1983): Proc Natl Acad Sci USA 80:439-443

Holmes KT, Williams PG, May GL, Gregory P, Wright LC, Dyne M, Mountford CE (1986): FEBS Lett 202:122-126

Homa ST, Conroy DM, Smith AD (1983): Biochim Biophys Acta 752:315-323

Hopkins GJ, West CE, Hard GC (1976): Lipids 11:328-333

Horrocks LA (1972): in: Ether Lipids: Chemistry and Biology, F Snyder (ed.). Academic Pres, New York, pp.177-272

Horrocks LA, Sharma M (1982): in: Phospholipids, JN Hawthorne, GB Ansell (eds.), Vol.4. Elsevier Biomedical Press, Amsterdam, pp.51-93

Horwitz AF, Hatten ME, Burger MM (1974): Proc Natl Acad Sci USA 71:3115-3119

Howard BV, Kritchevsky D (1969): Int J Cancer 4:393-402

Howard BV, Howard WJ, De la Llera M, Kefalides NA (1976): Atherosclerosis 23:521-534

Hui DY, Harmony JAK (1979): Biochim Biophys Acta 550:425-434

Hui DY, Harmony JAK, Innerarity TL, Mahley RW (1980): J Biol Chem 255:11775-11781

Hull SR, Laine RA, Kaizu T, Rodriguez I, Carraway KL (1984): J Biol Chem 259:4866-4877

Inch WR, McCredie JA, Knispel RR, Thompson RT, Pintar MM (1974): J Natl Cancer Inst 52:353-356

Itaya K, Hakomori S (1976): FEBS Lett 66:65-69

Itaya K, Hakomori S, Klein G (1976): Proc Natl Acad Sci USA 73:1568-1571

IUPAC-IUB Commission on Biochemical Nomenclature (CBN) (1977): Eur J Biochem 79:11-21

Iwanik MJ, Shaw KV, Ledwith BJ, Yanovich S, Shaw JM (1984): Cancer Res 44:1206-1215

Jackson DV, Bender RA (1978): in: Clinical Pharmacology of Anti-neoplastic Drugs, HM Pinedo (ed.). Elsevier/North Holland Biomedical Press, Amsterdam, pp.277-294

Jackson MB, Sturtevant JM (1978): Biochemistry 17:911-915

Jackson RL, Morrisett JD, Gotto AM Jr (1976): Physiol Rev 56:259-316

Jackson RL, Tajima S, Yamamura T, Yokoyama S, Yamamoto A (1986): Biochim Biophys Acta 875:211-219

Jacobs WLW (1971): Clin Chim Acta 31:175-179

Jain MK (1972): in: The Bimolecular Lipid Membrane: A System, Van Nostrand Reinhold Co, New York, pp.7-11

Jansen H, Van Tol A, Hülsmann WC (1980): Biochem Biophys Res Commun 92:53-59

Jesson JP, Meakin P, Knissel G (1973): J Am Chem Soc 95:618-620

Juliano RL, Ling V (1976): Biochim Biophys Acta 455:152-162

Kane JP, Hardman DA, Dimpfl JC, Levy JA (1979): Proc Natl Acad Sci USA 76:5957-5961

Karmali RA, Marsh J, Fuchs C (1984): J Natl Cancer Inst 73:457-461

Karnovsky MJ, Kleinfeld AM, Hoover RL, Klausner RD (1982): J Cell Biol 94:1-6

Katopodis N, Hirshaut Y, Geller N, Stock CC (1982): Cancer Res 42:5270-5275

Kaufman RL, Ginsburg V (1968): Exp Cell Res 50:127-132

Kawato S, Kinosita K Jr, Ikegami A (1978): Biochemistry 17:5026-5031

Keenan TW, Morré DJ (1970): Biochemistry 9:19-25

Khandijian EW, Turian G (1976): Cell Differentiation 5:171-188

Kim U, Baumler A, Carruthers C, Bielat K (1975): Proc Natl Acad Sci USA 72:1012-1016

Klock JC, Pieprzyk JK (1979): J Lipid Res 20:908-911

Kloppel FM, Keenan TW, Freeman MJ, Morré DJ (1977): Proc Natl Acad Sci USA 74:3011-3013

Koga S, Horwitz DL, Scanu AM (1969): J Lipid Res 10:577-588

Koizumi K, Shimizu S, Koizumi KT, Nishida K, Sato S, Ota K, Yamanaka N (1981): Biochim Biophys Acta 649:393-403

Kopnin BP (1981): Cytogenet Cell Genet 30:11-14

Kostner GM (1983): Adv Lipid Res 20:1-299

Krebs JJR, Hauser H, Carafoli E (1979): J Biol Chem 254:5308-5316

Krishnaraj R, Lin J, Kemp RG (1983): Cell Immunol 78:152-160

Kwok BCP, Shen BW, Dawson G (1981): J Biol Chem 256:9698-9704

Ladisch S, Gillard B, Wong C, Ulsh L (1983): Cancer Res 43:3808-3813

Lanza-Jacoby S, Miller EE, Rosato FE (1982): Lipids 17:944-949

Lee PM, Ketis NV, Barker KR, Grant CWM (1980): Biochim Biophys Acta 601:302-314

Lee T, Stephens N, Moehl A, Snyder F (1973): Biochim Biophys Acta 291:86-92

Leffert HL, Weinstein PB (1976): J Cell Biol 70:20-32

Lenard J, Singer SJ (1966): Proc Natl Acad Sci USA 56:1828-1835

Lengle EE (1979): J Natl Cancer Inst 62:1565-1567

Lengle EE, Krishnaraj R, Kemp RG (1979): Cancer Res 39:817-822

Levy GA, Schwartz BS, Curtiss LK, Edgington TS (1981): J Clin Invest 67:1614-1622

Levy RI, Lees RS, Fredrickson DS (1966): J Clin Invest 45:63-77

Liebes LF, Pelle E, Zucker-Franklin D, Silber R (1981): Cancer Res 41:4050-4056

Loor F (1980): Adv Immunol 30:1-120

Loughridge LW, Lewis MG (1971): Lancet 1:256-258

Low MG, Kincade PW (1985): Nature 318:62-64

Low MG, Ferguson MAJ, Futerman AH, Silman I (1986): TIBS 11:212-215

Luzzati V, Husson F (1962): J Cell Biol 12:207-219

Lynch HT, Schuelke GS, Wells IC, Cheng S, Kimberling WJ, Biscone KA, Lynch JF, Danes BS (1985): Cancer 55:410-415

Maler T, Riordan JR (1980): Biochim Biophys Acta 598:1-15

Maniatis T, Fritsch T, Sambrook J (1982): in: Molecular Cloning; A Laboratory Manual, Cold Spring Harbour Laboratory, pp150-206

Mannes GA, Maier A, Thieme C, Wiebecke B, Paumgartner G (1986): New Engl J Med 315:1634-1638

Marcus DM (1984): Molecular Immunology 21:1083-1091

Marique D, Hildebrand J (1973): Cancer Res 33:2761-2767

Marx JL (1986): Science 234:818-820

Mason PW, Jacobson BS (1985): Biochim Biophys Acta 821:264-276

Mathews FS, Levine M, Argos P (1971): Nature New Biol 233:15-16

Mathur SN, Spector AA (1976): Biochim Biophys Acta 424:45-56

Melera PW, Cronin-Sheridan AP (1976): Biochim Biophys Acta 432:300-311

Merritt WD, Richardson CL, Keenan TW, Morré DJ (1978): J Natl Cancer Inst 60:1313-1325

Meyers MB, Biedler JL (1981): Biochem Biophys Res Commun 99:228-235

Miller EC, Miller JA (1986): Cancer 58:1795-1803

Miller NE, Weinstein DB, Steinberg D (1977): J Lipid Res 18:438-450

Monneron A, d'Alayer J (1978): J Cell Biol 77:211-231

Morawiecki A (1964): Biochim Biophys Acta 83:339-347

Morrison WR, Smith LM (1964): J Lipid Res 5:600-608

Mountford CE, Holmes KT, Smith ICP (1986a): Prog Clin Biochem Med 3:73-112

Mountford CE, Grossman G, Gatenby PA, Fox RM (1980): Br J Cancer 41:1000-1003

Mountford CE, Grossman G, Hampson AW, Holmes KT (1982a): Biochim Biophys Acta 720:65-74

Mountford CE, Grossman G, Reid G, Fox RM (1982b): Cancer Res 42:2270-2276

Mountford CE, Mackinnon WB, Bloom M, Burnell EE, Smith ICP (1984a): J Biochem Biophys Methods 9:323-330

Mountford CE, Saunders JK, May GL, Holmes KT, Williams PG, Fox RM, Tattersall MHN, Bar JR, Russell P, Smith ICP (1986b): Lancet i:651-653

Mountford CE, Wright LC, Holmes KT, Mackinnon WB, Gregory P, Fox RM (1984b): Science 226:1415-1418

Muir A, Hensley WJ (1977): in: Measurement of Specific Proteins using a Standard Centrifugal Analyser. Proc 16th Annual Conference of the Australian Association of Clinical Biochemists

Murayama K, Levery SB, Shirrmacher V, Hakomori S (1986): Cancer Res 46:1395-1402

Murphy CR, Swift JG (1983): Acta Anat 116:174-179

Naoi M, Lee YC, Roseman S (1974): Anal Biochem 58:571-577

Narayen KA (1971): Int J Cancer 8:61-70

Narayan KA, Morris HP (1970): Int J Cancer 5:410-414

Newbold RF, Overell RW, Connell JR (1982): Nature 229:633-635

Newby AG, Luzio PJ, Hales CN (1975): Biochem J 146:625-633

Nicolau C, Dietrich W, Steiner MR, Steiner S, Melnick JL (1975): Biochim Biophys Acta 382:311-321

Nicolau C, Klenk HD, Reimann A, Hildenbrand K, Bauer H (1978): Biochim Biophys Acta 511:83-92

Nicolson GL (1976): Biochem Biophys Acta 457:57-108

Nicolson GL (1982): Biochim Biophys Acta 695:113-176

Nicolson GL (1984): Exp Cell Res 150:3-22

Nicolson GL, Poste G (1982): Curr Prob Cancer 7 No.6:3-83

Nilsson-Ehle P, Garfinkel AS, Schotz MC (1980): Annu Rev Biochem 49:667-693

Nydegger UE, Butler RE (1972): Cancer Res 32:1756-1760

Oldfield E, Chapman D (1972): FEBS Letts 23:285-297

Oldfield E, Gilmore R, Glaser M, Gutowsky HS, Hshung JC, Kang SY, King TE, Meadows M, Rice D (1978): Proc Natl Acad Sci USA 75:4657-4660

Oldstone MBA, Theofilopoulos AN, Gunvén P, Klein G (1974): Intervirology 4:292-302

Op den Kamp JAF (1979): Ann Rev Biochem 48:47-71

Oschry Y, Eisenberg S (1982): J Lipid Res 23:1099-1106

Otnaess AB, Holm T (1976): J Clin Invest 57:1419-1425

Owen JS, McIntyre N, Gillett MPT (1984): TIBS, 9:238-242

Paddy MR, Dahlquist FW (1982): Biophys J 37:110-112

Park BH, Fike RM, Kim U (1982): IRCS Med Sci 10:96-97

Parlo RA, Coleman PS (1984): J Biol Chem 259:9997-10003

Patsch JR, Gotto AM Jr, Olivecrona T, Eisenberg S (1978): Proc Natl Acad Sci USA 75:4519-4523

Pessin JE, Salter DW, Glaser M (1978): Biochemistry 17:1997-2004

Petitou M, Tuy F, Rosenfeld C, Mishal Z, Paintrand M, Jasnin C, Mathe G, Inbar M (1978): Proc Natl Acad Sci USA 75:2306-2310

Portoukalian J, Geneve J, Gerard JP, Doré JF (1982): in: Proceedings of the 13th International Cancer Congress, Abstract 2545, Seattle, p.446

Portoukalian J, Zwingelstein G, Abdul-Malak N, Doré JF (1978): Biochem Biophys Res Commun 85:916-920

Poste G, Nicolson GL (1980): Proc Natl Acad Sci USA 77:399-403

Pratt HPM, Saxon A, Graham ML (1978): Leukaemia Res 2:1-10

Price MR, Baldwin RW (1977): in: Dynamic Aspects of Cell Surface Organisation, G Poste, G Nicolson (eds.), Chapter 8, Elsevier, Amsterdam, pp.423-471

Prokazova NV, Kocharov SL, Shaposhnikova GI, Svezdina ND, Bergelson LD (1984): Eur J Biochem 141:527-529

Radsak K, Schwarzmann G, Wiegandt H (1982): Hoppe-Seyler's Z Physiol Chem 363:263-272

Ramshaw IA, Badenoch-Jones P (1985): Cancer Metastasis Rev 4:195-208

Ramshaw IA, Carlsen SA, Hoon D, Warrington RC (1982): Int J Cancer 30:601-607

Ramu A, Glaubiger D, Weintraub H (1984): Cancer Treat Rep 68:637-641

Ramu A, Glaubiger D, Magrath IT, Joshi A (1983): Cancer Res 43:5533-5537

Rajaram OV, White GH, Barter PJ (1980): Biochim Biophys Acta 617:383-392

Reading CL, Hutchins JT (1985): Cancer Metastasis Rev 4:221-260

Record M, El Tamer A, Chap H, Douste-Blazy L (1984): Biochim Biophys Acta 778:449-456

Redgrave TG (1970): J Clin Invest 49:465-471

Renooij W, van Golde LMG, Zwaal RFA, van Deenen LLM (1976): Eur J Biochem 61:53-58

Resch K, Schneider S, Szamel M (1981): Anal Biochem 117:282-292

Resch K, Schneider S, Szamel M (1983): Biochim Biophys Acta 733:142-153

Rifkin MR (1979): Proc Natl Acad Sci USA 75:3450-3454

Rintoul DA, Center MS (1984): Cancer Res 44:4978-4980

Riordan JR, Ling V (1985): Pharmac Ther 28:51-75

Riordan JR, Fahim S, Kantner N, Ling V (1982): J Cell Biochem Suppl 6:382

Robertson JD (1960): Prog Biophys and Biophys Chem 10:343

Robertson JD (1963): J Cell Biol 19:201-221

Roninson IB, Abelson HT, Housman DE, Howell N, Varshavsky A (1984): Nature 309:626-628

Rooney MW, Yachnin S, Kucuk O, Lis LJ, Kauffman JW (1985): Biochim Biophys Acta 820:33-39

Rosenfeld SI, Packman CH, Leddy JP (1983): J Clin Invest 71:795-808

Rosenthal MD (1981): Lipids 16:173-182

Rothman JE, Lenard J (1977): Science 195:743-753

Rye KA, Barter PJ (1986): Biochim Biophys Acta 875:429-438

Sandra A, Pagano RE (1978): Biochemistry 17:332-338

Satouchi K, Mizuno T, Samejima Y, Saito K (1984): Cancer Res 44:1460-1464

Schmidt CF, Barenholz Y, Huang C, Thompson TE (1978): Nature (London) 271:775-777

Schneeberger EE, Lynch RD, Geyer RP (1971): Exp Cell Res 69:193-206

Schroeder F, Gardiner JM (1984): Cancer Res 44:3262-3269

Schroeder F, Fontaine RN, Kinden DA (1982): Biochim Biophys Acta 690:231-242

Schroeder F, Fontaine RN, Feller DJ, Weston KG (1981): Biochim Biophys Acta 643:76-88

Schumacher HR, Szekely IE, Park SA, Rao UNM, Fisher DR, Patel SB (1973): Am J Path 73:27-39

Seelig A, Seelig J (1978): Hoppe-Seyler's Z Physiol Chem 359:1747-1756

Seelig J, Seelig A (1980): Q Rev Biophys 13:19-61

Shaposhnikova GI, Prokazova NV, Buznikov GA, Zvezdina ND, Teplitz NA, Bergelson LD (1984): Eur J Biochem 140:567-570

Sharom FJ, Grant CWM (1977): J Supramolec Struct 6:249-258

Sharom FJ, Grant CWM (1978): Biochim Biophys Acta 507:280-293

Shen D, Cardarelli C, Hwang J, Cornwell M, Richert N, Ishii S, Pastan I, Gottesman MM (1986): J Biol Chem 261:7762-7770

Shepherd J, Bicker S, Lorimer AR, Packard CJ (1979): J Lipid Res 20:999-1006

Shinitzky M (1984): in: Physiology of Membrane Fluidity, M Shinitzky (ed.), Vol.I, Chapter 1, pp.1-39. CRC Press Inc., Florida

Shore V, Shore B (1975): Biochem Biophys Res Commun 65:1250-1256

Simons K, Ehnholm C, Renkonen O, Bloth B (1970): Acta Path Microbiol Scand Section B 78:459-466

Simpson RW, Hirst GK (1961): Virology 15:436-451

Singer SJ (1971): in: Structure and Function of Biological Membranes, LI Rothfield (ed), Academic Press, New York, pp146-217

Singer SJ, Nicolson GJ (1972): Science 175:720-731

Skipski VP, Barclay M, Archibald FM, Lynch TP Jr, Stock CC (1971): Proc Soc Exp Biol Med 136:1261-1264

Skipski VP, Barclay M, Archibald FM, Stock CC (1975a): Prog Biochem Pharmacol 10:112-134

Skipski VP, Katopodis N, Prendergast JS, Stock CC (1975b): Biochem Biophys Res Commun 67:1122-1127

Skipski VP, Carter SP, Terebus-Kekish OI, Podlaski FJ Jr, Peterson RHF, Stock CC (1981): J Natl Canc Inst 67:1251-1258

Smith ICP (1979): Can J Biochem 57:1-14

Snyder F (1972): in: Ether Lipids: Chemistry and Biology, F Snyder (ed.). Academic Press, New York, pp.273-395

Sorlie PD, Feinleib M (1982): J Natl Cancer Inst 69:989-996

Sottocasa GL, Kuylenstierna B, Emster L, Bergstrand A (1967): J Cell Biol 32:415-438

Spiegel RJ, Magrath IT, Shutta JA (1981): Cancer Res 41:452-458

Springer GF, Desai PR (1977): Transplant Proc 9:1105-1111

Steck GL, Dawsen G (1974): J Biol Chem 249:2135-2142

Steck PA, Nicolson GL (1984): Transplantation Proceedings, Vol.XVI, pp.355-360

Steim JM, Tourtellotte ME, Reinert JC, McElhaney RN, Rader RL (1969): Proc Natl Acad Sci USA 63:104-109

Steiner S, Melnick JL, Kit S, Somers KD (1974): Nature 248:682-684

Stier A, Finch SAE, Bösterling B (1978): Febs Lett 91:109-112

Stroun M, Anker P, Maurice P, Gahan PB (1977): Int Rev Cytology 51:1-48

Stubbs CD, Kouyama T, Kinosita K Jr, Ikegami A (1981): Biochemistry 20:4257-4262

Stubbs CD, Tsang WM, Belin J, Smith AD, Johnson SM (1980): Biochemistry 19:2756-2762

Svennerholm L (1957): Biochim Biophys Acta 24:604-611

Svennerholm L (1963): J Neurochem 10:613-623

Szamel M, Goppelt M, Resch K (1985): Biochim Biophys Acta 821:479-487

Szamel M, Schneider S, Resch K (1981): J Biol Chem 256:9198-9204

Terpstra AHM, Woodward CJH, Sanchez-Muniz FJ (1981): Anal Biochem 111:149-157

Thomopoulos P, Berthelier M, Lagrange D, Chapman MJ, Laudat MH (1978): Biochem J 176:169-174

Tkaczuk P, Thornton ER (1979): Biochem Biophys Res Commun 91:1415-1422

Torrent-Quetglas M, Rivera-Fillat MP, Grau-Oliete MR (1981): Anal Biochem 114:228-234

Turner DA (1985): Seminars in Nuclear Medicine xv:210-223

Turner GA (1982): Invasion Metastasis 2:197-216

Ulmius J, Wennerström H, Lindblom G, Arvidson G (1975): Biochim Biophys Acta 389:197-202

Untracht SH, Shipley GG (1977): J Biol Chem 252:4449-4457

Upreti GC, de Antueno RJ, Wood R (1983): J Natl Cancer Inst 70:559-566

Urdal DJ, Hakomori S (1980): J Biol Chem 255:10509-10516

Valentine FT, Lawrence HS (1969): Science 165:1014-1016

Valk J, MacLean C, Algra PR (1985): in: Basic Priniples of Nuclear Magnetic Resonance Imaging. Elsevier, Amsterdan, New York, Oxford

Van Blitterswijk WJ (1984): in: Physiology of Membrane Fluidity, M Shinitzky (ed.), Volume II, Chapter 3. CRC Press Inc., Florida, pp.53-85

Van Blitterswijk WJ, de Veer G, Krol JH, Emmelot P (1982): Biochim Biophys Acta 688:495-504

Van Blitterswijk WJ, Emmelot P, Hilgers J, Kamlag D, Nusse R, Feltkamp CA (1975): Cancer Res 35:2743-2751

Van Blitterswijk WJ, Emmelot P, Hilkmann HAM, Oomen-Meulemans EPM, Inbar M (1977): Biochim Biophys Acta 467:309-320

Van Blitterswijk WJ, Emmelot P, Hilkmann HAM, Hilgers J, Feltkamp CA (1979): Int J Cancer 23:62-70

Van Blitterswijk WJ, Van Hoeven RP, Van der Meer BW (1981): Biochim Biophys Acta 644:323-332

Van den Bergh FAJTM, Tager JM (1976): Biochim Biophys Acta 441:391-402

Van Hoeven RP, Emmelot P (1972): J Membrane Biol 9:105-126

Van Hoeven RP, Emmelot P, Krol JH, Oomen-Meulemans EPM (1975): Biochim Biophys Acta 380:1-11

Van Tol A, Van Gent T, Jansen H (1980): Biochem Biophys Res Commun 94:101-108

Vance DE, Sweeley CC (1967): J Lipid Res 8:621-630

Verkleij AJ (1980): in: Electron Microscopy at Molecular Dimensions, W Baumeister, W Vogell (eds.). Springer-Verlag, New York, pp.328-337

Verkleij AJ, Ververgaert PHJ Th (1978): Biochim Biophys Acta 515:303-327

Vrignaud P, Montaudon D, Londos-Gagliardi D, Robert J (1986): Cancer Res 46:3258-3261

Wagner G, Kumar A, Wüthrich K (1981): Eur J Biochem 114:375-384

Waite M, Parce B, Morton R, Cunningham C, Morris HP (1977): Cancer Res 37:2092-2098

Wallach DFH (1975): in: Membrane Molecular Biology of Neoplastic Cells, Chapter 3, Elsevier Scientific Publishing Co., Amsterdam, pp.141-183

Wallach DFH, Kamat VB (1964): Proc Natl Acad Sci USA 52:721-728

Wallach DFH, Kamat VB (1966): in: Methods Enzymol, SP Colowick, NO Kaplan (eds.). Academic Press, New York, pp.164-172

Wallack MK, Brown AS, Rosato EF, Runin S, Johnson JI, Rosato FE (1978): J Surg Oncol 10:39-44

Watanabe K, Hakomori S (1976): J Exp Med 144:644-653

Watson JD (1977): in: Molecular Biology of the Gene (3rd edition), Chapter 18. WA Benjamin Inc., Menlo Park, California, pp.558-559

Weinberg RA (1982): Adv Cancer Res 36:149-163

Wennerström H, Lindblom G (1977): Q Rev Biophys 10:67-96

Wennerström H, Ulmius J (1976): J Mag Res 23: 431-435

Wharton DC, Tzagoloff A (1967): Methods Enzymol 10:245-250

Wheeler C, Rader R, Kessel D (1982): Biochem Pharmacol 31:2691-2693

Wieczorek AJ (1983): Hoppe-Seyler's Z Physiol Chem 364:1229

Wieczorek AJ, Rhyner G, Block LH (1985): Proc Natl Acad Sci USA 82:3455-3459

Wiegandt H (1985): in: New Comprehensive Biochemistry: Glycolipids, A Neuberger, LLM Van Deenen (eds.), Vol.10. Elsevier, Amsterdam, New York, Oxford, p1, p.106

Williams AF (1985): Nature 314:579-580

Williams AF, Gagnon J (1982): Science 216:696-703

Williams JP, Merrilees PA (1970): Lipids 5:367-370

Williams PG, Helmer MA, Wright LC, Dyne M, Fox RM, Holmes KT, May GL, Mountford CE (1985): FEBS Lett 192:159-164

Yamazaki M, Shinoda H, Hattori R, Mizuno D (1977): Gann 68:513-516

Yang HJ, Hakomori S (1971): J Biol Chem 246:1192-1200

Yau TM, Weber MJ (1972): Biochem Biophys Res Commun 49:114-120

Yeagle PL (1985): Biochim Biophys Acta 822:267-287

Yogeeswaran G (1983): Adv Cancer Res 38:289-350

Yogeeswaran G, Salk PL (1981): Science 212:1514-1416

Yogeeswaran G, Sheinin R, Wherrett JR, Murray RK (1972): J Biol Chem 247:5146-5158

Young WW Jr, Hakomori S (1981): Science 211:487-489

Vol. 13, No. 2, August 1986 BIOCHEMISTRY INTERNATIONAL
Pages 295-305

CELLULAR RESISTANCE TO VINBLASTINE IS ASSOCIATED WITH ALTERED RESPIRATORY FUNCTION

Lesley C. Wright, Marlen Dyne, Kerry T. Holmes, Tony Romeo*
and Carolyn E. Mountford
Ludwig Institute for Cancer Research (Sydney Branch), Blackburn Building,
University of Sydney, Sydney, N.S.W. 2006, Australia.
*Electron Microscope Unit, Madsen Building, University of Sydney,
Sydney, N.S.W. 2006, Australia.

Received May 26, 1986

SUMMARY

Human leukaemic T lymphoblasts made resistant to low levels (20 - 40 ng/ml) of vinblastine have altered respiratory capacity. Cellular oxygen uptake was greater in resistant cells compared with sensitive cells, and vinblastine (40 ng/ml) caused immediate inhibition of oxygen uptake in sensitive cells, but not in resistant cells. Isolated mitochondria reflected the changes observed in the intact cells. Rates of oxidation of cytochrome c, succinate and glutamine were higher in mitochondria from resistant cells and were little affected by challenge with vinblastine, whereas vinblastine at 40 ng/ml was completely inhibitory for sensitive cell mitochondria. Azide inhibited vinblastine efflux from sensitive and resistant cells in both the presence and absence of glucose. Levels of protein, total lipid, free cholesterol and cardiolipin were elevated in vinblastine-resistant lymphoblasts.

INTRODUCTION

Cellular resistance to anticancer drugs has long posed a problem in cancer management. Cell lines resistant to colchicine, vinca alkaloids and anthracyclines have several features in common. These include decreased cellular accumulation of drug, cross resistance to drugs other than the original selective agent (1,2), and over production of a 170,000 dalton glycoprotein in the plasma membrane (3).

In resistant cells active transport mechanisms involving energy metabolism have been proposed to account for the reduced cellular accumulation of drugs such as daunomycin, vincristine and vinblastine. (Review, see reference 1). However the roles of respiration and glycolysis in the acquisition of drug resistance have not been investigated.

The suggestion that cancer cells could have an impaired respiratory capacity and that inhibitors of mitochondrial respiration and oxidative phosphorylation might in general have anticancer effects was proposed as early

0158-5231/86/080295-11$01.00/0

as 1930 (4). The vinca alkaloid anticancer drug vinblastine, is known to cause a slight inhibition of respiration in L1210 leukaemic cells and an increase in aerobic glycolysis (5). In addition, oxygen uptake in the presence of glucose was partly inhibited in Sarcoma 180 and three Morris hepatoma lines by vinblastine and fluoropyruvate (6). These effects were reversed by glutamate. Skoda and co-workers (7) found that vinblastine but not vincristine inhibited the maturation of the precursor of mitochondrial aspartate aminotransferase, a key enzyme in cancer cell respiration of glutamine.

Since vinblastine has some effect on the respiration of malignant cells, we investigated the possibility that cellular resistance to vinblastine was linked with respiration. Using a human acute lymphoblastic leukaemic T cell line, CCRF-CEM, made resistant to low levels of vinblastine (20 - 40 ng/ml) we provide evidence that cellular resistance to vinblastine *in vitro* is associated with altered respiratory function which could affect drug efflux.

MATERIALS AND METHODS

Cell Culture: The acute lymphoblastic leukaemic T cell line, CCRF-CEM, was cultured in RPMI-1640 medium supplemented with 10% foetal calf serum. Cell doubling time was approximately 24 hours.

Drug Resistance: Lymphoblasts were made resistant to vinblastine by growing cells in the presence of increasing but sublethal concentrations of the drug. The IC_{50} (3) of CCRF-CEM cells not previously exposed to vinblastine was 3 ng/ml. The concentration of vinblastine in the growth medium was increased stepwise until, after a period of some weeks, cells were able to grow in 20 or 40 ng/ml of drug with a normal doubling time. The cells are designated VBL-20 or 40, respectively. All experiments described below were carried out with cells maintained in drug-free medium for at least two weeks. The resistance was not completely stable e.g. in VBL-20 there was a decrease in IC_{50} from 60 to approximately 30 ng/ml over an 8 week period. The p-glycoprotein reported by Beck *et al.* (3) is increased by three fold in VBL-20 cells compared with sensitive cells (our unpublished data).

Electron Microscopy: The pellets of 10^6 cells previously washed with phosphate buffered saline (PBS) were fixed with 2% glutaraldehyde in PBS, post-fixed with 1% osmium tetroxide in PBS, and stained *en bloc* with 0.5% aqueous uranyl acetate, dehydrated through a graded series of acetone and H_2O and embedded in Spurrs resin. Ultra thin sections were cut, stained with uranyl acetate and lead citrate, and examined in a Philips 400 Electron Microscope at 100 kv.

Lipid Analysis: Total lipid, phospholipid, triglyceride, cholesterol and cholesterol ester were all estimated as described previously (8). Cardiolipin was estimated in polar lipid extracts, separated from the total cell lipid by silica gel column chromatography. The individual phospholipid components were separated on plastic-backed silica gel (Merck) TLC sheets run in two directions, and the phosphorus content estimated for each spot (9).

Cell Respiration: Cell respiration was measured at 37°C in 2 ml volumes in a Rank oxygen electrode. Optimum rates were obtained using 0.5 - 1 x 10^8 cells. Oxygen uptake was measured in salt medium (8 mM morpholinopropane sulfonic acid (MOPS) pH 7.4 containing 145 mM NaCl, 5.6 mM KCl, with or without 10 mM glucose). The cells were washed three times in 0.9% NaCl before use. The trypan blue exclusion test was used to determine cell viability at the end of the experiments.

Cytochrome c Oxidase Activity: This was measured in cell homogenates, obtained by freeze-thawing in liquid nitrogen, and in isolated mitochondria by a spectrophotometric method (10). Linearity of enzyme activity with both time and protein concentration was established.

Lactate Production: This was measured in salt medium at 37°C using a UV spectrophotometric kit method (Boehringer-Mannheim, 139084).

Protein: The protein content of cell homogenates and mitochondria was measured using the Bio-Rad dye reagent (Bio-Rad 500-0001), with bovine serum albumin as a standard.

Mitochondrial Isolation: Mitochondria were isolated from cells by the method of Carpentieri and Sordahl (11) in medium containing 0.25 M sucrose, 5 mM Tris-HCl, 5 mM EGTA and 0.5% bovine serum albumin. Mitochondria were washed and resuspended in the same medium, but without EGTA. Respiratory activity was measured in a Rank oxygen electrode at 37°C in a 1.4 ml volume. The assay medium consisted of 0.25 M sucrose, 1.0 mM Tris-HCl (pH 7.2), 75 mM KCl, 2 mM Pi, 5 mM $MgCl_2$. Succinate (2 mM) or glutamine (5 mM) were used as substrates.

Uptake and Export of Vinblastine: Both sensitive and VBL-20 resistant cells were suspended for 1h in RPMI growth medium at 37°C with 20 ng/ml vinblastine containing 0.063 uCi/ml of [G-^{3}H]vinblastine sulphate. The cells were then washed twice in saline and once in MOPS salt medium at 4°C. They were made to a volume of 2 ml with salt medium alone (control) or with the addition of glucose and/or azide and incubated at 37°C for 20 min. Cells were pelleted by centrifugation at room temperature for 5 min. The cell pellets were dissolved in 3N NaOH at 60°C, neutralized with HCl and ACS scintillant added to both pellets and supernatants. Radioactivity was then counted in an LKB type 1217 Rackbeta scintillation counter.

Statistics: Unless stated otherwise figures in the text are means ± standard deviations from the mean.

RESULTS AND DISCUSSION

Differences in Cellular Oxygen Uptake

The deregulation of cholesterol synthesis in tumour cells leads to the diversion of mitochondrial citrate from participation in the TCA cycle (review see reference 12). The utilization of glucose as a respiratory substrate precursor is diminished and respiration can be supported by glutamine via mitochondrial aspartate aminotransferase activity (12). The possibility of a number of conflicting pathways operating simultaneously led us to believe that

differences in oxygen uptake between sensitive and resistant cells might be more easily revealed in the absence of exogenous substrates. Oxygen uptake was therefore measured in salt medium rather than in RPMI-1640 growth medium which contains abundant respiratory substrates including glucose and glutamine. The rate for the VBL-20 cells was found to be double that of the sensitive cells. For 8 experiments the rates were 57.7 ± 22.2 and 105 ± 17.7 nmol O_2 per 10^8 cells per min for sensitive and resistant cells respectively. Intactness of cells was confirmed by trypan blue exclusion and by the failure of added succinate to enhance the rate of oxygen uptake.

This difference in oxygen uptake could reflect less endogenous respiratory substrate(s) in the sensitive cells. If this were true the addition of a respiratory substrate such as glucose to the salt medium should restore both cell lines to similarly high rates of oxygen consumption. However, although the sensitive cells increased their oxygen consumption by 100% when glucose was added to the salt medium, we found that the VBL-20 cells reduced the rate by 21% indicating their preference for utilisation of glucose for either aerobic glycolysis and/or mitochondrial citrate export (12). Since highly glycolytic tumour cells usually have poorly developed mitochondria (12) it was not surprising that the sensitive cells had a greater rate of lactate production (374 ± 9 ug/10^8 cells/h) in salt medium than VBL-20 cells (178 ± 33 ug/10^8 cells/h).

Effects of Vinblastine on Cellular Oxygen Uptake

Sensitive and resistant cells were treated with varying levels of vinblastine (from 20 - 1060 ng/ml) during respiration in salt medium without glucose. In sensitive cells 20 ng/ml VBL was sufficient to reduce the oxygen uptake to 84% of the initial value. However, when a further 20 ng/ml was added the rate dropped to zero (Fig. 1). Higher concentrations (e.g. 200 ng/ml) resulted in rates immediately dropping to zero. The effect of adding vinblastine could not be overcome by subsequent addition of 5 mM glutamine.

VBL-40 cells, on the other hand, responded very differently with no inhibition being detected below 260 ng/ml. A slight decrease in the rate was noted with higher concentrations of the drug, but 28% of the initial rate was still present at 1060 ng/ml. Once again glutamine did not restore the activity when added after the vinblastine.

Chemical Analysis of Cells

Analysis of whole cells (Table 1) showed that the protein content of the

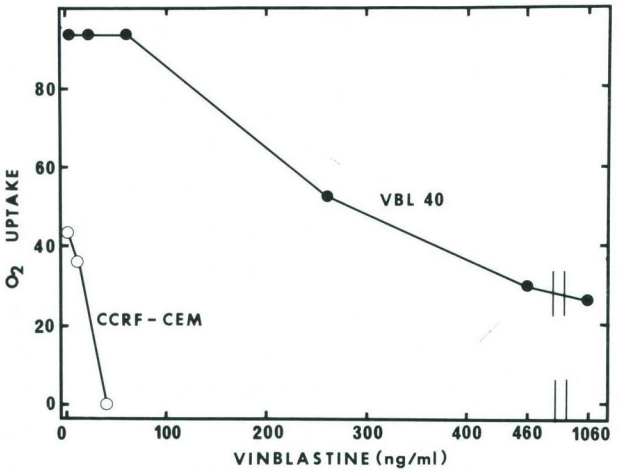

Fig. 1 Effects of vinblastine on the oxygen uptake of VBL-40 and sensitive cells in salt medium (no glucose). Rates of oxygen uptake are expressed as nmol/min/10^8 cells.

TABLE 1. Lipid and protein content of sensitive (CCRF-CEM) and resistant cells (VBL-20). Results are means ± S.D. from at least 5 experiments, except cardiolipin which was from 2 experiments. *Indicates results significantly different by the Mann-Whitney U Test. For the purposes of calculation, phosphorus was assumed to constitute 4% of phospholipid. The molecular weights of phospholipid triglyceride, and cholesterol ester were taken as 750, 885 and 650 respectively.

	SENSITIVE	RESISTANT
Total lipid ($mg/10^8$ cells)	1.37 ± 0.23	1.97 ± 0.46*
Free cholesterol ($nmol/10^8$ cells)	231 ± 40	320 ± 135*
Ester cholesterol ($nmol/10^8$ cells)	142 ± 53	162 ± 56
Phospholipid ($nmol/10^8$ cells)	940 ± 185	1245 ± 261
Triglyceride ($nmol/10^8$ cells)	135 ± 25	172 ± 48
Protein ($mg/10^8$ cells)	2.62 ± 0.4	4.54 ± 0.7*
Cardiolipin (% of phospholipid)	6.8 ± 0.1	8.7 ± 1.2*

resistant cells was increased. The total lipid content of the cells was elevated also with significant increases in free cholesterol and cardiolipin, which resides in the inner mitochondrial membrane (13). Because of its effects on the cytoskeleton, vinblastine treatment results in the accumulation of secretory vesicles containing VLDL in mouse hepatocytes (14) and it is possible that a similar interference with lipoprotein metabolism accounts for the increased cholesterol content observed in the resistant cells.

Fractionation of cellular membranes on a sucrose density gradient revealed that the increased cholesterol content, noted in Table 1, occurred in membrane fractions enriched in both plasma membrane and mitochondrial marker enzyme activities (our unpublished data). When tumour cell mitochondria were enriched with cholesterol they displayed increased succinate and glutamine-linked respiratory capacity with enhanced ADP-ATP exchange and increased mitochondrial ATPase activity (15). The behaviour of the mitochondria from resistant cells might be explicable on the basis of an increased cholesterol content. This has yet to be proven on purified mitochondria. Although the mean values were higher, the triglyceride, cholesterol ester and phospholipid content of VBL-20 cells was not significantly increased (Table 1). This contrasts with the 3.6 fold increase in cellular triglyceride content observed in doxorubicin-resistant P388 mouse leukaemia cells (16).

Ultrastructure of Sensitive and VBL Resistant Cells

Examination of CCRF-CEM sensitive and resistant cells by transmission electron microscopy revealed two major differences. The sensitive cells appeared to have mitochondrial profiles where the cristae were either absent or poorly developed (Fig. 2A), despite the double membrane remaining intact. This is normal for mitochondria of leukaemic lymphoblasts (17). In contrast, the mitochondrial profiles of the resistant cells appeared more numerous and have well developed cristae (Fig. 2B). Autophagocytic vacuoles bounded by a single membrane were seen more frequently in resistant cells. An increased organellar content is consistent with the increased cellular lipid and protein content of resistant cells (Table 1).

Fig. 2 ▷ A. Transmission electron micrograph of sensitive CCRF-CEM cells illustrating degenerate mitochondrial profiles (DM) and an autophagocytic vacuole (AV). Bar = 1 μm.
B. VBL-20 cells showing increased numbers of mitochondrial profiles (M). A number of small autophagocytic vacuoles (AV) can be seen in the top right hand cell. Bar = 1 μm.

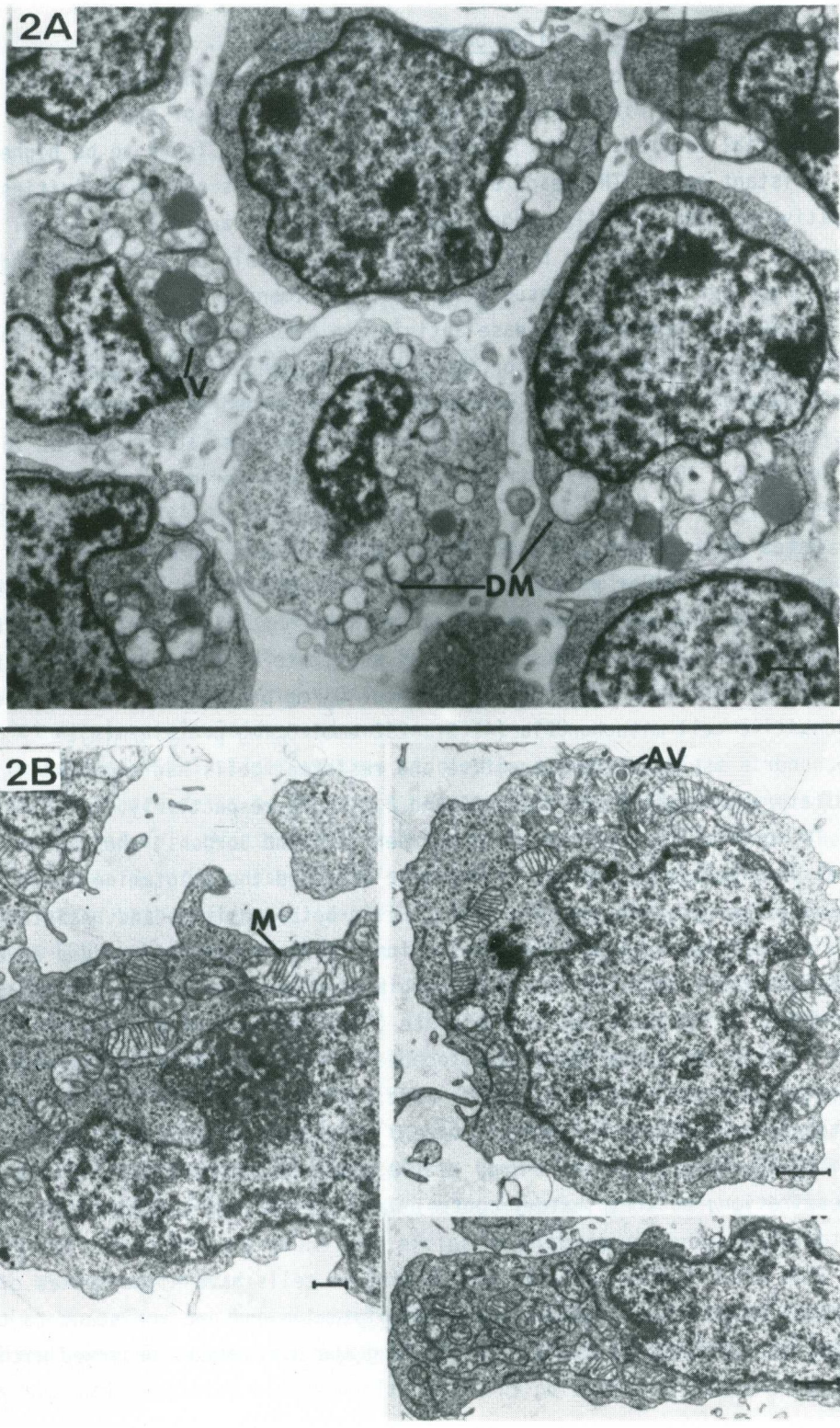
2A
V
DM
2B
M
AV

Effects of Vinblastine on Mitochondrial Respiration

The involvement of mitochondria in cellular resistance was further investigated using biochemical techniques. The activity of the inner mitochondrial membrane marker cytochrome c oxidase was found to be higher in the resistant cells. The means and standard deviations of the activities of sensitive and VBL-20 cell homogenates were 4.5 ± 0.3 and 7.8 ± 2.3 nmol substrate oxidised per min per mg protein respectively or 11.8 ± 2.6 and 35.4 ± 15.8 nmol per 10^8 cells respectively (6 experiments).

Because cytochrome c oxidase activity in homogenates might be influenced by the presence of activators or inhibitors, mitochondria isolated from sensitive and resistant cells were examined. Mitochondria isolated from sensitive and resistant cells have cytochrome c oxidase activities of 16.6 ± 0.9 and 34.6 ± 10.0 nmol substrate oxidized per min per mg protein respectively.

Rates of succinate oxidation by mitochondria were compared using suspensions of similar purity (i.e. where the increases in specific activity of cytochrome c oxidase from homogenate to mitochondria were similar). The rate of oxygen uptake using succinate as substrate by mitochondria isolated from VBL-20 resistant cells (84 ± 18.4 nmol O_2/mg protein/min) was double that of sensitive cell mitochondria (41.3 ± 2.2 nmol O_2/mg protein/min). Mitochondria isolated from sensitive and resistant cells had similar respiratory control ratios 2.1 ±.04 and 2.0 ± .05 respectively.

In contrast to the findings of Carpentieri and Sordahl, who studied both normal and leukaemic lymphoid cells (11), we found that glutamine acted as substrate (respiratory control ratio 2.2) in both sensitive and resistant cells with rates of about half the succinate rate. Vinblastine added at 20 ng/ml final concentration caused 50% inhibition of sensitive cell state 3 respiration using glutamine as substrate (Fig. 3). As in the whole cells, 40 ng/ml caused 100% inhibition. In mitochondria from VBL-40 cells the rates of oxidation of succinate and glutamine were higher than in VBL-20 mitochondria and there was a 37% inhibition of state 3 respiration by 20 ng/ml vinblastine (Fig. 3). Further aliquots of drug to 100 ng/ml caused no additional decrease in respiration, but respiratory control was lost. Higher concentrations were not tested.

Thus mitochondria isolated from resistant cells have higher rates of oxidation of succinate, cytochrome c and glutamine and are resistant to the effects of vinblastine, thereby paralleling the differences observed with whole cell oxygen uptake.

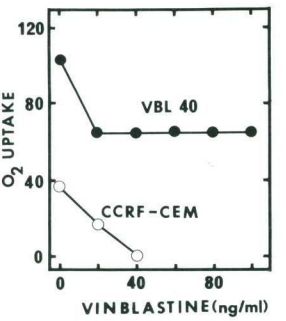

Fig. 3 Effects of vinblastine on the state 3 respiration of mitochondria isolated from sensitive CCRF-CEM cells and VBL-40 cells using glutamine (5 mM) as substrate. The rates of oxygen uptake are expressed as nmol/mg protein/min.

The Role of Respiration in Drug Efflux

Sensitive and VBL-20 cells were incubated with [^{3}H] labelled vinblastine (20ng/ml) for 1h in growth medium. The cellular accumulation of drug was nine-fold greater in the sensitive cells compared with the VBL-20 cells (5.4 ± 0.08 ng/h/10^8 cells and 0.6 ± 0.1 ng/h/10^8 cells respectively). Decreased cellular accumulation of drug is typical of cell lines resistant to colchicine, vinca alkaloids, and anthracyclines (1).

Leakage of vinblastine was then studied by transferring the vinblastine-loaded cells to drug-free salt medium. The efflux from VBL-20 cells was three-fold greater than from the sensitive cells (Table 2). The addition of azide or glucose either separately or together enhanced lactate production in both cell types (Table 2). Drug efflux, however, was diminished by about 50% with azide and the stimulus induced by glucose was also abolished. Ouabain inhibited lactate production by 11% in both cell types but did not reduce vinblastine efflux.

Metabolic inhibitors such as azide stimulate the accumulation of anthracyclines and vinca alkaloids in Ehrlich ascites and P388 leukaemia cells (1,2). Glucose enhances drug efflux in the presence of respiration inhibitors in these cells, suggesting that glycolysis is the main source of energy for active export (1,2). Our results in Table 2, however, show that in CCRF-CEM lymphoblasts the correlation of drug efflux is with respiratory capacity rather than glycolysis.

In conclusion, we have demonstrated that vinblastine (40 ng/ml) causes total and immediate arrest of oxygen uptake in cultured sensitive CCRF-CEM cells and their isolated mitochondria. However, neither the oxygen uptake of

TABLE 2. Release of [^{3}H] vinblastine and lactate into salt medium by sensitive and VBL-20 cells. Lactate production and isotope distribution in cells and supernatants were measured after 20 min incubation at 37°C. Values represent the means ± standard errors of two separate experiments.

	SENSITIVE		VBL-20	
	% [^{3}H] Vinblastine in Supernatant	Lactate ($\mu g/10^8$ cells)	% [^{3}H] Vinblastine in Supernatant	Lactate ($\mu g/10^8$ cells)
Control	9.5 ± 0.5	91	27 ± 2	67
+ 10 mM azide	4.5 ± 0.5	146	13 ± 1	145
+ 10 mM glucose	13 ± 1	492	41 ± 1	402
+ 10 mM glucose + 10 mM azide	6 ± 0	605	30 ± 1	546
+ 1.5 mM ouabain	12 ± 0	81	25 ± 0	60

cells resistant to 20-40 ng/ml of vinblastine nor the respiration of their isolated mitochondria was greatly affected. Interestingly, the vinblastine resistant lymphoblasts appeared to have greater numbers of mitochondrial profiles with intact cristae and their mitochondria displayed enhanced respiratory chain enzyme activities i.e. from cytochrome c and succinate to oxygen and from glutamine to oxygen.

In addition to the increased plasma membrane p-glycoprotein which is believed to be involved in control of membrane permeability (18) we have shown that there is also a respiration-dependent, active outward transport mechanism for vinblastine in leukaemic lymphoblasts. The increased activity of this efflux mechanism can now be linked with the greater respiratory capacity of resistant cells in the presence of vinblastine.

ACKNOWLEDGEMENTS

We are grateful to Dr John Pollak for his many helpful discussions.

REFERENCES

1. Danø,K., Skøvsgaard. T., Nissen, N.I., Fricke, E., and Di Marco, A. (1983) 13th International Cancer Congress, Part C, Biology of Cancer (2), pp.231-246, Alan R. Liss Inc., New York.
2. Inaba, M., and Sakurai, Y. (1979) Cancer Letters, 8, 111-115.
3. Beck, W.T., Mueller, T.J., and Tanzer, L.R. (1979) Cancer Res. 39, 2070-2075.
4. Warburg, O. (1930) The metabolism of tumours (Constable, A., ed.), London.
5. Hunter, J.C. (1963) Biochem. Pharmacol. 12, 283-291.
6. Regan, D.H., Lavietes, B.B., Regan, M.G., Demopoulos, H.B., and Morris, H.P. (1973) J. Natl. Cancer Res. Inst. 51, 1013-1017.
7. Skoda, R.C., Jaussi, R., and Christen, P. (1983) Biochem. Biophys. Res. Commun. 115, 144-152.
8. Mountford, C.E., Wright, L.C., Holmes, K.T., Mackinnon W.B., Gregory, P., and Fox, R.M. (1984) Science. 226, 1415-1418.
9. Wright, L.C., Dyne, M., Holmes, K.T., and Mountford, C.E. (1985) Biochem. Biophys. Res. Commun. 133, 539-545.
10. Wharton, D.C., and Tzagaloff, A. (1967) in Methods in Enzymology (Colowick, S.P. and Kaplan, N.O., eds.), Vol.10, pp.245-250, Academic Press, New York.
11. Carpentieri, U., and Sordahl, L.A. (1980) Cancer Res. 40, 221-224.
12. Coleman, P.S., and Lavietes, B.B. (1981) CRC Critical Rev. Biochem. 341-393.
13. Krebs, J.J.R., Hauser, H., and Carafoli, E. (1979) J. Biol.Chem. 254, 5308-5316.
14. Kovacs, A.L., Laszlo, L., and Kovacs, J. (1985) Exp. Cell. Res. 157, 83-94.
15. Parlo, R.A., and Coleman, P.S. (1984) J. Biol. Chem. 259, 9997-10003.
16. Ramu, A., Glaubiger, D., and Weintraub, H. (1984) Cancer Treatment Reports 68, 637-641.
17. Schumacher, H.R., Szekely, I.E., Park, S.A., Rao, U.N.M., Fisher, D.R., and Patel, S.B. (1973) Am. J. Path. 73, 27-39.
18. Garman, D., Albers, L., and Center, M.S. (1983) Biochem. Pharmacol. 32, 3633-3627.

Vol. 133, No. 2, 1985 BIOCHEMICAL AND BIOPHYSICAL RESEARCH COMMUNICATIONS
December 17, 1985 Pages 539-545

PHOSPHOLIPID AND ETHER LINKED PHOSPHOLIPID CONTENT ALTER WITH CELLULAR RESISTANCE TO VINBLASTINE

Lesley C. Wright, Marlen Dyne, Kerry T. Holmes and Carolyn E. Mountford

Ludwig Institute for Cancer Research (Sydney Branch), Blackburn Building, University of Sydney, Sydney, N.S.W 2006, Australia

Received October 31, 1985

The phospholipid and ether linked phospholipid content of leukaemic lymphocytes alters when the cells become resistant to low levels of the anti-cancer drug, vinblastine. Sphingomyelin and cardiolipin increase, and phosphatidyl ethanolamine and serine decrease in resistant cells. In addition, increases in 1-alkyl-2-acyl phosphatidyl choline and 1-alkenyl-2-acyl -phosphatidyl ethanolamine are concomitant with decreased 1,2-diacyl phosphatidyl choline and ethanolamine. Changes to the ultrastructure of the inner half of the plasma membrane bilayer, as a consequence of drug resistance, are illustrated by freeze-fracture electron microscopy.

The development of multi-drug resistance in the cancer patient is a major limitation to chemotherapy. Despite numerous in vitro studies of this phenomenon the mechanisms involved are not fully understood. However, cell lines resistant to colchicine, vinca alkaloids and anthracyclines have several features in common. These include decreased cellular accumulation of drug, cross resistance to drugs other than the original selective agent, and over production of a 170,000 dalton glycoprotein in the plasma membrane and a 19,000 dalton protein in the cytoplasm (1-5).

Increased sphingomyelin to phosphatidyl choline ratios have been reported in cellular lipids from P388 murine leukaemia cells made resistant to doxorubicin (6) and a higher degree of structural order has been shown in the plasma membrane lipids of these cells (7). In another study sensitive murine fibroblasts treated for 4 h with 100 μM vinblastine showed decreased plasma membrane phosphatidyl serine (8).

ABBREVIATIONS ALL: acute lymphoblastic leukaemic; PL: phospholipid; PE: phosphatidyl ethanolamine; PC: phosphatidyl choline; PS: phosphatidyl serine; SPH: sphingomyelin; PI: phosphatidyl inositol; PG: phosphatidyl glycerol; CL: cardiolipin.

0006-291X/85 $1.50

The purpose of the present study was to characterise the cellular phospholipid and ether-linked phospholipid content of vinblastine sensitive and resistant human ALL T lymphocytes as an indication of plasma membrane differences. In addition to confirming the increased sphingomyelin content reported for resistant P388 cells (6) we found decreased phosphatidyl ethanolamine and serine and increased cardiolipin. A significant increase in ether-linked phospholipid was recorded with cellular resistance to low levels of vinblastine (20 ng/ml). This observation, together with the altered plasma membrane topography demonstrated by freeze-fracture, has not been reported before.

MATERIALS AND METHODS

Cell Lines and Tissue Culture

Cells of the acute lymphoblastic (ALL) T cell line CCRF-CEM, both sensitive and resistant to vinblastine (described below), were grown in RPMI-1640 supplemented with 10% foetal calf serum as previously described (9).

Development of Vinblastine Resistant Cells

The cultured human leukaemic T cell line CCRF-CEM was made resistant to 20 ng/ml of vinblastine by growing cells in the continuous presence of increasing, sublethal concentrations of drug. All experiments were performed on cells which had been grown in drug-free medium for at least two weeks, by which time the vinblastine concentration inside the cells was estimated to be less than 0.5 ng/ml.

Lipid Isolation

Lipids were isolated from whole cells as previously described (10).

Phospholipid Composition

Polar lipids were separated from total cell lipids by chromatography on a silica gel 60 (Merck) column, then fractionated by two-dimensional TLC. The solvent systems used were (i) chloroform : methanol : acetic acid : water (25:8:8:1 v/v) and (ii) tetrahydrofuran : dimethoxymethane : methanol : water (20:12:8:2 v/v). The phospholipid content of each TLC spot was determined by the method of Duck-Chong (11).

Alkenyl and Alkyl Phospholipid Determination

Polar lipid extracts from whole cells were analysed by two dimensional TLC, essentially according to the method of El Tamer *et al.* (12). The acyl chain in position 1 of the diacyl phospholipids was hydrolysed by phospholipase A_1 from guinea pig pancreas, followed by acid fume hydrolysis of the 1-alkenyl-2-acyl species. The 1-alkyl-2-acyl species remained intact.

Electron Microscopy

Unfixed cell concentrates in phosphate buffered saline were frozen in liquid nitrogen-cooled Freon 22 and fractured at -100°C in a Balzer Freeze Etch Unit (BAF300). Replicas were examined in a Philips 400 electron microscope operating at 100 kV. The terminology of Branton *et al.* (13) is used in referring to membrane fracture faces.

The increase in surface area of the plasma membrane of the resistant cells was modelled as a number of hemispheres, and calculated by measuring distance

(X) in the direction of the shadow through to midpoint of the elevated areas (bulges).The radius (r) of the hemispheres was derived trigonometrically from the platinum shadow arriving at an angle of 45°. The surface area of a hemisphere would contribute an increase in surface area of $2\pi r^2-\pi r^2=\pi r^2$. A second measurement was made to ensure that in most cases the value of X which is the area of shadow plus the diameter was greater than the diameter of the hemisphere at right angles to the direction of shadowing. A total of 2 μ^2 of a cell membrane was measured containing 67 bulges. Stereo pairs at ± 6° were taken of the area measured and the cell curvature was found to be negligible therefore calculations were of a non-curved surface.

RESULTS

Phospholipid Analysis

Separation of the phospholipids by TLC, revealed differences in the relative quantities of lipid between sensitive and resistant cells. The resistant cells contained 2.5% more SPH, 2% more CL, 4% less PE and 1% less PS (Table 1), but there were no significant differences in PI or PG. The increase in the positively charged phospholipids (PC + SPH) by 4% is balanced by a 5% decrease in negatively charged phospholipid (PE + PS).

More striking differences were recorded when PE and PC were separated into their 1,2-diacyl, 1-alkenyl-2-acyl and 1-alkyl-2 acyl components (Table 2). Resistant cells had 10% more 1-alkyl-2-acyl PC and 27% more 1-alkenyl-2-acyl PE with concomitant decreases in 1,2-diacyl PC (10%) and 1,2-diacyl PE (27.5%). The amounts of 1-alkenyl-2-acyl PC and 1-alkyl-2-acyl PE remained the same.

The ether-linked phospholipid content of the resistant cells was 34% of the total phospholipid compared with 24% in the sensitive cells.

TABLE 1
PHOSPHOLIPID COMPOSITION

	SENSITIVE (% by weight of total)	RESISTANT
Origin + Lyso PC	0.3 ± 0	0.2 ± 0.1
Sphingomyelin (SPH)	3.0 ± 0.2	5.5 ± 0.3
Phosphatidyl Choline (PC)	44.3 ± 0.1	45.5 ± 1.4
Phosphatidyl Ethanolamine (PE)	30.7 ± 0.1	26.6 ± 0.4
Phosphatidyl Serine (PS)	5.8 ± 0.4	4.9 ± 0.1
Phosphatidyl Inositol (PI)	7.7 ± 0.4	8.1 ± 0.1
Phosphatidyl Glycerol (PG)	1.3 ± 0.9	0.9 ± 0.4
Cardiolipin (CL)	6.8 ± 0.1	8.7 ± 1.2

TABLE 2
DISTRIBUTION OF ACYL AND ETHER LINKED CHAINS IN PHOSPHOLIPIDS OF SENSITIVE AND RESISTANT LEUKAEMIC LYMPHOCYTES

	(% by weight of Phospholipid) SENSITIVE		RESISTANT		DIFFERENCE+ EXPRESSED AS % TOTAL	MEMBRANE*
	% of PC	% of PL	% of PC	% of PL	PL	FACE
PC						
Diacyl	80.2 ± 4.9	35.5	70.6 ± 4.7	32.1	- 3.4	outer
1-O-alkenyl	5.1 ± 1.4	2.3	5.1 ± 3.4	2.3	nil	outer
1-O-alkyl	14.7 ± 3.4	6.5	24.3 ± 1.6	11.1	+ 4.6	inner
PE						
Diacyl	50 ± 7.5	15.4	22.5 ± 9.0	5.9	- 9.5	outer
1-O-alkenyl	42.8 ± 7.2	13.1	69.7 ± 9.2	18.5	+ 5.4	both
1-O-alkyl	7.1 ± 0.3	2.2	7.8 ± 0.2	2.1	- 0.1	inner

+ Difference between sensitive and resistant;
* Lipid as located in Krebs II ascites cells (19).

Freeze Fracture Electron Microscopy

The faces developed from the fracture through the hydrophobic interior of the lipid bilayer of the plasma membrane are the outer or exoplasmic face (EF) and the inner or protoplasmic face (PF). Smooth fracture faces are considered to be formed by lipid bilayers (14) and the intramembraneous particles (IMPS) observed appear to be proteins intercalated in the membrane (15). IMPS can also be formed by lipopolysaccharides in the outer membrane of E. coli and by artificial lipid model systems (16).

The PF and EF faces of the resistant cells have 56% and 68% more IMPS respectively than the sensitive cells. The PF face of the plasma membrane of resistant cells is charaterized by the presence of elevated IMP free regions or bulges (Fig. 1B). The PF face of the sensitive cells does not have these elevated regions (Fig. 1A). The additional surface area provided by these bulges is calculated to be approximately 4% (see Materials and Methods).

DISCUSSION

An altered phospholipid composition and a higher ratio of SPH to PC accompanies cellular resistance to vinblastine (20 ng/ml) in the ALL T cell line

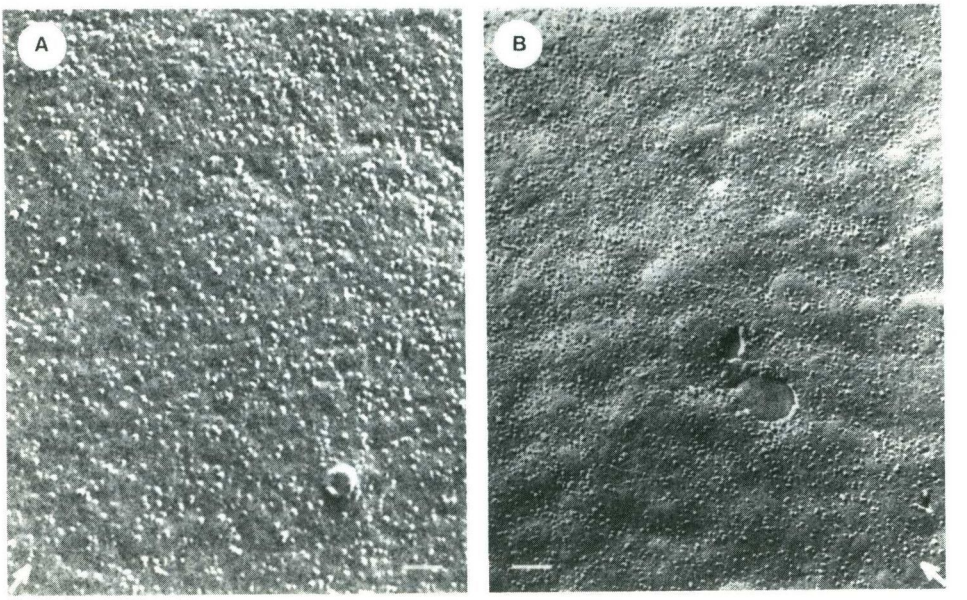

Fig. 1. Freeze fracture replicas of the protoplasmic face of the plasma membrane of CCRF-CEM. A(left): Sensitive cells. B(right): Vinblastine resistant cells. Arrow indicates the direction of shadowing. Bar = 100nm.

CCRF-CEM. The ratio of SPH to PC has been reported by Schmidt et al. (17) to be inversely proportional to the phospholipid structural order. In addition a decrease of 5% in the negatively charged phospholipids occurs with drug resistance.

The novel finding reported here is the alteration in ether and acyl phospholipid composition. These ether-linked lipids which are often elevated in cancer cells (18) account for 13% of the total phospholipid in sensitive cells and 27% in resistant cells. Diacyl and ether-linked phospholipids are membrane components, and plasma membranes, in particular, are rich in ether-linked phospholipids (19). Thus any changes detected in whole cell ether-linked phospholipids will reflect changes, qualitatively at least, in the plasma membrane (19).

Changes in cellular phospholipid composition due to drug resistance have been considered in the light of the distribution of phospholipids in the plasma membranes of Krebs II ascites cells (19) (Table 2). Differences in phospholipid subclasses between resistant and sensitive cells are expressed as a percentage

of the total phospholipid and some interesting observations are made, using the assumption that membrane lipid distribution in leukaemic lymphocytes resembles that of Krebs II ascites membranes.

The 1,2-diacyl PE and PC found on the external face is decreased by 12.9% when the cells become resistant to vinblastine. The 1-alkyl, 2-acyl PC (an inner face phospholipid) increases by 4.6%. The 1-O-alkenyl PE (plasmalogen), located on both faces, increases by 5.4% and therefore we have assumed an even distribution of a 2.7% increase in both halves of the bilayer. The net loss of major phospholipids from the outer half of the bilayer is therefore 10.2% and there is a concomitant gain of 7.2% lipid to the inner half of the bilayer (Table 2).

The overall increase in phospholipids as suggested by these calculations to be located on the inner face of the membrane could explain the elevated particle-free regions on the PF face of the plasma membrane in the electron micrographs. These elevated areas of lipid were calculated to increase the surface area by about 4%.

The increase in intramembranous particles in both PF and EF faces could reflect the increased p-glycoprotein content of the membranes, which has previously been associated with altered drug uptake (1). However, it must now be considered that increased levels of ether lipids would also alter permeability since ether lipids do not pack as closely in membranes as the corresponding diacyl species (20).

Two recent reports have linked increases in ether-containing membrane lipids with tumour progression (21,22). We have shown a similar association between drug resistance and ether-linked phospholipid and this raises the question of whether ineffective chemotherapy is leading to tumour progression.

ACKNOWLEDGMENTS

We would like to thank Professors Myer Bloom, Richard Fox, and Martin Tattersall for many helpful discussions and Dennis Dwarte for assistance with the electron microscopy.

REFERENCES

1. Beck, W.T., Mueller, T.J. and Tanzer, L.R. (1979) Cancer Res., 39, 2070-2075.

2. Biedler, J.L., Chang, T., Peterson, R.H.F., Melera, P.W., Meyers, M.B. and Spengler, B.A. (1983) In: Rational Basis for Chemotherapy, (B.A. Chabner, Ed.) pp71-92, Alan P. Liss Inc, New York.
3. Hill, B.T. and Whelan, R.D.H. (1982) Cancer Chemother. Pharmacol., 8, 163-169.
4. Ling, V., and Thompson, L.H. (1974) J. Cell Physiol., 83, 103-116.
5. Riordan, J.R., Fahim, S., Kartner, N. and Ling, V. (1982) Biochem. Supplement 6., 11th Annual UCLA Symposia Abstracts p.382.
6. Ramu, A., Glaubiger, D. and Weintraub, H. (1984) Cancer Treatment Reports, 68, 637-641.
7. Ramu, A., Glaubiger, D., Magrath, I.T. et al. (1983) Cancer Res., 43, 5533-5537.
8. Schroeder, F., Fontaine, R.N., Feller, D.J., and Weston, K.G. (1981) Biochim. Biophys. Acta, 643, 76-88
9. Mountford, C.E., Grossman, G., Reid, G. and Fox, R.M. (1982) Cancer Res., 42, 2270-2276.
10. Mountford, C.E., Wright, L.C., Holmes, K.T., Mackinnon, W.B., Gregory, P. and Fox, R.M. (1984) Science, 226, 1415-1418.
11. Duck-Chong, C. (1979) Lipids, 14, 492-497.
12. El Tamer, A., Record, M., Fauvel, J., Chap, H. and Douste-Blazy, L. (1984) Biochim. Biophys. Acta., 793, 213-220.
13. Branton, D., Bullivant, S., Gilula, N.B. et al. (1975) Science, 190, 54-56.
14. Verkleij, A.J. and Ververgaert, P.H.J. Th. (1978) Biochim. Biophys. Acta, 515, 303-327.
15. Murphy, C.R. and Swift, J.G. (1983) Acta. Anat., 116, 174-179.
16. Verkleij, A.J. (1980) In: Electron Microscopy at Molecular Dimensions, pp328-337, Baumeister W. and Vogell W. Ed. Springer-Verlag, New York.
17. Schmidt, C.F., Barenholz, Y. and Thompson, T.E. (1977) Biochemistry, 16, 2649-2656.
18. Snyder, F. (1972) in Ether Lipids: Chemistry and Biology (Snyder, F., Ed.) pp273-395, Academic Press, New York.
19. Record, M., El Tamer, A., Chap, H. and Douste-Blazy, L. (1984) Biochim. Biophys. Acta., 778, 449-456.
20. Boggs, J.M. (1980) Can. J. Biochem, 58, 755-770.
21. Roos, D.S., and Choppin, P.W. (1984) Proc. Natl. Acad. Sci., 81, 7622-7626.
22. Fallani, A., Bracco, M., Tombaccini, D., Mugnai, G. and Ruggieri, S. (1982) Biochim. Biophys. Acta., 711, 208-212.

Lipid domain in cancer cell plasma membrane shown by ^1H NMR to be similar to a lipoprotein

Philip G. Williams, Megan A. Helmer, Lesley C. Wright, Marlen Dyne, Richard M. Fox*, Kerry T. Holmes, George L. May and Carolyn E. Mountford+

Ludwig Institute for Cancer Research (Sydney Branch), Blackburn Building, University of Sydney, Sydney, NSW 2006, Australia

Received 6 September 1985

Human blood lipoproteins have been characterised by ^1H NMR methods and chemical analysis, and comparisons made with the properties of the triglyceride-rich plasma membrane domain found in cancer cells. By means of selective and non-selective T_1 experiments, the lipids in HDL and LDL are shown to be in diffusive exchange. In contrast, the lipids of chylomicra and VLDL do not exhibit lipid diffusion, and therefore resemble the neutral lipids of cancer cell plasma membranes. 2D scalar correlated NMR (COSY) spectra of cancer cells or solid tumours are similar to those obtained from VLDL and LDL. The long T_2 relaxation value observed for neutral lipid methylenes in metastatic cancer cells (> 300 ms) was not observed for any of the 4 lipoproteins studied. None of the lipoprotein classes gave a T_2 longer than 250 ms.

Lipoprotein *2D NMR* *Triglyceride* *(Cancer cell)* *Plasma membrane*

1. INTRODUCTION

High-resolution ^1H NMR spectra generated from lipids in the plasma membrane of cancer cells [1] are an indication of the biological status of those cells. The spectra have been used to monitor metastatic potential [2] and the onset of drug resistance (unpublished).

Two dimensional (2D) NMR [3] and chemical analysis of highly enriched plasma membranes have identified the membrane domain in question to be rich in triglyceride, with varying amounts of cholesterol ester [4]. Until recently triglyceride and cholesterol ester were considered unusual components of membranes [5].

The neutral lipid in the plasma membrane has an NMR linewidth of 10–30 Hz, and the application of selective and non-selective T_1 techniques [6] has detected no diffusive exchange with other lipids in the conventional bilayer [7]. Furthermore, the neutral lipids are able to tumble isotropically and independently of other membrane components [7].

Human lipoproteins provide a range of protein and lipid compositions and many of their properties are well documented [8–10]. These particles have been studied by T_1, T_2 and 2D NMR methods to determine if they provide a good model for the triglyceride rich plasma membrane domain in cancer cells.

2. MATERIALS AND METHODS

2.1. *Preparation of lipoprotein fractions*

Human blood (200 ml) was allowed to clot at room temperature for 2 h. Chylomicra were separated by flotation [11] and the remaining lipoprotein fractions were isolated according to Hatch and Lees [12]. All samples were dialysed against EDTA-Na_2 in D_2O (0.18%, pH 7.4) followed by 0.9% NaCl/0.01% NaN_3 in D_2O prior to NMR analysis.

+ To whom correspondence should be addressed
* Present address: Departments of Haematology and Oncology, Royal Melbourne Hospital, Parkville, VIC.3052, Australia

Published by Elsevier Science Publishers B.V. (Biomedical Division)
00145793/85/$3.30

2.2. *NMR spectroscopy*

^{1}H NMR spectra were recorded at 37°C using a Bruker WM-400 spectrometer equipped with an Aspect 2000 computer. 2D scalar correlated spectroscopy (COSY) experiments [3] and T_1 and T_2 measurements [7] have been described previously.

2.3. *Cell culture*

The cell line used for NMR analysis was the rat mammary adenocarcinoma line, J clone. Cells were grown in RPMI-1640 medium as described [7].

2.4. *Chemical analyses*

The protein content of the lipoprotein suspensions was obtained with the BioRad protein assay kit using bovine serum albumin as standard. The method of lipid extraction from dialysed lipoprotein samples was that of Gottfried [13], carried out at room temperature and in the presence of BHT (2,6-dibutyl-*p*-cresol). Non-lipid contaminants were removed by the method of Williams and Merrilees [14]. The lipid content of the extract was obtained by weighing an aliquot of the total lipid extract. The free cholesterol content of the lipid extracts was determined using an enzymic fluorometric method [15]. Total cholesterol content was measured by the same fluorometric method after saponification of the samples. Cholesterol ester content was calculated as the difference between total and free cholesterol content. Lipid phosphorus was determined on the total lipid extracts by a colorimetric method [16]. Triglyceride content was determined by using a colorimetric kit (Sigma technical bulletin no.405 [1983]).

3. RESULTS

The 4 main classes of human lipoproteins were isolated. Chemical analyses of protein and lipid content of the lipoprotein subclasses indicate that the fractions isolated are comparable with the literature. Cholesterol ester levels are lower than expected, and protein levels exceed those previously reported [8–10] (table 1). No attempt was made to purify the fractions. The sizes of the particles in each lipoprotein fraction, as determined by electron microscopy, are within the published values (table 1).

The 400 MHz ^{1}H NMR spectra of these 4 fractions are shown in fig.1 along with that obtained for a suspension of J clone cells. All spectra exhibit characteristics of a lipid spectrum with the -C=C-, $-N(CH_3)_3^+$, $(-CH_2)_n$ and CH_3 groups at 5.2, 3.2, 1.2 and 0.85 ppm, respectively [7]. However the HDL spectrum is very broad and it appears that the lipid spectrum is superimposed on a broad protein spectrum [17].

T_1 experiments were undertaken to determine if diffusion was taking place between the lipids. Based on the experiments by Brown and Davis [6],

Table 1

Chemical analysis of lipoprotein fractions

	% by wt[a]			
	Chylomicra	VLDL	LDL	HDL
Free cholesterol	0.15 ± 0.04	1.2 ± 0.12	2.2 ± 0.07	0.01 ± 0.0
Cholesterol ester	ND	3.1 ± 0.06	6.9 ± 0.30	0.1 ± 0.02
Phospholipid	5.2 ± 1.8	28.8 ± 0.33	41.7 ± 0.22	1.7 ± 0.23
Triglyceride	61.8 ± 3.9	49.3 ± 2.7	15.6 ± 0.59	0.3 ± 0.02
Protein	32.9 ± 6.7	17.6 ± 1.8	33.6 ± 3.7	97.9 ± 0.70
Particle size[b] (nm)	26–274	22–54	8–22	3–4

[a] The values represent the mean ± SE of 2 experiments except for chylomicra which is the mean ± SD for 3 experiments

[b] Particles were measured by negative staining electron microscopy. The preparations were stained with 1% ammonium molybdate solution (pH 8) and the electron micrographs obtained with a Philips 400 EM, operating at 100 kV and a maximum working magnification of 92000

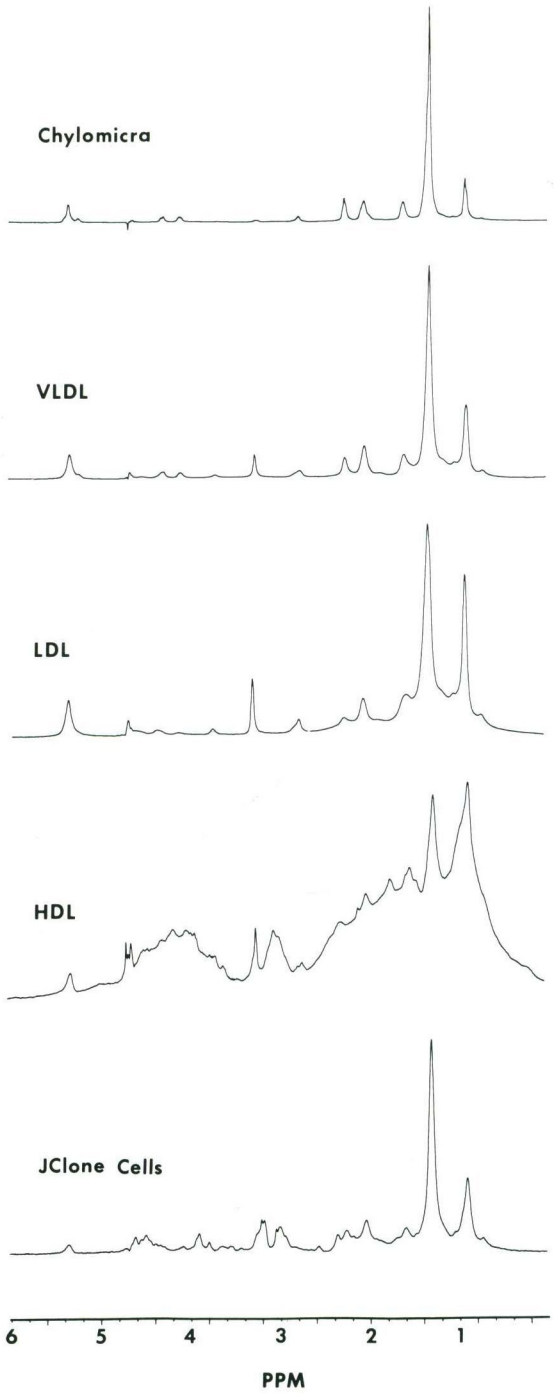

Fig.1. 400 MHz ^{1}H NMR spectra of chylomicra, VLDL, LDL, HDL and of the rat mammary adenocarcinoma cell line, J clone. Data were recorded at 37°C, with the sample spinning, using a sweep width of 4000 Hz. A line broadening of 3 Hz was applied.

the observation of single-exponential behaviour along with identical T_1 values for selective and non-selective inversion recovery experiments indicates that no exchange exists between protons contributing to the broad methylene resonance at 1.2 ppm [7]. This was the case for both chylomicra and VLDL, which had T_1 values of 0.55 ± 0.02 and 0.50 ± 0.02 s, respectively. In contrast LDL and HDL methylenes did not exhibit single exponential behaviour. Instead an initial rapid decay was observed due to transfer of magnetisation between the component lipids whilst the slope at longer times averages out over all orientations. Non-selective T_1 values for LDL and HDL were 0.37 ± 0.02 and 0.34 ± 0.02 s, respectively. The result for HDL and LDL was typical of that reported by Brown and Davis [6] for phospholipids.

Application of the CPMG pulse sequence to measure T_2 relaxation [7] showed that none of the 4 classes of lipoproteins has a T_2 in excess of 250 ms.

2D NMR clearly identifies the main component of chylomicra and VLDL to be triglyceride (fig.2). Triglyceride exhibits a unique cross-peak (G′) linking resonances at 4.1 and 4.3 ppm resulting from the geminal coupling of protons on carbons 1 and 3 of the glycerol backbone (structure, fig.2) [4]. This resonance is 0.1 ppm downfield from the corresponding glycerol resonance in the phosphatidylcholine spectrum [3]. All the cross-peaks marked in the chylomicra and VLDL spectra (fig.2) may be accounted for by triglyceride except for that denoted Z, which is from coupling between the methyl and methine protons of the alkyl side chain of the cholesterol molecule.

The spectra of LDL and HDL (fig.3) differ from the chylomicra and VLDL in that the unique triglyceride cross-peak G′, between 4.1 and 4.3 ppm is absent. However, a similar pattern is evident at a lower chemical shift and this may be due to phospholipid head groups or to protein. The acyl chain resonances A and B are less intense, and cross-peaks E and F from methylenes close to the carbonyl are absent altogether. The spectra of LDL and HDL are generally broader (as is also evident in the 1D spectra, fig.1) which is a reflection of their increased protein content (table 1).

The 2D COSY spectra of the lipoproteins (figs 2,3) may be compared with that obtained from a

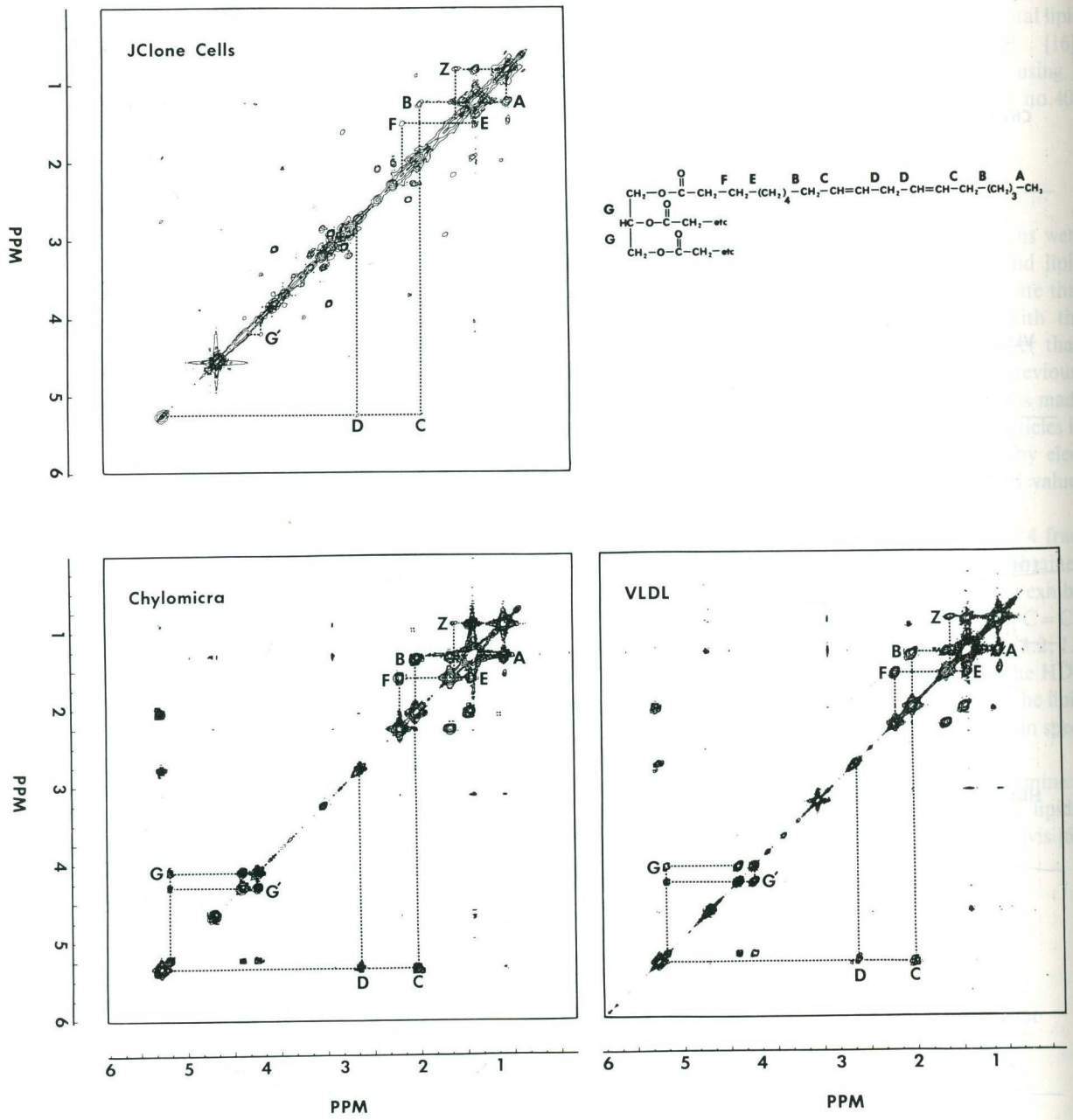

Fig.2. Symmetrised COSY spectra of chylomicra, VLDL and a suspension of J clone cells (1×10^8 cells) in phosphate-buffered saline in D_2O. Spectra were obtained at 37°C with the sample spinning and the residual HOD peak suppressed by gated irradiation. Lipid connectivities are indicated, and cross-peaks are designated according to the structure. Sine-bell and Gaussian (LB = −16, GB = 0.22) window functions were applied in the T_1 and T_2 domains, respectively, of the J clone spectrum, and sine-bell in both dimensions for the lipoprotein data. Z denotes the cross-peak linking the methyl and methine protons of the cholesterol alkyl chain.

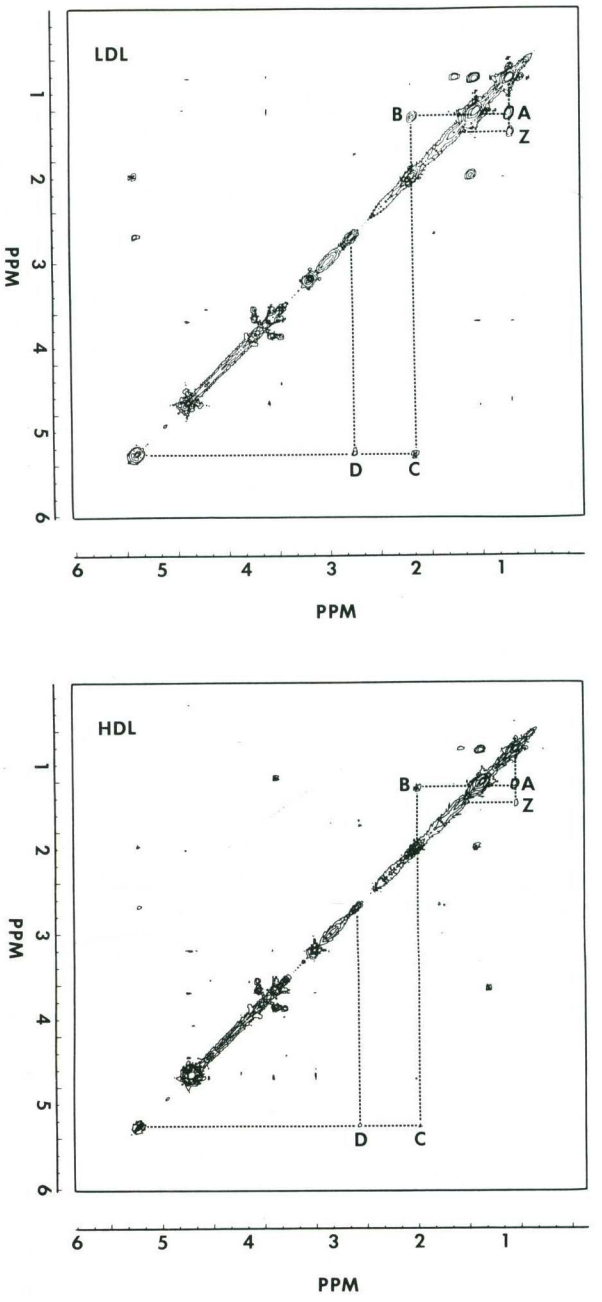

Fig.3. Symmetrised COSY spectra of LDL and HDL in phosphate-buffered saline in D_2O. Spectra were obtained at 37°C with the sample spinning and the residual HOD peak suppressed by gated irradiation. Lipid connectivities are indicated, and cross-peaks are designated according to the structure in fig.2. A sine-bell window function was applied in both the T_1 and T_2 domains.

suspension of rat mammary adenocarcinoma cells (J clone, fig.2). All the cross-peaks from the triglyceride molecule are present in the cells with the exception of G which is probably due to a lack of signal-to-noise. Cross-peak Z from the cholesterol alkyl chain is also visible in the cell spectrum. The remaining cross-peaks in the cell spectrum have been shown to arise from cytoplasmic components [4].

4. DISCUSSION

It was our intention to establish if any of the 4 main classes of lipoprotein resembled the triglyceride rich membrane domain found in the plasma membranes of cancer and other rapidly dividing cells [1]. Based on 2D NMR experiments, T_1 measurements and chemical analyses, both chylomicra and VLDL exhibit properties similar to the cancer cell membrane domain.

LDL and HDL have more phospholipid than triglyceride (table 1), with ratios of 2:1 and 10:1, respectively. Since phospholipid is a major constituent of the surface of all the lipoprotein particles, it is reasonable to assume that both lateral diffusion and exchange of lipid between particles could occur. However, in the case of the VLDL and chylomicra this diffusion is undetected since both particles are predominantly triglyceride. From these considerations the cell membrane domain appears more similar to VLDL and chylomicra than LDL or HDL, since no diffusive exchange of lipids has been observed in the cells and much of the ^1H NMR signal arises from neutral lipids. Until the cell membrane domain is isolated we are unable to establish its exact lipid and protein composition.

Another observation of particular interest to us was the absence of a long T_2 in any of the 4 classes of lipoproteins. Clearly the long T_2 measured for the triglycerides in the plasma membranes of cancer cells with the capacity to metastasize is due to a characteristic not present in lipoproteins from healthy donors.

It has been shown by others that many cancer patients have elevated levels of VLDL [18], and that most cancer cells have an increased number of LDL receptors on the cell surface which bind both LDL and VLDL [19]. Although a correlation between lipoprotein uptake and cancer was first postulated in the 1960's, only recently has the con-

nection between altered uptake and cellular behaviour patterns been made [20]. We do not yet know if the neutral lipids that give rise to the long T_2 values observed in cancer cell membranes are present in the lipoproteins of the cancer patient. Lipoproteins from the serum of patients with various types of cancer are now being investigated.

ACKNOWLEDGEMENTS

We would like to thank Professors Myer Bloom, John K. Saunders, Ian C.P. Smith, Martin H.N. Tattersall and Peter E. Wright for their helpful discussions. Many thanks to Judy Hood for typing the manuscript.

REFERENCES

[1] Mountford, C.E., Grossman, G., Reid, G. and Fox, R.M. (1982) Cancer Res. 42, 2270–2276.
[2] Mountford, C.E., Wright, L.C., Holmes, K.T., Mackinnon, W.B., Gregory, P. and Fox, R.M. (1984) Science 226, 1415–1418.
[3] Cross, K.J., Holmes, K.T., Mountford, C.E. and Wright, P.E. (1984) Biochemistry 23, 5895–5897.
[4] Mountford, C.E., Holmes, K.T., Wright, L.C., May, G.L., Williams, P.G. and Smith, I.C.P. (1985) in: NMR in Cancer (Allen, P. ed.) Pergamon, in press.
[5] Harsas, W., Murdoch, S. and Pollack, J.K. (1985) Biochem. Int. 10, 487–494.
[6] Brown, M.F. and Davis, J.H. (1981) Chem. Phys. Lett. 79, 431–435.
[7] Mountford, C.E., Mackinnon, W.B., Bloom, M., Burnell, E.E. and Smith, I.C.P. (1984) J. Biochem. Biophys. Methods 9, 323–330.
[8] Nelson, G.J. (1972) Blood Lipids and Lipoproteins: Quantitation, Composition and Metabolism, Wiley-Interscience, New York.
[9] Jost, P.C. and Griffiths, O.H. (1982) Lipid-Protein Interactions, vol.1, Wiley, New York.
[10] Kostner, G.M. (1983) Adv. Lipid Res. 20, 1–44.
[11] Parks, J.S., Atkinson, D., Small, D.M. and Rudell, L.L. (1981) J. Biol. Chem. 256, 12992–12999.
[12] Hatch, F.T. and Lees, R.S. (1968) Adv. Lipid Res. 6, 111–168.
[13] Gottfried, E.L. (1967) J. Lipid Res. 8, 321–327.
[14] Williams, J.P. and Merrilees, P.A. (1970) Lipids 5, 367–370.
[15] Heider, J.G. and Boyett, R.L. (1978) J. Lipid Res. 19, 514–518.
[16] Duck-Chong, C.G. (1979) Lipids 14, 492–497.
[17] Wuthrich, K. (1976) NMR in Biological Research: Peptides and Proteins, North-Holland, Amsterdam.
[18] Dilman, V.M., Bernstein, L.M., Ostroumova, M.N., Tsyrlina, Y.V. and Golubev, A.G. (1981) Br. J. Cancer 43, 637–643.
[19] Brown, M.S., Faust, J.R. and Goldstein, J.L. (1975) J. Clin. Invest. 55, 783–793.
[20] Chapman, H.A. and Hibbs, J.B. (1977) Science 197, 282–284.

REPRINTED FROM:

FEBS LETTERS

for the rapid publication of short reports in
biochemistry, biophysics and molecular biology

Volume 203, No. 2, 1986

A proteolipid in cancer cells is the origin of their high-resolution NMR spectrum

Lesley C. Wright, George L. May, Marlen Dyne and Carolyn E. Mountford*

Ludwig Institute for Cancer Research (Sydney Branch), Blackburn Building, University of Sydney, NSW 2006, Australia

pp. 164–168

Published by
Elsevier Science Publishers B.V.
on behalf of the Federation of European
Biochemical Societies

A proteolipid in cancer cells is the origin of their high-resolution NMR spectrum

Lesley C. Wright, George L. May, Marlen Dyne and Carolyn E. Mountford*

Ludwig Institute for Cancer Research (Sydney Branch), Blackburn Building, University of Sydney, NSW 2006, Australia

Received 28 May 1986

High-resolution proton nuclear magnetic resonance studies show that the spectrum of a proteolipid complex, isolated from the serum of patients with malignant diseases, is directly comparable with that obtained from intact cancer cells and solid tumours. These NMR signals have previously been shown to reveal differences between cancer cells with various biological characteristics such as metastatic capacity and drug sensitivity. The proteolipid contains cholesterol, phospholipid, triglyceride, glycolipids, ether-linked lipids, and an apoprotein of unusual electrophoretic mobility. We have yet to confirm the presence of the mRNA reported by others. NMR spectroscopy could be used as a rapid method of identifying the presence of this proteolipid complex in human serum and aiding the diagnosis of malignant disease.

NMR *Proteolipid* *(Human serum)* *Malignancy*

1. INTRODUCTION

High-resolution ^1H NMR signals from cancer cells correlate with their metastatic ability [1] and drug sensitivity [2] as well as being able to show malignant change prior to histological identification [3]. The origin of the NMR signal is the plasma membrane [4] and 2D NMR methods identify neutral lipid as being primarily responsible for this spectrum [5]. Lipoprotein complexes which have a core of neutral lipid [6] have been shown to have similar yet different characteristics to the plasma membrane lipid domain responsible for the high-resolution NMR spectra from malignant cells [7]. An RNA-proteolipid complex has recently been isolated from the serum of patients with malignant diseases and in the medium from cultures of malignant cells [8].

We have isolated a proteolipid and the remaining lipoproteins from the plasma of a patient with an ovarian tumour. The various lipoproteins, proteolipid, and a tumour biopsy have been studied by NMR methods. The proteolipid complex has been characterised further by lipid analysis, electron microscopy and biochemical assays.

* To whom correspondence should be addressed

2. MATERIALS AND METHODS

2.1. *Isolation of lipoproteins and proteolipid*

The total lipoprotein fraction was isolated as described by Goldstein et al. [9] from the serum of a patient with an ovarian cancer. An opalescent band, visible between LDL and HDL and containing the proteolipid complex, was isolated from the total lipoprotein fraction on a KBr gradient [8].

2.2. *Chemical analysis*

Total protein, lipid, triglyceride, phospholipid, free and esterified cholesterol were measured as described in [1]. RNA was determined by the orcinol method [10] with corrections for glycolipid interference. Extraction and quantitation of gangliosides (assumed to be mainly monosialoganglioside as judged by thin-layer chromatography) were performed as described [11]. Neutral glycosphingolipid was estimated by the orcinol method [12]. Total *O*-alkyl and *O*-alkenyl glycerolipids were determined as already reported

Published by Elsevier Science Publishers B.V. (Biomedical Division)
00145793/86/$3.50

[13]. Isolated lipoproteins and proteolipid were examined by electrophoresis on 1% agarose with 1 M barbital buffer, pH 9.0. Gels were stained with oil red O and positions of apo A- and apo B-containing lipoproteins were ascertained from a normal plasma control.

2.3. *Electron microscopy*

Particles were examined by negative-staining electron microscopy. The preparations were stained with 1% sodium phosphotungstate (pH 7.3) and the electron micrographs obtained with a Philips 400 electron microscope, operating at 100 kV and a maximum working magnification of $\times 92000$. For the distribution of particle diameters, 400 particles were measured from electron micrographs.

2.4. *NMR spectroscopy*

^{1}H NMR spectra were recorded at 37°C using a Bruker WM-400 spectrometer equipped with an Aspect 2000 computer. 2D scalar correlated spectroscopy (COSY) experiments [14] and T_1 and T_2 measurements [15] have been described.

2.5. *Enzyme studies*

Either RNase A (0.024 IU, Sigma, EC 3.1.1.34) or lipoprotein lipase (4.2 IU, bovine pancreas, Boehringer-Mannheim, EC 3.1.27.5) was added to 1 ml of proteolipid complex which contained 367 μg protein, and incubated for 1 h at 37°C prior to NMR study.

3. RESULTS AND DISCUSSION

3.1. *Chemical analysis*

The lipid, protein, and nucleic acid content of the band containing the proteolipid complex and the remaining lipoproteins isolated from the serum are shown in table 1. The composition of the isolated proteolipid complex is similar to that reported by Wieczorek et al. [8] except for a considerably smaller RNA content as measured by the orcinol method. This method does not confirm the presence of intact mRNA, since it detects only ribose. In addition, triglyceride and ether-linked lipids as well as gangliosides and an apoprotein with an unusual electrophoretic mobility (> pre-β) are present in this complex (table 1).

Glycolipid, both neutral and acidic, constitutes 20% of the proteolipid complex. It is also present in the LDL (23%) and HDL (11.2%) fractions of the plasma. Glycolipids are only present in trace amounts in lipoproteins from healthy donors [16]. However they have been found in neoproteolipids W and S [17] which were isolated from tumours

Table 1

Lipoprotein and proteolipid complexes isolated from the plasma of a patient with an ovarian tumour

	Size (nm)	Longest T_2 (ms)	Percentage of total weight									
			RNA	Protein		Triglyceride	Ganglioside	Neutral glycosphingolipid	Phospholipid	Cholesterol		Ether-linked lipid
										Free	Esterified	
VLDL and chylomicra[a]	26–156	188	–	apo B								
LDL	19– 23	111	nil	apo B	15.7	14.2	1.1	21.9	26.8	6.6	13.2	0.4
Proteolipid	22– 25 and 8– 11	852	4.1	apo A apo B unknown	19.9	13.5	4.5	15.5	25.2	6.1	10.7	0.4
HDL	6– 9	154	nil	apo A	45.2	8.7	1.3	9.9	23.8	1.9	8.4	0.6

[a] Protein and lipid not quantitated due to a low yield

and the serum of cancer patients. The relationship between the nucleic acid containing proteolipid and the neoproteolipid complexes is unclear since no nucleic acid analysis was undertaken on the latter.

3.2. *Electron microscopy*

From electron micrographs two particle sizes, 8–11 and 22–25 nm, in approximately equal numbers were identified in the opalescent band containing the proteolipid complex. We consider these two particle types to differ from the conventional LDL and HDL, since unusual electrophoretic mobility is observed in the opalescent band but not in LDL or HDL bands which are located on either side (table 1).

3.3. *NMR spectroscopy*

The NMR method used to distinguish metastatic cells from their malignant but non-metastatic counterparts in rats is the Meiboom-Gill modification of the Carr-Purcell (CPMG) pulse sequence which provides a spin-spin (T_2) relaxation time [15]. In metastatic cells the longest T_2 is of the order of 0.4–1 s whereas in non-metastatic cells and normal serum lipoproteins [7] it is less than 0.25 s [1].

The ^{1}H NMR spectra and T_2 relaxation profiles of resonances in the methylene region are shown in fig.1 for the total plasma lipoproteins (including the proteolipid complex), the isolated proteolipid complex alone and VLDL and LDL, from the same patient. Only the proteolipid complex has a long T_2 relaxation value of 0.85 s which contrasts with the lipoproteins which are all less than 0.2 s (table 1). Resonances c and d in the spectrum of the proteolipid, both of which have a long T_2, are not present in the spectrum of any conventional lipoproteins. This long T_2 can be measured not only in the isolated complex and total lipoprotein fraction, but also in the serum and the tumour itself. Biopsy samples of tumours on both ovaries from this patient were examined and T_2 values of 0.85 and 0.65 s recorded.

Cells and tumours both gave identical values for the selective and non-selective spin-lattice (T_1) relaxation experiments [15]. The same phenomenon was observed for the proteolipid complex where the T_1 was found to be 0.45 s. These measurements rule out either diffusion or spin ex-

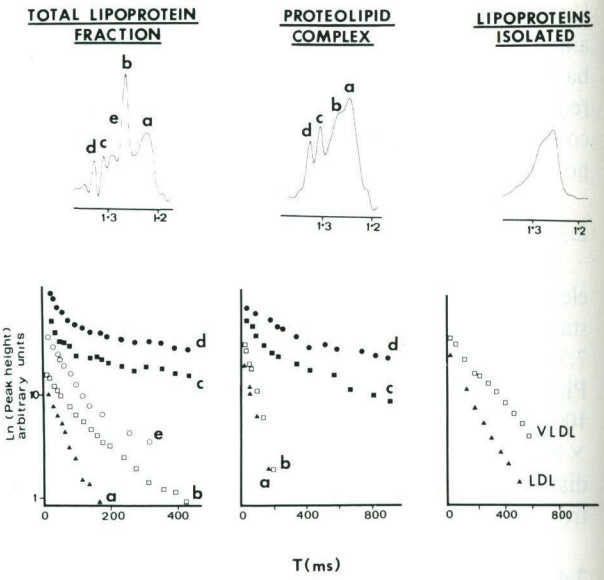

Fig.1. 400 MHz ^{1}H NMR spectra of the methylene region of: total lipoprotein fraction (including the proteolipid complex) isolated from the plasma (1); the opalescent band (containing the proteolipid complex) isolated from the total lipoprotein fraction on a KBr gradient [8] (2); lipoproteins (LDL and VLDL) which were isolated from the same plasma sample (3). The spectra are resolution enhanced by the Lorentzian-Gaussian method described in [15] using LB = −12; GB = 0.08. Below the NMR spectra the results of the CPMG T_2 relaxation experiment executed as described in [15] are shown. The natural log of each peak height is plotted against the delay between the first pulse and the nth echo. The T_2 values are calculated using a least squares method where $r^2 \geq 0.98$. The longest T_2 (ms) values of each profile are as follows: (1) a = 84, b = 181, c = 730, d = 660, e = 226; (2) a = 68, b = 63, c = 671, d = 970; (3) VLDL = 188, LDL = 111.

change between the molecules generating the spectrum. This was not the case for LDL or HDL from healthy donors where not only did the selective and non-selective measurements differ but a non-exponential decay was observed in the selective T_1 experiment [7]. This is an interesting comparison since the proteolipid is isolated between these two fractions on the KBr gradient. Nevertheless it is another physical measurement whereby the cells and tumours show identical behaviour to the proteolipid complex.

Attempts were made to identify the origins of the four methylene resonances which occur at 1.33,

1.31, 1.28 and 1.26 ppm in the spectrum of the proteolipid complex. RNase A had no effect on any of these resonances. This is consistent with the report by Wieczorek et al. [8] that RNase did not affect the nucleic acid content of the intact particle. Lipoprotein lipase, which degrades triglycerides caused resonances a and b at 1.26 and 1.28 ppm to decrease significantly in intensity. These two resonances have a short T_2 of less than 200 ms.

The assignment of resonances a and b to triglyceride is confirmed by 2D NMR methods (fig.2). 2D scalar correlated spectroscopy (COSY) methods allow assignment of resonances based on spin-spin (scalar) coupling. The off diagonal cross peaks denoted A–G (fig.2) indicate spin-spin coupling between protons on adjacent atoms.

The presence of cross peaks A–E (as summarised in scheme 1), and the cross peak G′ (at 4.3 ppm) which is unique to triglyceride, indicate the presence of this neutral lipid. In contrast to the cell spectrum, the assignments for which have been documented previously [5], cross peak F is not

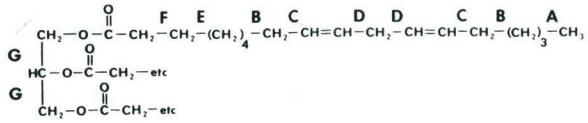

Scheme 1

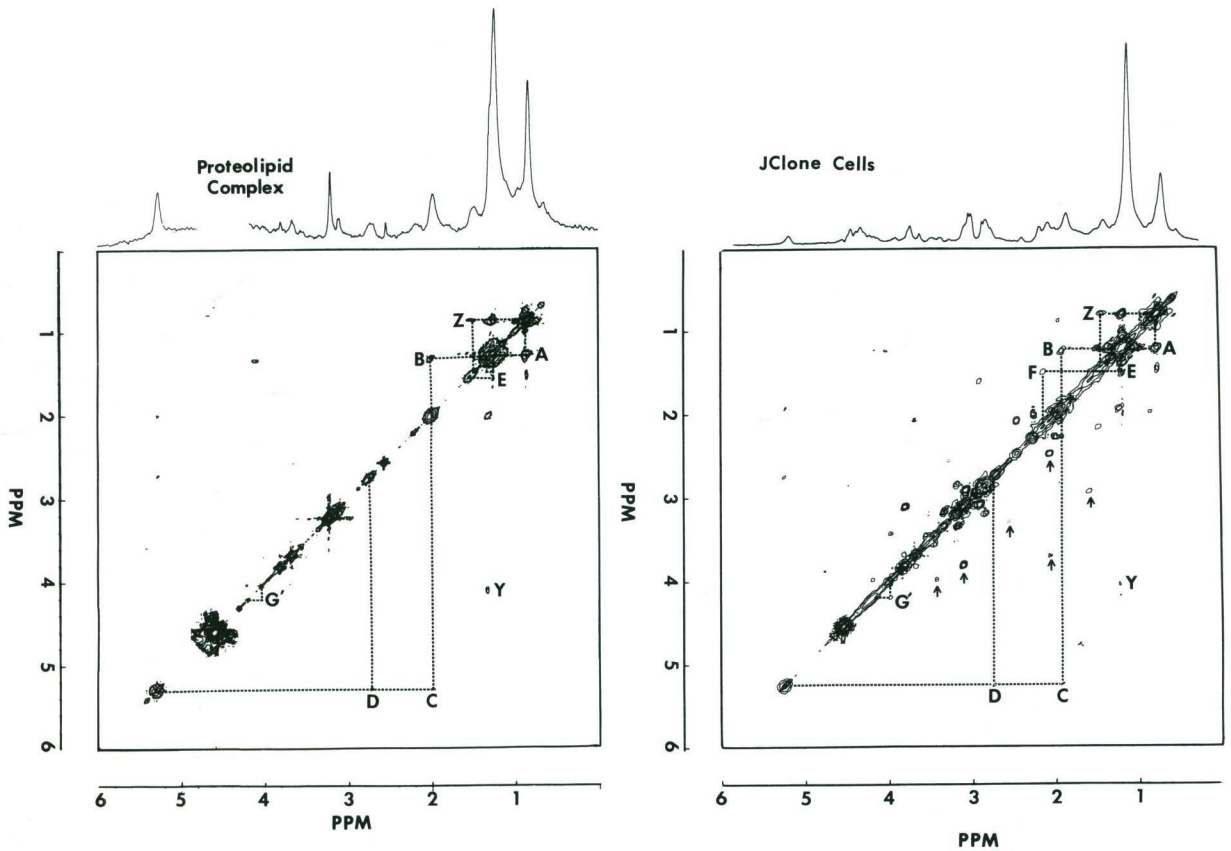

Fig.2. ^{1}H NMR spectra (400 MHz) of: proteolipid complex isolated on a KBr gradient [8] from the lipoprotein fraction of a patient with an ovarian tumour. Suspended in NaCl/D_2O (1); a suspension of the rat mammary adenocarcinoma J clone cells (1×10^8) suspended in PBS/D_2O (2). The one-dimensional spectra, transformed with a 3 Hz line broadening, are shown above the 2D scalar correlated spectroscopy (COSY) spectra executed as described in [14]. A Gaussian window function was applied in the t_2 domain (LB = −16; GB = 0.22) and a Sine-bell in the t_1 domain. Lipid acyl chain and glycerol connectivities assigned A–G are shown in scheme 1. Z denotes the cross peak between the methyl and methine protons of the alkyl side chain of the cholesterol ring system. Y is yet to be identified. The arrows in the cell spectrum point to cross peaks previously assigned to metabolites in the cell's cytoplasm [5].

observed in the spectrum of the proteolipid complex. The absence of this cross peak is likely to be due to a lack of signal since G′ is only just observable and triglyceride accounts for 18% of the total lipid in the proteolipid complex. Resonances c and d at 1.33 and 1.31 ppm have yet to be definitively assigned, but have chemical shifts consistent with the cross peak Y (fig.2).

We conclude that a proteolipid complex similar to that reported by Wieczorek et al. [8] accounts for almost all of the NMR signals from the plasma membrane of cancer cells, and for the unusually long T_2 relaxation value. Our data strongly suggest that a proteolipid is the plasma membrane lipid domain that gives high-resolution ^{1}H NMR signals. The presence of a proteolipid complex containing nucleic acid in the plasma membranes may provide an interesting explanation for the altered biological status of cancer cells as observed by NMR.

Furthermore, these observations may be relevant in NMR imaging which currently does not satisfactorily distinguish malignant from benign tumours [18]. Our data suggest that depending on the amount of proteolipid present in a tumour and its surrounds, the T_2 relaxation value will have contributions from this complex and may therefore be useful in tumour imaging.

ACKNOWLEDGEMENTS

We thank Professors M. Bloom and M.H.N. Tattersall, Drs K.T. Holmes, P.G. Williams and D. Sullivan and G. Shilson-Josling for helpful discussions and technical advice.

REFERENCES

[1] Mountford, C.E., Wright, L.C., Mackinnon, W.B., Holmes, K.T., Gregory, P. and Fox, R.M. (1984) Science 226, 1415–1418.

[2] Holmes, K.T., Fox, R.M., Wright, L.C. and Mountford, C.E. (1986) in: NMR in Cancer (Allen, P. ed.) Pergamon, in press.

[3] Mountford, C.E., Grossman, G., Gatenby, P.A. and Fox, R.M. (1980) Br. J. Cancer 41, 1000–1003.

[4] Mountford, C.E., Grossman, G., Reid, G. and Fox, R.M. (1982) Cancer Res. 42, 2270–2276.

[5] May, G.L., Wright, L.C., Holmes, K.T., Williams, P.G., Smith, I.C.P., Wright, P.E., Fox, R.M. and Mountford, C.E. (1986) J. Biol. Chem. 261, 3048–3053.

[6] Nelson, G.J. (1972) Blood Lipids and Lipoproteins: Quantitation, Composition and Metabolism, Wiley-Interscience, New York.

[7] Williams, P.G., Helmer, M.A., Wright, L.C., Dyne, M., Fox, R.M., Holmes, K.T., May, G.L. and Mountford, C.E. (1985) FEBS Lett. 192, 159–164.

[8] Wieczorek, A.J., Rhyner, G. and Block, L.H. (1985) Proc. Natl. Acad. Sci. USA 82, 3455–3459.

[9] Goldstein, J.L., Basu, S.K. and Brown, M.S. (1983) Methods Enzymol. 98, 241–260.

[10] Almog, R. and Shirey, T.L. (1978) Anal. Biochem. 91, 130–137.

[11] Bergelson, L.D. (1980) in: Lipid Biochemical Preparations (Bergelson, L.D. ed.) pp.244–245, Elsevier/North-Holland, Amsterdam.

[12] Hildebrand, J., Stryckmans, P. and Stoffyn, P. (1971) J. Lipid Res. 12, 361–366.

[13] Blank, M.L., Cress, E.A., Piantadosi, C. and Snyder, F. (1975) Biochim. Biophys. Acta 208, 208–218.

[14] Cross, K.J., Holmes, K.T., Mountford, C.E. and Wright, P.E. (1985) Biochemistry 23, 5895–5897.

[15] Mountford, C.E., Mackinnon, W.B., Burnell, E.E., Bloom, M. and Smith, I.C.P. (1984) J. Biochem. Biophys. Methods 9, 323–330.

[16] Van den Bergh, F.A.J.T.M. and Tager, J.M. (1976) Biochim. Biophys. Acta 441, 391–402.

[17] Skipski, V.P., Barclay, M., Archibald, F.M., Lynch, T.P. jr and Stock, C.C. (1971) Proc. Soc. Exp. Biol. 136, 1261–1264.

[18] Bottomley, P.A., Hardy, C.J., Argersinger, R.E. and Allen, G.R. (1985) Abstr. Soc. Mag. Res. in Med. 1, 29.

THE JOURNAL OF BIOLOGICAL CHEMISTRY
© 1986 by The American Society of Biological Chemists, Inc.

Vol. 261, No. 7, Issue of March 5, pp. 3048–3053, 1986
Printed in U.S.A.

Assignment of Methylene Proton Resonances in NMR Spectra of Embryonic and Transformed Cells to Plasma Membrane Triglyceride*

(Received for publication, August 20, 1985)

George L. May, Lesley C. Wright, Kerry T. Holmes, Philip G. Williams, Ian C. P. Smith‡, Peter E. Wright§, Richard M. Fox¶, and Carolyn E. Mountford‖

From the Ludwig Institute for Cancer Research (Sydney Branch), Blackburn Building, University of Sydney, Sydney, New South Wales 2006, Australia, the ‡Division of Biological Sciences, National Research Council, Ottawa K1A 0R6, Canada, and the §Department of Molecular Biology, Research Institute of Scripps Clinic, La Jolla, California 92037

Some biological characteristics of cancer cells and solid tumors are identifiable by the high resolution NMR relaxation behavior of their nonaqueous components. Chemical analysis and two-dimensional scalar correlated (COSY) NMR spectroscopy show these resonances arise from neutral lipid in the plasma membrane. Triglyceride is shown to be the main plasma membrane component giving rise to the NMR spectrum, while soluble nonmembrane components account for 90% of the remaining resonances in the spectrum of intact cells. The presence of triglyceride has been detected by chemical analysis in highly purified plasma membranes from two different cell lines. The COSY spectra of cancer cells are comparable with that obtained for the triglyceride-rich very low density human lipoprotein.

The high resolution ^1H NMR spectrum of a suspension of cancer cells or an excised solid tumor is characteristic of lipids (Mountford *et al.*, 1980, 1982b). Lorentzian-Gaussian resolution enhancement of the lipid methylene proton resonances near 1.2 ppm resolves four peaks, at 1.22, 1.23, 1.25, and 1.28 ppm, each of which can be examined separately in an NMR relaxation experiment. In transverse relaxation measurements, each of these shows several relaxation times, T_2. We recently reported that the resonance at 1.25 ppm, which shows a multiphasic plot, has a longest T_2 (denoted T_{2l}) of the order of 400–800 ms when the cells were known to have the capacity to generate secondary growths in other parts of the body (metastasize). In contrast, cells which remained as malignant but nonmetastatic primaries gave a T_{2l} of less than 200 ms for the same resonance (Mountford *et al.*, 1984a, 1984b). Furthermore, the behavior of these four methylene resonances is indicative of the exposure of the cancer cells to vinca alkaloid and other related anticancer drugs.[1] Identification of the chemical species which give rise to the NMR spectrum, and hence provide an indication of the biological capabilities of the cells, is therefore important.

We have established previously that these lipids are in or attached to the plasma membrane, tumble isotropically, and are in domains which are not in diffusive exchange with other lipids in the plasma membrane bilayer (Mountford *et al.*, 1984a, 1984b).

Chemical analysis of a crude plasma membrane preparation (enriched in plasma membrane markers 4-fold) from the rat mammary adenocarcinoma cell lines 13762 and J clone showed a significant quantity of triglyceride present in both cell lines, with the metastatic line 13762 having significantly more cholesterol ester. Other rapidly dividing cells have been shown to give a similar NMR spectrum (Block, 1973; Nicolau *et al.*, 1975, 1978; Mountford *et al.*, 1982b) and we have now extended the analytical studies to verify the presence of triglycerides in the crude plasma membrane preparations of all the rapidly dividing cells which we have investigated that give the NMR spectrum. In addition a highly purified plasma membrane, which is enriched 45-fold in plasma membrane markers, has been analyzed to ensure that the presence of triglyceride is not due to a contaminant.

The one-dimensional ^1H NMR spectra of cancer cells have narrow lines (≤10 Hz). However, assignment of the resonances to specific protons is difficult from one-dimensional spectra. In contrast, two-dimensional scalar correlated spectroscopy (COSY) provides a great deal of information not available from the one-dimensional spectrum (Wagner *et al.*, 1981; Arseniev *et al.*, 1982) by generating spectra which allow spin system assignments based on spin-spin (scalar) coupling. Using a modified pulse sequence (Cross *et al.*, 1984) we have found that suspensions of intact viable cancer cells may be studied by two-dimensional NMR methods. Two-dimensional scalar correlated spectroscopy has verified that the NMR spectrum arises predominantly from triglyceride in the plasma membranes and from soluble non-lipid components.

EXPERIMENTAL PROCEDURES

Cell Lines and Culture

Human peripheral blood lymphocytes, stimulated by pokeweed mitogen, were supplied and grown as previously described (Mountford *et al.*, 1982b). The preparation and culturing of chicken embryo fibroblasts followed reported procedures (Mountford *et al.*, 1982a). VBL20 is the acute lymphoblastic leukemic T cell line (CCRF-CEM) which has been made resistant to 20 ng/ml of the anti-cancer drug vinblastine. The cultured rat mammary adenocarcinoma metastatic cell line 13762 and the nonmetastatic clone, J clone, were supplied by Dr. I. Ramshaw, Australian National University and grown as previously described (Ramshaw *et al.*, 1982). All cells were grown at 37 °C in RPMI 1640 medium supplemented with 10% fetal calf serum. Cells were maintained and studied in the logarithmic phase of growth. The doubling time was 24–36 h.

Preparation of Samples for NMR Spectroscopy

Cell samples were prepared for NMR experiments as previously

* The costs of publication of this article were defrayed in part by the payment of page charges. This article must therefore be hereby marked "*advertisement*" in accordance with 18 U.S.C. Section 1734 solely to indicate this fact.

¶ Present address: Dept. of Haematology and Oncology, Royal Melbourne Hospital, Melbourne, Victoria, 3054, Australia.

‖ To whom correspondence should be addressed.

[1] K. T. Holmes, L. C. Wright, M. Dyne, R. M. Fox, and C. E. Mountford, unpublished experiments.

described (Mountford *et al.*, 1982b, 1984a). The samples were kept at 37 °C in the NMR tube for 1 h prior to commencement of the experiments to allow establishment of a stable state following increase in cell-cell contact. Cell viability was measured before and after each experiment. Only those data obtained from cells with at least 90% viability were used. The longest time for which this could be achieved was 3–4 h.

Triolein (Sigma) was dissolved (20 mg/ml) in $CDCl_3$ (99.96% isotopic purity, supplied by Wilmad Glass Co.) and the solution was degassed while freeze-thawing four times with liquid nitrogen.

Very low density lipoprotein (VLDL[2]) from healthy human donors was isolated by previously reported methods (Hatch and Lees, 1968). The particle size was measured by electron microscopy to be 27–32 nm, with a total variation of 22–54 and 31–78 nm on two experiments, which is within the normal range for human VLDL. The preparations were negatively stained with 1% ammonium molybdate solution and the electron micrographs were obtained with a Philips 400 EM operating at 100 kv and a working magnification × 92,000.

NMR Spectroscopy

^1H NMR spectra were recorded at 37 °C (cells, supernatant, and VLDL) or 25 °C (triolein) using a Bruker WM 400 spectrometer. Peaks were referenced to aqueous sodium 3-(trimethylsilyl)propanesulfonate or to the residual $CHCl_3$ resonance at 7.26 ppm as external or internal chemical shift references. The Meiboom-Gill modification of the Carr-Purcell pulse sequence (CPMG) (Meiboom and Gill, 1958) was used for spin-spin relaxation measurements as described (Mountford *et al.*, 1984a) and the COSY spectra were recorded with a pulse sequence modified to compensate for radiofrequency inhomogeneity (Cross *et al.*, 1984).

Membrane and Supernatant Preparations

Supernatant from VBL20 Cells—Washed cells (2.0×10^8) were lysed for 20 min at 4 °C in 2 ml of D_2O. The homogenate was centrifuged at 130,000 × *g* for 60 min and the supernatant fraction was removed.

Membrane Isolation—The preparation of crude plasma membranes was accomplished as reported (Mountford *et al.*, 1984b) with cell disruption by nitrogen cavitation at 800 p.s.i. for 15 min. The purification of the plasma membrane similarly involved cell disruption by nitrogen cavitation at 800 p.s.i. (15 min) of cells (4.5×10^9) washed three times in saline. The disruption was effected in a Parr pressure bomb with the cells suspended in 4 volumes of buffer consisting of 100 mM Tris-HCl, pH 7.4, 10 mM $MgCl_2$, 10% (w/v) sucrose, 10 μM leupeptin, and 1 mM phenylmethylsulfonyl fluoride. The cell lysate was centrifuged at 1000 × *g* (4 °C) for 5 min and the pellet was disrupted as before by nitrogen cavitation. The combined lysates (total homogenate) were again centrifuged at 1000 × *g* for 5 min. This pellet of unbroken cells and nuclei was discarded. The membranes were then sedimented by centrifugation of the 1000 × *g* supernatant at 140,000 × *g* for 1 h (4 °C) and resuspended in phosphate-buffered saline, pH 7.4. The suspension was further fractionated according to the method of Iwanik *et al.*, 1984. The membrane bands from the sucrose density gradients were removed by aspiration and diluted 1:4 with 10 mM HEPES, pH 7.2. All marker enzyme activities except 5′ nucleotidase and NADPH cytochrome *c* reductase were assayed on membranes which had been frozen overnight at −70 °C.

Marker Enzymes

The purity of the plasma membrane preparation was assessed by calculating the specific activity of the marker in the membrane and dividing by that in the homogenate. Protein content was measured with the Bio-Rad protein assay kit using bovine serum albumin as a standard. The following marker enzymes were assayed according to methods which have already been described: 5′ nucleotidase (Newby *et al.*, 1975), Na^+, K^+ adenosinetriphosphatase (Ames, 1965), and γ-glutamyltranspeptidase (Jacobs, 1971) as plasma membrane markers; acid phosphatase (Ames, 1965) as the marker for lysosomes; lactate dehydrogenase (Boehringer Mannheim GmbH diagnostica lactate dehydrogenase test kit, catalogue No. 124907), as a cytoplasmic marker; NADPH-cytochrome *c* reductase (Sottocasa *et al.*, 1967) as the marker for endoplasmic reticulum; and cytochrome *c* oxidase (Wharton and Tzagoloff, 1967) as the mitochondrial marker. DNA was used as the nuclear marker (Brunk *et al.*, 1979).

Chemical Analysis

Membranes were resuspended in 10 mM HEPES, pH 7.2, and the lipid was extracted (Gottfried, 1967; Williams and Merrilees, 1970). Values and standard errors were determined from assays run in duplicate on at least two different extractions. The free cholesterol and total cholesterol contents of the lipid extracts were determined by an enzymic fluorimetric method (Heider and Boyett, 1978). Cholesterol ester content was calculated by subtracting the free cholesterol from the total cholesterol content. Lipid phosphorus was determined colorimetrically on the total extracts (Duck-Chong, 1979), based on a mean molecular weight for phospholipid of 750. Triglyceride was also determined colorimetrically (Sigma Diagnostic Kit 405) using the molecular weight of triolein (885).

RESULTS AND DISCUSSION

The 400-MHz COSY spectrum of triolein in $CDCl_3$ is compared with that obtained from a suspension of cells in Fig. 1, *A* and *B*. The off diagonal cross-peaks, labeled A–G, indicate spin-spin coupling between protons on adjacent carbon atoms. The connectivities corresponding to each acyl chain cross-peak (*A–F*), summarized in Structures 1 (phospholipid) and 2 (triglyceride), can be seen in the spectrum of the leukemic T cell line VBL20 (Fig. 1*B*) confirming the assignment of lipid acyl chain resonances in the spectrum of cancer cell plasma membranes.

Two-dimensional NMR also identifies the lipid acyl chains as components of triglyceride. Triglyceride possesses a unique cross-peak G′ at 4.3 ppm resulting from the geminal protons of carbons 1 and 3 of the glycerol backbone (Structure 2 and Fig. 1*A*). This resonance is 0.1 ppm downfield from the corresponding glycerol resonance (Structure 1) in the phosphatidylcholine spectrum. Furthermore, no cross-peaks from a glycerol methylene adjacent to a phosphatidylcholine group, H, (Cross *et al.*, 1984) are in evidence in the cell spectrum, nor indeed is the cross-peak J due to the choline head group. The cross-peak D is not present in Fig. 1*A* as triolein has only one olefinic group in each acyl chain. However, the absence of C in the cell spectrum (Fig. 1*B*) is unexpected and while this cannot be due to the complete absence of carbon-carbon double bonds (as evidenced by the presence of D) it may suggest a low level of olefinic groups or that this cross-peak is not observed for dynamic reasons. The cross-peak G has never been observed for a cell system, possibly because of restricted motion of the glycerol backbone. Restricted motion may also explain the absence of cross-peaks from phospholipid headgroups and backbone.

In order to determine which cross-peaks in the cell spectrum originate from nonmembrane components such as metabolites, we lysed the cells. After the membranes and nuclei are spun down, the supernatant, which contains only soluble components, accounts for all of the remaining cross-peaks not generated by the triglyceride molecule in this cell line except that connecting resonances at 1.7 and 3.0 ppm (Fig. 1*C*). This latter cross-peak has been tentatively assigned to a resonance arising from the oligosaccharide head group of gangliosides, which display the same cross-peak.

The amounts of free cholesterol and cholesterol ester were variable in the crude plasma membrane preparations (Table I). A cross-peak connecting resonances at 0.9 and 1.4 ppm from the methyl and methine protons of the alkyl side chain of the cholesterol ring system, denoted *Z* in Fig. 2*B*, can be observed in the spectra of many cancer cells. This suggests the presence of cholesterol and/or cholesterol ester in the neutral lipid domain of the rat mammary adenocarcinoma cell line 13762 (Fig. 2*B*). In contrast, the VBL20 cell line (Fig.

[2] The abbreviations used are: VLDL, very low density lipoprotein; HEPES, 4-(2-hydroxyethyl)-1-piperazineethanesulfonic acid; CPMG, Meiboom-Gill modification of the Carr-Purcell pulse sequence.

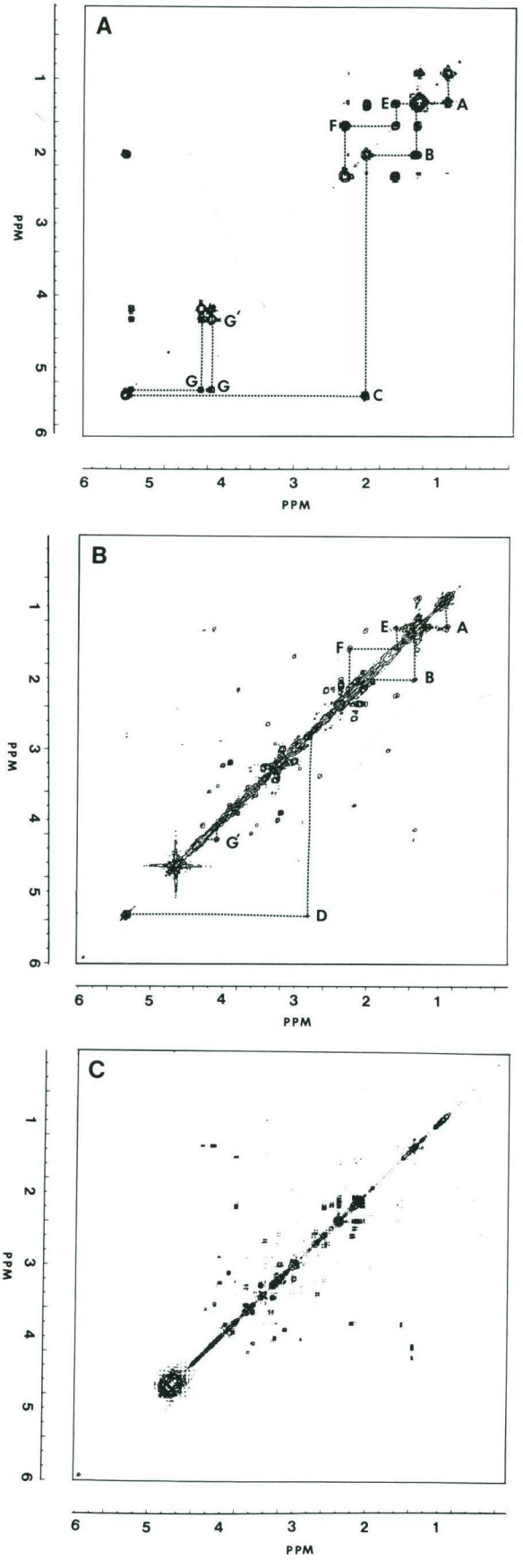

FIG. 1. **Symmetrized COSY spectra.** *A*, triolein in $CDCl_3$ solution (20 mg/ml). Lipid acyl chain and glycerol backbone connectivities are indicated. The assignments of the cross-peaks are shown in Structure 2 which is described in the text. A Sine-bell window function was applied in both the t_1 and t_2 domains. *B*, a suspension of VBL20 cells (1×10^8 cells) in phosphate-buffered saline in D_2O. Spectra were obtained at 37 °C with the sample spinning and suppression of the residual HOD peak by gated irradiation. Sine-bell and Gaussian (line broadening = −16, Gaussian broadening = 0.22) window functions were applied in the t_1 and t_2 domains, respectively (Cross *et al.*, 1984). Lipid acyl chain and glycerol backbone connectivities are indicated. (VBL20 is the acute lymphoblastic leukemic T cell line CCRF-CEM which has been made resistant to 20 ng/ml of vinblastine). *C*, supernatant from VBL20 cells (2.0×10^8). After washing, cells were lysed for 20 min at 4 °C in 2 ml of D_2O. The homogenate was centrifuged at 130,000 × *g* for 60 min and the supernatant was removed. The COSY spectrum was recorded as for VBL20 cells.

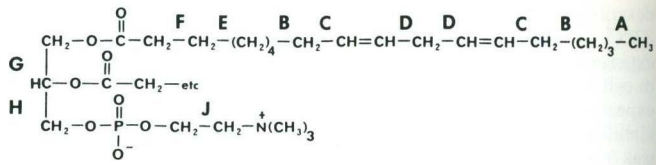

STRUCTURE 1

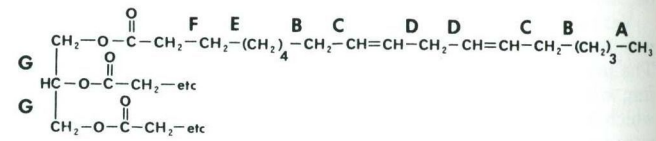

STRUCTURE 2

TABLE I

Neutral lipid composition of membranes of various cell lines

Crude plasma membranes from 2.5×10^8 cells were prepared as described by Mountford *et al.*, 1984b. The 13762 and J clone cell lines were enriched 4-fold and the other cell lines were prepared similarly. The analyses were carried out as described under "Experimental Procedures," and the values represent the mean ± S.E. as determined from assays run in duplicate on the number of experiments indicated in parentheses. Data are expressed as nmol/mg of lipid. The abbreviations used are: ALL, acute lymphoblastic leukemic; PBL, peripheral blood lymphocytes; PWM, pokeweed mitogen.

Cell line		Triglyceride	Free cholesterol	Cholesterol ester
Rat mammary adenocarcinoma				
Metastatic line 13762	(3)	86 ± 9	278 ± 21	45 ± 7
Nonmetastatic J Clone	(3)	77 ± 6	236 ± 9	6 ± 6
All T cell CCRF-CEM				
Sensitive	(5)	94 ± 5	182 ± 41	28 ± 11
Resistant to 20 ng/ml VBL	(5)	88 ± 16	167 ± 31	48 ± 23
Chicken fibroblast	(2)	163 ± 36	191 ± 22	55 ± 25
Human PBL stimulated with PWM	(2)	491 ± 25	256 ± 17	14–290[a]

[a] The range of values has been indicated due to large variation in results.

1, *B* and *C*) does not display this cross-peak, the absence of which may be accounted for either by dynamic effects or a difference in cholesterol and/or cholesterol ester composition.

Low levels of diglycerides have also been found in the membranes of some cancer cell lines.[3] Their two-dimensional spectra are essentially indistinguishable from those of triglycerides since the acyl chain connectivities are identical.

The chemical analyses of the crude plasma membranes of some cancer cells and of other rapidly dividing cells known to give narrow NMR lines are shown in Table I. The membrane triglyceride content and composition are comparable in most

[3] L. C. Wright, G. L. May, and C. E. Mountford, unpublished experiments.

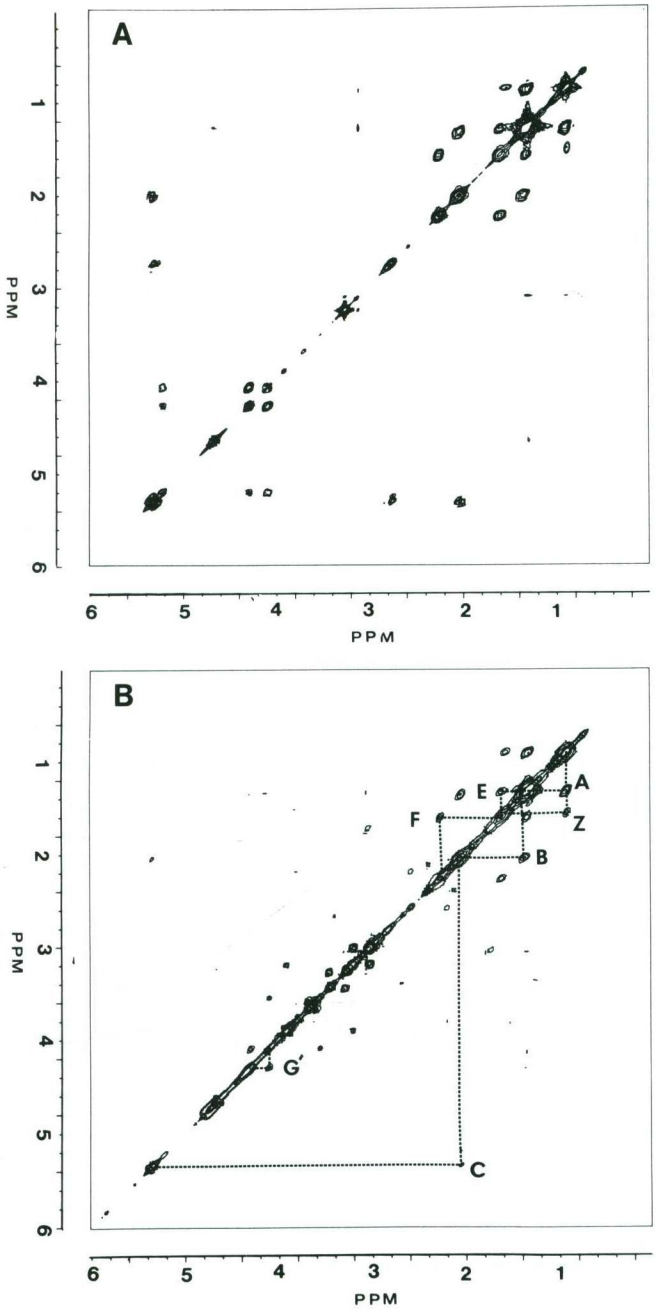

FIG. 2. **Symmetrized COSY spectra.** *A*, VLDL in D_2O (from healthy human donors). *B*, a suspension of 13762 cells (1×10^8 cells) in phosphate-buffered saline in D_2O. Spectra were obtained at 37 °C with the sample spinning and suppression of the residual HOD peak by gated irradiation. A Sine-bell window function was applied in both the t_1 and t_2 domains for *A*; and Sine-bell and Gaussian (line broadening = −16, Gaussian broadening = 0.22) window functions were applied in the t_1 and t_2 domains, respectively, for *B*. Lipid acyl chain and glycerol backbone connectivities are indicated. *Z* denotes the cross-peaks between the methyl and methine protons of the alkyl side chain of the cholesterol ring system.

cases, with chicken fibroblasts and stimulated human lymphocytes showing the greatest variation. Furthermore, cholesterol ester and free cholesterol levels display an even greater variability as evidenced by the standard errors.

The chemical analysis of the neutral lipid from the plasma membrane of the VBL20 cell line, purified 45-fold on a sucrose gradient, has confirmed the presence of unusually high levels of triglyceride in the plasma membrane. The extent of the enrichment and purity was determined by markers for plasma membrane and other cell constituents (Table IIA). Band 1, at the junction of the 10–30% sucrose layer, is shown to be the purest plasma membrane-containing fraction and, although the enrichment over the homogenate is approximately 45-fold, the ratio of plasma membrane markers to cytoplasmic, mitochondrial, and nuclear markers is many times greater. The major contamination appears to stem from endoplasmic reticulum as evidenced by the enrichment of NADPH cytochrome *c* reductase activity. Even so, the ratio of plasma membrane to endoplasmic reticulum markers in Band 1 is 11:1. Bands 2–4 are mixed membrane bands containing varying levels of mitochondrial, endoplasmic reticulum, lysosomal, and/or nuclear membranes in addition to plasma membrane. Chemical analysis of the major lipids (Table IIB) demonstrated that the levels of free cholesterol in the mixed membrane bands (B2 and B3) were in agreement with those found for the crude membrane preparations of VBL20 cells (Table I). In contrast, the level of free cholesterol in the B1 fraction was considerably higher and no cholesterol ester was detected in any of the bands. The presence of large amounts of free cholesterol is in itself an indication of membrane purity (Haeffner *et al.*, 1982) since the plasma membrane is the major site of cholesterol accumulation. The decrease in free cholesterol from B1 to B4 reflects the level of plasma membrane enrichment. In contrast, the cholesterol-to-phospholipid ratio shows an increase over the homogenate in bands 1–3. The levels of triglyceride in the bands (Table IIC) are most interesting since two of the mixed membrane bands (B2 and B3) again show agreement with those measured in the VBL20 crude membrane preparations (Table I) while triglyceride in B4 is slightly elevated and the purest plasma membrane-containing fraction (B1) has the highest levels of triglyceride. It is very unlikely that triglyceride has been trapped in the membrane bands from the triglyceride-rich floaters and supernatant fractions since for B1 the ratio of the plasma membrane marker 5′ nucleotidase to the cytoplasmic marker lactate dehydrogenase is 5000:1. The data further suggest that triglyceride may be present in all the membranes and indeed increased amounts of triglyceride or diglyceride have been found recently in mitochondrial membranes of rat liver, the rapidly dividing fetal cells containing four times as much as the adult cells (Harsas *et al.*, 1985). It has been suggested by others (Verkleij, 1984; Sen *et al.*, 1981) that membranes containing increased proportions of neutral lipids such as triglycerides would exhibit changes in their permeability properties reflecting a decrease in the bilayer content of the membranes.

We have also found elevated levels of triglyceride in a 9-fold enriched plasma membrane preparation from a rat mammary adenocarcinoma 13762 subline. Chemical analysis shows the B1 fraction to contain 376 nmol/mg of lipid. The data thus support the NMR assignments in Fig. 2.

The T_{2l} of greater than 600 ms, found to correlate with the presence of malignant cells with the capacity to metastasize, is very long and can only be accounted for by fast molecular motion in an unusual environment (Mountford *et al.*, 1984a). The location and environment of the triglyceride in the membrane has been investigated by spin-spin relaxation experiments. Different solvent systems have been studied in an attempt to determine the type of environment conducive to this type of relaxation mechanism.

Triglycerides (and diglycerides) as well as cholesterol esters of differing acyl chain content in $CDCl_3$ were found to give a single exponential decay with the T_2 varying from 1 s to 300 ms. (The acyl chains from cholesterol esters and triglycerides

TABLE II

Analysis of neutral lipid from a highly purified plasma membrane of VBL20 cells

TABLE IIA

Marker enzyme activity

Plasma membranes were isolated from 4.5×10^9 cells by disruption by nitrogen cavitation followed by fractionation on a sucrose density gradient. The enzyme activities were determined as described under "Experimental Procedures" for the initial suspension (homogenate) after cell disruption and the four density gradient bands as well as the supernatant from the density gradient centrifugation and a band of lipid which separated on top of the supernatant (designated floaters). The enrichment was calculated by the specific activity of the marker in each fraction divided by that in the homogenate. The values represent mean ± S.E. of two experiments. Band 1 is at the interface of the 10 and 30% sucrose layers; Band 2 is at the interface of the 30 and 48% layers; Band 3 is at the interface of the 48 and 60% sucrose layers; and Band 4 is the pellet at the bottom of the 60% sucrose layer.

Enzyme marker	Enrichment					
	Band 1	Band 2	Band 3	Band 4	Floaters	Supernatant
5′-Nucleotidase	44.9 ± 17.7	19.4 ± 5.0	15.5 ± 2.2	14.6 ± 5.3	0.46 ± 0.09	ND[c]
γ-Glutamyltranspeptidase	12.6 ± 3.3	11.1 ± 2.9	5.0 ± 0.4	0.6 ± 0.6	ND	0.15 ± 0.15
Na^+,K^+ adenosinetriphosphatase	10.5 ± 3.4	14.4 ± 5.0	5.8 ± 2.5	2.4 ± 0.3	ND	ND
Acid phosphatase	1.2 ± 0.4	1.9 ± 0.1	1.4 ± 0.1	1.0 ± 0.4	1.1 ± 0.3	2.0 ± 0.9
Lactate dehydrogenase	0.009 ± 0.001	0.08 ± 0.01	0.087 ± 0.005	0.035 ± 0.004	3.0 ± 1.2	2.5 ± 0.7
NADPH cytochrome *c* reductase	4.0 ± 0.2	6.8 ± 1.4	9.0 ± 0.6	6.7 ± 2.6	1.5 ± 0.2	0.9 ± 0.2
Cytochrome *c* oxidase	0.39 ± 0.3	3.5 ± 0.7	7.2 ± 1.2	6.4 ± 0.6	ND	ND
DNA	0.079 ± 0.007	0.11 ± 0.02	0.39 ± 0.03	1.1 ± 0.5	0.021 ± 0.004	0.015 ± 0.003

TABLE IIB

Cholesterol and phospholipid composition

The homogenate and four membrane bands from the density gradient centrifugation were analyzed according to the methods described under "Experimental Procedures" and the values represent the mean ± S.E. as determined from assays run in duplicate on two different extractions. No cholesterol ester was detected in the bands. Data are expressed as nmol/mg of lipid.

Fraction	Free cholesterol	Phospholipid	Cholesterol-to-phospholipid ratio
Homogenate	122 ± 12	1010 ± 16	0.12 ± 0.01
B1	263 ± 50	1403 ± 71	0.19 ± 0.05
B2	184 ± 10	856 ± 95	0.22 ± 0.02
B3	157 ± 30	922 ± 201	0.17 ± 0.01
B4	75 ± 5	1101 ± 15	0.07 ± 0.01

TABLE IIC

Triglyceride composition

The homogenate and four bands were analyzed, as well as the supernatant from the density gradient fractionation and a band of lipid which separated on top of the supernatant (designated floaters). The methods are as described under "Experimental Procedures" and the values represent the mean ± S.E. as determined from assays run in duplicate on two different extractions.

Fraction	Lipid	Protein	Recovery[a]
	nmol/mg	*nmol/mg*	*%*
Homogenate	274 ± 18	130 ± 25	
Floaters	640 ± 17	893 ± 26	54 ± 5[b]
Supernatant	297 ± 187	31 ± 12	
B1	139 ± 30	378 ± 193	13 ± 3
B2	79 ± 17	230 ± 71	11.5 ± 1.5
B3	90 ± 14	173 ± 21	12.5 ± 1.5
B4	114 ± 11	130 ± 35	9 ± 1

[a] Distribution of triglyceride is measured as a per cent of the total triglyceride recovered. The 1000-g pellet was not assayed.

[b] Recovery in supernatant floaters plus supernatant.

[c] ND, not detected.

were found to behave identically). Neutral lipids with one double bond at position 9 generate two clusters of resonances at 1.28 and 1.30 ppm from the nuclei at positions 2–7 and 12–17, respectively, in the chain (Frost and Gunstone, 1975). The results of a CPMG experiment, over the delay range 0–2 s for triolein (18:1) in chloroform, is shown in Fig. 3*A*.

The metastatic 13762 (Fig. 3*B*) and nonmetastatic J clone lines (Fig. 3*C*) both have four resonances under the broad methylene envelope at 1.2 ppm. CPMG experiments over the delay range 0–200 ms generate two rates of decay for each of the four resonances. A long T_{21} for the resonance at 1.25 ppm identifies the metastatic line 13762 from its nonmetastatic counterpart J clone. In contrast to the triglyceride in $CDCl_3$, these resonances cannot readily be followed over the delay range 200–2000 ms due to lack of signal intensity. Other cell lines, including human ovarian and colon cells (Mountford, *et al.*, 1984b), have been found to demonstrate a similar pattern whereby the metastatic cells generate a T_{21} of greater than 400 ms while their nonmetastatic counterparts have a T_{21} of less than 200 ms.[4] Triolein dispersed in D_2O does not yield a T_2 in excess of 200 ms.

Human lipoproteins are rich in cholesterol ester and triglyceride and have been shown to give narrow line ^1H NMR spectra. A possibility for the anomalously narrow ^1H NMR lines in our cells is that the neutral lipid domains may be akin to those in lipoproteins. The COSY spectra in Fig. 2 show that, except for the cross-peaks G (which have never been observed for a cell system) and D (which has a very low intensity in the 13762 cells and is not always observed), the cell spectrum is accounted for in terms of the triglyceride-rich VLDL spectrum plus that of the cellular metabolites. If lipoproteins are implicated, it is conceivable that protein conformational changes may account for the lengthening of T_2s encountered in the living cell.

In conclusion, a narrow NMR resonance originating from the plasma membrane of a cancer cell is unexpected, but it is explicable in terms of fundamental physics and chemistry. We have shown that there is chemical evidence for the presence of neutral lipid domains in the plasma membrane. The NMR signal can be accounted for by isotropically tumbling lipid which is not in diffusive exchange with the more conventionally structured membrane lipid. The type of lipid, identified by chemical analysis and two-dimensional NMR, is triglyceride (and diglyceride) and free or esterified cholesterol.

Other neutral molecules will be attracted preferentially to

[4] L. Kean, K. T. Holmes, P. G. Williams, G. L. May, M. Dyne, and C. E. Mountford, unpublished experiments.

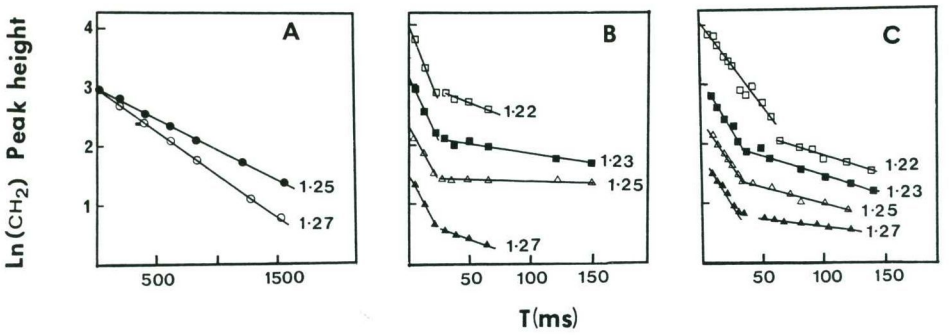

FIG. 3. **Transverse relaxation data, in which the natural log of the -CH_2- intensity is plotted against the delay between the first pulse and the *n*th echo in the Meiboom-Gill modification of the Carr-Purcell pulse sequence (Brindle *et al.*, 1979).** *A*, triolein in $CDCl_3$ solution (20 mg/ml). *B*, a suspension of 13762 cells (1×10^8 cells) in phosphate-buffered saline in D_2O. *C*, a suspension of J clone cells (1×10^8 cells) in phosphate-buffered saline in D_2O. The cell samples were prepared and the pulse sequence was executed as described under "Experimental Procedures." Spectral accumulations (32) were recorded with the water resonance suppressed by gated irradiation (Jesson *et al.*, 1973) in the case of *B* and *C*. No resolution enhancement is applied to *A*, while *B* and *C* have Lorentzian-Gaussian resolution enhancement (line broadening = −11, Gaussian broadening = 0.04). The chemical shifts are denoted beside each plot.

the oily membrane domain of the type described above. If this domain were large enough to traverse the plasma membrane, it could be a method of transporting many different types of molecules, including anesthetics and drugs into the cell.

Acknowledgments—We are indebted to Prof. Martin Tattersall for the suggestion that we study cancer metastasis and for his continued interest and support. We gratefully acknowledge Prof. Myer Bloom and Dr. John Saunders for their considerable contribution of time and thought to this program, and Dr. Ian Ramshaw for supplying the original metastasis model and his continued interest and advice. In addition we would like to thank Marlen Dyne for electron micrographs and technical assistance, Liz Kean for the tissue culture, Pat Gregory for animal facilities, and Judy Hood for her enthusiastic typing of the manuscript.

REFERENCES

Ames, B. N. (1965) *Methods Enzymol.* **8,** 115–118
Arseniev, A. S., Wider, G., Jonbert, F. J., and Wüthrich, K. (1982) *J. Mol. Biol.* **159,** 323–351
Block, R. (1973) *FEBS Lett.* **34,** 109–112
Brindle, K. M., Brown, F. F., Campbell, I. D., Grathwohl, C., and Kuchel, P. W. (1979) *Biochem. J.* **180,** 37–44
Brunk, C. F., Jones, K. C., and James, T. W. (1979) *Anal. Biochem.* **92,** 497–500
Cross, K. J., Holmes, K. T., Mountford, C. E., and Wright, P. E. (1984) *Biochemistry* **23,** 5895–5897
Duck-Chong, C. G. (1979) *Lipids* **14,** 492–497
Frost, D. J., and Gunstone, F. D. (1975) *Chem. Phys. Lipids* **15,** 53–85
Gottfried, E. L. (1967) *J. Lipid Res.* **8,** 321–327
Haeffner, E. W., Heck, B., and Kolbe, K. (1982) *Biochim. Biophys. Acta* **693,** 280–286
Harsas, W., Murdoch, S., and Pollak, J. K. (1985) *Biochem. Int.* **10,** 487–494
Hatch, F. T., and Lees, R. S. (1968) *Adv. Lipid Res.* **6,** 1–68
Heider, J. G., and Boyett, R. L. (1978) *J. Lipid Res.* **19,** 514–518
Iwanik, M. J., Shaw, K. V., Ledwith, B. J., Yanovich, S., and Shaw, J. M. (1984) *Cancer Res.* **44,** 1206–1215
Jacobs, W. L. W. (1971) *Clin. Chim. Acta.* **31,** 175–179
Jesson, J. P., Meakin, P., and Knissel, G. (1973) *J. Am. Chem. Soc.* **95,** 618–620
Meiboom, S., and Gill, D. (1958) *Rev. Sci. Instrum.* **29,** 688–691
Mountford, C. E., Grossman, G., Gatenby, P. A., and Fox, R. M. (1980) *Br. J. Cancer* **41,** 1000–1003
Mountford, C. E., Grossman, G., Hampson, A. W., and Holmes, K. T. (1982a) *Biochim. Biophys. Acta.* **720,** 65–74
Mountford, C. E., Grossman, G., Reid, G., and Fox, R. M. (1982b) *Cancer Res.* **42,** 2270–2276
Mountford, C. E., Mackinnon, W. B., Bloom, M., Burnell, E. E., and Smith, I. C. P. (1984a) *J. Biochem. Biophys. Methods* **9,** 323–330
Mountford, C. E., Wright, L. C., Holmes, K. T., Mackinnon, W. B., Gregory, P., and Fox, R. M. (1984b) *Science* **226,** 1415–1418
Newby, A. G., Luzio, P. J., and Hales, C. N. (1975) *Biochem. J.* **146,** 625–633
Nicolau, C., Dietrich, W., Steiner, M. R., Steiner, S., and Melnick, J. L. (1975) *Biochim. Biophys. Acta* **382,** 311–321
Nicolau, C., Klenk, H.-D., Reimann, A., Hildenbrand, K., and Bauer, H. (1978) *Biochim. Biophys. Acta* **511,** 83–92
Ramshaw, I. A., Carlsen, S. A., Hoon, D., and Warrington, R. C. (1982) *Int. J. Cancer* **30,** 601–607
Sen, A., Williams, W. P., Brain, A. P. R., Dickens, N. J., and Quinn, P. J. (1981) *Nature* **293,** 488–490
Sottocasa, G. L., Kuylenstierna, B., Emster, L., and Bergstrand, A. (1967) *J. Cell. Biol.* **32,** 415–438
Verkleij, A. J. (1984) *Biochim. Biophys. Acta* **779,** 43–63
Wharton, D. C., and Tzagoloff, A. (1967) *Methods Enzymol.* **10,** 245–250
Williams, J. P., and Merrilees, P. A. (1970) *Lipids* **5,** 367–370
Wagner, G., Kumar, A., and Wüthrich, K. (1981) *Eur. J. Biochem.* **114,** 375–384